Institut für Nutzpflanzenwissenschaften und Ressourcenschutz (INRES)
Fachbereich Pflanzenzüchtung

Genetic analysis of drought stress adaptation in bread wheat diversity

Dissertation

zur Erlangung des Grades

Doktor der Agrarwissenschaften (Dr. agr.)

der Landwirtschaftlichen Fakultät

der Rheinischen Friedrich-Wilhelms-Universität Bonn

vorgelegt von

Mohammad Kamruzzaman

aus

Pabna, Bangladesh

Bonn 2022

Angefertigt mit Genehmigung der Landwirtschaftlichen Fakultät der Universität Bonn

Referent:	Prof. Dr. Ali Ahmad Naz
Koreferent:	Prof. Dr. Annaliese Mason
Fachnahes Mitglied:	Prof. Dr. Mathias Becker
Vorsitzender:	Prof. Dr. Jens Léon
Tag der mündlichen Prüfung:	11.10.2022

Acknowledgment

I would like to express my deepest sense of gratitude to Prof. Dr. Ali Ahmad Naz for providing the opportunity to work under his supervision and cordial help throughout this research work. I am grateful to Prof. Dr. Jens Léon for his support and valuable suggestions, during my research. I am also thankful to Prof. Dr. Annaliese Mason for being my second supervisor, sharing the research ideas and providing valuable comments on my thesis. I also thank her for providing the experimental facility. I would also like to thank Prof. Dr. Mathias Becker for his research idea and for accepting my request to be part of the examination committee.

I would like to thank Dr. Asis Shrestha for showing me laboratory methods related to this work, for valuable suggestions, and for helping during the experiment. My sincere gratitude also goes to Dr. Agim Ballvora for providing the research materials and technical guidance for this work. I would like acknowledge Dr. Said Dadshani and Dr. Patrice Ahossi Koua for sharing marker data. I am also grateful to Mr. Nurealam Siddique for sharing his field research materials, fruitful discussion and suggestion to improve work quality. Special thanks to Dr. Harun-or Rashid, Principal Scientific Officer, BINA, Mymensingh, Bangladesh for reading the thesis and providing a valuable suggestion for improvement. I would also like to acknowledge Dr. Benedict Oyiga for reading and providing critical comments on my thesis. I would like to acknowledge Dr. Michael Schneider to help during experiment and to read this thesis paper and provide excellent suggestion.

I am also thankful to Mekides Abebe Beyene and Gullar Gadimaliyeva for helping me during the experiments. I would like send my appreciation to the staff of Campus Klein Altendorf for helping me to manage the experiment inside the rainout shelter. I would also like to thank the Department of Plant Breeding and its technical/administrative staff for their support and experimental facility. Special thanks to Karin Woitol, Jan Schoenenbach and Martina Ruland for organizing laboratory materials. I would like to thank Dr. Hasina Begum and Mohammad Bahman Sadeqi for helping me during the experiment.

I would like acknowledge my office authority, Bangladesh Institute of Nuclear Agriculture (BINA), Mymensingh, and Ministry of Agriculture, Bangladesh to approve my deputation. I would also take this opportunity to thank National Agricultural Technology Program (NATP), Phase-2, PIU-BARC, Bangladesh for providing scholarship and research funds to this PhD project.

Finally, I must express my appreciation to my family for their love and encouragement throughout my studies. This accomplishment would not have been possible without these wonderful people. Thank you.

Dedication

I dedicate this thesis to my belated mother, who was my best friend. I lost her during my thesis time. May Almighty Allah (SWT) rewards her departed soul in Jannah!

Table of contents

Summary

The accumulations of proline (Pro) and hydrogen peroxide (H_2O_2) are the typical response of plant against drought stress, therefore genetic analysis of these responses are crucial to establishing new varieties in crops like wheat. A genetic study namely genome-wide association study (GWAS) was performed to elucidate loci and candidate genes linked to drought-induced Pro and H_2O_2 accumulation and H_2O_2-induced root-shoot growth in bread wheat. GWAS identified a total of 11 significant marker-trait associations (MTAs) on 1A and 1B chromosomes for relative Pro values in a glasshouse experiment. The same study was performed in the field environment, and the study identified the most significant MTAs on 5B, and 1B chromosomes associated with 71 and 34 markers for Pro and H_2O_2 stress tolerance index (STI), respectively. The GWAS was also performed for H_2O_2-induced root-shoot variability to identify linked candidate loci and genes. Significant MTA was identified on 3B, 2A, 5A, 3B, 5D, 5A, and 6B chromosomes for relative root length, STI root length, relative shoot length, STI shoot length, relative root fresh weight, relative shoot fresh weight, STI shoot fresh weight, respectively. Linkage disequilibrium analyses revealed that European cultivars are linked with higher Pro accumulation under drought conditions. An opposite outcome between European and Non-Europe cultivars was observed for STI of Pro and H_2O_2. Similarly, distinct genetic relatedness was observed between the traditional and modern cultivars for root-shoot-associated STI and relative values. Minor alleles of single-marker and haplotypes were associated with higher Pro and H_2O_2 accumulation under drought and also with higher STI and the relative value for root-shoot traits. The candidate genes identified in significant loci regions were mostly involved in metal ion binding, transmembrane transport, oxidation-reduction process, protein phosphorylation, protein kinase, DNA, and ADP binding processes. The candidate loci, homolog search, and protein amylases revealed the loci and genes identified for drought-induced Pro and H_2O_2 and H_2O_2-induced root-shoot traits are reported first time in wheat. The alleles showed the contrasting phenotype that could be utilized to understand precisely their role under drought. Collectively, identified genetic factors associated with Pro and H_2O_2 biosynthesis lays a fundamental basis for future functional characterization of the identified genes.

Kurzfassung

Die Anhäufung von Prolin (Pro) und Wasserstoffperoxid (H_2O_2) ist die typische Reaktion von Pflanzen auf Trockenstress. Daher ist die genetische Analyse dieser Reaktionen von entscheidender Bedeutung für die Etablierung neuer Sorten bei Nutzpflanzen wie Weizen. Eine genetische Studie, nämlich eine genomweite Assoziationsstudie (GWAS), wurde durchgeführt, um Loci und Kandidatengene zu ermitteln, die mit der trockenheitsbedingten Pro- und H_2O_2-Akkumulation und dem H_2O_2-induzierten Wurzel-Sprossen-Wachstum bei Brotweizen in Verbindung stehen. GWAS identifizierte insgesamt 11 signifikante Marker-Merkmal-Assoziationen (MTAs) auf den Chromosomen 1A und 1B für relative Pro-Werte in einem Gewächshausversuch. Die gleiche Studie wurde im Freiland durchgeführt, und die Studie identifizierte die signifikantesten MTAs auf 5B- und 1B-Chromosomen, die mit 71 bzw. 34 Markern für Pro und H_2O_2-Stresstoleranzindex (STI) assoziiert sind. Die GWAS wurde auch für H_2O_2-induzierte Wurzel-Spross-Variabilität durchgeführt, um damit verbundene Kandidaten-Loci und Gene zu identifizieren. Signifikante MTA wurde auf den Chromosomen 3B, 2A, 5A, 3B, 5D, 5A und 6B für die relative Wurzellänge, die STI-Wurzellänge, die relative Trieblänge, die STI-Trieblänge, das relative Wurzel-Frischgewicht, das relative Triebluftgewicht bzw. das STI-Triebluftgewicht festgestellt. Analysen des Kopplungsungleichgewichts ergaben, dass europäische Sorten mit einer höheren Pro-Akkumulation unter Trockenheitsbedingungen verbunden sind. Ein entgegengesetztes Ergebnis zwischen europäischen und außereuropäischen Sorten wurde für STI von Pro und H_2O_2 beobachtet. Ebenso wurde eine deutliche genetische Verwandtschaft zwischen den traditionellen und den modernen Sorten für die Wurzel-Sprossen-assoziierten STI- und Relativwerte festgestellt. Minor-Allele von Einzelmarkern und Haplotypen wurden mit einer höheren Pro- und H_2O_2-Akkumulation unter Trockenheit und auch mit einem höheren STI und dem relativen Wert für Wurzel-Spross-Eigenschaften in Verbindung gebracht. Die Kandidatengene, die in den signifikanten Loci-Regionen identifiziert wurden, waren meist an Metallionenbindung, Transmembrantransport, Oxidations-Reduktionsprozessen, Proteinphosphorylierung, Proteinkinase, DNA- und ADP-Bindungsprozessen beteiligt. Die Suche nach Kandidatenloci, Homologen und Proteinamylasen ergab, dass die Loci und Gene, die für trockenheitsinduzierte Pro- und H_2O_2- und H_2O_2-induzierte Wurzel-Spross-Eigenschaften identifiziert wurden, zum ersten Mal in Weizen vorkommen. Die Allele zeigten einen kontrastreichen Phänotyp, der genutzt werden könnte, um ihre Rolle bei Trockenheit genau zu verstehen. Insgesamt bilden die identifizierten genetischen Faktoren, die mit der Pro- und H_2O_2-Biosynthese in Verbindung stehen, eine grundlegende Basis für die zukünftige funktionelle Charakterisierung der identifizierten Gene.

List of Tables

List of figures

List of supplementary figures

List of Supplementary Table

List of abbreviations

ABA	Abscisic acid
FDR	false discovery rate
GLM	general linear model
MLM	Mixed linear model
GWAS	Genome-wide Association Study
GST	glutathione-S-transferase
MTA	Marker-trait association
LD	Linkage Disequilibrium
MAF	Minor Allele Frequency
OAT	ornithine-delta-aminotransferase
P5CDH	Δ1-pyrroline-5-carboxylate dehydrogenase
P5CR	P5C reductase
P5CS	pyrroline-5-carboxylate synthetase
PDH	proline dehydrogenase
bZIP	basic-domain leucine zipper
MAPK	mitogen activated protein kinase
QQ	Quantile-Quantile
QTL	Quantitative Trait Loci
ROS	Reactive oxygen species
GST	glutathione-S-transferase
SNP	Single nucleotide polymorphism
TASSEL	Trait Analysis by Association, Evolution, and Linkage
IWGSC	International wheat genome sequencing consortium
RPV	Relative proline value
STI	Stress tolerance index
RL	Root length
SL	Soot length
SFW	Shoot fresh weight
RFW	Root fresh weight
H_2O_2	Hydrogen peroxide
GY	Grain yield

Chapter 1. General introduction

1.1. Wheat is an important crop for food security

Wheat is an important component of agricultural history and food security. About 10000 years back when wheat was assumed to grow first in the Fertile Crescent, an area in the Middle East, and later it was disseminated to another part of the world at a fast pace (Venske et al., 2019). There are several species of the wheat genus (Triticum). The most widespread is common or bread wheat (*Triticum aestivum* L.), which accounts for 95% of the total areas cultivated. Due to having the capability to grow under minimum water status, it has an advantage over other crops. However, it is currently cultivated on about 219 million hectares that mainly covers temperate, Mediterranean-type, and subtropical parts of both hemispheres, from 67°N in Norway, Finland, and Russia to 45°S in Argentina, which comprises 17% of all crop areas. China, India, Russia, the USA, and France are the main wheat-producing countries (Figure 1.1). The global production is around 750 million tons (Figure 1.1). It is the basic staple food of 40% world's population and provides humans with 18% of their daily intake of calories and 20% of their protein (Sowell et. al., 2022). The average yield of wheat ranges from 2.6 t/ha to 6.5 t/ha depending on the type of cultivation area. For example, average wheat production is higher in East Asia and the European Union (4.3–5.3 t/ha). The average wheat production in South Asia is 3.0 t/ha and in Africa is 2.6 t/ha. Annually per person consumption of wheat varies widely from 170 kg in Central Asia to 27 kg in Eastern and Southern Africa (Shiferaw et al., 2013). China and India each consume 17-18% of global wheat (RaboResearch, 2017). Around 500 kcal energy per capita per day comes from wheat (Dixon et al., 2009). World has experienced so many unfavorable episodes during 1960s, which mainly came from shortage of food. In 1960s, the increasing population and food demand was severe in developing countries. This event reinforced a dramatic increase in cereal production in many countries. Several genetic traits were selected to improve the yield, stability, and large-scale adaptability of rice, corn, and wheat (Khush, 2001). This time brought forth greater productivity in wheat, mainly because of incorporation of dwarf gene (Zhang et al., 2014). The introgression of dwarfing genes from a Japanese cultivar 'Norin 10' leaded to increase in yield potential (Khush, 2001). Even currently, more than 70% of commercially grown wheat are harboring this 'Norin 10' dwarfing genes (Hedden, 2003).

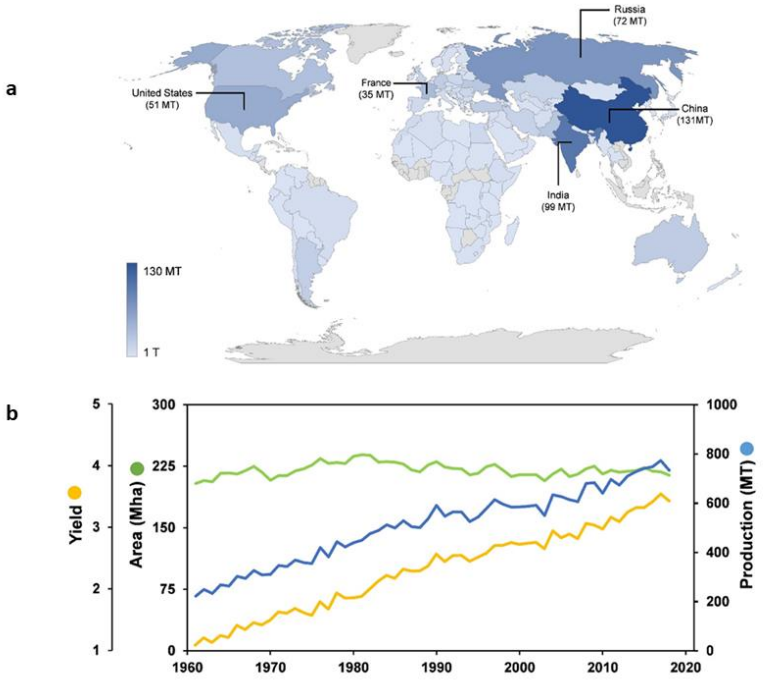

Figure 1.1. Global scenario of wheat production. (a) Total wheat production in megaton (MT) in the year 2018 per country. (b) The world wheat production, harvested area, and yield between 1960 and 2018. The picture was adopted from de Sousa et al., (2021)

In recent decades, global food production has been suffered from different abiotic stresses. Very recently, COVID-19 situation also limits the agricultural trading globally. These factors are considerable thread for global food security. Moreover, the climate resilience of wheat has been noticed to decline in most European countries during the past 10 years, probably due to the reduced diversity in the genetic pool of cultivars (Kahiluoto et al., 2019). Grain production needs to be doubled to feed a world population that is estimated to reach approximately 9 billion by 2050. To meet the predicted demands of wheat in developing countries, exploring new technologies for increasing the rate of genetic gain and mining genetic variability and diversity need to be achieved (Asseng et al., 2017).

1.2. Drought stress is a major challenge for global crop production

Drought is a period of unusually determined extreme weather that sustains long enough to pose a negative impact on agricultural production on local to global scales (Zipper et al., 2016). It may last for a few days to months or years. There are four categories of drought, namely meteorological, hydrological, agricultural, and socioeconomic (Wilhite and Glantz, 1985). The first three categories are physical and directly related the crop weather and climate. Meteorological drought is the water shortage for a long time and region based. Agricultural drought is the shortage of water in the soil,

in groundwater reservoirs that cannot meet the evapotranspiration demand of the crops to maintain optimum growth and production. Hydrological drought is the deficiencies of water from the hydrological system such as soil moisture, streamflow, and groundwater and reservoir levels (Zipper et al., 2016). When plants are subject to water deficit conditions they compensate for the stress by reducing shoot biomass and exhibiting significant yield loss of up to 70% (Kleine and Müller, 2014; Sallam et al., 2019). Several drought episodes, short term to the long term, occurred in the 20th century worldwide. Those events went through severe food crises and loss of lives. Moreover, world agriculture has been suffering from global warming for a few decades.

Drought is responsible for significant yield loss globally (Lobell et al., 2014). Several studies anticipated that the drought episodes would be more frequent in the coming days because of water loss due to less precipitation and more evaporation (Sheffield and Wood, 2008; Trenberth et al., 2013; Dhanyalakshmi et al., 2019). A study highlighted that more than 7% greater yield damage occurs only for drought. It causes 8-11% more crop damage in developed countries than in developing ones (Lesk et al., 2016). The study also estimated that droughts during 1964-2007 caused a cereal loss of 1820 million Mg. This loss was equivalent to global maize and wheat production in 2013, and to the loss during 1985-2007, which is two times larger than that during the droughts of 1964-1984. Wang et al., (2018) estimated an average of 2.2 dry months each year, and the dry area increased by 1.1% per decade across the world which experiences the drought. They also assumed that the least developing countries of Asia and Africa will be more sufferers of drought since they do not have enough support and infrastructure to cope with the calamities. Lobell et al., (2011) reported that high temperature and drought from 1980 to 2008 declined the global yield of maize and wheat by 3.8%, and 5.5%, respectively. Verón et al., (2015) reviewed that the yield loss during the 1971-2012 period amounted to 5.4 % of average yields for maize, 5.1 % for wheat, and 2.6 % for soybean due to shortage of precipitation.

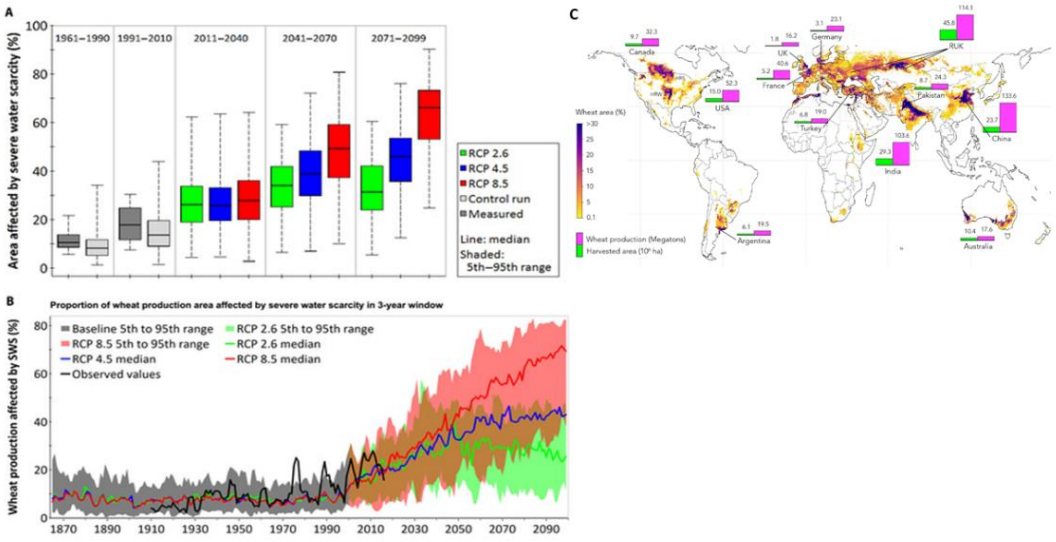

Figure 1.2. Estimated proportion of global wheat-growing area affected by SWS between 1861 and 2100. (A) Global wheat affected by SWS (B) Annual values of areas affected by SWS during year from 1911 to 2016. (C) Worldwide wheat cropping area (%), total harvested area, and wheat production of the top 12 global wheat producers. Abbreviations: representative concentration pathways=RCP; SWS= severe water scarcity. Figure source: Trnka et al., 2019; Helman and Bonfil, 2022.

Kim et al., (2019) estimated the production losses of maize, rice, soy, and wheat from 1983 to 2009 which were reduced by 0.8% per year due to drought-related attributes. The combined effects of high temperatures and drought significantly reduced the yields of maize, soybeans, and wheat by 11.6, 12.4, and 9.2%, respectively in 2014 compared to the year 1963 (Matiu et al., 2017). Qaseem et al., (2019) reported that the grain yield of wheat was reduced by 44.66% under drought treatment. Similar findings were also documented by Daryanto et al., (2016). They showed that 40% moisture loss results in yield reduction of wheat and maize by 20.6%, and 39.3% respectively.

Global warming has increased the frequency and intensity of severe water scarcity (SWS) events, which may negatively affect wheat production. Currently, wheat is grown in all six continents except Antarctica. The leading producers include China, the Russian Federation, Ukraine, Kazakhstan (RUK), India, USA, France, Canada, Pakistan, Germany, Argentina, Turkey, Australia, and United Kingdom (Figure 1C) which was collectively 600 megatons in 2019 (Figure 1.2). A projection was made without considering climate change mitigation which reported that up to 60% of the current wheat-growing area will face simultaneous SWS events by the end of this century (Figure 1.2) (Trnka et al., 2019). Leng and Hall (2019) reported a simulation model which estimated that compared to the present condition, there is a risk of the yield of 9%-12%, 5.6%-6.3%, 18.1%-19.4%, and 15.1%-16.1 for wheat, maize, rice, and soybeans by the end of 21st

century, respectively. However, the extreme climatic condition has been predicted a crop reduced production by 50% in 2050 and that will be 90% in 2100 (Leng and Hall, 2019). Moreover, the food and agriculture organization has estimated a 43% increase in the global annual demand for cereals from approximately 2.1 Giga tons in 2006 to 3.0 Giga tons by 2050. All these situations call for urgent mitigation strategies to reduce water loss, and develop drought adaptive crop varieties.

1.3. The genetic diversity of wheat-a potential basis for drought adaptation

Wheat is an ideal crop for studying the diversity as it evolved through allopolyploid speciation, adaptation, and domestication (Gustafson et al., 2009). Due to having high adaptive fitness, wheat has been acclimatized to diverse climates including subtropical and Mediterranean regions. More than 25,000 varieties of bread wheat has been adapted to temperate environments (Shewry, 2018). Modern hexaploid bread wheat (*T. aestivum* L.) has gained complex genomic composition (Dubcovsky and Dvorak, 2007). The bread wheat comprises of three genomes (A, B, and D), and contains 42 (AABBDD, $2n = 6x = 42$) chromosomes, respectively. These genomic compositions were descendent from the wild progenitors. Two allopolyploid speciation events are associated with bread wheat. The A genome was derived from the progenitor *T. turgidum* ssp. dicoccoides (AA; 2n = 2x = 14). But the B sub-genome progenitor has not certainly been discovered precisely yet (Peng et al., 2011).

The bread wheat was derived from hybridization between cultivated tetraploid wheat (*T. turgidum*) and the goat grass *Aegilops tauschii* (DD, 2n=2x=14) (Salamini et al., 2002). The third sub-genome (D) progenitor *Aegilops tauschii* constitutes a genetic diversity for improving the performance and environmental resilience of bread wheat (Gaurav et al., 2021). With the genetic resources of both ancestral diploids, cultivated bread wheat is generally more vigorous, giving higher yields and adapting to a wider range of environmental conditions as compared to its progenitors (Venske et al., 2019). It is due to the integration episodes at genome and chromosome levels which increased genetic diversity (Danilova et al., 2019). Another report says the genetic diversity can be increased by introgression up to two to three orders of magnitude which is more than mutation (Ellstrand et al., 2013). In modern agriculture, breeding programs and research activities of crops like rice, soybean, maize, etc. have been suffering from genetic erosion derived from genetic bottlenecks (Eyre-Walker et al., 1998; Hyten et al., 2006). Here, wheat shows better genetic diversity for plant breeding research. As mentioned above, the genome of wheat contains 21 chromosomes which

makes the genome size about 18 Giba base pairs, which is approximately 136 times larger than that of *Arabidopsis* and is larger than other important crops like rice and maize. All these shreds of evidences point out that wheat has more genetic potential that can be exploited to develop drought tolerance varieties.

1.4. Proline accumulation in plants under drought and adaptive role for acclimation

Plants often suffer from drought stress that causes morphological, physiological, and biochemical changes. These changes collectively lead to destabilized plant growth, which ultimately cause yield loss (Sallam et al. 2019). Reactive oxygen species (ROS) adversely affect plant growth under stress conditions. To cope with that, the defense machinery of plants become active and accumulate larger quantities of compatible solutes (Serraj and Sinclair, 2002). Compatible solutes are low molecular weight, highly soluble organic compounds that are usually non-toxic at cellular concentrations. These solutes protect cells through cellular osmotic adjustment, ROS detoxification, membrane integrity and DNA/protein stabilization. Proline (Pro) is a compatible solute, multifunctional, low molecular weight amino acid, which has several protective roles for stressed cells. It maintains redox balance, plasma membrane integrity, ROS detoxification, and osmotic adjustment of stressed cells and acts as a driver for NADP+/NADPH redox balance during osmotic stress (Sharma et al., 2011; Kishor et al., 2015). Due to having such a versatile role, it is one of the widely studied molecules in the field of plant science (Szabados and Savouré, 2010; Kishor et al., 2015). The housekeeping or minimum level is always involved in normal plant growth. Its accumulation goes high in a plant cell when the generation is higher than the degradation. A study estimated that under control conditions Pro comprises less than 5% of the total free amino acids pool. Whereas under stress condition, the concentration elicits up to 80% of the amino acid pool (Shahbaz et al., 2013). Sharma and Verslues, (2010) observed that under normal condition Pro maintains normal physiology of plants while under drought conditions it elicits up to 100 folds. Pro biosynthesis is triggered by dehydration or any stress but the rehydration or stress withdrawal triggers the catabolism process. Therefore, its metabolism in control-stress-control conditions follows a cyclic fashion. However, higher Pro accumulation has been documented in drought, salinity, low temperature, heavy metal, UV radiation, etc. stresses (Bassi and Sharma, 1993; Hare et al., 1998; Munns, 2005; Fedotova and Dmitrieva, 2016). The generation of Pro in plant occurs through glutamic acid pathway. According to that pathway, the amino acid glutamate is initially reduced to glutamic- γ-semi aldehyde (GSA) by the pyrolline-5-carboylate synthase enzyme. This GSA

spontaneously converted to pyrroline-5-carboxylate (P5C). This P5C is finally reduced to Pro by the P5C reductase enzyme (Verbruggen et al, 1993). These reactions for biosynthesis take place in the chloroplast. In catabolic reaction, the enzyme Pro dehydrogenase (ProDH) that located in mitochondria, oxidizes Pro to P5C and finally, P5C dehydrogenase converts P5C to glutamate (Rai and Penna, 2013) (Figure 1.3). Alternatively, Pro can be produced from ornithine through Orn-δ-aminotransferase (δOAT) which transfers the δ-amino group of ornithine to α-ketoglutarate, thereby forming GSA in Mitochondria. GSA is in equilibrium with the cyclic P5C. Therefore, P5C is here a common intermediate for Pro biosynthesis and degradation (Delauneys et al., 1993). In contrast, recent finding has shown that the P5C is generated through δOAT and ultimately gives glutamate (Figure 1.3). It is noted that Pro biosynthesis via the glutamate pathway occurs rarely (Funck et al., 2008). Savouré et al., (1995) observed that the expression of the P5CS gene was regulated osmotically, upon salt treatment in *Arabidopsis* the transcript level of it increased. Yoshiba et al., (1995) reported that upregulation of P5CS occurred through osmotic stress but not through P5CR, which suggested that the conversion of glutamate to P5C is the rate-limiting step of Pro biosynthesis.

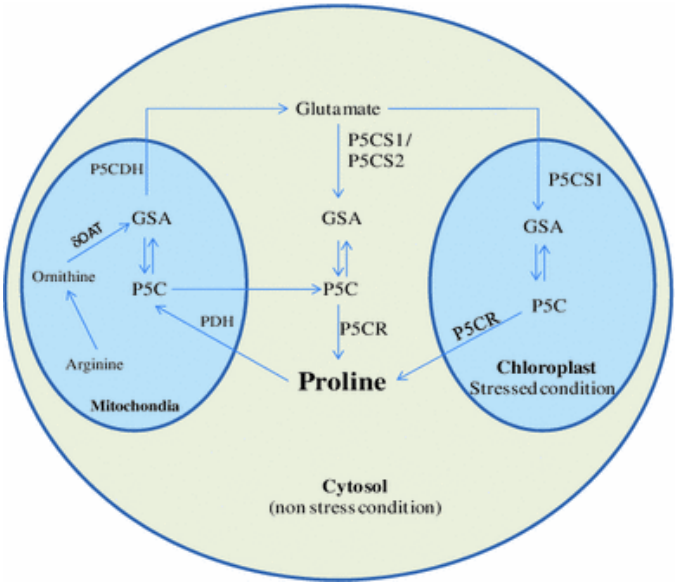

Figure 1.3. Biosynthetic pathways of Pro in plants. Source: Rai and Penna, 2013

Plants utilize the elevated Pro in a balanced way. Initially, the Pro rises during drought then utilized by plants to cope with the drought. But unfortunately, some drought-susceptible cultivars like 'Scarlett' failed to utilize the reserved Pro efficiently due to wilting symptoms on leaves appearing early, and leaf death which results in Pro reduction under drought stress condition in barley (Sayed

et al., 2012). The degradation of Pro into P5C and GSA toxic intermediates may cause cell death (Hellmann et al., 2000). However, improved drought tolerance has been reported in advanced backcrossed lines derived from the genetic cross between the cultivar, Scarlett, and wild barely, ISR42-8 (Muzammil et al., 2018). Several studies pointed out that, Pro act as a source of carbon, nitrogen, and energy during the recovery of the plant (Trotel et al., 1996; Szabados and Savouré, 2010). Mattioli et al., (2008) reported that Pro acts as signal molecules that control the various genes expression and enhance plant growth and development such as flowering and seed set during water stress. Osmo-protectant role of Pro has been documented by several studies under drought stress conditions (Delauney et al., 1993; Yoshiba et al., 1995). Those studies also revealed that the Pro regulation at the transcriptional level is regulated by the expression of some genes. High Pro accumulation was reported in pigeon pea under polyethylene glycol (PEG) induced water stress conditions (Fazeli et al., 2006).

Iyer and Caplan, (1998) revealed that Pro accumulation can increase the expression of the drought stress genes in rice. Sayed et al., (2012) reported that Pro can act as a reliable marker under drought stress conditions because the QTLs that harbored Pro-related genes were associated with high Pro content under drought. In several plants, ABI1 and the CaM4 calmodulin-MYB2 pathways are linked and regulate the regulatory pathways of P5CS1 transcription (Knight et al., 1997; N et al., 1997; Parre et al., 2007). Bhaskara et al., (2012) reported three mutants such as PP2Cs, highly ABA-Induced 1 (HAI1), HAI2, and HAI3 increased the accumulation of Pro under the low water potential.

A report identified that overexpression of wheat F-box protein-containing gene *TaFBA1* regulates Pro biosynthesis (Li et al., 2018). Their findings suggested that *TaFBA1* may improve enzymatic antioxidant levels and regulate gene expression by interacting with other proteins, which leads to enhanced stress tolerance in plants. Few reports revealed that zinc finger proteins (ZFPs) are involved in Pro biosynthesis during abiotic stress including salt and drought, stress responses, and ROS scavenging processes (Luo et al., 2012; Wang et al., 2016). Jiang et al., (2015) identified the crucial roles of pentatricopeptide repeat proteins which is a positive regulators of plant responses to abiotic stresses and displayed tolerance to drought and salt through the high level of Pro accumulation. Likewise, the gene encodes serine-threonine kinase has been reported to regulate drought tolerance via modulating ABA sensitivity, acts as a positive regulator of the ABA-mediated drought-stress tolerance, and produced higher Pro in mutant after dehydration treatment

(Lim et al., 2020). Ju et al., (2013) identified a functional E3 ubiquitin ligase that participated negatively in Pro production in wild type but the mutant form increased Pro contents and enhances drought tolerance in *Arabidopsis*. Many pieces of evidence laid to an idea that higher levels of Pro in different plant species are associated with increased drought tolerance. Due to its enigmatic and distinct role, the criterion that higher Pro accumulation in genotypes is associated with drought tolerance was not successfully implemented across plant species (Stewart CR, 1980). But it is clear that Pro has an adaptive role in drought stress conditions and its regulation is controlled by the cumulative effects of many stress-related genes. Therefore, it is important to explore the role of genetic elements that regulate Pro in plant/wheat for adaptation to drought.

1.5. Hydrogen peroxide is linked with many signaling and developmental pathways in plants

Hydrogen peroxide (H_2O_2) is a byproduct of aerobic metabolism in plants and can be synthesized either enzymatically or non-enzymatically (Mittler, 2002). The enzymatic process includes the enzymes such as oxalate, amine oxidases, and flavin-containing enzymes, and cell wall peroxidases (Hu et al., 2003; Cona et al., 2006; Francoz et al., 2015) (Figure 1.4). Till the last decade, H_2O_2 was thought to be a toxic reactive oxygen species (ROS) responsible for damage to a variety of cellular components. It became clear later on that H_2O_2 can also act as a potent signaling molecule, and is involved in a plethora of physiological functions (Petrov and Van Breusegem, 2012). However, among the ROS, H_2O_2 has a relatively long life span and therefore is measurable in plants. It is synthesized mainly from its precursor O_2^- in mitochondria, chloroplast, and peroxisome through photorespiration, electron transport chains (ETC), and redox reaction (Niu and Liao, 2016). In addition, nicotinamide adenine dinucleotide phosphate (NADPH) oxidases may involve producing superoxide that is converted to H_2O_2 by superoxide dismutase (SOD) (Brewer et al., 2015). Remans et al., (2010) reported that H_2O_2 formation in plants is mostly related to the stimulation of NADPH oxidase under heavy metal stresses. Ben Rejeb et al., (2015) observed that H_2O_2 produced through NADPH oxidases increased Pro content under salt or mannitol stress in *Arabidopsis thaliana*. Few other enzymes such as glucose oxidases, sulfite oxidases, and glycolate oxidases can oxidize their substrates to produce H_2O_2 (Brychkova et al., 2012; Chang and Tang, 2014) (Figure 1.4). The non-enzymatic reactions are linked with photosynthesis and respiration. Non-enzymatic H_2O_2 is produced continually through electron transport reactions both in mitochondria and chloroplasts (Figure 1.4). H_2O_2 is an important regulatory component in different signaling pathways, and it is coupled with the different developmental and physiological processes

in plants (Barba-Espín et al., 2011). Cell-to-cell movement of H_2O_2 occurs through aquaporin channels for signal transduction (García-Mata and Lamattina, 2013). It has been reported that there is crosstalk among H_2O_2, NO, and Ca^{2+}, which makes a complex signaling network to regulate different developmental and physiological processes in plants. For example, Li and Xue, (2010) reported that Ca^{2+} signaling played as a downstream molecule of H_2O_2 and nitric oxide (NO) signal pathway during adventitious rooting of mung bean. Similarly, Liao et al., (2012) found a relationship between H_2O_2, NO, and Ca^{2+}/CaM. The exogenous application of NO and H_2O_2 promoted adventitious root formation through increasing endogenous Ca^{2+} and calmodulin (CaM) levels in marigold. Hu et al., (2007) reported that cross-talk between Ca^{2+}-CaM and H_2O_2 also played a significant role in antioxidant defense in ABA signaling in maize leaves. Another signal transduction component, the mitogen-activated protein kinase (MAPK) pathway is associated with abiotic stress responses and extracellular stimuli that are transduced into intracellular changes (Zhou et al., 2014). Exposure of cells to exogenous H_2O_2 leads to activation of MAPK pathways (Zuo et al., 2016).

However, the generation of elevated amount of H_2O_2 under drought and any other stress exhibited as cross-tolerance to the same and other different stress conditions (Neill et al., 2002). For example, a recent study reported that 60 mM exogenous H_2O_2 treatment can improve drought tolerance in wheat (Bhardwaj et al., 2021). It improves abiotic stress tolerance by modulating the expression of resistance genes and antioxidant enzyme activities. Jing et al. (2009) observed that exogenous H_2O_2 treatment to cucumber plants promotes drought tolerance by reducing membrane damage and increasing anti-oxidant activities.

In response to a variety of stress stimuli and crosstalk and modulation of gene expression in different signaling pathways by H_2O_2 has received much attention (Bowler and Fluhr, 2000). Li et al., (2011) stated expression of genes modulated H_2O_2 was involved in ROS control, transcriptional regulation, signal transduction, carbohydrate, protein, and lipid metabolism. A large number of genes involved in defense, signal transduction, stress perception, transcription, and general metabolism have been identified, revealing a highly dynamic and redundant network of genes associated with enzymes involved in ROS production and ROS-scavenging. WRKY and zinc finger transcription factors are largely controlling the activities of ROS-related defense genes. In *Arabidopsis*, zinc finger proteins ZAT7 and ZAT12 were found strongly up-regulated by oxidative stress in apx knockout mutants in response to H_2O_2 (Rizhsky et al., 2004). Polidoros and

Scandalios, (1999) observed that high concentrations of H_2O_2 rapidly induced catalase (CAT) and glutathione-S-transferase-1 (GST1) gene. Later, they also observed that H_2O_2 induced the expression of a GST gene in the leaves of maize seedlings (Polidoros et al., 2013). A global analysis of gene expression study stated that 1-2% of gene expression is regulated in response to H_2O_2 treatment under drought and other stress conditions (Desikan et al., 2000), which in other words, suggested that H_2O_2 metabolism is regulated by many genes.

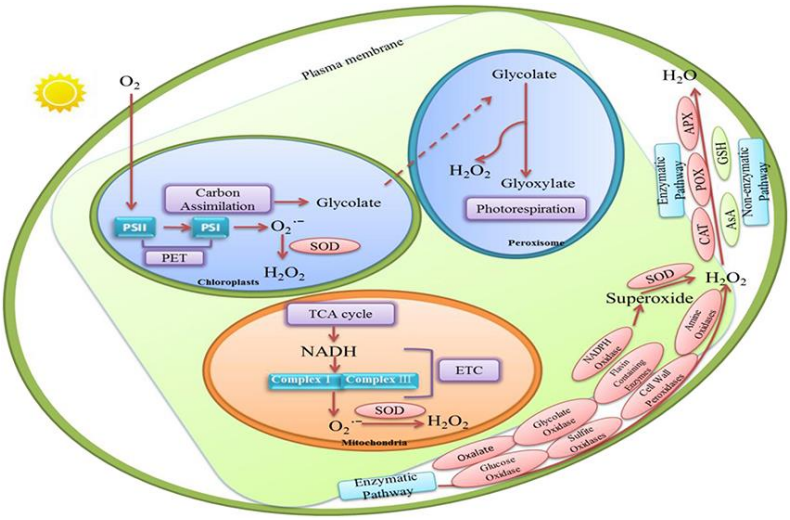

Figure 1.4. The various routes of hydrogen peroxide (H_2O_2) production and removal in plant cells, the photo was adapted from Niu and Liao, (2016).

Continuous H_2O_2 production under normal conditions is required for physiological processes comprising photosynthesis, opening, and closing of stomata, senescence, cell growth and development (Deng et al., 2012). Under normal conditions, H_2O_2 accumulation has been reported as 60 µM- 7 mM in *Arabidopsis*, 20 µM in Maize, and 60 µM in Kentucky bluegrass (Veljovic-Jovanovic et al., 2002;Tewari et al., 2004; He et al., 2005). High concentration of H_2O_2 production has been reported in drought, salinity, cold, high temperature, heavy metal, and UV radiation in plants (Cruz De Carvalho, 2008; Zhou et al., 2012; Liu et al., 2018). Its overproduction under stress condition triggers oxidative burst to organic molecules that causes programmed cell death, albeit the toxic level is balanced by the antioxidant system (Corpas et al., 2001).

1.6. Genome-wide association study-an important tool to identify candidate genes of a trait of study

Understanding the genetic architecture of a complex trait is a fundamental basis to understand its biology. Most of the traits of agricultural importance are complex and largely influenced by many genetic factor and environmental conditions as well as their interactions (MacKay et al., 2009). Genome-wide association study (GWAS) is a technique that has been adopted to gain insight into the genetic architecture of the complex trait. Physical mapping of several polyploidy species and sequencing of the wheat genome by the international wheat genome sequencing consortium (IWGSC) further accelerate genome-wide studies in wheat and other polyploidy species (Fleury et al., 2010; Feuillet and Eversole, 2007). GWAS performs testing genetic variants across the genomes of many individuals of a population to identify genotype-phenotype association (Alseekh et al., 2021). Genotyping usually uses simple-sequence repeats or a single nucleotide polymorphic (SNP) array. SNPs arrays are incorporated with imputation (Johnson et al., 2013). Association tests then employ F-statistics to identify genomic regions that are linked with the phenotype of interest.

The first GWAS was performed in human disease, a variant of the complement factor H gene associated with age-related macular degeneration (Klein et al., 2005). Soon after its development, it had been successfully used in dissecting a bunch of complex phenotypes including human and animal diseases, physiological, and agronomic traits in plants (Huang et al., 2010; Horton et al., 2012; Chen et al., 2016). GWAS has been successfully employed to uncover genes governing stress tolerance in many plant species (Ueda et al., 2015; Yuan et al., 2019; Liu et al., 2020). It exhibits a high-resolution genomic map for a studied trait, since it includes the recombination history of a large number of individuals of a species (Brachi et al., 2011).

But due to constrain by the population structure and unequal relatedness between individuals (kinship), GWAS showed spurious associations in previously used the general linear model (GLM). To address this problem considerable efforts have been made to assess population structure statistically (Devlin and Roeder, 1999; Liu et al., 2016). Later it was corrected through a mixed linear model (MLM) that incorporated the population stratification as a fixed effect, kinship among individuals via the variance-covariance structure of the random effect for the individual (Yu et al., 2005; Zhao et al., 2007). Thus, MLM fits for correcting the inflation by the small genetic effects and controlling the bias caused by population structure. GWAS approach requires a larger

population size as it estimates small effect sizes and thus explains a modest proportion of heritability (Manolio et al., 2009). Therefore, large population size is important as reduces the portion missing heritability. Larger population size when combined with an increased number of SNPs chance of a successful result increases (Visscher et al., 2012; Ahlqvist et al., 2015). Moreover, thus it can resolve many of the limitations such as missing signals, population stratification, ultra-rare mutation identification as well as gene-to-gene and gene-to- environment interactions (Steinthorsdottir et al., 2014; Lek et al., 2016).

Due to having an important role in food security, using GWAS has drawn special attention to wheat. Water shortage limits its global production drastically. A study was conducted with 361 wheat genotypes to develop drought-tolerant cultivars (Rabbi et al., 2021). The study identified a total of 69 consistent QTL involved with drought tolerance-related traits. Chromosomes 1A, 3A, 3B, 4B, 4D, 5B, 6A, and 6B harbored the major QTL for drought tolerance. Six potential novel QTL were identified on chromosomes 3D, 4A, 5B, 7A, and 7B for days to heading, plant height, and thousand kernel weight under drought stress, respectively. Another study on drought tolerance-related traits identified marker-trait association on chromosomes 1B, 2A, 2B, 2D, 3A, 3B, 3D, 4B, 5A, 5B, 6B, and 7B, respectively (Maulana et al., 2018), 12 stable QTL among those responded to drought stress. Some significant single-nucleotide polymorphisms (SNPs) coincided with candidate genes playing roles in plant abiotic stress responses. Similar studies have been reported for shoot biomass, root biomass, root-shoot ratio and grain yield, relative water contents, grain per spike, and yield per plant under drought stress conditions (Pfeifer et al., 2014; Mwadzingeni et al., 2017; Mathew et al., 2019). However, all these studies focused on agronomic traits. To our knowledge GWAS with drought-associated metabolites in wheat and other cereals with a global diversity panel has not been performed. Due to having an immense adaptive role in drought, studies with Pro and H_2O_2 are important. Although, phenotyping with the large number of accessions for Pro and H_2O_2 is laborious. Studies should be emphasized in these areas to get insight into their precise role in drought adaptation. Verslues et al. (2014) reported some effector genes related to Pro metabolism in *Arabidopsis* and more recently in *Eucalyptus* by other authors through GWAS (Mora-Poblete et al. 2021). To our knowledge, there is no GWAS available for drought- induced H_2O_2 accumulation in plants. A recent GWAS report has shown that diversified response to H_2O_2 exposure across the *Arabodopsis* accessions was lying in a selective aquaporins ability to channel H_2O_2 across the membranes (Sadhukhan et al., 2017). Based on previous findings, we can think

about few research questions. What is role of Pro and H_2O_2 under drought stress and how diversified they are in wheat? What are the genetic regulators of Pro and H_2O_2 accumulation diversity in wheat? Are Pro accumulation diversity controlled by the same genetic factor or different under glasshouse and field environments? What are the genetic factors linked to the tolerance mechanisms mediated by H_2O_2 induced wheat seedling growth?

Keeping all these research questions in consideration, the present study was formulated with the following specific objectives:

- to assess the variation of Pro accumulation among the cultivars induced by drought in the glasshouse environment
- to identify candidate loci and genes linked with Pro variability induced by drought in the glasshouse environment
- to assess the variation of Pro and H_2O_2 accumulation among the cultivars induced by drought in the natural field environment
- to identify candidate loci and genes linked with Pro and H_2O_2 variability induced by drought in the natural field environment
- to uncover the natural genetic variability of root-shoot traits induced by H_2O_2 and
- to identify the candidate loci and genes for natural genetic variability of root-shoot traits induced by H_2O_2

The result of the study is described into following three chapters:

Chapter 2: Genetic mapping of candidate loci for drought-induced Pro accumulation in bread wheat

Chapter 3: Pinpointing genomic loci for drought-induced Pro and hydrogen peroxide accumulation in bread wheat under field conditions

Chapter 4: Hydrogen peroxide-induced root-shoot variations in bread wheat and mapping of candidate loci by GWAS

1.7. References

Ahlqvist E, Van Zuydam NR, Groop LC, McCarthy MI (2015) The genetics of diabetic complications. Nat Rev Nephrol 2015 115 11: 277–287

Alseekh S, Kostova D, Bulut M, Fernie AR (2021) Genome-wide association studies: assessing trait characteristics in model and crop plants. Cell Mol Life Sci 2021 7815 78: 5743–5754

Asseng S, Cammarano D, Basso B, Chung U, Alderman PD, Sonder K, Reynolds M, Lobell DB (2017) Hot spots of wheat yield decline with rising temperatures. Glob Chang Biol 23: 2464–2472

Barba-Espín G, Diaz-Vivancos P, Job D, Belghazi M, Job C, Hernández JA (2011) Understanding the role of H2O2 during pea seed germination: a combined proteomic and hormone profiling approach. Plant Cell Environ 34: 1907–1919

Bassi R, Sharma SS (1993) Proline accumulation in wheat seedlings exposed to zinc and copper. Phytochemistry 33: 1339–1342

Bhardwaj RD, Singh N, Sharma A, Joshi R, Srivastava P (2021) Hydrogen peroxide regulates antioxidant responses and redox related proteins in drought stressed wheat seedlings. Physiol Mol Biol Plants 27: 151–163

Bhaskara GB, Nguyen TT, Verslues PE (2012) Unique drought resistance functions of the highly ABA-induced clade a protein phosphatase 2Cs. Plant Physiol 160: 379–395

Bonner CA, Williams DS, Aldrich HC, Jensen RA (1996) Antagonism by l-glutamine of toxicity and growth inhibition caused by other amino acids in suspension cultures of Nicotiana silvestris. Plant Sci 113: 43–58

Bowler C, Fluhr R (2000) The role of calcium and activated oxygens as signals for controlling cross-tolerance. Trends Plant Sci 5: 241–246

Brachi B, Morris GP, Borevitz JO (2011) Genome-wide association studies in plants: the missing heritability is in the field. Genome Biol 2011 1210 12: 1–8

Brewer TF, Garcia FJ, Onak CS, Carroll KS, Chang CJ (2015) Chemical approaches to discovery and study of sources and targets of hydrogen peroxide redox signaling through nadph oxidase Proteins. http://dx.doi.org/101146/annurev-biochem-060614-034018 84: 765–790

Brychkova G, Yarmolinsky D, Fluhr R, Sagi M (2012) The determination of sulfite levels and its oxidation in plant leaves. Plant Sci 190: 123–130

Chakraborty U, Pradhan D High temperature-induced oxidative stress in Lens culinaris, role of antioxidants and amelioration of stress by chemical pre-treatments. doi: 10.1080/17429145.2010.513484

Chang Q, Tang H (2014) Optical determination of glucose and hydrogen peroxide using a nanocomposite prepared from glucose oxidase and magnetite nanoparticles immobilized on graphene oxide. Microchim Acta 181: 527–534

Chen W, Wang W, Peng M, Gong L, Gao Y, Wan J, Wang S, Shi L, Zhou B, Li Z, et al (2016) Comparative and parallel genome-wide association studies for metabolic and agronomic traits in cereals. Nat Commun 2016 71 7: 1–10

Cona A, Rea G, Botta M, Corelli F, Federico R, Angelini R (2006) Flavin-containing polyamine oxidase is a hydrogen peroxide source in the oxidative response to the protein phosphatase inhibitor cantharidin in Zea mays L. J Exp Bot 57: 2277–2289

Corpas FJ, Barroso JB, Del Río LA (2001) Peroxisomes as a source of reactive oxygen species and nitric oxide signal molecules in plant cells. Trends Plant Sci 6: 145–150

Cruz De Carvalho MH (2008) Drought stress and reactive oxygen species: Production, scavenging and signaling. Plant Signal Behav 3: 156

Dixon J, Braun HJ, Kosina P, Crouch J, (eds.) (2009) Wheat facts and futures 2009. Mexico, DF: CIMMYT. Available online: https://repository.cimmyt.org/handle/10883/1265

Danilova T V., Poland J, Friebe B (2019) Production of a complete set of wheat–barley group-7 chromosome recombinants with increased grain β-glucan content. Theor Appl Genet 132: 3129–3141

Daryanto S, Wang L, Jacinthe PA (2016) Global Synthesis of Drought Effects on Maize and Wheat Production. PLoS One 11: e0156362

Delauney AJ, Hu CAA, Kishor PBK, Verma DPS (1993) Cloning of ornithine δ-aminotransferase cDNA from Vigna aconitifolia by trans-complementation in Escherichia coli and regulation of proline biosynthesis. J. Biol. Chem.

Delauneys AJ, Hu C-AA, Kishor PBK, Pal D, Vermaq S (1993) The journal of biological chehistrv cloning of ornithine & aminotransferase cDNA from *Vigna aconitifolia* by Trans-complementation in *Escherichia coli* and regulation of proline biosynthesis. J Biol Chem 268: 18673–18678

Deng X-P, Cheng Y-J, Wu X-B, Kwak S-S, Chen W, Eneji AE (2012) Exogenous hydrogen peroxide positively influences root growth and exogenous hydrogen peroxide positively influences root growth and metabolism in leaves of sweet potato seedlings. AJCS 6: 1572–1578

Desikan R, Neill SJ, Hancock JT (2000) Hydrogen peroxide–induced gene expression in Arabidopsis thaliana. Free Radic Biol Med 28: 773–778

Deuschle K, Funck D, Hellmann H, Däschner K, Binder S, Frommer WB (2001) A nuclear gene encoding mitochondrial Delta-pyrroline-5-carboxylate dehydrogenase and its potential role in protection from proline toxicity. Plant J 27: 345–356

Deutsch CA, Tewksbury JJ, Tigchelaar M, Battisti DS, Merrill SC, Huey RB, Naylor RL (2018) Increase in crop losses to insect pests in a warming climate. Science (80) 361: 916–919

Devlin B, Roeder K (1999) Genomic control for association studies. Biometrics 55: 997–1004

Dhanyalakshmi KH, Mounashree DC, Vidyashree DN, Earanna N, Nataraja KN (2019) Options and opportunities for manipulation of drought traits using endophytes in crops. Plant Physiol Reports 24: 555–562

Dubcovsky J, Dvorak J (2007) Genome plasticity a key factor in the success of polyploid wheat under domestication. Science (80-) 316: 1862–1866

Ellstrand NC, Meirmans P, Rong J, Bartsch D, Ghosh A, De Jong TJ, Haccou P, Lu BR, Snow AA, Neal Stewart C, et al (2013) Introgression of crop alleles into wild or weedy populations. http://dx.doi.org/101146/annurev-ecolsys-110512-135840 44: 325–345

Evans JR, Lawson T (2020) From green to gold: agricultural revolution for food security. J Exp Bot 71: 2211–2215

Eyre-Walker A, Gaut RL, Hilton H, Feldman DL, Gaut BS (1998) Investigation of the bottleneck leading to the domestication of maize. Proc Natl Acad Sci U S A 95: 4441–4446

Fazeli F, Ghorbanli M, Niknam V (2006) Effect of drought on water relations, growth and solute accumulation in two sesame cultivars. Pakistan J Biol Sci 9: 1829–1835

Fedotova M V., Dmitrieva OA (2016) Proline hydration at low temperatures: its role in the protection of cell from freeze-induced stress. Amino Acids 48: 1685–1694

Feuillet C, Eversole K (2007) Physical mapping of the wheat genome: A coordinated effort to lay the foundation for genome sequencing and develop tools for breeders. Isr J Plant Sci 55: 307–313

Fleury D, Luo MC, Dvorak J, Ramsay L, Gill BS, Anderson OD, You FM, Shoaei Z, Deal KR, Langridge P (2010) Physical mapping of a large plant genome using global high-information-content-fingerprinting: the distal region of the wheat ancestor Aegilops tauschii chromosome 3DS. BMC Genomics 2010 111 11: 1–10

Francoz E, Ranocha P, Nguyen-Kim H, Jamet E, Burlat V, Dunand C (2015) Roles of cell wall peroxidases in plant development. Phytochemistry 112: 15–21

Funck D, Stadelhofer B, Koch W (2008) Ornithine-δ-aminotransferase is essential for Arginine Catabolism but not for Proline Biosynthesis. BMC Plant Biol 8: 1–14

García-Mata C, Lamattina L (2013) Gasotransmitters are emerging as new guard cell signaling molecules and regulators of leaf gas exchange. Plant Sci 201–202: 66–73

Gaurav K, Arora S, Silva P, Sánchez-Martín J, Horsnell R, Gao L, Brar GS, Widrig V, Raupp J, Singh N, et al (2021) Evolution of the bread wheat D-subgenome and enriching it with diversity from Aegilops tauschii. bioRxiv 2021.01.31.428788

Gustafson P, Raskina O, Ma X, Nevo E (2009) Wheat evolution, domestication, and improvement. Wheat Sci Trade 3–30

Hare PD, Cress WA, Van Staden J (1998) Dissecting the roles of osmolyte accumulation during stress. Plant Cell Environ 21: 535–553

He Y, Liu Y, Cao W, Huai M, Xu B, Huang B (2005) Effects of salicylic acid on heat tolerance associated with antioxidant metabolism in *Kentucky bluegrass*. Crop Sci 45: 988–995

Hedden P (2003) The genes of the Green Revolution. Trends Genet 19: 5–9

Hellmann H, Funck D, Rentsch D, Frommer WB (2000) Hypersensitivity of an arabidopsis sugar signaling mutant toward exogenous proline application. Plant Physiol 123: 779–789

Helman D, Bonfil DJ (2022) Six decades of warming and drought in the world's top wheat-producing countries offset the benefits of rising CO2 to yield. Sci Reports 2022 121 12: 1–

10

Horton MW, Hancock AM, Huang YS, Toomajian C, Atwell S, Auton A, Muliyati NW, Platt A, Sperone FG, Vilhjálmsson BJ, et al (2012) Genome-wide patterns of genetic variation in worldwide Arabidopsis thaliana accessions from the RegMap panel. Nat Genet 44: 212

Hu X, Bidney DL, Yalpani N, Duvick JP, Crasta O, Folkerts O, Lu G (2003) Overexpression of a gene encoding hydrogen peroxide-generating oxalate oxidase evokes defense responses in sunflower. Plant Physiol 133: 170–181

Hu X, Jiang M, Zhang J, Zhang A, Lin F, Tan M (2007) Calcium-calmodulin is required for abscisic acid-induced antioxidant defense and functions both upstream and downstream of H2O2 production in leaves of maize (Zea mays) plants. New Phytol 173: 27–38

Huang X, Wei X, Sang T, Zhao Q, Feng Q, Zhao Y, Li C, Zhu C, Lu T, Zhang Z, et al (2010) Genome-wide association studies of 14 agronomic traits in rice landraces. Nat Genet 2010 4211 42: 961–967

Hyten DL, Song Q, Zhu Y, Choi IY, Nelson RL, Costa JM, Specht JE, Shoemaker RC, Cregan PB (2006) Impact of genetic bottlenecks on soybean genome diversity. Proc Natl Acad Sci USA 103: 16666–16671

Iyer S, Caplan A (1998) Products of Proline Catabolism Can Induce Osmotically Regulated Genes in Rice 1. Plant Physiol 116: 203–211

IPCC: climate change 2014: synthesis report. Contribution of working groups I, II and III to the fifth assessment report of the intergovernmental panel on climate change [core writing team, R.K. Pachauri and L.A. Meyer (eds.)] (2014) IPCC, Geneva, Switzerland, pp 151

Jiang S-C, Mei C, Liang S, Yu Y-T, Lu K, Wu Z, Wang X-F, Zhang D-P (2015) Crucial roles of the pentatricopeptide repeat protein SOAR1 in Arabidopsis response to drought, salt and cold stresses. Plant Mol Biol 88: 369–385

Johnson EO, Hancock DB, Levy JL, Gaddis NC, Saccone NL, Bierut LJ, Page GP (2013) Imputation across genotyping arrays for genome-wide association studies: assessment of bias and a correction strategy. Hum Genet 132: 509

Ju HW, Min JH, Chung MS, Kim CS (2013) The atrzf1 mutation of the novel RING-type E3 ubiquitin ligase increases proline contents and enhances drought tolerance in Arabidopsis. Plant Sci 203–204: 1–7

Kahiluoto H, Kaseva J, Balek J, Olesen JE, Ruiz-Ramos M, Gobin A, Kersebaum KC, Takáč J, Ruget F, Ferrise R, et al (2019) Decline in climate resilience of european wheat. Proc Natl Acad Sci U S A 116: 123–128

Khush GS (2001) Green revolution: the way forward. Nat Rev Genet 2001 210 2: 815–822

Kim W, Iizumi T, Nishimori M (2019) Global Patterns of Crop Production Losses Associated with Droughts from 1983 to 2009. J Appl Meteorol Climatol 58: 1233–1244

Kishor PBK, Hima Kumari P, Sunita MSL, Sreenivasulu N (2015) Role of proline in cell wall synthesis and plant development and its implications in plant ontogeny. Front Plant Sci 6: 1–17

Kiyosue T, Yoshiba Y, Yamaguchi-Shinozaki K, Shinozaki K (1996) A nuclear gene encoding mitochondrial proline dehydrogenase, an enzyme involved in proline metabolism, is upregulated by proline but downregulated by dehydration in Arabidopsis. Plant Cell 8: 1323–1335

Klein RJ, Zeiss C, Chew EY, Tsai JY, Sackler RS, Haynes C, Henning AK, SanGiovanni JP, Mane SM, Mayne ST, et al (2005) Complement factor H polymorphism in age-related macular degeneration. Science 308: 385–389

Kleine S, Müller C (2014) Drought Stress and Leaf Herbivory Affect Root Terpenoid Concentrations and Growth of Tanacetum vulgare. J Chem Ecol 40: 1115–1125

Knight H, Trewavas AJ, Knight MR (1997) Calcium signalling in Arabidopsis thaliana responding to drought and salinity. Plant J 12: 1067–1078

Lehmann S, Funck D, Szabados L, Rentsch D (2010) Proline metabolism and transport in plant development. Amin Acids 2010 394 39: 949–962

Lek M, Karczewski KJ, Minikel E V., Samocha KE, Banks E, Fennell T, O'Donnell-Luria AH, Ware JS, Hill AJ, Cummings BB, et al (2016) Analysis of protein-coding genetic variation in 60,706 humans. Nat 2016 5367616 536: 285–291

Leng G, Hall J (2019) Crop yield sensitivity of global major agricultural countries to droughts and the projected changes in the future. Sci Total Environ 654: 811–821

Lesk C, Rowhani P, Ramankutty N (2016) Influence of extreme weather disasters on global crop production. Nat 2016 5297584 529: 84–87

Li JT, Qiu ZB, Zhang XW, Wang LS (2011) Exogenous hydrogen peroxide can enhance tolerance of wheat seedlings to salt stress. Acta Physiol Plant 33: 835–842

Li Q, Wang W, Wang W, Zhang G, Liu Y, Wang Y, Wang W (2018) Wheat F-box protein gene TAFBA1 is involved in plant tolerance to heat stress. Front Plant Sci 9: 521

Li SW, Xue L (2010) The interaction between H2O2 and NO, Ca2+, cGMP, and MAPKs during adventitious rooting in mung bean seedlings. Vitr Cell Dev Biol - Plant 46: 142–148

Liao WB, Zhang ML, Huang GB, Yu JH (2012) Ca2+ and CaM are involved in NO- and H2O2-induced adventitious root development in marigold. J Plant Growth Regul 31: 253–264

Lim J, Lim CW, Lee SC (2020) Pepper novel serine-threonine kinase CADIK1 regulates drought tolerance via modulating ABA sensitivity. Front Plant Sci 11: 1133

Liu L, Jiang Z, Zhang S, Zhao H, Yang W, Siedow JN, Pei ZM (2018) Both NaCl and H2O2 long-term stresses affect basal cytosolic Ca2+ levels but only NaCl alters cytosolic Ca2+ signatures in arabidopsis. Front Plant Sci 871: 1390

Liu X, Huang M, Fan B, Buckler ES, Zhang Z (2016) Iterative usage of fixed and random effect models for powerful and efficient genome-wide association studies. PLOS Genet 12: e1005767

Liu Z, Li H, Gou Z, Zhang Y, Wang X, Ren H, Wen Z, Kang BK, Li Y, Yu L, et al (2020) Genome-wide association study of soybean seed germination under drought stress. Mol Genet Genomics 295: 661–673

Lobell DB, Roberts MJ, Schlenker W, Braun N, Little BB, Rejesus RM, Hammer GL (2014) Greater sensitivity to drought accompanies maize yield increase in the U.S. Midwest. Science (80-) 344: 516–519

Lobell DB, Schlenker W, Costa-Roberts J (2011) Climate trends and global crop production since 1980. Science (80-) 333: 616–620

Luo MC, Deal KR, Akhunov ED, Akhunova AR, Anderson OD, Anderson JA, Blake N, Clegg MT, Coleman-Derr D, Conley EJ, et al (2009) Genome comparisons reveal a dominant mechanism of chromosome number reduction in grasses and accelerated genome evolution in Triticeae. Proc Natl Acad Sci U S A 106: 15780–15785

Luo X, Cui N, Zhu Y, Cao L, Zhai H, Cai H, Ji W, Wang X, Zhu D, Li Y, et al (2012) Over-expression of GsZFP1, an ABA-responsive C2H2-type zinc finger protein lacking a QALGGH motif, reduces ABA sensitivity and decreases stomata size. J Plant Physiol 169: 1192–1202

MacKay TFC, Stone EA, Ayroles JF (2009) The genetics of quantitative traits: challenges and prospects. Nat Rev Genet 2009 108 10: 565–577

Mani S, Van de Cotte B, Van Montagu M, Verbruggen N (2002) Altered Levels of Proline Dehydrogenase Cause Hypersensitivity to Proline and Its Analogs in Arabidopsis. Plant Physiol 128: 73–83

Manolio TA, Collins FS, Cox NJ, Goldstein DB, Hindorff LA, Hunter DJ, McCarthy MI, Ramos EM, Cardon LR, Chakravarti A, et al (2009) Finding the missing heritability of complex diseases. Nat 2009 4617265 461: 747–753

Marchini J, Howie B (2010) Genotype imputation for genome-wide association studies. Nat Rev Genet 2010 117 11: 499–511

Mathew I, Shimelis H, Shayanowako AIT, Laing M, Chaplot V (2019) Genome-wide association study of drought tolerance and biomass allocation in wheat. PLoS One. doi: 10.1371/journal.pone.0225383

Matiu M, Ankerst DP, Menzel A (2017) Interactions between temperature and drought in global and regional crop yield variability during 1961-2014. PLoS One 12: e0178339

Mattioli R, Marchese D, D'Angeli S, Altamura MM, Costantino P, Trovato M (2008) Modulation of intracellular proline levels affects flowering time and inflorescence architecture in Arabidopsis. Plant Mol Biol 66: 277–288

Maulana F, H A, JD A, TT K, W H, XF M (2018) Genome-Wide Association Mapping of Seedling Heat Tolerance in Winter Wheat. Front Plant Sci. doi: 10.3389/FPLS.2018.01272

Metwally SA, Shoaib RM, Hashish KI, El-Tayeb TA (2019) In vitro ultraviolet radiation effects on growth, chemical constituents and molecular aspects of Spathiphyllum plant. Bull Natl Res Cent 2019 431 43: 1–9

Mittler R (2002) Oxidative stress, antioxidants and stress tolerance. Trends Plant Sci 7: 405–410

Mora-Poblete F, Ballesta P, Lobos GA, Molina-Montenegro M, Gleadow R, Ahmar S, Jiménez-Aspee F (2021) Genome-wide association study of cyanogenic glycosides, proline, sugars,

and pigments in Eucalyptus cladocalyx after 18 consecutive dry summers. Physiol Plant 172: 1550–1569

Munns R (2005) Genes and salt tolerance: bringing them together. New Phytol 167: 645–663

Muzammil S, Shrestha A, Dadshani S, Pillen K, Siddique S, Léon J, Naz AA (2018) An Ancestral allele of pyrroline-5-carboxylate synthase1 promotes proline accumulation and drought adaptation in cultivated barley. Plant Physiol 178: 771–782

Mwadzingeni L, Shimelis H, Rees DJG, Tsilo TJ (2017) Genome-wide association analysis of agronomic traits in wheat under drought-stressed and non-stressed conditions. PLoS One. doi: 10.1371/journal.pone.0171692

N S, E A, L O, S B, A Z, J S, C K, L S (1997) Differential expression of two P5CS genes controlling proline accumulation during salt-stress requires ABA and is regulated by ABA1, ABI1 and AXR2 in Arabidopsis. Plant J 12: 571–581

Nanjo T, Fujita M, Seki M, Kato T, Tabata S, Shinozaki K (2003) Toxicity of free proline revealed in an arabidopsis T-DNA-tagged mutant deficient in proline dehydrogenase. Plant Cell Physiol 44: 541–548

Neill S, Desikan R, Hancock J (2002) Hydrogen peroxide signalling. Curr Opin Plant Biol 5: 388–395

Niu L, Liao W (2016) Hydrogen peroxide signaling in plant development and abiotic responses: Crosstalk with nitric oxide and calcium. Front Plant Sci 7: 230

Parre E, Ghars MA, Leprince AS, Thiery L, Lefebvre D, Bordenave M, Richard L, Mazars C, Abdelly C, Savouré A (2007) Calcium signaling via phospholipase c is essential for proline accumulation upon ionic but not nonionic hyperosmotic stresses in Arabidopsis. Plant Physiol 144: 503–512

Peng JH, Dongfa •, Nevo S• E, Peng JH, Sun D, Nevo E (2011) Domestication evolution, genetics and genomics in wheat. Mol Breed 2011 283 28: 281–301

Peng S, Huang J, Sheehy JE, Laza RC, Visperas RM, Zhong X, Centeno GS, Khush GS, Cassman KG (2004) Rice yields decline with higher night temperature from global warming. Proc Natl Acad Sci U S A 101: 9971–9975

Petrov VD, Van Breusegem F (2012) Hydrogen peroxide—a central hub for information flow in plant cells. AoB Plants 2012: 14

Pfeifer M, Kugler KG, Sandve SR, Zhan B, Rudi H, Hvidsten TR, Mayer KFX, Olsen OA, Rogers J, Doležel J, et al (2014) Genome interplay in the grain transcriptome of hexaploid bread wheat. Science (80-). doi: 10.1126/science.1250091

Polidoros AN, Mylona P V., Pasentsis K, Scandalios JG, Tsaftaris AS (2013) The maize alternative oxidase 1a (Aox1a) gene is regulated by signals related to oxidative stress. http://dx.doi.org/101179/135100005X21688 10: 71–78

Polidoros AN, Scandalios JG (1999) Role of hydrogen peroxide and different classes of antioxidants in the regulation of catalase and glutathione S-transferase gene expression in maize (Zea mays L.). Physiol Plant 106: 112–120

Qaseem MF, Qureshi R, Shaheen H, Pakistan R, Rawalpindi P (2019) Effects of pre-anthesis drought, heat and their combination on the growth, yield and physiology of diverse wheat (*Triticum aestivum* L.) genotypes varying in sensitivity to heat and drought stress. Sci Reports 2019 91 9: 1–12

RaboResearch (2017) Global wheat consumption. Utrecht: Rabobank. Available online: https://research.rabobank.com/far/en/sectors/grains-oilseeds/global_wheat_demand_article_1.html

Rabbi SMHA, Kumar A, Mohajeri Naraghi S, Simsek S, Sapkota S, Solanki S, Alamri MS, Elias EM, Kianian S, Missaoui A, et al (2021) Genome-wide association mapping for yield and related traits under drought stressed and non-stressed environments in wheat. Front Genet 12: 836

Rai AN, Penna S (2013) Molecular evolution of plant P5CS gene involved in proline biosynthesis. Mol Biol Rep 40: 6429–6435

Ben Rejeb K, Lefebvre-De Vos D, Le Disquet I, Leprince AS, Bordenave M, Maldiney R, Jdey A, Abdelly C, Savouré A (2015) Hydrogen peroxide produced by NADPH oxidases increases proline accumulation during salt or mannitol stress in Arabidopsis thaliana. New Phytol 208: 1138–1148

Remans T, Opdenakker K, Smeets K, Mathijsen D, Vangronsveld J, Cuypers A (2010) Metal-specific and NADPH oxidase dependent changes in lipoxygenase and NADPH oxidase gene expression in Arabidopsis thaliana exposed to cadmium or excess copper. Funct Plant Biol 37: 532–544

Rizhsky L, Davletova S, Liang H, Mittler R (2004) The zinc finger protein ZAT12 is required for cytosolic ascorbate peroxidase 1 expression during oxidative stress in Arabidopsis. J Biol Chem 279: 11736–11743

Sadhukhan A, Kobayashi Y, Nakano Y, Iuchi S, Kobayashi M, Sahoo L, Koyama H (2017) Genome-wide association study reveals that the Aquaporin NIP1;1 contributes to variation in hydrogen peroxide sensitivity in *Arabidopsis thaliana*. Mol Plant 10: 1082–1094

Salamini F, Özkan H, Brandolini A, Schäfer-Pregl R, Martin W (2002) Genetics and geography of wild cereal domestication in the near east. Nat Rev Genet 2002 36 3: 429–441

Sallam A, Alqudah AM, Dawood MFA, Baenziger PS, Börner A (2019) Drought stress tolerance in wheat and barley: Advances in physiology, breeding and genetics research. Int J Mol Sci. doi: 10.3390/ijms20133137

Savouré A, Jaoua S, Hua XJ, Ardiles W, Van Montagu M, Verbruggen N (1995) Isolation, characterization, and chromosomal location of a gene encoding the delta 1-pyrroline-5-carboxylate synthetase in Arabidopsis thaliana. FEBS Lett 372: 13–19

Sayed MA, Schumann H, Pillen K, Naz AA, Léon J (2012) AB-QTL analysis reveals new alleles associated to proline accumulation and leaf wilting under drought stress conditions in barley (*Hordeum vulgare* L.). BMC Genet 13: 1–12

Segura V, Vilhjálmsson BJ, Platt A, Korte A, Seren Ü, Long Q, Nordborg M (2012) An efficient multi-locus mixed-model approach for genome-wide association studies in structured

populations. Nat Genet 2012 447 44: 825–830

Serraj R, Sinclair TR (2002) Osmolyte accumulation: can it really help increase crop yield under drought conditions? Plant Cell Environ 25: 333–341

Shahbaz M, Mushtaq Z, Andaz F, Masood A (2013) Does proline application ameliorate adverse effects of salt stress on growth, ions and photosynthetic ability of eggplant (*Solanum melongena* L.). Sci Hortic (Amsterdam) 164: 507–511

Sharma S, Verslues PE (2010) Mechanisms independent of abscisic acid (ABA) or proline feedback have a predominant role in transcriptional regulation of proline metabolism during low water potential and stress recovery. Plant Cell Environ 33: 1838–1851

Sharma S, Villamor JG, Verslues PE (2011) Essential role of tissue-specific proline synthesis and catabolism in growth and redox balance at low water potential. Plant Physiol 157: 292–304

Sheffield J, Wood EF (2008) Projected changes in drought occurrence under future global warming from multi-model, multi-scenario, IPCC AR4 simulations. Clim Dyn 31: 79–105

Shewry PR (2018) Do ancient types of wheat have health benefits compared with modern bread wheat? J Cereal Sci 79: 469–476

Shiferaw B, Smale M, Braun HJ, Duveiller E, Reynolds M, Muricho G (2013) Crops that feed the world 10. Past successes and future challenges to the role played by wheat in global food security. Food Secur 5: 291–317

Soriano JM, Villegas D, Aranzana MJ, García Del Moral LF, Royo C (2016) Genetic structure of modern durum wheat cultivars and mediterranean landraces matches with their agronomic performance. PLoS One 11: e0160983

de Sousa T, Ribeiro M, Sabença C, Igrejas G (2021) The 10,000-year success story of wheat! Foods 2021, 10: 2124

Steinthorsdottir V, Thorleifsson G, Sulem P, Helgason H, Grarup N, Sigurdsson A, Helgadottir HT, Johannsdottir H, Magnusson OT, Gudjonsson SA, et al (2014) Identification of low-frequency and rare sequence variants associated with elevated or reduced risk of type 2 diabetes. Nat Genet 46: 294–298

Stewart CR HA (1980) Proline accumulation as a metabolic response to water stress. In NC Turner, PJ Kramer, eds, adaptation of plants to water and high temperature stress. John Wiley & Sons, Ltd

Sowell, Andrew R., Bryn Swearingen, and Claire Hutchins. Wheat Outlook: April 2022, WHS-22d, U.S.

Department of Agriculture, Economic Research Service, April 12, 2022.

Suneja Y, Gupta AK, Bains NS (2019) Stress adaptive plasticity: *Aegilops tauschii* and *Triticum dicoccoides* as potential donors of drought associated morpho-physiological traits in wheat. Front Plant Sci 10: 211

Szabados L, Savouré A (2010) Proline: a multifunctional amino acid. Trends Plant Sci 15: 89–97

Tam V, Patel N, Turcotte M, Bossé Y, Paré G, Meyre D (2019) Benefits and limitations of

genome-wide association studies. Nat Rev Genet 2019 208 20: 467–484

Tewari RK, Kumar P, Tewari N, Srivastava S, Sharma PN (2004) Macronutrient deficiencies and differential antioxidant responses—influence on the activity and expression of superoxide dismutase in maize. Plant Sci 166: 687–694

Trenberth KE, Dai A, Van Der Schrier G, Jones PD, Barichivich J, Briffa KR, Sheffield J (2013) Global warming and changes in drought. Nat Clim Chang 2014 41 4: 17–22

Trnka M, Feng S, Semenov MA, Olesen JE, Kersebaum KC, Rötter RP, Semerádová D, Klem K, Huang W, Ruiz-Ramos M, et al (2019) Mitigation efforts will not fully alleviate the increase in water scarcity occurrence probability in wheat-producing areas. Sci Adv. doi: 10.1126/sciadv.aau2406/suppl_file/aau2406_sm.pdf

Trotel P, Bouchereau A, Niogret MF, Larher F (1996) The fate of osmo-accumulated proline in leaf discs of Rape (*Brassica napus* L.) incubated in a medium of low osmolarity. Plant Sci 118: 31–45

Ueda Y, Frimpong F, Qi Y, Matthus E, Wu L, Höller S, Kraska T, Frei M (2015) Genetic dissection of ozone tolerance in rice (*Oryza sativa* L.) by a genome-wide association study. J Exp Bot 66: 293–306

Venske E, Dos Santos RS, Busanello C, Gustafson P, Costa de Oliveira A (2019) Bread wheat: a role model for plant domestication and breeding. Hered 2019 1561 156: 1–11

Verbruggen N, Villarroel R, Van Montagu M (1993) Osmoregulation of a pyrroline-5-carboxylate reductase gene in Arabidopsis thaliana. Plant Physiol. doi: 10.1104/pp.103.3.771

Verón SR, de Abelleyra D, Lobell DB (2015) Impacts of precipitation and temperature on crop yields in the Pampas. Clim Change 130: 235–245

Verslues PE, Lasky JR, Juenger TE, Liu TW, Nagaraj Kumar M (2014) Genome-wide association mapping combined with reverse genetics identifies new effectors of low water potential-induced proline accumulation in Arabidopsis. Plant Physiol. doi: 10.1104/pp.113.224014

Visscher PM, Brown MA, McCarthy MI, Yang J (2012) Five Years of GWAS Discovery. Am J Hum Genet 90: 7–24

Wang F, Tong W, Zhu H, Kong W, Peng R, Liu Q, Yao Q (2016) A novel Cys2/His2 zinc finger protein gene from sweetpotato, IbZFP1, is involved in salt and drought tolerance in transgenic Arabidopsis. Planta 243: 783–797

Wang Z, Li J, Lai C, Wang RY, Chen X, Lian Y (2018) Drying tendency dominating the global grain production area. Glob Food Sec 16: 138–149

Webber H, Ewert F, Olesen JE, Müller C, Fronzek S, Ruane AC, Bourgault M, Martre P, Ababaei B, Bindi M, et al (2018) Diverging importance of drought stress for maize and winter wheat in Europe. Nat Commun 2018 91 9: 1–10

Wen YJ, Zhang H, Ni YL, Huang B, Zhang J, Feng JY, Wang SB, Dunwell JM, Zhang YM, Wu R (2018) Methodological implementation of mixed linear models in multi-locus genome-

wide association studies. Brief Bioinform 19: 700–712

Wilhite DA, Glantz MH (1985) Understanding: The drought phenomenon: The role of definitions. Water Int 10: 111–120

Yano K, Yamamoto E, Aya K, Takeuchi H, Lo PC, Hu L, Yamasaki M, Yoshida S, Kitano H, Hirano K, et al (2016) Genome-wide association study using whole-genome sequencing rapidly identifies new genes influencing agronomic traits in rice. Nat Genet 48: 927–934

Yoshiba Y, Kiyosue T, Katagiri T, Ueda H, Mizoguchi T, Yamaguchi-Shinozaki K, Wada K, Harada Y, Shinozaki K (1995) Correlation between the induction of a gene for delta 1-pyrroline-5-carboxylate synthetase and the accumulation of proline in Arabidopsis thaliana under osmotic stress. Plant J 7: 751–760

Yu J, Pressoir G, Briggs WH, Bi IV, Yamasaki M, Doebley JF, McMullen MD, Gaut BS, Nielsen DM, Holland JB, et al (2005) A unified mixed-model method for association mapping that accounts for multiple levels of relatedness. Nat Genet 2005 382 38: 203–208

Yuan Y, Cairns JE, Babu R, Gowda M, Makumbi D, Magorokosho C, Zhang A, Liu Y, Wang N, Hao ZF, et al (2019) Genome-wide association mapping and genomic prediction analyses reveal the genetic architecture of grain yield and flowering time under drought and heat stress conditions in maize. Front Plant Sci 9: 1919

Zhang C, Gao L, Sun J, Jia J, Ren Z (2014) Haplotype variation of Green Revolution gene Rht-D1 during wheat domestication and improvement. J Integr Plant Biol 56: 774–780

Zhao K, Aranzana MJ, Kim S, Lister C, Shindo C, Tang C, Toomajian C, Zheng H, Dean C, Marjoram P, et al (2007) An Arabidopsis Example of Association Mapping in Structured Samples. PLOS Genet 3: e4

Zhou J, Wang J, Shi K, Xia XJ, Zhou YH, Yu JQ (2012) Hydrogen peroxide is involved in the cold acclimation-induced chilling tolerance of tomato plants. Plant Physiol Biochem PPB 60: 141–149

Zhou J, Xia XJ, Zhou YH, Shi K, Chen Z, Yu JQ (2014) RBOH1-dependent H2O2 production and subsequent activation of MPK1/2 play an important role in acclimation-induced cross-tolerance in tomato. J Exp Bot 65: 595–607

Zhu B, Su J, Chang M, Verma DPS, Fan YL, Wu R (1998) Overexpression of a Δ1-pyrroline-5-carboxylate synthetase gene and analysis of tolerance to water- and salt-stress in transgenic rice. Plant Sci 139: 41–48

Zipper SC, Qiu J, Kucharik CJ (2016) Drought effects on US maize and soybean production: spatiotemporal patterns and historical changes. Environ Res Lett 11: 094021

Zong JM, Li XW, Zhou YH, Wang FW, Wang N, Dong YY, Yuan YX, Chen H, Liu XM, Yao N, et al (2016) The AaDREB1 Transcription Factor from the Cold-Tolerant Plant Adonis amurensis Enhances Abiotic Stress Tolerance in Transgenic Plant. Int J Mol Sci. doi: 10.3390/IJMS17040611

Zuo T, Yu J, Wang WX, Zhao KL, Chen C, Deng WH, He XB, Wang P, Shi Q, Guo WY (2016) Mitogen-activated protein kinases are activated in placental injury in rat model of acute pancreatitis in pregnancy. Pancreas 45: 850–857

Chapter 2. Genetic mapping of candidate loci for drought-induced proline accumulation in bread wheat

2.1. Abstract

Proline (Pro) is an important metabolite, which plays an adaptive role in plants under drought stress. Understanding the genetic basis of drought-induced Pro accumulation remains elusive in crop plants, especially in wheat. Here, we investigated Pro accumulation under control and drought conditions using a diversity panel comprises of 150 wheat cultivars. Drought stress significantly increased Pro accumulation than well-water treated plants. Drought-inducible Pro variability was dissected using genome-wide association study (GWAS) that identified significant marker-trait associations, especially on 1A and 1B chromosomes. Population structure analysis revealed the cultivars originated from Europe were associated with higher Pro content. Further, linkage disequilibrium analysis identified minor allele of haplotypes and single-markers were linked with higher Pro accumulation under drought. The identified candidate genes were involved in metabolic, transport, and biosynthetic pathways. Next, an *in silico* transcript analysis found the high expression of candidate genes in shoot/leaves under drought stress conditions. Overall, the key genomic regions controlling drought-inducible Pro accumulation can be used in improving plant adaptation to drought.

2.2. Introduction

Drought is a major limiting factor for crop growth and production, which causes up to 70% grain yield reduction globally. Almost all stages of plants are directly or indirectly affected by drought stress (Golldack et al., 2014; Webber et al., 2018). It has been estimated that around 17% of the total cultivated area is diversely affected by drought (Dai, 2012; Arun-Chinnappa et al., 2017). It is anticipated that, this scenario will be worst due to the rapid global climatic changes in coming years, thereby crop production will be declined (Lobell et al., 2008). Therefore, it is imperative to identify and develop drought-tolerant cultivars that balance productivity in the future to secure sustainable food supply (Maqbool, Aslam, & Ali, 2017). Plant adaptation response to drought includes tolerance, avoidance, recovery, and escape mechanisms (Chen et al., 2015; Khan et al., 2016). Plant drought resistance is the escape through short life cycle or developmental flexibility (early germination, faster plant growth) (Maulana et al., 2018), avoidance is the means of enhanced water uptake, reduced leaf area by rolling, reduced water loss and decline in shoot and root growth

(Tardieu & Parent, 2017), and the recovery is the resurrection of growth after exposure to the extreme drought stress (Maulana et al., 2018).

The mechanisms of drought adaptation are complex and cumulatively controlled by many genes with minor effects, and by the environments and the interaction between genes and environments (Stich and Melchinger, 2010). Thus, the dissection of underlying candidate genes for complex trait is challenging. With state-of-the-art in population genetics, different approaches are now available to depict genetic footprint and complex genetic architecture. Genome-wide association studies (GWAS) have been adopted to gain insight into the genetic architecture of complex genome like wheat. It has been successfully employed to uncover genes governing stress tolerance in many plant species (Bowne et al., 2012; Maulana et al., 2020; Siddiqui et al., 2021). Moreover, GWAS exhibits a high resolution genomic map for a studied trait, since it includes recombination history of large number of individuals of a species (Brachi et al., 2011).

The morphological, physiological, biochemical and molecular changes during drought stress collectively lead to destabilized plant growth, which ultimately causes yield loss (Sallam et al. 2019). Reactive oxygen species (ROS) adversely affects the growth when accumulated excessively under drought conditions. In response to them, plant's defense machineries activated, including production of several metabolites, among them, proline (Pro) has been reported to play a pivotal role in adaptation (Shrestha et al., 2021). Pro is a multifunctional, low molecular weight amino acid. There are two well-known pathways of Pro biosynthesis in plants. Most reported pathway is glumatic acid, where glumate is reduced to glutamic- γ-semialdehyde (GSA) by pyrolline-5-carboylate synthase enzyme. This GSA spontaneously converted to pyrroline-5-carboxlate (P5C). Finally this P5C is reduced to L-Pro by P5C reductase enzyme (Verbruggen et al, 1993). The enzyme Pro dehydrogenase (ProDH) oxidizes L-Pro to P5C, and P5C dehydrogenase converts P5C to L-glutamate (Boggess et al. 1978; Elthon and Stewart, 1981). The primary role of Pro is to maintain membrane stability and to protect macromolecule structure during osmotic stress (Szabados and Savouré, 2010; Forlani et al., 2019). Several studies reported that Pro acts as molecular chaperon, maintain pH balance and helps to maintain NADP+/NADPH redox balance under osmotic stress (Sharma et al., 2011; Kishor et al., 2015). Variation of Pro in a species for adaptation to local environmental condition represents its metabolic plasticity. Different upstream and downstream signaling genes in Pro accumulation pathways are regulating such metabolic plasticity (Suneja et al., 2019).

Under normal condition, Pro is accumulated to a minimal levels for maintaining normal physiology of plants, while under drought it elicits up to a 100 folds, which leads to an idea that higher levels of Pro in different plant species would be associated with increased drought tolerance (Sharma and Verslues, 2010). Several efforts have been made to fix the criterion that higher Pro accumulation in genotypes is associated with drought tolerance. But, due to due to enigmatic and contrasting role across plant species, the criterion met with limited success (Stewart and Hanson, 1980). In *Arabidopsis*, drought tolerance accessions produce higher Pro than susceptible accessions (Sharma et al. 2011). Pro accumulation scenario was the same for the rice under drought (Dien et al., 2019), therefore both findings suggest that higher levels of Pro accumulation under drought is an indicator of the drought tolerance. Whereas in barley, susceptible genotypes produced higher Pro than tolerant genotypes under drought, which indicates higher Pro accumulation is a drought indicator (Sayed et al., 2012). However, further gene level studies suggested that rather than just accumulation, Pro is important for drought resistance as well (Sharma et al., 2011). Due to having diverse role under drought and other stresses it could be incorporated into genetic studies for improvement for plants adaptation to drought stress, thus, can be an important tool in plant breeding program for developing climate resilient crop varieties. It is rapid, less expensive method and measurable at seedlings stage with only few days exposure to drought stress (Bates et al., 1973). Many reports have been available regarding the elevated levels of Pro accumulation under drought stress condition including in citrus, maize, coconut, amaranths, and other crops (Molinari et al., 2004; Kandowangko et al., 2009; Gomes et al., 2010; Slabbert and Krüger, 2014). Moreover, higher Pro accumulation in plants has been reported for salinity, freezing, and high temperature stresses (Huang et al., 2013; Lalk and Dörffling, 1985; Ergin et al., 2016). Its accumulation capacity has been suggested to be controlled by multiple genes (Maleki et al., 2010).

Despite having important role, genetic dissection for Pro in plants are not sufficient so far. Verslues et al. (2014) reported some effector genes related to Pro metabolism in *Arabidopsis* through GWAS and more recently in *Eucalyptus* by other authors (Mora-Poblete et al., 2021). To our knowledge it is lacking in crops, particularly in wheat such study has not yet been performed. Wheat is an economically important crop for understanding stress adaptation owing to global distribution and dramatic variability of drought responsive traits (Kulkarni et al., 2017). It has a complex genome which is about 136 times bigger than that of *Arabidopsis*. Therefore, it is ideal for gaining better insight into Pro architecture in such a complex genomic background. To achieve this, the objectives

of the study aimed to: (1) determine natural genetic diversity under control and drought condition, (2) uncover the novel loci/ genomic regions contributed to drought induced Pro accumulation, and (3) analyze transcript expression of candidate genes *in silico* under drought condition.

2.3. Materials and methods

2.3.1. Plant materials and growth condition

The study consists of a diversity panel of a total of 150 bread winter wheat (*Triticum aestivum* L.) cultivars, that have been registered from 1963 to 2013 (Voss-Fels et al., 2019). 60% of the wheat cultivars originated from Germany, and rest 40% cultivars came from 25 different countries including USA, United Kingdom, Mexico, France, Denmark, Serbian, Chili, Australia and Ukraine. The details of studied plant materials are provided in Supplementary Table 2. S1.

The experiment was conducted in a growth chamber condition. A 14/10 hours light and dark cycle with a constant of 22°C temperature and 50-60% air moisture were maintained during experimental period. The experiments were repeated three consecutive times under the same growth conditions, which could be assigned as three replications and consisting of 3-4 biological replications. The trials were conducted in a completely randomized design. To maintain uniformity, seeds were germinated first in petri dishes and germinated seedlings were then transplanted in a 96 well plastic plate: each hole has length and width= 5 cm, and depth = 7.5 cm, into which equal amount of soil mixture was filled that contains a mixture of topsoil (40%) and natural sand (60%) (Terrasoil; Cordel & Sohn) and one single seedling. To make homogenous soil mixture, topsoil and natural sand were mixed very well into plastic bucket by hands before plate set up. Equal amount of moisture was maintained into each hole (8 ml), which is equivalent to 70% field capacity, on a daily basis till first two weeks of seedlings growth. Recommended dose of balanced fertilizers (7% N, 3% P_2O_5 and 6% K_2O) were also applied to the plates through mixing with tap water to maintain healthy seedling growth. All the plates were randomized daily by changing the position into growth chamber which were followed until final sample collection. After two weeks (at 4^{th} -leaf -stage), one set of plants (n= 150) in plastic plates were assigned to drought by stopping the regular water, which is designated as drought treatment. Another set of this panel was kept under normal watering designated as control treatment. Both treatments were continued for 7 days. Then, the whole aerial part of each individual plants was collected through scissors and wrapped into aluminum foil paper and snap frozen into liquid nitrogen immediately. Thus, all individual

seedlings from both treatments were collected and stored at -80°C refrigerator until Pro determination. Further, a small-scale pot experiment was conducted with 20 cultivars contrasting to Pro content: 10 highest and 10 lowest Pro producing cultivars. They were grown into pots (9cm×9cm×8cm) to check their differential Pro generating capacities upon same treatments by maintaining 70% field capacity (volume basis) in both treatments till drought start. The treatments control or drought, growth chamber environment, sample collection method, and Pro determination were followed in same way as described above.

2.3.2. Pro determination

Pro was determined according to Bates et al. (1973) with a slight modifications. In brief, 3% salphosalicylic acid and the ninhydrin reagents (2.5 g ninhydrin in 60 ml glacial acetic acid and 40 ml 6 M phosphoric acid) were used for Pro determination procedure. Firstly, samples were grinded in liquid nitrogen, and then 90-100 g chilled powder were taken into 2.0 ml micro centrifuge tube. Then, 1.5 ml 3% salphosalicylic acid was added and vortex vigorously. The mixture was centrifuged at 12000 g for 5 minutes. Then, 200 µl of supernatant was taken into new 2 ml micro centrifuge tube and 200 µl acetic acid and 200 µl ninhydrin reagents were added. The mixture was incubated at 95°C temperature for 1 hr. After incubation, the reaction was stopped by putting into ice immediately. Then, 600 µl of pure tolune was added, vortexed and left at room temperature for 30 minutes. The absorbance of chromatophore was measured at 520 nm using a microplate reader (TECAN Infinite 200 Pro, TECAN Group Limited, Switzerland). Sample Pro level was calculated using a standard curve approach derived from standard solutions.

2.3.3. Phenotypic data analysis

Some outliers from the dataset by were excluded to achieve the criteria of the mean of all genotypes ± 3 standard deviations according to Ueda et al. (2015) for further analyses. Then, descriptive statistics including coefficient of variation (CV%), mean, maximum, minimum, skewness, kurtosis, boxplot and histogram of Pro value were performed through R statistical computing software (version 3.5.1). To assess the effects of treatment, genotype and their interaction on phenotypic traits, linear model, one-way ANOVA (type "II") were used, where treatment was considered as fixed effect and replication and cultivar were regarded as random effect. The variance components were used for calculating broad sense heritability (H^2). The following formula was used for calculating H^2:

$H2 = \frac{Vg}{Vg+Verr/r}$; Where Vg is genotypic variance and Verr is the error variance and r is the number of replications.

Relative values were calculated using following formula:

Relative Pro value (RPV) $= Ys - Yp$; where Y_s is the mean Pro value for individual drought stressed cultivars, and Yp is for mean Pro value of individual cultivar under control condition (Hossain et al. 1990).

2.3.4. Genome-wide association study

To perform GWAS, we used RPVs as phenotypic data which was calculated through SAS 9.4 program. The single nucleotide polymorphic (SNP) markers which cover across 21 chromosomes of wheat were obtained following the genomic DNA extraction process, and mostly described by Begum et al. (2020), and Voss-Fels et al. (2019) were employed for the association study. SNPs data imputation was performed by SAS program v.9.4, which represents 15K SNP chip of 10,431 bi-allelic SNPs with <10% missing value and minor allele frequency >0.05. Mixed linear Model (MLM) was employed, which included kinship matrix (K) as an additive genetic effect and first three principal components as a fixed effect to avoid false positives association (Zhang et al., 2010). Then, a threshold *P*-value of 0.001 [$-\log_{10}(p) = 3$)] was used to declare as threshold for significant associations according to previous studies (Tadesse et al., 2015; Gao et al., 2016). The SNPs that satisfy the threshold *P*-value were selected as candidate loci region for putative gene search as previously described using the same association panel (Siddiqui et al., 2021).

2.3.5. Genome-wide linkage disequilibrium (LD) estimation

LD analysis of this population panel was performed with the same marker set (described above) through Trait Analysis by Association, Evolution and Linkage (TASSEL) 5.2 program. The options of the program during analysis were by default: sliding window, with size of 50 includes 5, 05,775 comparisons. Accumulated r^2 value from the analysis were used for plotting graph through putting the r^2 against the genetic distance in Mbp in r package (library: ggplot2). LD decay rates across A, B, and D genomes and their distribution were observed by setting a cut off of $r^2 = 0.1$ as the critical distance up to which a gene locus extends (Oyiga et al., 2020). Locally weighed polynomial regression (LOESS) curves were fitted into the scatter plot using smooth line of R (R Development Core Team, 2011).

2.3.6. Analysis of local LD, putative candidate gene and *in silico* candidate gene expression

After performing LD decay analysis across genomes (A, B and D), the local LD analysis was executed through Haploview 4.2 program by selecting significant marker with the markers adjacent to it, according to Barrett et al. (2005). LD block were considered as loci when it displayed in heat-map with upper confidence bounds of D' value exceeded 0.98 and the lower bound exceeded 0.7 (Gabriel et al., 2002). A student's t-test assuming two samples unequal variances was conducted to compare the means of Pro between contrasting haplotypes. However, LD blocks harboring significant SNPs were defined as the candidate loci, and genes located in these loci were assembled. The significant SNPs but not belonging to an LD block, a 1.0 Mbp window of both side across chromosome was taken to search putative candidate genes according to previous report by Begum et al. (2020). Gene annotation and gene ontology (GO) were obtained from the International Wheat Genome Sequencing Consortium (IWGSC) of 'Chinese Spring' RefSeq v1.0 in the Wheat URGI database (https://wheat-urgi.versailles.inra.fr) (Alaux et al. 2018). Analysis of orthologs between wheat and Arabidopsis was conducted within Triticeae-Gene Tribe through one to one selection task (Chen et al. 2020) (http://wheat.cau.edu.cn/TGT/). The expression level of putative candidate genes was accessed from IWGSC Refseq1.1 in the Wheat Expression browser (http://www.wheat-expression.com/) in a multiple gene searching window. Log2 (tpm) value from browser samples (n= 3 to 17) were used as the expression unit for in silico expression analysis as it provides better resolution to compare multiple genes among several categories. High level age (seedling, vegetative, reproductive), tissue of four levels (spike, grain, leaves/shoots, roots) with stress were set as criterion for filtering the expression value for genes for drought stress and control conditions. Then, log2 (tpm) values of the genes were used for visualization of expression in heat-map by using TB tools (Toolbox for biologist) v 1.09854 (Chen et al., 2020).

2.4. Results

2.4.1. Diversity-set revealed a significant variation for drought-inducible Pro accumulation

Drought stress was imposed for 7-days attributed to the observe plant- to- plant Pro variation among the genotypes. After phenotypic data analysis, we found a clear treatment effect among the genotypes. Pro accumulation under control condition ranged from 20.0 to 92.0 μg/g fresh weight with a mean value of 42.5 and median 42.0. In contrast, higher values were observed under drought

which ranged from 601.0 to 4378.0 μg/g fresh weight with a mean of 2366.0 and median 2334.0 (Table 2.1 and Figure 2.1a). ANOVA analysis showed significant effect of genotype, treatments and genotype treatment interaction, respectively (Table 2.1). Both control and drought treatment exhibited high heritability of 0.76 and 0.91, respectively, indicating that, the trait is stable and mostly controlled by the genetic factors. The RPV calculated for association study were ranged from 100 to 4550 with a mean of 2205 (Table 2.1).

Table 2.1. Summary statistics of Pro accumulation in 150 cultivars under control and drought conditions

Source of Variation	Treatment		Relative Pro Value	ANOVA		
	Control (ug/g FW)	Drought (ug/g FW)		Genotype	Treatment	Genotype*Treatment
Mean	42.5	2366.0	2205.0			
Median	42.0	2334.0	2072.0	***	***	***
Minimum	20.0	601.0	100.0			
Maximum	92.0	4378.0	4550.0			
Quantile1	37.0	1901.0	1535.0			
Quantile3	47.0	2873.0	2205.0			
Skewness	1.31	0.19	0.31			
Kurtosis	5.76	2.93	2.38			
Standard Dev	8.39	667.90	971.17			
CV (%)	19.73	28.22	41.59			
H^2	0.76	0.91	-			

***Significant at the probability level of 0.01; H^2= Broad sense heritability; HFW=Fresh weight

Moreover, it was observed that drought treatment increased Pro level on an average 56 times as compared to the average of control treatment (Supplementary Table 2. S3). Whereas, the lowest elevated level under drought was recorded as 19 times in a Mexico originated cultivar Siete Cerros 66 released in 1966, and the highest was 98 times in Great Britain originated cultivar Einstein (Supplementary Table 2. S2.2). We also calculated the correlation between control and drought treatment and observed no linear correlation between both treatments (R2=0.07) between control and drought treatment (Supplementary Figure 2. S4).

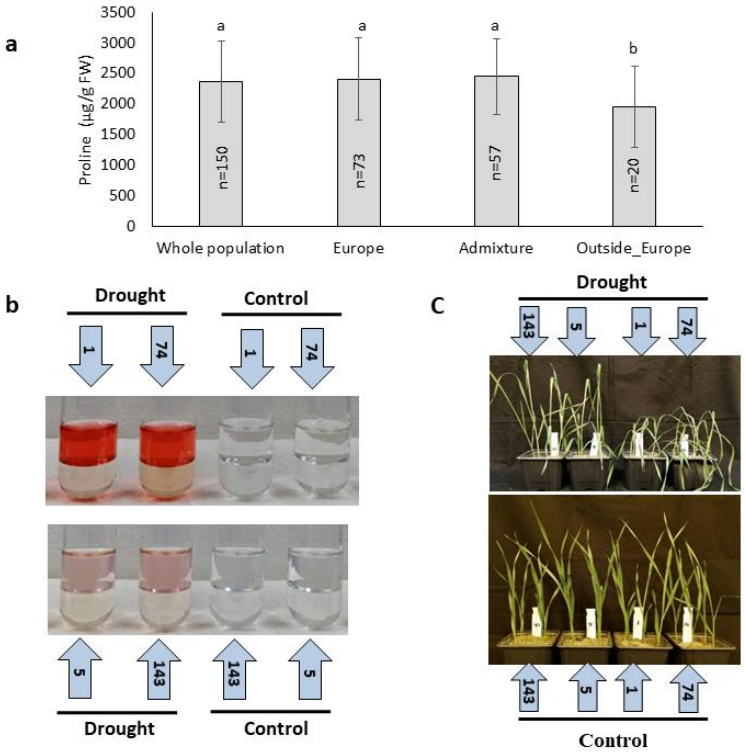

Figure 2. 1. Pro accumulation in whole population, different sub-populations and in contrasting cultivars. Pro accumulation in whole diversity panel and its different sub-populations (a). Pro accumulation in contrasting cultivars, 1 and 74 are representing as high Pro contributing cultivars, and 5 and 143 are representing as low Pro contributing cultivars (b). Visual observation of seedling under 7 day's drought and control treatment (c). In (a), mean values and standard deviation are plotted; n indicates the number of lines representing each group. Bars not sharing the same letter were significantly different at $P < 0.05$; FW=Fresh weight

In addition, this phenotypic variation is supported by Pro contents when tested more precisely with only ten highest and ten lowest Pro producing cultivars (Supplementary Figure 2. S3). This result exhibited same potentiality by the cultivars for Pro in response to drought.

2.4.2. Higher Pro accumulation was pronounced in cultivars originated from Europe

Population structure analysis of this diversity panel revealed that the cultivars are clustered into two distinct sub-population according to their origin (Begum et al., 2020). A major cluster was formed by 73 genotypes originating from Europe. The second distinct cluster included 20 genotypes originating from outside Europe (Supplementary Figure S2.1). Therefore, we accessed whether the genotype Pro accumulation is linked to the observed population stratification under drought stress, as Pro under drought was more promising. We categorized Pro value according to sub-population and performed student t-test assuming unequal variance. We also included the

admixture group and whole population in the analysis. The result showed a clear connection of Pro with population structure (Figure 2.1a). The European sub-population accumulated significantly higher Pro than those originating from outside-Europe under drought condition. If we consider only two groups, Europe and outside Europe for this analysis, we observed about 79% of total population are high Pro contributing cultivars. This percentage is 86 when the admixture group was included. By contrast, rest of 14 % population was the low Pro contributing cultivars and originated mostly from outside Europe. However, this structural effect could affect the GWAS result. Hence, was accounted for by including PCA and kinship matrix to reduce the structural effect.

The LD decay in whole population and sub-populations were calculated and were used to ascertain whether the Pro difference between sub-populations is coming from genetic recombination (Supplementary Figure S2). We observed that, LD decay of whole population is rapid in D genome and slow in B genome. LD decay of whole population of this panel was previously reported as 10.4, 14.7 and 33.04 mega base pairs (Mbp) across the A, D and B genome ($r2 = 0.1$ as background level) (Begum et al., 2020). The admixture group exhibited similar LD decay pattern of whole population. Whereas, the European and non-European subpopulation's LD decay patterns exhibited contrasting difference. LD decay pattern of European subpopulation was similar to the whole population across A and D genomes except for B genome which is slower within 10 Mbp. But outside Europe subpopulation exhibited distinct pattern of that. LD decay pattern of this population is slower across all genome and the highest of that was observed in D genome and within 25 Mbp (Supplementary Figure 2. S2).

2.4.3. QTL for drought-inducible Pro accumulation were detected primarily on chromosome 1A and 1B

The marker set described above was filtered with MAF > 0.05 before employing to GWAS. The average polymorphism information content (PIC) and heterozygosity were calculated as 0.31 and 0.0, respectively (Table 2.2). B genome has the highest number of SNPs (5165) which were 50% of total followed by genome A which contains 38%. The lowest number of SNPs were in D genome (1274) which possess 12% of total marker (Table 2.2). Chromosome wide observation reveals that chromosome 2B has the highest number of markers (960), while 4D has the lowest (40) (Table 2.2). The B genome contains a greater number of SNPs than the A and D genomes.

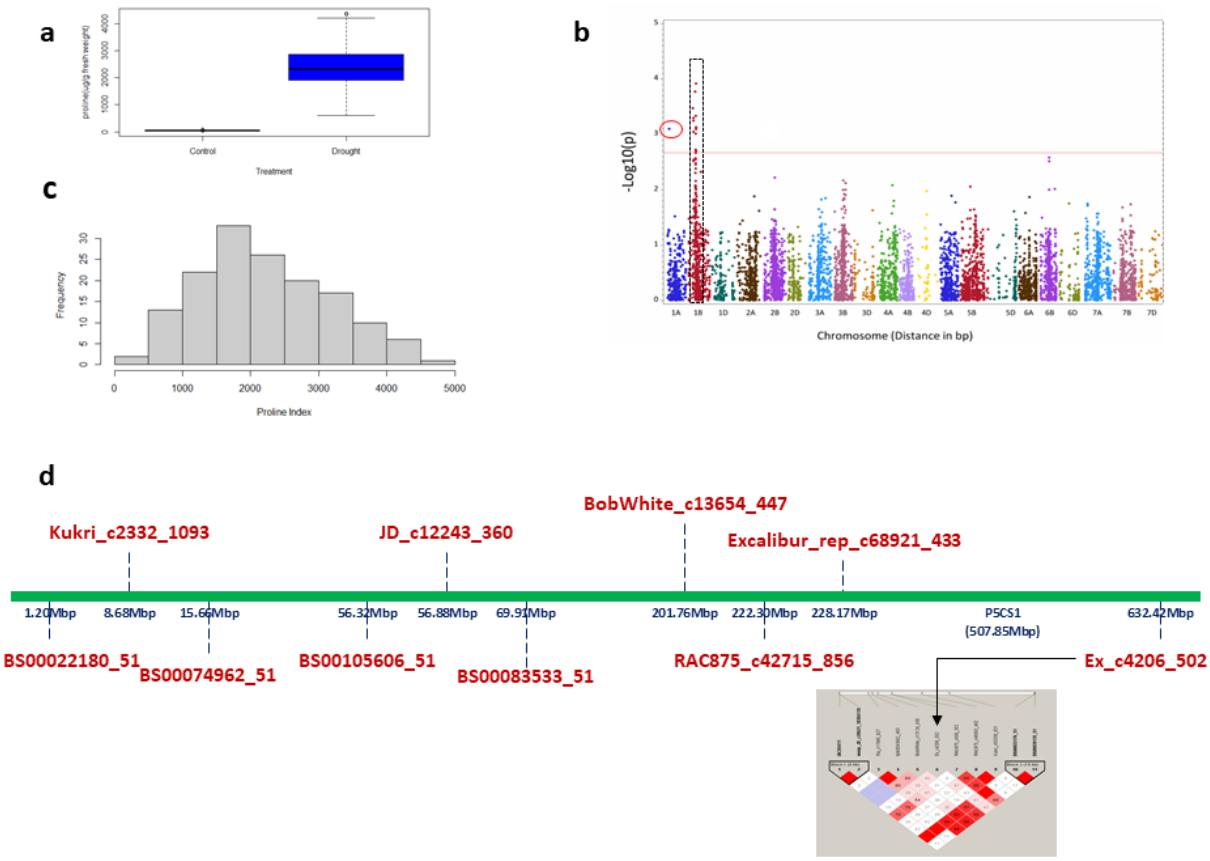

Figure 2.2. Analysis of marker-trait associations for drought inducible Pro accumulation. Box plot showing the distribution of Pro value both under normal and drought condition (a). Manhattan plot displaying the marker-trait associations (b). Frequency distribution of relative Pro value (c). Physical positions of significant SNPs (total 620.38 Mbp region) in 1B chromosome and the location of P5CS1 gene; Haploview showed a window of 10 markers positions adjacent to the nearest significant SNP marker, Ex_c4206_502, which is lying in high LD decay region and did not establish any LD block with none of its adjacent marker (s) that overlaps the Pro gene *P5CS1* (*Pyrolline-5-carboylate synthase*) (d). In (b), the horizontal line indicates the false discovery rate (FDR) threshold. The SNPs above the red line represent significant SNPs.

As RPVs exhibited near to a normal distribution pattern, they were directly used for association study without data transformation (Figure 2.2b). The GWAS found a significant association between marker and trait. The peak positions were identified at chromosome 1A and 1B in Manhattan plot (Figure 2. 2c), which comprised in total 11 significant SNPs. Among them 10 were identified at chromosome 1B (Figure 2.2d) and one at 1A. The topmost significant SNP marker JD_c12243_360, located at 64.04 cM distance and physically at 56,879,853 base pair position, can explain 10.02% genetic variance (Table 2.3). Haplotype block analysis with all significant markers in 1B region identified 3 significant markers established LD block with adjacent markers (Table

2.3). The markers did not form any LD block, a window of 1Mbp regions on both side was scanned to search candidate genes (Supplementary Figure 2. S5). Whereas, for LD block forming markers, candidate gene search was performed in LD block regions. In addition, we assessed the effect of minor allele, major allele and favorable allele on Pro accumulation by the cultivars, both for haplotype blocks and single markers. The analyses observed that in majority cases "minor allele" was the allele which showed the highest effect on Pro accumulation. Significant marker BS00074962_51 in 1B chromosome formed LD block with three adjacent markers, thereby made three distinct haplotypes (CACT, CATC and TCCT). Pairwise comparison revealed that, haplotype CATC (major and favorable allele) is responsible for significantly higher Pro value among the population than the haplotype TCCT (minor allele) (Figure 2.3).

Table 2.2. Genome and chromosome wise marker distribution and diversity

Genome	Chromosome	Number of markers	Heterozygosity	PIC
A	1	569	0	0.344
	2	553	0	0.342
	3	519	0	0.291
	4	423	0	0.327
	5	622	0	0.297
	6	632	0	0.297
	7	674	0	0.317
		3992[a]	**0**	**0.317[b]**
B	1	819	0	0.348
	2	960	0	0.283
	3	783	0	0.312
	4	372	0	0.285
	5	840	0	0.288
	6	750	0	0.305
	7	641	0	0.302
		5165[a]	**0**	**0.298[b]**
D	1	294	0	0.346
	2	371	0	0.306
	3	149	0	0.321
	4	50	0	0.288
	5	138	0	0.288
	6	139	0	0.307
	7	133	0	0.316
		1274[a]	**0**	**0.310**
Total		10431	0[b]	0.341[b]

[a]Total of sub-genome; [b]mean of sub-genome

Whereas, the haplotype block of another significant marker BS00105606_51 revealed three distinct haplotypes, among them the minor and favorable allele GTA exhibited highest Pro content. Similarly, the third significant marker BS00083533_51 exhibited three haplotypes across the population, wherein TTTG was minor (n=15) but responsible for highest Pro values (Figure 2.3). Next, the single marker analyses were also identified similar results: average Pro content of major alleles exhibited significantly less than that of minor alleles (Table 2.3 and Supplementary Table 2. S3). The functional association of top most significant marker (JD_c12243_360) was assessed for RPVs (Supplementary Table 2. S7). The average Pro content of C allele was significantly higher than the contrasting allele T ($P< 0.05$). The cultivar 'Einstein' possessing T allele had highest PRV. In contrast, the cultivar 'Claire' possessed C allele contributing to less RPVs (Supplementary Table 2.S7 and Figure 2.1b, c).

LD blocks regions collectively contained a total of 97 protein coding genes including 13 genes encode for pentatricopeptide repeat-containing protein and four genes encode F-box family protein. Total gene list is curated in Supplementary Table 2. S4. The single marker regions possess 284 protein coding genes including 28 genes code for pentatricopeptide repeat-containing protein, 11 code F-box family protein, 9 code for chymotrypsin inhibitor and 3 genes code for serine/threonine-protein kinase. Few other like E3 ubiquitin-protein ligase protein, zinc finger family protein encoding genes were also observed. These promising candidate genes were selected based on previous literatures that include genes/gene family/coding proteins involved in Pro metabolism; the detailed of them are illustrated in following section. Topmost significant SNP locus (JD_c12243_360) is associated with 42 genes including several genes for F-box, and pentatricopeptide repeat-containing protein (Supplementary Table 2. S4). The second rank loci (BS00105606_51) has 9 genes that encode for pentatricopeptide repeat-containing protein and 3 encode for F-box family protein in its LD block regions. There are 9 chymotrypsin inhibitor encoding genes were detected in LD block region of 3rd rank significant loci (BS00074962_51).

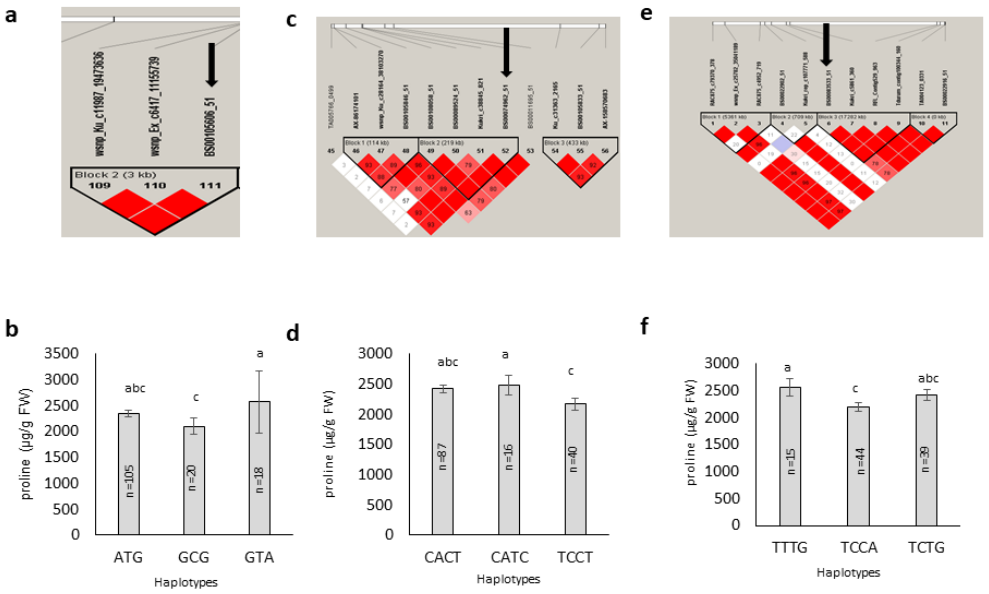

Figure 2.3. Local linkage disequilibrium (LD) analysis of the peak area on chromosome 1B. In the LD matrix darker red indicates higher pairwise LD between two markers, and the dashed line indicates an LD block. Comparison of phenotypic values between haplotype groups formed for the 2nd rank marker BS00105606_51 included in the LD block shown in panel (vertical black arrow) (a). Mean values and standard errors are plotted; n indicates the number of lines representing each of the haplotypes (b). Comparison of phenotypic values between haplotype groups formed for the 3rd rank marker BS00074962_51 included in the LD block shown in panel (vertical black arrow) (c). Mean values and standard errors are plotted; n indicates the number of lines representing each of the haplotypes (d). Comparison of phenotypic values between haplotype groups formed for the 11th rank marker BS00083533_51 included in the LD block shown in panel (vertical black arrow) (e). Mean values and standard errors are plotted; n indicates the number of lines representing each of the haplotypes (f); bars not sharing the same letter were significantly different at $P < 0.05$; FW=Fresh weight.

Similarly, 4th to 11th rank significant loci present in 1B chromosome (except for 9th rank significant marker locus) also contain several promising candidate genes in their loci regions including pentatricopeptide repeat-containing protein, F-box family protein, zinc finger family protein, MYB transcription factor, thioredoxin family protein, serine/threonine-protein kinase, RING-finger ubiquitin ligase. One significant SNP locus, which is 9th rank significant SNP, is located at 1A chromosome. The flanking region of it consists of 49 protein coding genes. Among them, 8 genes encode serine/threonine-protein kinase protein, one MADS-box transcription factor family protein (*TraesCS1A01G013100),* and F-box family protein (*TraesCS1A01G014200*) the gene encodes.

Apart from that, the most reported and known gene for Pro is P5CS1. However, it is located between the significant markers Excalibur_rep_c68921_433 and Ex_c4206_502, and the physical distance between these two significant markers is 404.25 Mb. The gene P5CS1 was not present in 1.0 Mbp regions in either markers**.** We further considered the report by Begum et al. (2020), where LD decay for this population for B genome was measured 33.04 Mb.

Table 2.3. Significant 11 SNPs and their genetic and physical position for drought induced Pro content among 150 cultivars

Marker	Ch.	GP	GV	PP	MAF	P-value	Major Allele	Minor Allele	Mean A*	Mean B*
JD_c12243_360	1B	64.09	10.01	56879853	0.091	0.0001202	T (n=131)	C (n=18)	2342	2570
BS00105606_51	1B	57.59	10.02	56316838	0.093	0.0001698	ATG (n=105)	GCG (n=20), GTA (n=18)		
BS00074962_51	1B	40.93	9.95	15658634	0.083	0.0003377	CACT (n=87)	CATC (n=16), TCCT (n=40)		
Excalibur_rep_c68921_433	1B	62.95	9.8	228170353	0.160	0.000465	C (n=121)	T (n=27)	2317	2618
RAC875_c42715_856	1B	43.85	9.55	222301499	0.078	0.0005063	C (n=127)	T (n=12)	2294	2701
BobWhite_c13654_447	1B	43.85	9.65	201757787	0.087	0.0005668	A(n=126)	G (n=14)	2627	2288
Ex_c4206_502	1B	108.41	10.05	632420641	0.107	0.0007028	G (n=120)	A (n=20)	2263	2577
BS00022180_51	1B	64.09	9.2	1203909	0.100	0.0007441	C (n=120)	T (n=16)	2344	2648
Kukri_c37212_1286	1A	26.59	9.71	8242603	0.096	0.0007974	G (n=131)	T (n=18)	2308	2728
Kukri_c2332_1093	1B	64.09	8.9	8675010	0.084	0.0007989	G (n=121)	A(n=14)	2240	2627
BS00083533_51	1B	62.58	9.5	69906151	0.089	0.0009631	TCCA (n=44)	TCTG (n=39), TTTG (n=15)		

Note. Abbreviations: GP (Genetic Position); PP (Physical Position); GV (Genetic Variance); Ch. (Chromosome); Mean A* (Mean Pro value of Major Allele); Mean B* (Mean Pro Value of Minor Allele)

Then, we assessed the LD decay of local region by constructing 12. 15 Mb span LD blocks with 11 markers including the significant one Ex_c4206_502. We observed a substantial LD decay exist between Ex_c4206_502 and nearest adjacent marker (r2=0.10) towards Excalibur_rep_c68921_433 (Figure 2.2d). This local LD decay indicates both significant markers which are distantly apart from each other are in high LD decay region. These also indicates the gene *P5CS1* is in high LD decay regions and demands for developing more markers to illustrate the role and molecular basis of it in wheat.

2.4.4. *In silico* transcript analysis of promising genes revealed higher expression level in response to drought stress

The expression levels of promising candidate genes associated with Pro metabolisms were examined.

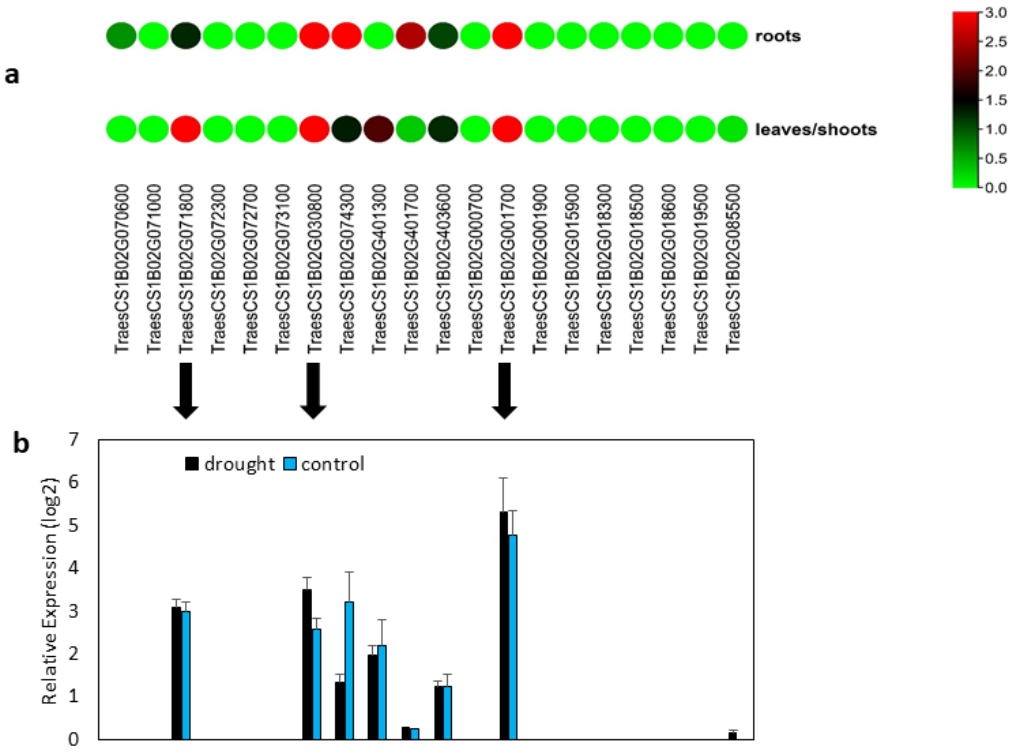

Figure 2.4. Expression patterns of 20 promising candidate genes. Expression in different tissues of Chinese Spring leaf, root stem/leaves (a). Relative expression of candidate genes under control (black bar) and drought (blue bar) conditions (b). Genes having no expression under control condition showing blank white area in (b).

We investigated 20 promising candidate genes including *TraesCS1B02G071800* was highly expressed in shoot/leaves, *TraesCS1B02G074300* in root, *TraesCS1B02G030800* and

TraesCS1B02G001700 in both root and shoot/leaves under drought stress condition (Figure 2.4a, b). Furthermore, a relative expression analyses of these genes showed higher expression levels in leaves/ shoots. Interestingly, we observed that the genes *TraesCS1B02G071800* (*Integral membrane protein*), *TraesCS1B02G030800* (*ABC transporter ATP-binding protein*) and *TraesCS1B02G001700* (*Cytochrome P450*) were highly expressed under drought when compared with non- stress conditions, while other genes exhibited variable levels of expression.

2.5. Discussion

In present study, we used a global collection of 150 cultivars that have already been demonstrated the adaptation to drought, ozone and nitrogen use efficiency (Voss-Fels et al., 2019; Begum et al., 2020; Koua et al., 2021; Siddiqui et al., 2021). Here, we were interested to dissect genetic variation and unravel underlying loci regions associated with Pro accumulation induced by drought. However, the key discussions are illustrated in following sub-headings below.

2.5.1. Pro can be a reliable marker and could be utilized in genetic improvement for plants adaptation to drought stress

Under drought conditions, average Pro content elicited up to 56 times as compared to the control treatment (Supplementary Table 2. S3), which is in line with a previous study by Sharma and Verslues (2010). According to them Pro content under drought stress may exceed up to 100 fold. Although determination of Pro is laborious and sample collection needs extra precautions, handling of aerial part, particularly whole shoot is easier. This approach facilitates faster detection at seedling stage of plant growth and thus the assessment of a cultivar under drought does not need to wait till harvesting. Previous studies on barley (Ziijriga et al., 1989) and wheat (Heerden & Villiers, 2013) reported that epidermis and vascular bundles had preferentially higher Pro content under stress conditions. These evidences along with our findings suggested that Pro can be a reliable marker for assessment of the potentiality of a wheat cultivar adapted to drought. Moreover, we found that, minor allele's cultivars are linked significantly higher Pro under drought as compared to the major allele cultivars. This information will be helpful for further genetic study and improvement of cultivars for better adaption to drought. We identified contrasting alleles in response to RPV for the topmost significant marker. C allele is contributing significantly higher RP content than T allele (Supplementary Table 2. S7). These cultivars and contrasting alleles may improve better wheat adaptation to drought.

2.5.2. Diversity panel revealed accelerated phenotypic variation for Pro in response to drought stress

Both control and drought treatments demonstrated a clear plant-to-plant Pro differences. The effect of genotype and environment interaction was significant, which indicates drought treatment causes large phenotypic variations among the cultivars. In addition, there was no significant linear correlation exist between drought and control treatment, pointing out the presence of a great genetic diversity within the population. According to Valliyodan et al. (2017) the natural variation among the drought related traits help to identify best resources for genetic studies.

Therefore, the panel utilized is an important resource that can clearly distinguish Pro related genetic study. In additon, a small-scale experiment with ten highest and ten lowest Pro accumulating cultivars exhibited a similar trend of Pro accumulation which indicates the phenotypic data obtained for the Pro are stable and reproducible. A continuous phenotypic variation was also observed for Pro content indicating polygenic inheritance of the trait. The present study also revealed that the Europe originated cultivars had significantly higher Pro content. Next, the LD decay analyses identified the genetic basis of distinct phenotypic difference between Europe and Non Europe originated cultivar groups (Supplementary Figure S2.2). The genetic basis was illustrated by the distinct LD decay pattern between the groups, which is in line with a previous study by Reinert et al. (2016).

2.5.3. GWAS identifies candidate loci and underlying genes in 1A and 1B chromosomes

For GWAS, we employed the MLM, including three principal components and a kinship matrix, which reduced the probability of false positives result (Begum et al., 2020). MLM is the better fitted model than General Linear Model (GLM) and suitable for trait like Pro (Ueda et al., 2015). For the RPVs, the Manhattan plot exhibited consistent peak in 1A and 1B regions. In addition, we noticed that 10,431 polymorphic SNP markers distributed across three genomes (A, B and D) of wheat, the number of markers is highest at B genome followed by genome A, while lowest number of markers present in D genome (Table 2.2). The highest marker trait association (MTA) were also identified at B genome in present study. This result is in agreement with the findings of Alipour et al. (2017). Recently, a study with genotyping set of 369 Iranian wheat accessions using 16,506 SNPs identified highest number of SNPs on B genome, while the lowest number of SNPs were located in D. The lowest number in D genome is indicating a lower genetic

diversity because of the lower frequency of recombination rates (Eltaher et al. 2018). However, after considering the threshold level [$-\log_{10}$ (p) =3.0], we identified 11 significant loci associated with RPVs (Table 2.3).

It has been suggested that natural variation of a trait in a species might be controlled by genes of the same families in other species (X. Y. Huang & Salt, 2016). The loci regions in this study consist of many genes which are associated with metabolic, transport and biosynthetic process. For example, several genes encode F-box family protein. F-box gene is a signaling-related gene which plays a significant role in stress resistance of plants. A previous report revealed that F-box gene *FOA1* harbors the Pro related transcription factors ABF3 and ABRE elements in the promoter region, thereby regulate Pro biosynthesis (Peng et al., 2012). F-Box gene has also been reported in wheat associated with Pro content (Li et al., 2018). Few other genes like zinc finger proteins (ZFPs), that are known to be involved in abiotic stress and have adaptive role in salt and drought stresses, through Pro biosynthesis (Luo et al., 2012; Wang et al., 2016). These proteins may act as an up-stream signaling molecule for Pro biosynthesis, thus suggested an influential role in other effector genes for Pro biosynthesis (Luo et al. 2012; Wang et al., 2016). Accordingly, pentatricopeptide repeat protein, chymotrypsin protease inhibitor, serine-threonine kinase are known for adaptive role during stress conditions through an elevated level of Pro (Jiang et al., 2015; Lim et al., 2020; Tiwari et al., 2015). In addition, *in silico* transcript analysis of few promising genes including *TraesCS1B02G030800* (*ABC transporter ATP-binding protein*) and *TraesCS1B02G001700* (*Cytochrome P450*) (Figure 2.4a, b), and identified similar proteins (MYB transcription factor, ABC transporter, Cytochrome P450, thioredoxin, MADS-box family protein etc.) in *Arabidopsis thaliana* and *Eucalyptus cladocalyx* (Verslues et al., 2014; Mora-Poblete et al., 2021) suggested that those genes might have regulatory role in Pro biosynthetic pathways.

2.5.4. Co-localization markers associated with grain yield QTLs

We compared our significant loci to previously reported yield related QTLs/loci in wheat. Interestingly, we observed that significant markers loci JD_c12243_360, BS00105606_51 and BS00083533_51 lie within the yield associated QTLs, Yld.cim-1BS.2 and Yld.cim-1BS.6; and the locus BS00074962_51 lies between Yld.cim-1BS.1 QTL (Supplementary Table S2.6) (Juliana et al., 2021). Loci for grain yield was also reported in 1A and 1B (673640580 to 675741400 bp) (Li et al., 2019). The nearest SNP locus (Ex_c4206_502) is located at 41 Mb upstream of that in 1B, in the present study. Therefore, these loci are considered as pleotropic. These QTLs are coincided

with few pentatricopeptide repeat-containing protein-coding genes, that are involved in chloroplast development (Zhang et al., 2017; Li et al., 2021). Few other genes in these QTL regions encodes receptor like- kinase protein that are involve in drought tolerance, and Glucan endo-1,3-beta-glucosidasem, which is involved in carbohydrate metabolic process. These pathways are directly associated with photosynthesis and grain yield formation process (Wang et al., 2014; Holding et al., 2010). Pro has been documented as an important component in regulating general protein synthesis in plants and thus contribute to grain formation (Wang et al. 2014; Holding et al. 2010). All these observations suggested that loci responsible for Pro contents are also linked with grain yield formation.

2.5.5. Comparison of wheat with *Arabidopsis* loci identifies unique loci for Pro

Genetic dissection for Pro has been documented in Barley and *Arabidopsis* under drought stress conditions using with bi-parental accessions and recombinant inbred lines population, respectively. Several significant QTLs/loci were also identified (Sayed et al., 2012; Verslues et al., 2014). We compared those identified loci and genes with wheat, but no homologs were identified in present study (Supplementary Table 2. S5). It is already known that shoot Pro must be different from root Pro at same environmental condition (Hayat et al., 2012). Present study utilized aerial part but those reported studies in barley and *Arabidopsis* included the root or other parts. Therefore, it is possible that the regulatory elements identified in this study for shoot are different from root in *Arabidopsis*. However, complete Pro profiling including both root and shoot under the same environmental condition is needed to be performed in future which can explain the reasons more precisely. These results suggested that the loci identified for wheat Pro contents are not conserved and assumed to be unique in wheat and in particular for shoot (Supplementary Table S2.5). A possible explanation regarding this might be that many genes contributing to Pro are not conserved among the species, and many of them may introgress from related species for their better fitness to the local environment, and thus under diverse environment variable fitness events could be happened. Notably, *P5CS1* (*Delta-1-pyrroline-5-carboxylate synthase*) gene has been reported responsible for Pro accumulation in plants (Mattioli et al., 2008). Homologs of this gene is located between two significant SNPs in 1B chromosome but far from either of the SNPs and belongs to a high LD decay region. Their functional characterizations are yet to publish.

2.6. Conclusions

Pro accumulation in wheat is an adaptive cue during drought stress, while the accumulation is controlled by multiple genes. This study identified large genetic variation of Pro induced by drought. Pro accumulation under drought condition was significantly higher in European originated cultivars as compared to the cultivars came from outside of Europe. The study further highlighted significant loci on 1A and 1B chromosomes and underlying putative candidate genes. Most of them have not been reported yet got their role in drought stress adaptation in wheat. Therefore, our findings provide a fundamental basis of loci and candidate genes contributing to natural variation for drought-inducible Pro accumulation in wheat. Further functional studies underlying gene/genes are required to illustrate their regulatory role and function in the Pro metabolic pathways in wheat and other cereals.

2.7. References

Alaux M, Rogers J, Letellier T, Flores R, Alfama F, Pommier C, Mohellibi N, Durand S, Kimmel E, Michotey C, et al (2018) Linking the international wheat genome sequencing consortium bread wheat reference genome sequence to wheat genetic and phenomic data. Genome Biol 19: 111

Alipour H, Bihamta MR, Mohammadi V, Peyghambari SA, Bai G, Zhang G (2017) Genotyping-by-sequencing (GBS) revealed molecular genetic diversity of Iranian wheat landraces and cultivars. Front Plant Sci 8: 1293

Arun-Chinnappa KS, Ranawake L, Seneweera S (2017) Impacts and management of temperature and water stress in crop plants. Abiotic Stress Manag Resilient Agric 221–233

Barrett JC, Fry B, Maller J, Daly MJ (2005) Haploview: analysis and visualization of LD and haplotype maps. Bioinformatics 21: 263–265

Bates LS, Waldren RP, Teare ID (1973) Rapid determination of free proline for water-stress studies. Plant Soil 1973 391 39: 205–207

Begum H, Alam MS, Feng Y, Koua P, Ashrafuzzaman M, Shrestha A, Kamruzzaman M, Dadshani S, Ballvora A, Naz AA, et al (2020) Genetic dissection of bread wheat diversity and identification of adaptive loci in response to elevated tropospheric ozone. Plant Cell Environ 43: 2650–2665

Boggess SF, Koeppe DE, Stewart CR (1978) Oxidation of proline by plant mitochondria. Plant Physiol 62: 22–25

Bowne JB, Erwin TA, Juttner J, Schnurbusch T, Langridge P, Bacic A, Roessner U (2012) Drought responses of leaf tissues from wheat cultivars of differing drought tolerance at the metabolite level. Mol Plant 5: 418–429

Brachi B, Morris GP, Borevitz JO (2011) Genome-wide association studies in plants: the missing heritability is in the field. Genome Biol 2011 1210 12: 1–8

Chen C, Chen H, Zhang Y, Thomas HR, Frank MH, He Y, Xia R (2020) TBtools: an integrative toolkit developed for interactive analyses of big biological data. Mol Plant 13: 1194–1202

Chen D, Wang S, Cao B, Cao D, Leng G, Li H, Yin L, Shan L, Deng X (2015) Genotypic variation in growth and physiological response to drought stress and re-watering reveals the critical role of recovery in drought adaptation in maize seedlings. Front Plant Sci. doi: 10.3389/FPLS.2015.01241

Dai A (2012) Increasing drought under global warming in observations and models. Nat Clim Chang 2012 31 3: 52–58

Dien DC, Thu TTP, Moe K, Yamakawa T (2019) Proline and carbohydrate metabolism in rice varieties (Oryza sativa L.) under various drought and recovery conditions. Plant Physiol Reports 2019 243 24: 376–387

Eltaher S, Sallam A, Belamkar V, Emara HA, Nower AA, Salem KFM, Poland J, Baenziger PS (2018a) Genetic diversity and population structure of f3:6 nebraska winter wheat genotypes using genotyping-by-sequencing. Front Genet 9: 76

Eltaher S, Sallam A, Belamkar V, Emara HA, Nower AA, Salem KFM, Poland J, Baenziger PS (2018b) Genetic diversity and population structure of F3:6 Nebraska winter wheat genotypes using genotyping-by-sequencing. Front Genet 9: 76

Elthon TE, Stewart CR (1981) Submitochondrial location and electron transport characteristics of enzymes involved in proline oxidation. Plant Physiol 67: 780

Ergin S, Gülen H, Kesici M, Turhan E, Ipek A, Köksal N (2016) Effects of high temperature stress on enzymatic and nonenzymatic antioxidants and proteins in strawberry plants. Turkish J Agric For 40: 908–917

Erginbas-Orakci G, Sehgal D, Sohail Q, Ogbonnaya F, Dreisigacker S, Pariyar SR, Dababat AA (2018) Identification of novel quantitative trait loci linked to crown rot resistance in spring wheat. Int J Mol Sci. doi: 10.3390/ijms19092666

Forlani G, Trovato M, Funck D, Signorelli S (2019) Regulation of proline accumulation and its molecular and physiological functions in stress defence. Osmoprotectant-mediated abiotic

stress toler. plants. Springer International Publishing, pp 73–97

Gabriel SB, Schaffner SF, Nguyen H, Moore JM, Roy J, Blumenstiel B, Higgins J, DeFelice M, Lochner A, Faggart M, et al (2002) The structure of haplotype blocks in the human genome. Science (80-) 296: 2225–2229

Gao L, Turner MK, Chao S, Kolmer J, Anderson JA (2016) Genome wide association study of seedling and adult plant leaf rust resistance in elite spring wheat breeding lines. PLoS One. doi: 10.1371/JOURNAL.PONE.0148671

Golldack D, Li C, Mohan H, Probst N (2014) Tolerance to drought and salt stress in plants: Unraveling the signaling networks. Front Plant Sci 0: 151

Gomes FP, Oliva MA, Mielke MS, Almeida AAF, Aquino LA (2010) Osmotic adjustment, proline accumulation and cell membrane stability in leaves of Cocos nucifera submitted to drought stress. Sci Hortic (Amsterdam) 126: 379–384

Hayat S, Hayat Q, Alyemeni MN, Wani AS, Pichtel J, Ahmad A (2012) Role of proline under changing environments: A review. Plant Signal Behav 7: 1456

Heerden PDR van, Villiers OT de (2013) Evaluation of proline accumulation as an indicator of drought tolerance in spring wheat cultivars. http://dx.doi.org/101080/02571862199610634368 13: 17–21

Hellmann H, Funck D, Rentsch D, Frommer WB (2000) Hypersensitivity of an Arabidopsis sugar signaling mutant toward exogenous proline application. Plant Physiol 122: 357–367

Holding DR, Meeley RB, Hazebroek J, Selinger D, Gruis F, Jung R, Larkins BA (2010) Identification and characterization of the maize arogenate dehydrogenase gene family. J Exp Bot 61: 3663–3673

Hossain ABS, Sears RG, Cox TS, Paulsen GM (1990) Desiccation tolerance and its relationship to assimilate partitioning in winter wheat. Crop Sci 30: 622–627

Huang XY, Salt DEE (2016) Plant ionomics: from elemental profiling to environmental adaptation. Mol Plant 9: 787–797

Huang Z, Zhao L, Chen D, Liang M, Liu Z, Shao H, Long X (2013) Salt stress encourages proline accumulation by regulating proline biosynthesis and degradation in jerusalem artichoke plantlets. PLoS One 8: e62085

Jiang S-C, Mei C, Liang S, Yu Y-T, Lu K, Wu Z, Wang X-F, Zhang D-P (2015) Crucial roles of the pentatricopeptide repeat protein SOAR1 in Arabidopsis response to drought, salt and cold stresses. Plant Mol Biol 88: 369–385

Ju HW, Min JH, Chung MS, Kim CS (2013) The atrzf1 mutation of the novel RING-type E3 ubiquitin ligase increases proline contents and enhances drought tolerance in Arabidopsis. Plant Sci 203–204: 1–7

Juliana P, Singh RP, Poland J, Shrestha S, Huerta-Espino J, Govindan V, Mondal S, Crespo-Herrera LA, Kumar U, Joshi AK, et al (2021) Elucidating the genetics of grain yield and stress-resilience in bread wheat using a large-scale genome-wide association mapping study with 55,568 lines. Sci Reports 2021 111 11: 1–15

Kandowangko NY, Suryatmana G, Nurlaeny N, Simanungkalit R (2009) Proline and abscisic acid content in droughted corn plant inoculated with azospirillum sp. and arbuscular mycorrhizae fungi. HAYATI J Biosci 16: 15–20

Khan A, Sovero V, Gemenet D (2016) Genome-assisted breeding for drought resistance. Curr Genomics 17: 330

Kishor PBK, Hima Kumari P, Sunita MSL, Sreenivasulu N (2015) Role of proline in cell wall synthesis and plant development and its implications in plant ontogeny. Front Plant Sci. doi: 10.3389/fpls.2015.00544

Koua AP, Oyiga BC, Baig MM, Léon J, Ballvora A (2021) Breeding driven enrichment of genetic variation for key yield components and grain starch content under drought stress in winter wheat. Front Plant Sci 0: 1703

Kulkarni M, Soolanayakanahally R, Ogawa S, Uga Y, Selvaraj MG, Kagale S (2017) Drought response in wheat: Key genes and regulatory mechanisms controlling root system architecture and transpiration efficiency. Front Chem 5: 106

Li F, Wen W, Liu J, Zhang Y, Cao S, He Z, Rasheed A, Jin H, Zhang C, Yan J, et al (2019) Genetic architecture of grain yield in bread wheat based on genome-wide association studies. BMC Plant Biol 2019 191 19: 1–19

Li H, Yang Y, Wang H, Liu S, Jia F, Su Y, Li S, He F, Feng C, Niu M, et al (2021) The receptor-like kinase erecta confers improved water use efficiency and drought tolerance to poplar via modulating stomatal density. Int J Mol Sci. doi: 10.3390/IJMS22147245

Li Q, Wang W, Wang W, Zhang G, Liu Y, Wang Y, Wang W (2018) Wheat F-box protein gene tafba1 is involved in plant tolerance to heat stress. Front Plant Sci 9: 521

Lim J, Lim CW, Lee SC (2020) Pepper novel serine-threonine kinase CADIK1 regulates drought tolerance via modulating aba sensitivity. Front Plant Sci 11: 1133

Lobell DB, Burke MB, Tebaldi C, Mastrandrea MD, Falcon WP, Naylor RL (2008) Prioritizing

climate change adaptation needs for food security in 2030. Science (80-) 319: 607–610

Luo X, Cui N, Zhu Y, Cao L, Zhai H, Cai H, Ji W, Wang X, Zhu D, Li Y, et al (2012) Over-expression of GsZFP1, an ABA-responsive C2H2-type zinc finger protein lacking a QALGGH motif, reduces ABA sensitivity and decreases stomata size. J Plant Physiol 169: 1192–1202

Maleki A, Saba J, Shekari F (2010) Inheritance of proline content in bread wheat (Triticum aestivum L.) under rainfed conditions. undefined

Mattioli R, Marchese D, D'Angeli S, Altamura MM, Costantino P, Trovato M (2008) Modulation of intracellular proline levels affects flowering time and inflorescence architecture in Arabidopsis. Plant Mol Biol 66: 277–288

Maulana F, Ayalew H, Anderson JD, Kumssa TT, Huang W, Ma FX(2018) Genome-wide association mapping of seedling heat tolerance in winter wheat. Front Plant Sci. doi: 10.3389/FPLS.2018.01272

Maulana F, Huang W, Anderson JD, Ma X-F (2020) Genome-wide association mapping of seedling drought tolerance in winter wheat. Front Plant Sci 0: 1626

Molinari HBC, Marur CJ, Filho JCB, Kobayashi AK, Pileggi M, Júnior RPL, Pereira LFP, Vieira LGE (2004) Osmotic adjustment in transgenic citrus rootstock Carrizo citrange (Citrus sinensis Osb. x Poncirus trifoliata L. Raf.) overproducing proline. Plant Sci. doi: 10.1016/j.plantsci.2004.07.007

Mora-Poblete F, Ballesta P, Lobos GA, Molina-Montenegro M, Gleadow R, Ahmar S, Jiménez-Aspee F (2021) Genome-wide association study of cyanogenic glycosides, proline, sugars, and pigments in Eucalyptus cladocalyx after 18 consecutive dry summers. Physiol Plant 172: 1550–1569

Peng J, Yu DS, Wang LQ, Xie MM, Yuan CY, Wang Y, Tang DY, Zhao XY, Liu XM (2012) Arabidopsis F-box gene FOA1 involved in ABA signaling. Sci China Life Sci 55: 497–506

Reinert S, Kortz A, Léon J, Naz AA (2016) Genome-wide association mapping in the global diversity set reveals new QTL controlling root system and related shoot variation in barley. Front Plant Sci 7: 1061

Sallam A, Alqudah AM, Dawood MFA, Baenziger PS, Börner A (2019) Drought stress tolerance in wheat and barley: Advances in physiology, breeding and genetics research. Int J Mol Sci. doi: 10.3390/ijms20133137

Sayed MA, Schumann H, Pillen K, Naz AA, Léon J (2012) AB-QTL analysis reveals new alleles

associated to proline accumulation and leaf wilting under drought stress conditions in barley (Hordeum vulgare L.). BMC Genet 13: 1–12

Sharma S, Verslues PE (2010a) Mechanisms independent of abscisic acid (ABA) or proline feedback have a predominant role in transcriptional regulation of proline metabolism during low water potential and stress recovery. Plant Cell Environ 33: 1838–1851

Sharma S, Verslues PE (2010b) Mechanisms independent of abscisic acid (ABA) or proline feedback have a predominant role in transcriptional regulation of proline metabolism during low water potential and stress recovery. Plant Cell Environ 33: 1838–1851

Sharma S, Villamor JG, Verslues PE (2011) Essential role of tissue-specific proline synthesis and catabolism in growth and redox balance at low water potential. Plant Physiol 157: 292–304

Shrestha A, Cudjoe DK, Kamruzzaman M, Siddique S, Fiorani F, Léon J, Naz AA (2021) Abscisic acid-responsive element binding transcription factors contribute to proline synthesis and stress adaptation in Arabidopsis. J Plant Physiol 261: 153414

Siddiqui MN, Teferi TJ, Ambaw AM, Gabi MT, Koua P, Léon J, Ballvora A (2021) New drought-adaptive loci underlying candidate genes on wheat chromosome 4B with improved photosynthesis and yield responses. Physiol Plant. doi: 10.1111/PPL.13566

Slabbert MM, Krüger GHJ (2014) Antioxidant enzyme activity, proline accumulation, leaf area and cell membrane stability in water stressed Amaranthus leaves. South African J Bot 95: 123–128

Stich B, Melchinger AE (2010) An introduction to association mapping in plants. CAB Rev Perspect Agric Vet Sci Nutr Nat Resour. doi: 10.1079/PAVSNNR20105039

Suneja Y, Gupta AK, Bains NS (2019) Stress Adaptive Plasticity: Aegilops tauschii and Triticum dicoccoides as potential donors of drought associated morpho-physiological traits in wheat. Front Plant Sci 10: 211

Szabados L, Savouré A (2010) Proline: a multifunctional amino acid. Trends Plant Sci 15: 89–97

Tadesse W, Ogbonnaya FC, Jighly A, Sanchez-Garcia M, Sohail Q, Rajaram S, Baum M (2015) Genome-wide association mapping of yield and grain quality traits in winter wheat genotypes. PLoS One. doi: 10.1371/journal.pone.0141339

Tardieu F, Parent (2017) Predictable “meta-mechanisms” emerge from feedbacks between transpiration and plant growth and cannot be simply deduced from short-term mechanisms. Plant Cell Environ 40: 846–857

Tiwari LD, Mittal D, Chandra Mishra R, Grover A (2015) Constitutive over-expression of rice

chymotrypsin protease inhibitor gene OCPI2 results in enhanced growth, salinity and osmotic stress tolerance of the transgenic Arabidopsis plants. Plant Physiol Biochem 92: 48–55

Ueda Y, Frimpong F, Qi Y, Matthus E, Wu L, Höller S, Kraska T, Frei M (2015) Genetic dissection of ozone tolerance in rice (Oryza sativa L.) by a genome-wide association study. J Exp Bot 66: 293

Verbruggen N, Villarroel R, Van Montagu M (1993) Osmoregulation of a pyrroline-5-carboxylate reductase gene in Arabidopsis thaliana. Plant Physiol. doi: 10.1104/pp.103.3.771

Verslues PE, Lasky JR, Juenger TE, Liu TW, Nagaraj Kumar M (2014) Genome-wide association mapping combined with reverse genetics identifies new effectors of low water potential-induced proline accumulation in Arabidopsis. Plant Physiol. doi: 10.1104/pp.113.224014

Voss-Fels KP, Stahl A, Wittkop B, Lichthardt C, Nagler S, Rose T, Chen T-W, Zetzsche H, Seddig S, Majid Baig M, et al (2019) Breeding improves wheat productivity under contrasting agrochemical input levels. Nat Plants 2019 57 5: 706–714

Wang F, Tong W, Zhu H, Kong W, Peng R, Liu Q, Yao Q (2016) A novel Cys2/His2 zinc finger protein gene from sweetpotato, IbZFP1, is involved in salt and drought tolerance in transgenic Arabidopsis. Planta 243: 783–797

Wang G, Zhang J, Wang G, Fan X, Sun X, Qin H, Xu N, Zhong M, Qiao Z, Tang Y, et al (2014) Proline responding1 Plays a Critical Role in Regulating General Protein Synthesis and the Cell Cycle in Maize. Plant Cell 26: 2582

Webber H, Ewert F, Olesen JE, Müller C, Fronzek S, Ruane AC, Bourgault M, Martre P, Ababaei B, Bindi M, et al (2018) Diverging importance of drought stress for maize and winter wheat in Europe. Nat Commun 2018 91 9: 1–10

Zhang J, Xiao J, Li Y, Su B, Xu H, Shan X, Song C, Xie J, Li R (2017) PDM3, a pentatricopeptide repeat-containing protein, affects chloroplast development. J Exp Bot 68: 5615–5627

Zhang Z, Ersoz E, Lai CQ, Todhunter RJ, Tiwari HK, Gore MA, Bradbury PJ, Yu J, Arnett DK, Ordovas JM, et al (2010) Mixed linear model approach adapted for genome-wide association studies. Nat Genet. doi: 10.1038/ng.546

Ziijriga GE, Argandora VH, Corcuera LJ (1989) Distribution of glycine-betaine and proline in water stressed and unstressed barley leaves. Phytochemistry 28: 419420

Chapter 3: Pinpointing genomic loci for drought-induced proline and hydrogen peroxide accumulation in bread wheat under field conditions

3.1. Abstract

Proline (Pro) and hydrogen peroxide (H_2O_2) play critical functions in plants during drought adaptation, although their phenotyping with large populations is labor-intensive. Therefore, genetic mapping for drought-induced Pro and H_2O_2 under field conditions is very limited in crop plants. A genome-wide association study (GWAS) was performed using a diversity panel comprises of 184 bread wheat cultivars under natural field (control) and rain-out shelter (drought) environments to identify candidate loci and genes regulating Pro and H_2O_2 accumulations induced by drought. GWAS identified top significant marker-trait associations (MTAs) for Pro on chromosomes 1A and 5B, and for H_2O_2 on 2A, and 1B in response to drought and stress tolerance index (STI), respectively. Among 143 identified significant MTAs, 36 and 2 were linked with drought and 71 and 34 for STI of Pro and H_2O_2, respectively. Next, linkage disequilibrium analysis revealed minor alleles of single-marker and haplotypes were associated with higher Pro and H_2O_2 accumulation under drought. Several putative candidate genes for Pro and H_2O_2 content showed protein kinase, transporter, and protein-binding activities. Thus, identified genetic factors associated with Pro and H_2O_2 biosynthesis underlying drought adaptation lays a fundamental basis for functional studies and future marker-assisted breeding programs.

3.2. Introduction

Global climate change features a number of environmental instabilities that are potential threat for agriculture (Leng and Hall, 2019). Among them, water scarcity is a crucial aspect for crop production. When plants subject to water deficit condition, it compensate the stress by reducing shoot biomass and by yield loss up to 70% (Kleine and Müller, 2014; Sallam et al., 2019). Water scarcity will be more severe in coming days, therefore, to combat such crisis studies related to drought adaptation must be emphasized. The drought tolerance mechanisms in plants are complex because many stress related genes are cumulatively involved in with minor effects (Stich and Melchinger, 2010). Moreover, the environments and the interaction between genes and environments have influence on these mechanisms (Stich and Melchinger, 2010). To understand these mechanisms and underlying regulatory elements, appropriate genetic tool is required. Previously traditional QTL mapping was used for association studies which could identify a

chromosomal regions linked with the trait of interest (Collard et al., 2005). Followed by the QTL mapping the linked markers were used to understand the nature of trait among the accessions. Thus, it was difficult to understand the key regulators involved in stress adaptive mechanisms by QTL mapping precisely. However, different modern genetic approaches are now available to dissect the complex traits. Among them, genome-wide association study (GWAS) is an approach that has been extensively used in recent years for plants (Brachi et al. 2011). A trait of interest can be dissected successfully through GWAS both under normal and stress condition (Bowne et al., 2012; Maulana et al., 2020). GWAS utilizes hundreds of thousands markers (SNPs or SSR) through incorporating the phenotypic value for the association mapping, thus makes the genomic regions narrow precisely (Brachi et al. 2011). Although, proline (Pro) and hydrogen peroxide (H_2O_2) are regulated by many genes, the dissection through GWAS can successfully be employed to identify candidate loci and genes (Stich and Melchinger, 2010). A recent GWAS has shown that diversified response to H_2O_2 exposure across the *Arabodopsis* accessions were lying in a selective aquaporins ability to channel H_2O_2 across the membranes (Sadhukhan et al., 2017). Verslues et al. (2014) attempted a GWA study with diverse accessions of model plant of *Arabidopsis* from root to identify genes responsible for Pro accumulation variation under salt stress. These evidences provide the basis of employing GWAS for Pro and H_2O_2 under drought stress in present study.

Pro is a proteinogenic amino acid that is synthesized in cytosol, chloroplasts, and cytoplasmic compartments in plants both under control and stress condition (Szabados and Savouré, 2010). The housekeeping level of this amino acid is involved in metabolism required for normal plant growth. The interesting aspect is, the dehydration event triggers its biosynthesis whereas the rehydration triggers the catabolism. Thus, Pro accumulation in control-stress-control conditions follows a cyclic fashion in plants. The common pathway for the biosynthesis in plant is glutamic acid pathway. According to that pathway, initially the amino acid glutamate is reduced to glutamic- γ-semialdehyde (GSA) by pyrolline-5-carboylate synthase enzyme. This GSA spontaneously converted to pyrroline-5-carboxlate (P5C). Finally, this P5C is reduced to L-Pro by P5C reductase enzyme (Verbruggen et al, 1993). In the catabolic reaction, the enzyme Pro dehydrogenase (ProDH) oxidizes L-Pro to P5C in mitochondria and finally P5C dehydrogenase converts P5C to L-glutamate (Boggess and Koeppe, 1978; Elthon and Stewart, 1981). Several studies documented the role of Pro as molecular chaperon, pH adjuster, and as a driver for NADP+/NADPH redox balance in osmotic stress (Sharma et al., 2011; Kishor et al., 2015). Variation of Pro in a species

under local environmental condition represents its metabolic plasticity (Ignea et al., 2017). This metabolic plasticity for Pro accumulation is regulated by different upstream and downstream signaling genes (Suneja et al., 2019). Under drought condition Pro content elicits up to a 100 folds (Sharma and Verslues, 2010), which leads to an idea that higher levels of Pro in different plant species would be associated with increased drought tolerance. Several efforts have been made to fix the criterion that higher Pro accumulation in genotypes is associated with drought tolerance. But due to having both enigmatic and distinct role, the criterion met with limited success across plant species (Stewart CR, 1980).

H_2O_2 is an abundant reactive oxygen species (ROS) in plants. Among ROS, H_2O_2 is relatively stable and measurable (Zhou et al., 2006). It is generated from its precursor O_2^- mainly in mitochondria, chloroplasts and peroxisomes. As an important regulatory components in different signaling pathways, it is involved in different developmental and physiological process in plants. A global analysis of gene expression study revealed that 1-2% of genes expression was regulated in response to H_2O_2 treatment under drought and other stress conditions (Desikan et al., 2000), which suggested that many genes are involved in H_2O_2 metabolism. However, the raised amount of H_2O_2 under drought and any other stress results in a cross tolerance to the same and other different stress condition (Neill et al., 2002). As for example, a recent study reported that 60 mM exogenous H_2O_2 treatment can improve drought tolerance in wheat. Bhardwaj et al., (2021) observed that H_2O_2 improves abiotic stress tolerance by modulating the expression of resistance genes and antioxidant enzyme activities. At low concentration it is beneficial and acts a signaling molecule in different physiological process including photosynthesis, opening and closing of stomata, senescence, cell growth and development (Deng et al., 2012). The role of low concentrations H_2O_2 under control condition has been reported in *Arabidopsis*, maize, and in Kentucky bluegrass (Veljovic-Jovanovic et al., 2002; Tewari et al., 2004; He et al., 2005). However, overproduction may occur under stress condition which triggers oxidative burst to organic molecules that causes program cell death (Corpas et al., 2001). High concentration of H_2O_2 production has been reported not only in drought stress but also in other stress condition including salinity, cold, high temperature, heavy metal, and UV radiation in plants (Zhou et al., 2006; Cruz De Carvalho, 2008; Liu et al., 2018). Remans et al., (2010) reported that H_2O_2 is related to the stimulation of NADPH oxidation in plants under stress condition. H_2O_2 treatment can lead to

significant accumulation of Pro through stimulation of NADPH oxidation and induction of P5CS activity and a decrease in catabolic PDH activity (Yang et al., 2009).

Physiological aspects are equally important like morphological traits, since morphological attributes are directly linked with physiology and regulatory genes (Tshikunde et al., 2019). Susceptible and tolerant cultivars are basically driven by contrasting physiology and gene function. Whereas, morphological characterization is prolonged, the physiological characterization are prompt and precise. Many studies have already been reported for morphological attributes, but the physiological status can be incorporated as comprehensive approach and thereby crop improvement program can be boosted (Sreeman et al., 2018). Phenotyping for physiological traits like Pro and H_2O_2 under field condition is laborious especially for a large number of accessions. But, the phenotyping can serve a great purpose in understanding adaptive role during drought.

Studies towards identifying the key regulators of Pro and H_2O_2 are quite insufficient. To our knowledge, such evidence for the crop plants particularly for wheat is absent. Moreover, this kind of studies under field condition is interesting because findings will be more realistic. The genome size of wheat genome is about 18 Giga base pairs which is approximately 136 times larger than that of *Arabidopsis* and also larger than other important crops like rice and maize. Therefore, wheat has more genetic potential, and would be more informative for Pro and H_2O_2 study. Taking all above aspects in consideration, the present study aimed to (1) assess the diversity of Pro and H_2O_2 accumulation under control and drought condition, (2) determine the correlation of Pro and H_2O_2 with yield attributes, and (3) identify loci for drought induced Pro and H_2O_2 accumulation under field condition.

3.3. Materials and methods

3.3.1. Plant materials and experimental set up

The study was conducted with a global collection of 184 winter wheat cultivars, which comprise of 60% cultivars originated from Germany and rest 40% came from United States of America (USA), United Kingdom, Mexico, France, Denmark, Serbian, Chili, Australia and Ukraine (Supplementary Table 3. S1). The experiment was performed at campus Klein-Altendorf (50.4°N; 6.99°E; 160 m above sea level), the experimental station of the University of Bonn, during summer season 2019/2020. The experimental set up followed a split-plot design where the treatments,

control and drought were in main plots. Within the main treatments the cultivars were further sub-divided into two blocks following randomized complete block design (RCBD). About 25 seeds were sown into single rows in a randomized way. The management and intercultural practices and were followed by Siddiqui et al., (2021). Two sets of cultivars were prepared. One set was grown under the open field condition which is designated as 'control treatment', and another set was grown under rain-out shelter, designated as 'drought treatment'. But until the treatment start both sets were grown under same water level and management practices. The rain-out shelter had an overhead sprinklers programmed to deliver ~5.00 mm water per day. Plants were grown till heading stage (BBCH 51) and then stopped watering for 9 days on the set grown under the rain out shelter to facilitate drought. After nine days, water limiting symptoms started to appear among the cultivars under drought treatment, while the leaves of cultivars under control treatment were still normal. However, the penultimate leaves from three individuals of each cultivar from each block were polled together. Thus, two replications were made from two block which included total 6 individuals from each cultivar. The samples were wrapped through aluminum foil paper and put immediately into liquid nitrogen and further stored at -80°C freezer. The average moisture content of the plots was determined by an EM50 Data Logger (ICT International) at the depth of 0-30 cm of the experimental plots both under control and drought conditions and presented in Supplementary Table 3. S4.

3.3.2. Pro and H_2O_2 determination

Pro was estimated according to Bates et al. (1973) with minor modifications. In brief, ninhydrin reagent (2.5 g ninhydrin in 60 ml glacial acetic acid and 40 ml 6 M phosphoric acid) and 3% of salphosalicylic acid were prepared freshly. Samples were crushed in liquid nitrogen and 90-100 g of chilled powder was taken into 2.0 ml micro centrifuge tube. Then, 1.5 ml of 3% salphosalicylic acid was mixed and centrifuged at 12000 g for 5 minutes. 200 µl of supernatant was mixed with 200 µl acetic acid and 200 µl ninhydrin reagent. Next, the mixture was incubated at 95°C temperature for 60 minutes. After incubation, the reaction was immediately stopped by putting into ice for 5 minutes. Then, 600 µl of pure toluene was mixed and left at room temperature for 30 minutes. The chromatophore reading was recorded at 520 nm wavelength with 10 reads per well through 96 well plastic plate using a microplate reader (TECAN Infinite 200 Pro, TECAN Group Limited, Switzerland). Samples Pro were determined through standard curve method and content was expressed as µg/g fresh weight of plant.

H_2O_2 was determined according to previously described method (Velikova et al., 2000) with some modifications. Leaf tissues were grinded into powder through liquid nitrogen and the 90-100 g powder was homogenized into 500 µl of 0.1% trichloroacetic acid (TCA) into 2.0 µl micro centrifuge tube and centrifuged at 12000 g for 10 minutes. Then, 200 µl supernatant was mixed with 200 µl of 10 mM potassium phosphate buffer and 1 M 400 µl potassium iodide into a new 2.0 ml micro centrifuge tube through vortexing. The sample absorbance were recorded at 390 nm using the same microplate reader as used for Pro. Sample H_2O_2 were determined through standard curve method and content was expressed as µg/g fresh weight of plant.

3.3.3. Correlation analysis with Pro, H_2O_2 and yield attributes

The average values of yield attributes such as grain yield (GY), plant dry biomass weight (PBW), shoot dry mass weight (SDW), spike number (SN), kernels number (KN), thousand kernel weight (TKW) of the same panel were retrieved form a recent publication (Koua et al., 2021, Supplemental table 5). Similarly, average values of Pro and H_2O_2 were estimated. Then, the analysis of the relationships among those yield attributes, Pro and H_2O_2 content under drought stress condition was performed. The pearson's correlation coefficients (r) were calculated using R program and correlation table was made using 'xtable' package with the function 'corstars'.

3.3.4. Data analysis

Statistical analysis was performed by R statistical computing software (version 3.5.1) and Microsoft excel 2013. The maximum, minimum, mean, and coefficient of variation (CV %) were calculated for Pro and H_2O_2 content. To determine the treatment, genotype and their interaction on phenotypic traits, two-way ANOVA was applied using a mixed model, where replication as a random effect with the genotype, treatment and interaction effect were regarded as fixed effects (Kadam et al., 2017) using the R program, especially packages "nlme", and "emmeans" (R Development Core Team 2018). Stress tolerance index (STI) was calculated using following formula:

$STI= (Yp \times Ys)/(Xp)^2$; where Ys = phenotypic value of a genotype under drought-stressed condition; Yp = phenotypic value of a genotype under non-stressed condition, and Xp = mean phenotypic value of genotypes under non-stressed condition (Fernandez, 1992).

3.3.5. Genome wide association studies

Pro and H_2O_2 content under control and drought condition and STI were used to perform GWAS. But to improve normativity of data, H_2O_2 content was transformed to square root before conducting the GWAS. Total 24,216 SNP markers covering across 21 chromosomes of wheat were obtained following the genomic DNA extraction process, and mostly described by previous publication (Voss-Fels et al., 2019; Dadshani et al., 2021) were employed for the association study. To remove missing SNPs with a minor allele frequency (MAF) of < 5%, SNPs data imputation was performed in TASSEL 5.2, LinkImpute (LD-kNNi) method (Money et al., 2015). Association mapping was performed by using TASSEL version 5.2 following a compressed MLM by incorporating the population structures with five principal components together with the kinship matrix where kinship matrix (K) were used as an additive genetic effect and first three principal components as a fixed effect to avoid false positives association and to correct the population structure (Zhang et al., 2010). After the Bonferroni correction, only two SNPs of Pro under drought condition can pass the significant threshold but an stringent threshold that over-corrects the marker trait association, therefore, did not followed (Sukumaran et al., 2018), rather a threshold *P*-value of 0.001 [$-\log_{10}(p) = 3.0$] was declared as a significant threshold according to previous studies (Tadesse et al., 2015; Gao et al., 2016). Manhattan plots were visualized using the R package "CMplot". After this criterion, the SNPs that satisfy the threshold *P*-value were considered as true positives and used for candidate gene search.

3.3.6. Linkage disequilibrium (LD) and haplotype analysis

LD analysis was performed based on the significant markers identified in the GWAS study using Haploview 4.2 to define candidate loci/haplotype block (Barrett et al., 2005). LD heat-map was generated based on confidence bounds of the *D'* values ranged between > 0.98 to 0.7 (Gabriel et al., 2002). Generally, LD blocks harbors both significant SNPs and non- significant markers together. We considered the whole blocks for haplotype analysis. Student's t-test was performed both for single significant markers and the haplotypes alleles to compare statistical differences between alleles. The significant marker alleles that exhibited distinct STI of Pro and H_2O_2 are listed in Supplementary Table 3. S3.

3.3.7. Putative candidate genes search

Genes located within the loci regions were selected as candidate genes which are listed in Supplementary Table 3. 8. The significant SNPs do not belong to any LD block, 1.0 Mega base pair (Mbp) window on both side of them were asserted as loci regions for putative candidate genes (Begum et al., 2020). Gene annotation and gene ontology (GO) were obtained from the International Wheat Genome Sequencing Consortium (IWGSC) of 'Chinese Spring' RefSeq v1.0 in the Wheat URGI database (https://wheat-urgi.versailles.inra.fr) (Alaux et al., 2018). Candidate genes were further investigated using past literatures to understand their possible functions. Analysis of orthologs between wheat and *Arabidopsis* was conducted within Triticeae-Gene Tribe through one to one selection task (Chen et al., 2020) (http://wheat.cau.edu.cn/TGT/).

3.4. Results

3.4.1. Diversity panel showed huge phenotypic variation for drought induced Pro and H_2O_2 accumulation

In order to observe phenotypic diversity induced by drought we estimated and analyzed Pro and H_2O_2 content both under control and drought conditions. We observed that there is a huge accumulation variation among the cultivars for Pro and H_2O_2 under both control and drought conditions. Pro accumulation under control condition recorded minimum of 28 µg/g FW and maximum of 179 µg/g FW with a mean value 84 µg/g FW (Table 3. 1). Drought condition exhibited minimum of 85 µg/g FW and maximum of 2420 µg/g FW, having a mean of 929 µg/g FW. Similar accumulation type was also observed in case of H_2O_2 content (Table 3. 1). The coefficient of variation was higher in drought condition than that of in control condition for both Pro and H_2O_2. Interestingly, average Pro content in drought condition was observed 11.10 times higher than the control condition. H_2O_2 accumulation under drought was estimated 0.63 times higher than to control. Analysis of variance results showed that genotypes, genotypes and treatments interactions were highly significant ($P< 0.001$) (Table 3. 1). Under drought condition, the lowest Pro producing cultivar was Zobel and the highest was observed in the variety Kurt (Supplementary Table 3. S2). For H_2O_2, 'Urban' was the lowest H_2O_2 and 'Elixer' was the highest H_2O_2 producing cultivars under drought condition (Supplementary Table 3. S2). Both highest and lowest Pro and H_2O_2 producing cultivars were originated from Germany.

Table 3.1. Descriptive statistics and analysis of variance (ANOVA) based on average phenotypic values (µg/g fresh weight) of Pro and H_2O_2 under control, drought stress conditions

Traits	Max	Min	Mean	CV (%)	*C	Two-way ANOVA		
						G	T	G×T
Pro_Con	165.40	27.92	83.72	11.97				
Pro_Dro	2420.55	84.51	929.49	27.16	11.10	***	***	***
Pro_STI	77.54	0.66	13.85	-				
H_2O_2_Con	133.05	46.20	84.50	10.58				
H_2O_2_Dro	216.53	78.09	132.52	13.86	0.63	***	***	***
H_2O_2_STI	3.82	0.73	1.56	-				

Abbreviation: Pro_Con= proline content under control condition; Pro_Dro= Proline content under drought condition; H_2O_2_Con=H_2O_2 content under control condition; H_2O_2_Dro= H_2O_2 content under drought condition; G=Genotype; T=Treatment;*C, times changes of phenotypic value in drought in comparison to the control

Analysis of variance results showed that genotypes, genotypes and treatments interactions were highly significant (P< 0.001) (Table 3. 1). Under drought condition, the lowest Pro producing cultivar was 'Zobel' and the highest was observed in the variety 'Kurt'. For H_2O_2, 'Urban' was the lowest H_2O_2 and 'Elixer' was the highest H_2O_2 producing cultivars under drought condition (Supplementary Table 3. S2). Both highest and lowest Pro and H_2O_2 producing cultivars were originated from Germany.

3.4.2. Phenotypic observation of drought-induced Pro and H_2O_2 accumulation for cultivar-origin and modern-traditional categories

To observe the effect of sub-group on phenotype, we further analyzed Pro content under drought condition and the STI of both Pro and H_2O_2 according to the origin of cultivars (Europe and Non-Europe), and the year of cultivars released after (modern) or before the year 2000 (traditional). Student t-test was performed to compare between the groups. It was observed that there was no significant Pro difference between Europe and Non-Europe sub-groups under drought stress (Figure 3.1a).

But the modern cultivar sub-group had significantly lower (P< 0.05) Pro content than that of the traditional sub-group. In the case of STI Pro, significant differences were found between Europe and Non-Europe, and between modern and traditional sub-groups (Figure 3. 3b). We performed

similar analysis for STI H_2O_2. The analysis found a contrasting phenotypic difference between Europe and Non-Europe cultivar groups (Figure 3. 1c).

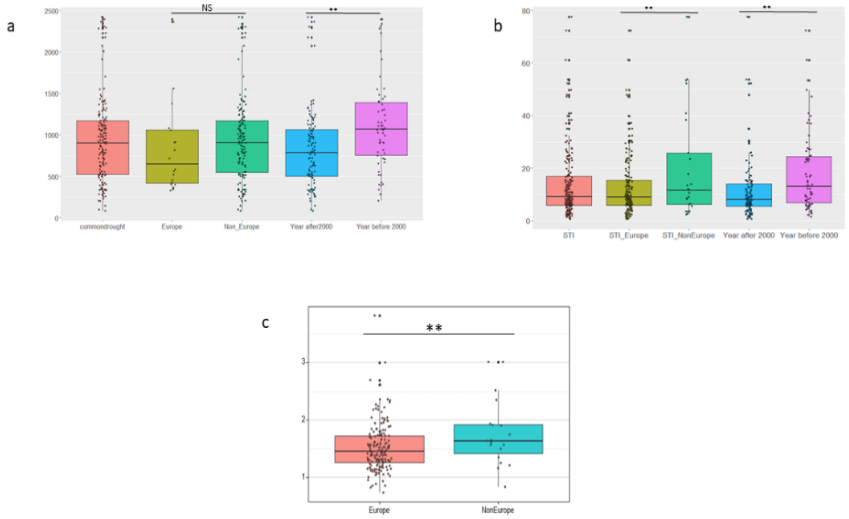

Figure 3. 1. Proline accumulation of 184 the cultivars among different sub-groups. Proline accumulation of European and Non-European sub-group and cultivar sub-group registered before (traditional) and after the year 2000 (modern) under drought stress treatment in the field (a); STI of proline between STI of Europe (STI for Europe) and STI of Non-Europe (STI for Non-Europe) and between the cultivar group modern and traditional (b); STI value of hydrogen peroxide between Europe and Non-European group (c). **, Significant (P< 0.05); NS, Non-significant

3.4.3. Correlation analyses reveals weak correlation of Pro and H_2O_2 with yield attributes under drought condition

To know whether Pro and H_2O_2 are linked with yield attributes we studied correlation among yield-related attributes, Pro and H_2O_2 under drought stress. We found a variable correlations among Pro, H_2O_2 and yield attributes. We found that Pro has both positive and negative correlation with yield parameters under drought condition (Supplementary Table 3. S7). The highest positive correlation was observed between Pro and PH combination. In contrast, the highest negative correlation was identified between Pro and GY. For H_2O_2 content under drought, the highest positive correlation exhibited between H_2O_2 and SN and the highest negative correlation was between TKW and H_2O_2 (Supplementary Table 3. S7). In general our findings revealed that correlations among Pro, H_2O_2 and yield attributes under drought stress were not strong.

3.4.4. GWAS identified the candidate loci for drought induced Pro and H_2O_2 accumulation

Marker-trait association (MTA) identified total 125 markers that passed the thresh hold [*P*= 0.001 or $-\log_{10}$ (p) = 3.0] for Pro content under drought, STI, and Pro accumulation under control conditions. The significant MTA was observed across different chromosomes (Figure 3. 2a, 3.3a; Supplementary Figure 3. S1a). Total 36 significant markers lying on 1A, 3B, 4A, 5A, 6D, 6B and 7B chromosomes were identified for Pro content under drought condition (Figure 3. 1a). These markers explained 3.4 to 5.5% phenotypic variation (Table 3. 2, 3. 3; Supplementary Table 3. S5, 3. S6). The top most significant marker, wsnp_Ex_rep_c106111_90308719 (*P*=0.000003) located on 1A (8.23 Mbp) chromosome established a haplotype block (Pro_1A_Hap1). This chromosome harbored total 9 significant markers. The hotspot region of significant markers for Pro content under drought was 4A which comprised of 12 markers across 41.95 to 46.12 Mbp chromosomal region. We observed that 19 SNPs out of 36 overlapped with candidate genes, which possessed 52% of significant SNPs.

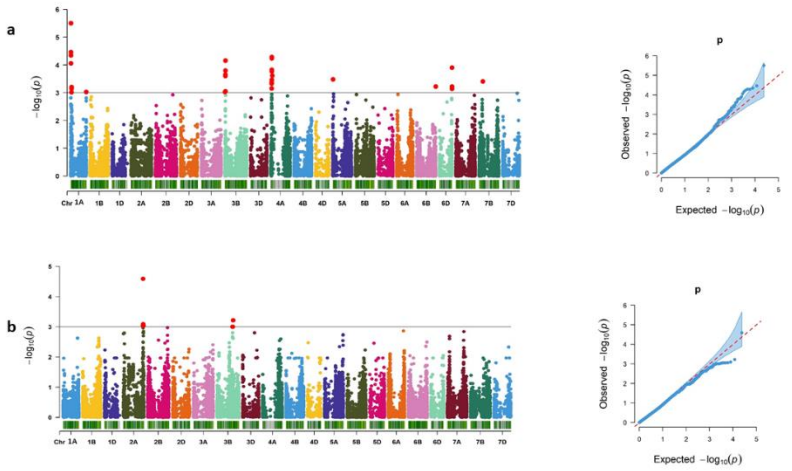

Figure 3. 2. Manhattan plots of GWAS on Pro and H_2O_2 content under drought condition. Manhattan plot (left) and QQplot (right) of Pro content under drought condition (a) and Manhattan plot (left) and QQplot (right) of H_2O_2 content under drought condition (b). $-\log_{10}$ (P) = 3.0 is the significant threshold level for MTA. The red dots on Manhattan plots above the horizontal grey line are representing significant markers

For STI of Pro, total 71 significant markers were identified, which explained 6.30 to 12.12% phenotypic variation (Table 3. 2, 3.3; Supplementary Table 3. S5, 3. S6). The topmost significant marker AX-158525047 (*P*=0.000008), was located on 5B chromosome (490.61 Mbp), which

showed the highest phenotypic variation among all significant markers (12.12%) (Figure 3. 3a; Table 3. 2). Other MTA was detected on 2A, 2B, 3A, 3B, 4B, 5A, 5B, 5D and 6A chromosomes, respectively. The hotspot region for STI of Pro was identified on 5B chromosome which contained 30 significant markers that encompassed a span of 490.61 Mbp to 565.76 Mbp chromosomal region. We observed that 28% of SNPs overlapped the genes (Table 3. 2).

Under the control treatment, 18 significant markers were associated with Pro. The MTA was observed on 1A, 2A, 3B, 4A, 4B, 5A, 5B, 5D, 6B, 7B chromosomes, respectively. These markers accounted for 3.33 to 4.26% phenotypic variation (Table 3. 2, 3. 3; Supplementary Table 3. S5, 3. S6). AX-158524974 located at 5B was the top significant marker (*P*= 0.0002) which was accounted for 4.26% phenotypic variation (Supplementary Table 3. S5). The hotspot region is associated with 4 significant markers that located on 5B chromosome (588.51 to 712.60 Mbp). MTA of H_2O_2 identified total 53 significant markers including 16 markers for control, 2 for drought and 34 for STI (Table 3. 2, 3; Supplementary Table 3. S5, 3. S6). Under drought condition, H_2O_2 is associated with 2 significant markers. The top most significant markers was AX-158557366 (*P*=0.00004) which located on 2A chromosome (749.10 Mbp), and exhibited 10.17% phenotypic variation (Figure 3. 2b; Table 3.2). Another significant marker AX-158550818 (P= 0.0009) was located on 5A chromosome (702.75 Mbp).

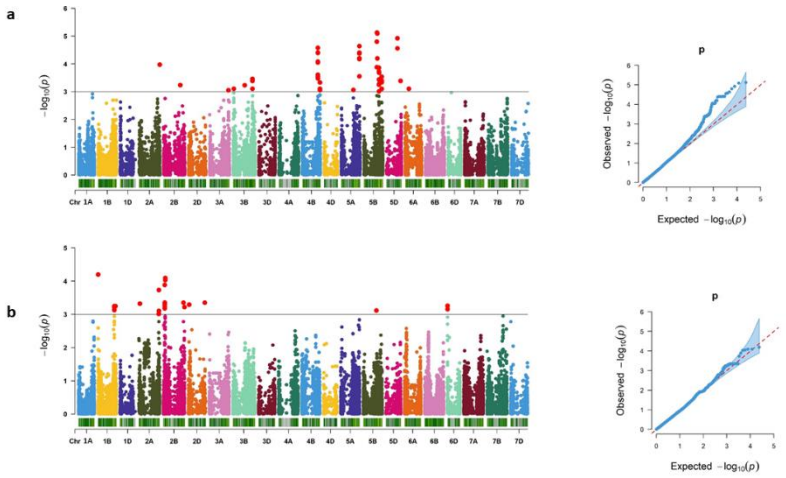

Figure 3.3. Manhattan plots of GWAS for STI of Pro and H_2O_2. Manhattan plot (left) and QQplot (right) of proline STI (a); Manhattan plot (left) and QQplot (right) of hydrogen peroxide STI (b). $-\log_{10}(P) = 3.0$ is the significant threshold level for MTA. The red dots on Manhattan plots above the horizontal grey line are representing significant markers

For H_2O_2 STI, the association study identified MTA across 1B, 2A, 2B, 2D, 5B and 6D chromosomes (Figure 3. 3b). Those markers were responsible for 6.22 to 8.33% phenotypic variation (Table 3. 2, 3. 3; Supplementary Table 3. S5, 3. S6). The top most signal was observed on 1B, 43.20 Mbp position. The marker Kukri_c79308_278 (*P*= 0.00008) was the top most significant marker which formed a haplotype block (HP_1B_Hap1) (Table 3. 3). The hotspot region for significant marker was located on 2B chromosome which comprised of 19 markers across 51.92 Mbp to 800.06 Mbp chromosomal region. Moreover, we observed that 32 out of 57 markers overlapped with putative candidate genes (either intron or exon), which comprised 56 % of significant SNPs (Supplementary Table 3. S8b). For H_2O_2 under control condition, significant markers were identified on 1B, 2A, 2B, 2D, 6B and 6D chromosomes and those marker caused 7.0 to 8.22% phenotypic variation (Table 3. 2, 3. 3; Supplementary Table 3. S5, 3. S6). The top most significant SNP, Kukri_c79308_278 (*P*= 0.00006) was located on 1B chromosome (4.32 Mbp) and formed a haplotype block (HP_1B_Hap1) (Table 3.3). Total 12 markers on 2B chromosome were associated with control Pro, hence 2B was the hotspot region for H_2O_2 accumulation under control condition. Overall observation also revealed that, significant MTA were highest in the A genome followed by the B and D genomes, respectively.

3.4.5. Major and minor alleles of significant markers showed variable associations with Pro and H_2O_2 accumulation

Contrasting alleles of a trait are an important source for plant breeding programs. To estimate the allelic effect initially we observed significant markers either established linkage disequilibrium (LD) block with nearby markers or remained single (Table 3. 2, 3. 3; Supplementary Table 3. S5, 3. S6). LD analysis revealed that 89 SNPs formed 25 haplotype blocks and 36 markers remained as single-markers. Under drought condition, significant markers on 1A, 3B, 4A, 6D and 7B chromosomes formed 3, 2, 3, 1, 1 haplotype blocks, respectively (Table 3.3). Among them, biggest haplotype block, Pro_4A_Hap1 was formed on 4A chromosome which comprised of 13 markers. For control Pro, significant markers formed one haplotype block in each of 1A, 5A and 7B chromosomes (Supplementary Table 3. S6). For STI of Pro, haplotype blocks was formed on 3B, 4B, 5A and 5B chromosomes, respectively. Pro_4B_Hap1, a haplotype block on 4B chromosome was revealed as the largest block (2.49 Mbp) which contained 20 markers (Table 3.3). Total 34 significant SNPs were located within haplotype blocks.

Table 3. 2. Marker, chromosome (Chr), position, *P*-value, phenotypic variation, allele, favorable (Fav.) allele, t-test value regarding Pro and H_2O_2 accumulation under drought stress and for STI of Pro and H_2O_2

Trait	Marker	Chr	Position	P-value	Phenotypic var (%)	Allele (Major: Minor)	Fav. allele	t-test value
Pro_drought	RFL_Contig1027_442	1A	8244106	3.48E-05	5.5	A:G	G	0.02
	AX-158569423	1A	8248738	8.81E-05	5.0	G:A	A	0.03
	BS00084022_51	1A	31781700	9.57E-04	3.4	T:C	T	0.02
	CAP12_rep_c3868_270	3B	986619	9.42E-04	3.4	C:A	A	0.03
	AX-158541844	3B	20538743	6.95E-05	5.1	G:T	T	<0.01
	AX-158538340	3B	20717449	8.92E-04	3.5	A:G	G	<0.01
	AX-158541844	3B	20538743	6.95E-05	5.1	G:T	T	<0.01
	AX-158538340	3B	20717449	8.92E-04	3.5	A:G	G	<0.01
	AX-158541845	3B	20718475	1.60E-04	4.7	G:A	A	0.01
	AX-111526074	3B	20719624	1.60E-04	4.7	G:A	A	<0.01
	BS00009970_51	4A	45338226	3.46E-04	4.1	T:C	T	<0.01
	AX-111497637	4A	46292909	5.82E-05	5.2	C: T	C	<0.01
	wsnp_Ex_c57094_58953404	5A	9657523	3.30E-04	4.1	A:G	G	<0.01
	Excalibur_c2991_320	6D	469919670	1.25E-04	4.6	C:T	C	<0.01
Pro_STI	AX-110412102	2A	775936337	1.07E-04	9.4	A:G	G	<0.01
	AX-158540981	2B	632394417	5.82E-04	6.7	A:G	G	<0.01
	AX-158523479	3A	712134412	8.94E-04	6.3	C:T	T	<0.01
	BS00003522_51	3B	432844940	5.91E-04	6.7	A:G	G	<0.01
	Ku_c1575_338	3B	726481592	7.93E-04	7.4	G:A	G	0.02
	AX-158550762	5A	451456903	8.66E-04	6.3	T:C	T	0.03
	Jagger_c3991_101	5B	488820722	1.33E-04	8.3	T:C	C	<0.01
	GENE_3437_148	5B	489280672	1.59E-05	10.8	T:C	C	<0.01
	AX-158525047	5B	490619499	7.52E-06	12.12	C:T	T	<0.01
H_2O_2_drought	AX-158557366	2A	749105336	3.95E-05	10.17	A:G	G	<0.01
H_2O_2_STI	AX-111649657	1B	614277801	8.74E-04	6.31	A:G	G	<0.01
	AX-89670926	1B	614293304	6.68E-04	6.62	G:A	G	<0.01
	AX-86183817	1B	614452475	6.50E-04	6.64	G:A	G	<0.01

AX-110434034	1B	614612411	5.83E-04	6.75	C:T	T	<0.01
AX-158602322	2A	34152277	5.20E-04	6.88	A:G	G	<0.01
AX-158596005	2A	751004758	8.52E-04	6.85	C:T	T	<0.01
Kukri_c30020_302	2A	751094015	2.10E-04	8.33	C:T	T	<0.01
Excalibur_c9752_289	2B	760950856	5.06E-04	6.91	C:T	T	<0.01
AX-158597023	2B	761322528	5.06E-04	6.91	C:T	T	<0.01
AX-158596842	2B	800060795	4.34E-04	7.23	G:A	A	<0.01
BobWhite_c11059_169	2D	32053537	5.65E-04	6.82	A:C	C	<0.01
Tdurum_contig42636_995	5B	491957849	9.70E-04	6.22	C:T	T	<0.01

Abbreviation: Pro_drought= Proline content under drought condition; H_2O_2_drought= H_2O_2 content under drought condition

Table 3. 3. Haplotypes block, number of markers in haplotype block (NMHB), chromosome (Chr), haplotype block (HB) size, haplotype allele and favorable allele regarding Pro and H_2O_2 accumulation under drought and for the STI

Trait	Haplotype block	NMHB	Chr	HB size (bp)	Haplotype alleles (Ma: Mi)	Favorable allele
Pro_Dro	Pro_1A_Hap1	3	1A	404126	TGT: CTC	CTC
	Pro_1A_Hap2	6	1A	10436	ACCTGG: GTTGGT	GTTGGT
	Pro_1A_Hap3	6	1A	197978	CCAAAT: CCGGCT	CCAAAT
	Pro_3B_Hap1	4	3B	1281	GGCG: AGCG	AGCG
	Pro_3B_Hap2	6	3B	197149	CGCCCG: CGTCCG	CGTCCG
	Pro_4A_Hap1	13	4A	2587578	GCCTAATCCTGTC: GCCTAATCTTGTC	GCCTAATCCTGTC
	Pro_4A_Hap2	4	4A	75535	CCTA: TTCG	TTCG
	Pro_4A_Hap3	5	4A	1780008	ACTTG: GACCA	ACTTG
	Pro_6D_Hap1	3	6D	292341	CGT: TAC	TAC
	Pro_7B_Hap1	4	7B	631054	CTAG: CTGA	CTGA
Pro_STI	Pro_3B_Hap3	3	3B	2175	AGG: GGA	GGA
	Pro_3B_Hap4	7	3B	1050651	AGCATGC: CAAGCAC	AGCATGC
	Pro_4B_Hap1	20	4B	2493409	CACCCTACTCTGCGTATGTG: TGTTTCGTCTCTTACGCTCA	CACCCTACTCTGCGTATGTG
	Pro_4B_Hap2	8	4B	332843	AAATTATG: CGGCCGCA	AAATTATG
	Pro_5A_Hap1	11	5A	408220	CGCCATTAACG: TATAGCCGGTA	CGCCATTAACG
	Pro_5B_Hap1	6	5B	787764	GCCCAC: ATATGC	ATATGC
	Pro_5B_Hap2	4	5B	284390	GTGG: TGAA	TGAA
	Pro_5B_Hap3	8	5B	2005360	AGCGTAAT: CATAGCGG	CATAGCGG
	Pro_5B_Hap4	8	5B	2619512	CGACGACC: TAGTGGTT	TAGTGGTT
	Pro_5B_Hap5	4	5B	7048	GGAT: AGGC	AGGC
	Pro_5B_Hap6	18	5B	3739633	CAATCATATATCTCCAAG: TGGCCATCCGCTCATCGG	TGGCCATCCGCTCATCGG

	Pro_5B_Hap7	18	5B	933082	CTCCCCCGCTGTAACACA: CTCCCCCGCTGTAACATA	CTCCCCCGCTGTAACACA
H_2O_2_Dro	HP_5A_Hap1	3	5A	15706	ATT: GCT	GTC
H_2O_2_ STI	HP_1B_Hap1	3	1B	24816	GTA: ACG	ACG
	HP_1B_Hap2	3	1B	9056	CGA: AAG	AAG
	HP _2B_Hap1	11	2B	2193600	GCGCTGTTTGT: ATATCACCCAT	ATATCACCCAT
	HP _2B_Hap2	6	2B	3877092	AATCCG: CATCCG	AATCCG
	HP _2D_Hap1	3	2D	1304253	ACC: GTC	GTC
	HP _6D_Hap1	4	6D	21999	ACCC: GTTT	GTTT

Abbreviation: Pro_Dro= Proline content under drought condition; H_2O_2_Dro= H_2O_2 content under drought condition

H_2O_2 accumulation variation under drought condition was associated with one haplotype block, HP_5A_Hap1, which was located on 5A chromosome. For H_2O_2 STI, 6 haplotype blocks were detected on 1B, 2B, 2D and 6D chromosomes (Table 3. 3). H_2O_2 under control condition was linked with 3 haplotype blocks across 1B, 2B and 6B chromosomes among them HP_2B_Hap1 was the largest haplotype (2.19 Mbp). LD analysis found that 70%, 77% and 100% minor alleles of single-markers and 77%, 58% and 61.63% of haplotypes were associated with high Pro content drought, STI and Pro content under control conditions, respectively. Similar results were observed for H_2O_2 content. Under drought condition high H_2O_2 content was associated with minor allele of HP_5A_Hap1 haplotype. Similarly, more than 60% of minor alleles of single markers and haplotypes were associated with high STI and H_2O_2 content under control conditions. Therefore, in general our findings showed that the minor alleles of haplotypes and single-markers were linked with higher Pro and H_2O_2 content and with the high STI of Pro and H_2O_2.

3.4.6. Markers pleiotropy identified common markers between traits

To identify pleotropic markers, analysis was performed with loci identified for different traits. We identified 12 SNPs pleiotropy that shared more than one traits. One SNP locus AX-111526074 located on 3B chromosome shared Pro STI and Pro content under drought condition. Similarly, the markers Kukri_c79308_278 and AX-158602322 located on 1B and 2A, respectively and the markers AX-158575274, AX-158547448, AX-158597348, BS00009807_51, IAAV3165, Kukri_c37311_136, wsnp_Ex_c10596_17293192, and wsnp_Ex_c10596_17293363 located on 2B chromosome shared Pro content under control condition and STI of H_2O_2. The marker, RFL_Contig1027_442 associated with Pro content under drought was identified as pleotropic. This marker was previously identified for yield by Nedelkou et al., (2017). There was no marker that shared Pro and H_2O_2 content under drought condition.

3.4.7. Candidate loci harbored putative candidate genes

Candidate gene analysis was performed to find out the potential candidate genes linked with Pro and H_2O_2 accumulation under drought and the STI of Pro and H_2O_2. To make a short list of putative candidate genes we retrieved the genes (either exon or intron regions) that overlapped with the significant SNPs or haplotype block regions (Table 3. 4). 1Mb upstream and downstream regions of significant SNP locus was scanned to find out candidate genes. The full list of genes is provided in Supplementary Table 3. S8.

Table 3. 4. A short-list of putative candidate gene related to Pro and H_2O_2 accumulation under drought and for STI. The genes are in overlapped with the significant markers or haplotype block regions

Trait	Marker/Haplotype	Chr	Position (bp)	Candidate gene	Protein	Gene Ontology
Pro_Dro	RFL_Contig1027_442	1A	8244106	*TraesCS1A01G015200*	Tubulin-folding cofactor E protein	GO:0043014: alpha tubuline binding
	AX-158569423	1A	8248738	*TraesCS1A01G015300*	Ras-like protein	NA
	BS00009970_51	4A	45338226	*TraesCS4A01G053700*	CaM_binding domain-containing protein	
	Pro_1A_Hap1	1A	7835834 to 8239960	*TraesCS1A01G014400*	Serine/threonine-protein kinase	GO:0004672 MF: protein kinase activity
				TraesCS1A01G014500	Serine/threonine-protein kinase	GO:0004672 MF: protein kinase activity
				TraesCS1A01G014900	Serine/threonine-protein kinase	GO:0004672 MF: protein kinase activity
				TraesCS1A01G015000	Serine/threonine-protein kinase	GO:0004672 MF: protein kinase activity
	Pro_1A_Hap2	1A	33365205 to 33375641	*TraesCS1A01G051900*	transmembrane protein	NA
	Pro_1A_Hap3	1A	586717462 to 586915440	*TraesCS1A01G051000*	F-box protein	NA
				TraesCS1A01G051100	F-box/LRR-repeat protein	NA
				TraesCS1A01G051600	F-box family protein	GO:0005515 MF: protein binding
	Pro_3B_Hap1	3B	18820910 to18822191	*TraesCS3B01G039100*	MYB transcription factor	GO:0003677 MF: DNA binding
				TraesCS3B01G039200	NBS-LRR disease resistance protein	GO:0043531 MF: ADP binding
	Pro_7B_Hap1	7B	144074930 to 144705984	*TraesCS7B01G122600*	Aquaporin	GO:0005215 MF: transporter activity
				TraesCS7B01G122800	Receptor-like protein kinase	GO:0004672 MF: protein kinase activity
				TraesCS7B01G122900	Zinc finger family protein	GO:0003676 MF: nucleic acid binding
	Pro_6D_Hap1	6D	470391193 to 470683534	*TraesCS6D01G401100*	Pentatricopeptide repeat-containing protein	GO:0005515 MF: protein binding
	Pro_4A_Hap1	4A	40442320 to 43031174	*TraesCS4A01G049900*	Protein kinase	GO:0004672 MF: protein kinase activity

				TraesCS4A01G050000	Phosphatase 2C family protein	GO:0003824 MF: catalytic activity
				TraesCS4A01G050100	Tetratricopeptide repeat protein 1	GO:0005515 MF: protein binding
				TraesCS4A01G050400	Pentatricopeptide repeat-containing protein, putative	GO:0005515 MF: protein binding
				TraesCS4A01G050500	Metal transporter	GO:0005215 MF: transporter activity
Pro_STI	AX-110412102	2A	775936337	*TraesCS2A01G584400*	WAT1-related protein	GO:0016020 CC: membrane
	Ku_c1575_338	3B	726481592	*TraesCS3B01G475800*	Auxin response factor	GO:0003677 MF: DNA binding
	AX-158550762	5A	451456903	*TraesCS5A01G235300*	Hexosyltransferase	GO:0016758
	AX-158525047	5B	490619499	*TraesCS5B01G307200*	DNA polymerase delta subunit 4	GO:0006260 BP: DNA replication
	GENE_3437_148	5B	489280672	*TraesCS5B01G305100*	PF02181: Formin Homology 2 Domain	G
	Jagger_c3991_101	5B	488820722	*TraesCS5B01G304800*	cytochrome P450, family 702, subfamily A, polypeptide 6	NA
	Excalibur_c9846_458	5B	505482207 to 506269971	*TraesCS5B01G320600*	Pentatricopeptide repeat-containing protein	GO:0005515 MF: protein binding
	Pro_3B_Hap4	3B		*TraesCS3B01G475800*	Auxin response factor	GO:0003677 MF: DNA binding
				TraesCS3B01G476500	F-box protein	NA
				TraesCS3B01G476700	Auxin response factor	NA
				TraesCS3B01G476800	Prefoldin subunit 5	NA
				TraesCS3B01G476900	F-box protein family	GO:0005515 MF: protein binding
				TraesCS3B01G477000	E3 ubiquitin protein ligase drip2	NA
	Pro_4B_Hap1	4B		*TraesCS4B01G292700*	Transmembrane protein, putative	NA
				TraesCS4B01G292900	AP2-like ethylene-responsive transcription factor	GO:0003677 MF: DNA binding
	Pro_5A_Hap1	5A		*TraesCS5A01G516800*	Basic-leucine zipper (bZIP) transcription factor family protein	NA
	Pro_5B_Hap1	5B		*TraesCS5B01G320600*	Pentatricopeptide repeat-containing protein	GO:0005515 MF: protein binding
	Pro_5B_Hap3	5B		*TraesCS5B01G387400*	F-box family protein	GO:0005515 MF: protein binding
	HP_1B_Hap1	1B		*TraesCS1B01G007800*	TAF domain-containing protein	GO:0046982 MF: protein heterodimerization
H_2O_2_STI	AX-86183817	1B	614452475	*TraesCS1B01G382000*	Lys-63-specific deubiquitinase BRCC36	GO:0005515 MF: protein binding

	AX-158596005	2A	751004758	*TraesCS2A01G537100*	Superoxide dismutase	GO:0004784 MF: superoxide dismutase activity
	Excalibur_c9752_289	2B	760950856	*TraesCS2B01G570500*	phosphatidylinositol 4-kinase gamma-like protein	GO:0016301 MF: kinase activity
	HP _2B_Hap1	2B	51928949 to 73198699	*TraesCS2B01G090200*	F-box family protein	GO:0005515 MF: protein binding
				TraesCS2B01G091500	Cytochrome P450	GO:0005506 MF: iron ion binding
				TraesCS2B01G566900	Serine/threonine-protein kinase	GO:0004672 MF: protein kinase activity
	HP _2B_Hap2	2B	758593004 to 760933257	*TraesCS2B01G567000*	Serine/threonine-protein kinase	GO:0004672 MF: protein kinase activity
				TraesCS2B01G567100	Serine/threonine-protein kinase	GO:0004674 MF: protein serine/threonine kinase activity
				TraesCS2B01G567500	Serine/threonine-protein kinase	GO:0004672 MF: protein kinase activity
				TraesCS2B01G567600	Superoxide dismutase	GO:0004784 MF: superoxide dismutase activity
				TraesCS2B01G567700	Serine/threonine-protein kinase	GO:0004674 MF: protein serine/threonine kinase activity
				TraesCS2B01G567800	Serine/threonine-protein kinase	GO:0004672 MF: protein kinase activity
				TraesCS2B01G568000	Serine/threonine-protein kinase	GO:0004672 MF: protein kinase activity
				TraesCS2B01G568500	Serine/threonine-protein kinase	GO:0004672 MF: protein kinase activity
				TraesCS2B01G568600	Serine/threonine-protein kinase	GO:0004672 MF: protein kinase activity
	HP _6D_Hap1	6D	3119406 to 3141405	*TraesCS6D01G007800*	receptor kinase 1	GO:0004672 MF: protein kinase activity
				TraesCS6B01G138800	F-box plant-like protein, putative	NA
				TraesCS6B01G138900	F-box plant-like protein, putative	NA
H_2O_2_Dro	HP_5A_Hap1	5A	702750820 to 702766526	*TraesCS5A01G548800*	DEAD-box ATP-dependent RNA helicase 50	GO:0005524: ATP binding

Abbreviation: Pro_Dro= Proline content under drought condition; H_2O_2_Dro= H_2O_2 content under drought condition

Two topmost significant SNPs, RFL_Contig1027_442 and AX-158569423 for Pro content under drought coincided with the genes *TraesCS1A01G015200* and *TraesCS1A01G015300* that encode tubulin-folding cofactor E protein and Ras-like proteins, respectively (Table 3. 4). The third significant was linked with CaM binding domain-containing protein. Three haplotype blocks in 1A for Pro content drought were linked with four serine/threonine-protein kinase coding genes that were involved in protein kinase activity (GO: 0004672) (Table 3. 4). Pro_1A_Hap2 was associated with a gene encoded for transmembrane protein. Haplotype region of Pro_1A_Hap3 was coincided with F-box family protein coding genes, and the haplotype Pro_3B_Hap1 was associated with MYB transcription factor and NBS-LRR disease resistance gene. Significant markers underlying Pro_4A_Hap1 block was associated with protein kinase (*TraesCS4A01G049900*) and phosphatase 2C family protein coding (*TraesCS4A01G050000*) and tetratricopeptide repeat protein genes (*TraesCS4A01G050100* and *TraesCS4A01G050400*). These genes were involved in protein binding (GO: 0005515), DNA binding (GO: 0003677) and adenosine diphosphate (ADP) binding (GO: 0043531) activity. The haplotype Pro_6D_Hap1 was associated with pentatricopeptide repeat-containing protein (*TraesCS6D01G401100*) gene which was involved in protein binding (GO: 0005515) activity. The haplotype Pro_7B_Hap1 was coincided with zinc finger family protein (*TraesCS7B01G122900*) and Receptor-like protein kinase (*TraesCS7B01G122800*). Moreover, several F box family protein genes were observed in other significant SNPs for Pro content under drought condition (Table 3. 4 and Supplementary Table 3. S8a).

In the case STI of Pro, total 56 protein coding genes overlapped with significant SNPs and haplotype blocks. Of them, 62 genes were associated with 11 haplotype blocks (Supplementary Table 3. S8b). Significant marker locus AX-110412102 was coincided with WAT1-related protein coding gene (*TraesCS2A01G584400*). Another significant SNP AX-110412102 was overlapped with auxin response factor (*TraesCS3B01G475800*). Other significant SNPs on 5B chromosomes were overlapped with DNA polymerase delta subunit 4 (*TraesCS5B01G307200*), formin like (*TraesCS5B01G305100*), and cytochrome P450 (*TraesCS5B01G304800*) proteins. Other haplotypes were linked with putative candidate genes such as F-box protein coding, AP2-like ethylene-responsive transcription factor (*TraesCS4B01G292900*), basic-leucine zipper (bZIP) transcription factor family protein (*TraesCS5A01G516800*) and pentatricopeptide repeat-containing protein (*TraesCS5B01G320600*) (Table 3. 4). Several candidate genes were also identified in 1Mb regions of significant SNPs, for example, Lys-63-specific deubiquitinase,

superoxide dismutase, sulfotransferase proteins, ethylene-responsive transcription factor coding genes. In addition we compared the genes identified in our present study with the homologs and orthologs with genes identified in Arabidopsis to find out the conserved regions between species (Supplementary Table 3. S9). Interestingly, only few genes were identified as homologs in wheat but those are not the genes we identified in the present study.

In the case of STI of H_2O_2, the significant marker AX-86183817 encompassed Lys-63-specific deubiquitinase protein coding gene. The significant marker AX-158596005 was linked with the gene *TraesCS2A01G537100* encoded for superoxide dismutase (Table 3. 4). Among the haplotype block regions, nine serine/threonine-protein kinase gene and one superoxide dismutase protein coding gene were located within HP_2B_Hap2 block region. Several putative candidate genes for example disease resistance protein, zinc finger, pentatricopeptide repeat-containing protein were also identified within 1Mb regions of significant SNPs (Supplementary Table 3. 8b). Overall, the candidate gene analysis found several genes that linked with Pro and H_2O_2 accumulation variation under drought and with STI of Pro and H_2O_2 as potential candidates.

3.5. Discussion

3.5.1. Diversity panel exhibits augmented phenotypic variation for Pro and H_2O_2 in response to drought stress

Diversity of population is an important criterion for plant breeding research especially to develop drought-tolerant crop varieties (Swarup et al., 2021). Present study showed the phenotypic variability of drought induced Pro and H_2O_2 accumulation under field environment. We observed a clear plant-to-plant Pro and H_2O_2 differences under both control and drought treatments, although the variation is wider under the drought stress condition. The effect of genotype and environment interaction was significant, which indicates the drought treatment enhances Pro accumulation. A continuous phenotypic variation was also observed for both Pro and H_2O_2 content, which is indicating a polygenic inheritance. Pro accumulation followed a significant difference between modern and traditional sub-groups. The modern cultivars group was noticed to accumulate lower Pro than that of traditional group. Moreover, variation for Pro accumulation under drought was wider in traditional sub-group. In case of STI of H_2O_2, the European sub-group exhibited significantly higher STI of H_2O_2 than Non-European sub-group. Our findings are in agreement with a previous report by Reinert et al. (2016), which identified distinct LD decay among the sub-

population of barley. In our case the possible reason might be a distinct LD decay pattern across the three genomes exist between Europe and Non-Europe, traditional and modern sub-groups. Our result also indicates that the European sub-group is more responsive to drought than Non-European, although the adaptive role needs to be addressed further.

3.5.2. Pro and H_2O_2 accumulation under drought stress might be a physiological marker for screening the cultivars and genetic improvement

Pro has been known to be correlated with drought stress (Forlani et al., 2019). Several studies regarding genetic (Xia et al., 2017), transcriptomic and proteomic analyses (Gupta et al., 2016; Hoermiller et al., 2017) augmented the importance of Pro in stress tolerance. Housekeeping amount of Pro has been reportedly associated with signaling pathways of plant developmental and maturation process, which leads to enhanced vegetative growth and grain yield (Mattioli et al., 2020; Jira-Anunkul and Pattanagul, 2021). The H_2O_2 has been regarded as a regulator of underlying different stress response mechanisms (Niu and Liao, 2016). Many signal transduction pathways are also triggered by H_2O_2 into plant cells under drought condition. The correlations among Pro and H_2O_2 and yield attributes were not strong in our study. Therefore, our results point out that Pro and H_2O_2 accumulation in leaves under drought stress in field condition might not be a direct determinant of yield attributes under drought condition rather might have adaptive role or become an indicator of drought for plants during drought in the field environment. We found Pro content under drought conditions increased by 11 time as compared to the control treatment. The finding is similar to a previous study by Sharma and Verslues (2010), where Pro accumulation has been reported elicited up to 100 fold under drought condition as compared to the control conditions. Studies on barley (Ziijriga et al. 1989) and wheat (Heerden and Villiers, 2013) reported that epidermis and vascular bundles had preferentially higher Pro content under stress conditions. These evidences are supporting our results and suggest that Pro and H_2O_2 can be a reliable marker for assessment of a wheat cultivar under drought stress. Moreover, we identified contrasting alleles of STI of H_2O_2 and Pro which represents relative performance of the each cultivars in response to drought. The study found that the minor alleles of significant markers are linked significantly with higher Pro and H_2O_2 content under drought as compared to the major alleles (Table 3. 2, 3.3). For Pro, the ‘C’ allele of the topmost significant marker is associated with less STI, whereas the ‘T’ allele is showing high STI (Supplementary Table 3.S3). The cultivar ‘Akteur’ is representing the lowest STI and the ‘Centurk’ represents the highest STI of Pro. Similarly, the topmost significant

marker for STI H_2O_2 is linked with a haplotype, the 'GTA' allele of which is linked with low STI and the 'ACG' is for high. The cultivar 'Urban' showed lowest STI and the cultivar 'Mironovs' possessed highest STI of H_2O_2. These results indicate that the drought induces more Pro and H_2O_2 accumulation. Collectively our findings reveal that Pro and H_2O_2 accumulation under drought stress might be a physiological marker in plants and the contrasting alleles can be utilized for marker-assisted breeding programs.

3.5.3. GWAS identifies candidate loci and genes linked with Pro and H_2O_2 in response to drought stress

Dissecting the genetic regulators underlying drought-induced Pro and H_2O_2 variations is one of our prime targets for its further functional studies. The present study reveals a large genetic diversity within the population which is important for GWAS and further genetic studies. According to Valliyodan et al. (2017) the natural variation among the drought related traits help to identify best resources for genetic studies. In this study we employed a GWAS to identify candidate loci associated with Pro and H_2O_2 variations in response to drought. We identified candidate loci and associated several candidate genes for Pro and H_2O_2. Top most two significant markers for Pro content under drought condition are coincided with Ras like protein which is involved in GTP binding function. Ras protein plays a pivotal role in signal transduction and the ortholog in Arabidopsis has been identified as a drought responsive gene and the over expression is associated with the drought tolerance (Chen et al., 2021). Transmembrane protein (TP) coding genes have been identified in few haplotype regions. TP is involved in Pro transport and few transmembrane proteins have been reported in different species (Wang et al., 2015; Fujiwara et al., 2010). CaM_binding domain-containing protein coding was found to be linked with significant SNPs. Calmodulin is a ubiquitous calcium-binding protein that can regulate diverse cellular functions by modulating the activity of various enzymes and proteins, this gene has been recorded for tolerance to stress by facilitating Pro accumulation (Hyuk Yoo et al., 2004). All the evidences supported our genes encode for Ras protein, TP, CaM binding domain proteins identified for Pro accumulation variation under drought are the potential candidates.

Few haplotypes for STI of Pro is associated with F-box protein coding genes. A previous report revealed the overexpression F-box protein gene in tobacco improved the stress tolerance (An et al., 2019). F-Box gene has also been reported associated with Pro content in wheat (Li et al., 2018).

Therefore, candidate F-box genes in the present study might have possibility to be involved in Pro metabolism. The gene *TraesCS4B01G292900* (AP2-like ethylene-responsive transcription factor) was associated with other few haplotypes. AP2/ERF is one of the ideal candidate for crop improvement since their overexpression in plants enhances tolerances to drought, salt and freezing (Xu et al., 2011; Debbarma et al., 2019). A recent GWAS study identified that ethylene-responsive transcription factor genes are involved in Pro metabolism in Eucalyptus (Mora-Poblete et al., 2021). Both STI of Pro and H_2O_2 are associated with Cytochrome P450 proteins. This P450s produce H_2O_2 through uncoupling process and play an important role in stress tolerance (Yan et al., 2016). Few genes identified in our loci region encode for zinc finger proteins (ZFPs). ZFPs are large protein family and involved in Pro biosynthesis, stress responses and ROS scavenging mechanisms (Luo et al., 2012; Wang et al., 2016). Several genes in our candidate loci regions encode for pentatricopeptide repeat and serine-threonine kinase proteins. These proteins have been reported as a positive regulator of plant responses to abiotic stresses and display a tolerance to drought by higher level of Pro accumulation (Jiang et al., 2015; Lim et al., 2020). A previous GWAS identified pentatricopeptide repeat and serine-threonine kinase protein coding genes that were linked with Pro metabolism in *Arabidopsis* (Verslues et al., 2014). Therefore, pentatricopeptide repeat and serine-threonine kinase protein-coding genes might have correlation with Pro metabolism in wheat.

Significant locus AX-158596005 associated with STI of H_2O_2 encompassed a gene that encodes for superoxide dismutase (SOD) protein. SOD is a ubiquitous antioxidant enzyme that converts the superoxide radical to H_2O_2. This protein has been documented for association in drought (Tyagi et al., 2017). Few significant SNPs for STI of H_2O_2 are associated with disease resistance proteins. Disease resistance protein has an adaptive machinery for plant that is involved in response to stresses. In a previous study identified that, N1P1, a disease resistance coding gene is involved in H_2O_2 signaling (Sadhukhan et al., 2017). The topmost significant locus for STI of H_2O_2 is linked with the E3 ubiquitin-protein ligase ORTHRUS 2. The biological function of this gene is involved in protein ubiquitination pathway, which is part of protein modification, this function is supported by a previous study (Pradhan et al., 2020), which revealed that H_2O_2 causes protein modification, thereby, changes the protein function. All these evidences support our findings and suggest the identified genes for STI of H_2O_2 are the potential candidates that regulate H_2O_2 in response to the drought.

3.6. Conclusions

Pro and H_2O_2 accumulation during stress condition plays multi-dimensional role, therefore, study on underlying key genetic components in an interesting area of research. This study identified large genetic variation of Pro and H_2O_2 induced by drought. The traditional sub-group accumulated higher Pro than that of modern sub-group under drought condition. The STI of H_2O_2 European sub-group exhibited significantly higher STI than Non-European. GWAS identified significant MTAs on different chromosomes for Pro and H_2O_2 under drought stress condition and for STI of Pro and H_2O_2, respectively. Minor alleles of single-markers and haplotypes are linked with higher Pro and H_2O_2 content under drought. Identified loci are reported first time in wheat under drought condition. These loci and contrasting alleles can be incorporated in further functional studies and genetic improvement of cultivars under drought stress.

3.7. References

Alaux M, Rogers J, Letellier T, Flores R, Alfama F, Pommier C, Mohellibi N, Durand S, Kimmel E, Michotey C, et al (2018) Linking the International Wheat Genome Sequencing Consortium bread wheat reference genome sequence to wheat genetic and phenomic data. Genome Biol 19: 111

An J, Li Q, Yang J, Zhang G, Zhao Z, Wu Y, Wang Y, Wang W (2019) Wheat F-box Protein TaFBA1 Positively Regulates Plant Drought Tolerance but Negatively Regulates Stomatal Closure. Front Plant Sci 10: 1242

Barrett JC, Fry B, Maller J, Daly MJ (2005) Haploview: analysis and visualization of LD and haplotype maps. Bioinformatics 21: 263–265

Bates LS, Waldren RP, Teare ID (1973) Rapid determination of free proline for water-stress studies. Plant Soil 1973 391 39: 205–207

Begum H, Alam MS, Feng Y, Koua P, Ashrafuzzaman M, Shrestha A, Kamruzzaman M, Dadshani S, Ballvora A, Naz AA, et al (2020) Genetic dissection of bread wheat diversity and identification of adaptive loci in response to elevated tropospheric ozone. Plant Cell Environ 43: 2650–2665

Bowne JB, Erwin TA, Juttner J, Schnurbusch T, Langridge P, Bacic A, Roessner U (2012)

Drought Responses of Leaf Tissues from Wheat Cultivars of Differing Drought Tolerance at the Metabolite Level. Mol Plant 5: 418–429

Chen C, Chen H, Zhang Y, Thomas HR, Frank MH, He Y, Xia R (2020) TBtools: An Integrative Toolkit Developed for Interactive Analyses of Big Biological Data. Mol Plant 13: 1194–1202

Chen D, He L, Lin M, Jing Y, Liang C, Liu H, Gao J, Zhang W, Wang M (2021) A ras-related small GTP-binding protein, RabE1c, regulates stomatal movements and drought stress responses by mediating the interaction with ABA receptors. Plant Sci. doi: 10.1016/J.PLANTSCI.2021.110858

Corpas FJ, Barroso JB, Del Río LA (2001) Peroxisomes as a source of reactive oxygen species and nitric oxide signal molecules in plant cells. Trends Plant Sci 6: 145–150

Dadshani S, Mathew B, Ballvora A, Mason AS, Léon J (2021) Detection of breeding signatures in wheat using a linkage disequilibrium-corrected mapping approach. Sci Reports 2021 111 11: 1–12

Debbarma J, Sarki YN, Saikia B, Boruah HPD, Singha DL, Chikkaputtaiah C (2019) Ethylene Response Factor (ERF) Family Proteins in Abiotic Stresses and CRISPR–Cas9 Genome Editing of ERFs for Multiple Abiotic Stress Tolerance in Crop Plants: A Review. Mol Biotechnol 2019 612 61: 153–172

Deng X-P, Cheng Y-J, Wu X-B, Kwak S-S, Chen W, Eneji AE (2012) Exogenous hydrogen peroxide positively influences root growth and exogenous hydrogen peroxide positively influences root growth and metabolism in leaves of sweet potato seedlings. AJCS 6: 1572–1578

Desikan R, Neill SJ, Hancock JT (2000) Hydrogen peroxide–induced gene expression in Arabidopsis thaliana. Free Radic Biol Med 28: 773–778

Fernandez GCJ (1992) Effective selection criteria for assessing plant stress tolerance. Adapt food Crop to Temp water Stress. doi: 10.22001/WVC.72511

Forlani G, Trovato M, Funck D, Signorelli S (2019) Regulation of Proline Accumulation and Its

Molecular and Physiological Functions in Stress Defence. Osmoprotectant-Mediated Abiotic Stress Toler. Plants. Springer International Publishing, pp 73–97

Fujiwara T, Mitsuya S, Miyake H, Hattori T, Takabe T (2010) Characterization of a novel glycinebetaine/proline transporter gene expressed in the mestome sheath and lateral root cap cells in barley. Planta 232: 133–143

Gabriel SB, Schaffner SF, Nguyen H, Moore JM, Roy J, Blumenstiel B, Higgins J, DeFelice M, Lochner A, Faggart M, et al (2002) The structure of haplotype blocks in the human genome. Science (80-) 296: 2225–2229

Gao L, Turner MK, Chao S, Kolmer J, Anderson JA (2016) Genome Wide Association Study of Seedling and Adult Plant Leaf Rust Resistance in Elite Spring Wheat Breeding Lines. PLoS One. doi: 10.1371/JOURNAL.PONE.0148671

Grallath S, Weimar T, Meyer A, Gumy C, Suter-Grotemeyer M, Neuhaus JM, Rentsch D (2005) The AtProT family. Compatible solute transporters with similar substrate specificity but differential expression patterns. Plant Physiol 137: 117–126

Gupta A, Sarkar AK, Senthil-Kumar M (2016) Global transcriptional analysis reveals unique and shared responses in arabidopsis thaliana exposed to combined drought and pathogen stress. Front Plant Sci 7: 686

He Y, Liu Y, Cao W, Huai M, Xu B, Huang B (2005) Effects of Salicylic Acid on Heat Tolerance Associated with Antioxidant Metabolism in Kentucky Bluegrass. Crop Sci 45: 988–995

Heerden PDR van, Villiers OT de (2013) Evaluation of proline accumulation as an indicator of drought tolerance in spring wheat cultivars. http://dx.doi.org/101080/02571862199610634368 13: 17–21

Hoermiller II, Naegele T, Augustin H, Stutz S, Weckwerth W, Heyer AG (2017) Subcellular reprogramming of metabolism during cold acclimation in Arabidopsis thaliana. Plant Cell Environ 40: 602–610

Hyuk Yoo J, Young Park C, Cheol Kim J, Do Heo W, Sun Cheong M, Cheol Park H, Chul Kim

M, Cheol Moon B, Soo Choi M, Hwan Kang Y, et al (2004) Direct interaction of a divergent CaM isoform and the transcription factor, MYB2, enhances salt tolerance in Arabidopsis. J Biol Chem 280: 3697–3706

Ignea C, Athanasakoglou A, Andreadelli A, Apostolaki M, Iakovides M, Stephanou EG, Makris AM, Kampranis SC (2017) Overcoming the plasticity of plant specialized metabolism for selective diterpene production in yeast. Sci Reports 2017 71 7: 1–11

Jiang S-C, Mei C, Liang S, Yu Y-T, Lu K, Wu Z, Wang X-F, Zhang D-P (2015) Crucial roles of the pentatricopeptide repeat protein SOAR1 in Arabidopsis response to drought, salt and cold stresses. Plant Mol Biol 88: 369–385

Jira-Anunkul W, Pattanagul W (2021) Effects of hydrogen peroxide application on agronomic traits of rice (Oryza sativa L.) under drought stress. Plant, Soil Environ 67 (2021): 221–229

Kadam NN, Tamilselvan A, Lawas LMF, Quinones C, Bahuguna RN, Thomson MJ, Dingkuhn M, Raveendran M, Struik PC, Yin X, et al (2017) Genetic Control of Plasticity in Root Morphology and Anatomy of Rice in Response to Water Deficit. Plant Physiol 174: 2302–2315

Kleine S, Müller C (2014) Drought Stress and Leaf Herbivory Affect Root Terpenoid Concentrations and Growth of Tanacetum vulgare. J Chem Ecol 40: 1115–1125

Koua AP, Oyiga BC, Baig MM, Léon J, Ballvora A (2021) Breeding driven enrichment of genetic variation for key yield components and grain starch content under drought stress in winter wheat. Front Plant Sci https://www.frontiersin.org/article/10.3389/fpls.2

Li Q, Wang W, Wang W, Zhang G, Liu Y, Wang Y, Wang W (2018) Wheat F-Box Protein Gene TaFBA1 Is Involved in Plant Tolerance to Heat Stress. Front Plant Sci 9: 521

Luo X, Cui N, Zhu Y, Cao L, Zhai H, Cai H, Ji W, Wang X, Zhu D, Li Y, et al (2012) Over-expression of GsZFP1, an ABA-responsive C2H2-type zinc finger protein lacking a QALGGH motif, reduces ABA sensitivity and decreases stomata size. J Plant Physiol 169: 1192–1202

Mattioli R, Palombi N, Funck D, Trovato M (2020) Proline Accumulation in Pollen Grains as

Potential Target for Improved Yield Stability Under Salt Stress. Front Plant Sci 11: 1699

Maulana F, Huang W, Anderson JD, Ma X-F (2020) Genome-Wide Association Mapping of Seedling Drought Tolerance in Winter Wheat. Front Plant Sci 0: 1626

Money D, Gardner K, Migicovsky Z, Schwaninger H, Zhong GY, Myles S (2015) LinkImpute: Fast and accurate genotype imputation for nonmodel organisms. G3 Genes, Genomes, Genet 5: 2383–2390

Mora-Poblete F, Ballesta P, Lobos GA, Molina-Montenegro M, Gleadow R, Ahmar S, Jiménez-Aspee F (2021) Genome-wide association study of cyanogenic glycosides, proline, sugars, and pigments in Eucalyptus cladocalyx after 18 consecutive dry summers. Physiol Plant 172: 1550–1569

Nedelkou IP, Maurer A, Schubert A, Léon J, Pillen K (2017) Exotic QTL improve grain quality in the tri-parental wheat population SW84. PLoS One 12: e0179851

Neill S, Desikan R, Hancock J (2002) Hydrogen peroxide signalling. Curr Opin Plant Biol 5: 388–395

Niu L, Liao W (2016) Hydrogen Peroxide Signaling in Plant Development and Abiotic Responses: Crosstalk with Nitric Oxide and Calcium. Front Plant Sci 7: 230

Pradhan S, Ali Babar M, Bai G, Khan J, Shahi D, Avci M, Guo J, McBreen J, Asseng S, Gezan S, et al Genetic dissection of heat-responsive physiological traits to improve adaptation and increase yield potential in soft winter wheat. doi: 10.1186/s12864-020-6717-7

Reinert S, Kortz A, Léon J, Naz AA (2016) Genome-wide association mapping in the global diversity set reveals new QTL controlling root system and related shooGenome-wide association mapping in the global diversity set reveals new QTL controlling root system and related shoot variation in barleyt . Front Plant Sci 7: 1061

Remans T, Opdenakker K, Smeets K, Mathijsen D, Vangronsveld J, Cuypers A, Remans T, Opdenakker K, Smeets K, Mathijsen D, et al (2010) Metal-specific and NADPH oxidase dependent changes in lipoxygenase and NADPH oxidase gene expression in Arabidopsis thaliana exposed to cadmium or excess copper. Funct Plant Biol 37: 532–544

Sadhukhan A, Kobayashi Y, Nakano Y, Iuchi S, Kobayashi M, Sahoo L, Koyama H (2017) Genome-wide Association Study Reveals that the Aquaporin NIP1;1 Contributes to Variation in Hydrogen Peroxide Sensitivity in Arabidopsis thaliana. Mol Plant 10: 1082–1094

Sallam A, Alqudah AM, Dawood MFA, Baenziger PS, Börner A (2019) Drought stress tolerance in wheat and barley: Advances in physiology, breeding and genetics research. Int J Mol Sci. doi: 10.3390/ijms20133137

Schwacke R, Grallath S, Breitkreuz KE, Stransky E, Stransky H, Frommer WB, Rentsch D (1999) LeProT1, a Transporter for Proline, Glycine Betaine, and g-Amino Butyric Acid in Tomato Pollen. Plant Cell 11: 377

Sharma S, Verslues PE (2010a) Mechanisms independent of abscisic acid (ABA) or proline feedback have a predominant role in transcriptional regulation of proline metabolism during low water potential and stress recovery. Plant Cell Environ 33: 1838–1851

Sharma S, Verslues PE (2010b) Mechanisms independent of abscisic acid (ABA) or proline feedback have a predominant role in transcriptional regulation of proline metabolism during low water potential and stress recovery. Plant Cell Environ 33: 1838–1851

Siddiqui MN, Teferi TJ, Ambaw AM, Gabi MT, Koua P, Léon J, Ballvora A (2021) New drought-adaptive loci underlying candidate genes on wheat chromosome 4B with improved photosynthesis and yield responses. Physiol Plant. doi: 10.1111/PPL.13566

Sreeman SM, Vijayaraghavareddy P, Sreevathsa R, Rajendrareddy S, Arakesh S, Bharti P, Dharmappa P, Soolanayakanahally R (2018) Introgression of physiological traits for a comprehensive improvement of drought adaptation in crop plants. Front Chem 6: 92

Stewart CR HA (1980) Proline accumulation as a metabolic response to water stress. In NC Turner, PJ Kramer, eds, Adaptation of Plants to Water and High Temperature Stress. John Wiley & Sons, Ltd

Stich B, Melchinger AE (2010) An introduction to association mapping in plants. CAB Rev Perspect Agric Vet Sci Nutr Nat Resour. doi: 10.1079/PAVSNNR20105039

Sukumaran S, Reynolds MP, Sansaloni C (2018) Genome-Wide Association Analyses Identify QTL Hotspots for Yield and Component Traits in Durum Wheat Grown under Yield Potential, Drought, and Heat Stress Environments. Front Plant Sci 0: 81

Suneja Y, Gupta AK, Bains NS (2019) Stress Adaptive Plasticity: Aegilops tauschii and Triticum dicoccoides as Potential Donors of Drought Associated Morpho-Physiological Traits in Wheat. Front Plant Sci 10: 211

Swarup S, Cargill EJ, Crosby K, Flagel L, Kniskern J, Glenn KC (2021) Genetic diversity is indispensable for plant breeding to improve crops. Crop Sci 61: 839–852

Tadesse W, Ogbonnaya FC, Jighly A, Sanchez-Garcia M, Sohail Q, Rajaram S, Baum M (2015) Genome-wide association mapping of yield and grain quality traits in winter wheat genotypes. PLoS One. doi: 10.1371/journal.pone.0141339

Tewari RK, Kumar P, Tewari N, Srivastava S, Sharma PN (2004) Macronutrient deficiencies and differential antioxidant responses—influence on the activity and expression of superoxide dismutase in maize. Plant Sci 166: 687–694

Tshikunde NM, Mashilo J, Shimelis H, Odindo A (2019) Agronomic and Physiological Traits, and Associated Quantitative Trait Loci (QTL) Affecting Yield Response in Wheat (Triticum aestivum L.): A Review. Front Plant Sci 10: 1428

Tyagi S, Sharma S, Taneja M, Shumayla, Kumar R, Sembi JK, Upadhyay SK (2017) Superoxide dismutases in bread wheat (Triticum aestivum L.): Comprehensive characterization and expression analysis during development and, biotic and abiotic stresses. Agri Gene 6: 1–13

Velikova V, Yordanov I, Edreva A (2000) Oxidative stress and some antioxidant systems in acid rain-treated bean plants: Protective role of exogenous polyamines. Plant Sci 151: 59–66

Verbruggen N, Villarroel R, Van Montagu M (1993) Osmoregulation of a pyrroline-5-carboxylate reductase gene in Arabidopsis thaliana. Plant Physiol. doi: 10.1104/pp.103.3.771

Verslues PE, Lasky JR, Juenger TE, Liu TW, Nagaraj Kumar M (2014) Genome-wide association mapping combined with reverse genetics identifies new effectors of low water

potential-induced proline accumulation in Arabidopsis. Plant Physiol. doi: 10.1104/pp.113.224014

Voss-Fels KP, Stahl A, Wittkop B, Lichthardt C, Nagler S, Rose T, Chen T-W, Zetzsche H, Seddig S, Majid Baig M, et al (2019) Breeding improves wheat productivity under contrasting agrochemical input levels. Nat Plants 2019 57 5: 706–714

Wang F, Tong W, Zhu H, Kong W, Peng R, Liu Q, Yao Q (2016) A novel Cys2/His2 zinc finger protein gene from sweetpotato, IbZFP1, is involved in salt and drought tolerance in transgenic Arabidopsis. Planta 243: 783–797

Wang H, Tang X, Wang H, Shao HB (2015) Proline accumulation and metabolism-related genes expression profiles in Kosteletzkya virginica seedlings under salt stress. Front Plant Sci 6: 792

Xia Y, Li R, Bai G, Siddique KHM, Varshney RK, Baum M, Yan G, Guo P (2017) Genetic variations of HvP5CS1 and their association with drought tolerance related traits in barley (Hordeum vulgare L.). Sci Reports 2017 71 7: 1–10

Xu ZS, Chen M, Li LC, Ma YZ (2011) Functions and Application of the AP2/ERF Transcription Factor Family in Crop ImprovementF. J Integr Plant Biol 53: 570–585

Yan Q, Cui X, Lin S, Gan S, Xing H, Dou D (2016) GmCYP82A3, a Soybean Cytochrome P450 Family Gene Involved in the Jasmonic Acid and Ethylene Signaling Pathway, Enhances Plant Resistance to Biotic and Abiotic Stresses. PLoS One 11: e0162253

Zhang Z, Ersoz E, Lai CQ, Todhunter RJ, Tiwari HK, Gore MA, Bradbury PJ, Yu J, Arnett DK, Ordovas JM, et al (2010) Mixed linear model approach adapted for genome-wide association studies. Nat Genet. doi: 10.1038/ng.546

Zhou B, Wang J, Guo Z, Tan H, Zhu X (2006) A simple colorimetric method for determination of hydrogen peroxide in plant tissues. Plant Growth Regul 2006 492 49: 113–118

Ziijriga GE, Argandora VH, Corcuera LJ (1989) Distribution of glycine-betaine and proline in water stressed and unstressed barley leaves. Phytochemistry 28: 419420

Chapter 4. Hydrogen peroxide-induced root-shoot variations in bread wheat and mapping of candidate loci by GWAS

4.1. Abstract

Hydrogen peroxide (H_2O_2) is a signalling molecule that plays a crucial role in plant growth and development. Understanding genetic factors regulating H_2O_2-mediated root-shoot growth is very limited, especially in crops. Here, we estimated genetic diversity for root-shoot traits under control and H_2O_2 treatment using a diversity panel comprised of 150 wheat cultivars. The H_2O_2 treatment significantly reduced root-shoot growth. Next, a genome-wide association study was performed using the relative value and stress tolerance index (STI) of root-shoot traits. A total of 108 marker-trait association was identified including the topmost association found on chromosomes 3B, 2A, 5A, 3B, 5D, 5A, 6B, 4B and 3B for relative root length, STI root length, relative shoot length, STI shoot length, relative root fresh weight, relative shoot fresh weight, STI shoot fresh weight, relative and STI root-shoot ratio, respectively. Linkage disequilibrium analysis identified the major alleles of significant markers for all traits except for relative root length and relative root-shoot ratio were linked with high relative value and STI. The candidate genes were mostly involved in metal ion binding, transmembrane transport, oxidation-reduction process, protein phosphorylation, DNA, and ADP binding processes. Identified genomic regions for root-shoot traits in response to H_2O_2 could be utilized in the future for functional studies.

4.2. Introduction

During the life cycle, plants frequently undergo various abiotic stresses that negatively affect growth and productivity. They produce different reactive oxygen species (ROS) in response to those stresses. But the adaptive mechanisms recognize and respond to those external stimuli to adjust accordingly, although the strength of adaptation depends on plant species and type of stresses. Hydrogen peroxide (H_2O_2) is one of the main components of ROS and an important signalling molecule that mediates systemic signal networks under control and stress conditions (Petrov and Breusegem, 2012). It is comparatively long-lived and freely diffusible through the cell membrane. Its transportation from organelles of origin to the site of action is mediated through the channel protein-coding gene aquaporin (Sadhukhan et al., 2017). Cellular production occurs through enzymatic and non-enzymatic processes. The enzymatic process includes mainly NADPH oxidases, cell wall peroxidases, glycolate, amine oxidases, flavin-containing enzymes, and glucose oxidases (Brychkova et al., 2012; Chang and Tang, 2014; Francoz et al., 2015). Whereas, the non-enzymatic process includes several oxidation-reduction

reactions (Borisova et al., 2012). Interestingly, plants under non-stress conditions produce H_2O_2 which is required for normal growth and development (Deng et al., 2012). However, raised amount of H_2O_2 production has been documented for mechanical injury, pathogen attack, exposure to extreme temperature, ozone, and drought (Jubany-Marí et al., 2009; Liu et al., 2013). Under those situations, H_2O_2 up-regulated the genes involved in the defence response, hypersensitive response, proteases, transcription and translation, and mitochondrial metabolisms. These evidences have established a tight association of H_2O_2 with both signalling pathways and tolerance mechanisms. For example, a study revealed that nitroxide-inuced-S-nitrosylation activated an ascorbate peroxidase (APX) in *Arabidopsis thaliana* which enhanced H_2O_2 resistance, but the APX activity levels affected the sensitivity of H_2O_2 signalling pathway (Yang et al., 2015). Moreover, raised amount of H_2O_2 under a stress can exhibit a cross tolerance to the same and other different stresses (Neill et al., 2002). H_2O_2 mediated tolerance and cross-tolerance occurs through the activation of signal transduction components like calcium-dependent protein kinases (CDPKs) and mitogen activated protein (MAP) kinases under different biotic and abiotic stresses (Wurzinger et al., 2011). The H_2O_2 induced tolerance has been documented for wheat, rice under drought and salt stress (Uchida et al., 2002; Wahid et al., 2008; Liheng et al., 2009; Pongprayoon et al., 2013). Similarly, H_2O_2 induced cold and salt tolerance has been reported in tomato and maize, respectively (Zhou et al., 2012; Neto et al., 2005).

Root-shoot growth of plants are quickly responsive to exogenous H_2O_2 application. Toxic levels of H_2O_2 reduce the cell production through extensive cellular damage (Anjum et al., 2016). Reduction in cell growth results in less root-shoot growth in plants (Voothuluru et al., 2020). Another report indicated that H_2O_2 reduced the expression of mRNA activity of ROS-scavenging and anti-oxidant level (Voothuluru et al., 2020). H_2O_2 modulates the activity of genes involved in ROS control, transcriptional regulation, signal transduction, protein, carbohydrate, and lipid metabolism during acclimation in stress environments (Li et al., 2011; Liu et al., 2016). The regulatory elements for H_2O_2 signalling pathways and their role in cell-to-cell communication are not fully clear till now (Miller et al., 2009). Few downstream transcription factors of H_2O_2 signalling pathways have been identified as responsive to biotic (e.g., zinc-finger TFs such as ZAT12) (Rizhsky et al., 2004) or abiotic (e.g. salt stress responsive JUNGBRUNNEN1) (Wu et al., 2012) stresses. A genome wide expression study revealed that H_2O_2 plays a key role in the transcriptional up-regulation of small heat shock proteins during high-light stress (Vanderauwera et al., 2005). The co-up-regulated genes were highly related to plastid/nucleus functions and gene regulation function, such as nucleotide,

protein, DNA, and chromatin binding, and transcription regulator activity, and transcription process (Cheng et al., 2013). A transcriptome analysis study has shown that 1-2% of genes expression in *Arabidopsis* is regulated in response to H_2O_2 treatment under drought and other stress conditions (Desikan et al., 2000), and one-third of the transcription factor mRNA are altered after exposure to H_2O_2 (Gadjev et al., 2006). These genes are generally involved in cell wall protection, desiccation tolerance, production of ROS scavenging enzymes and DNA damage repair. Their expression modulation was observed through the activation of mitogen activated protein kinase (MAPK) pathway (Zhang and Zhang, 2022).

Abiotic stress related, Ca^{2+} signalling is also one of the main targets of H_2O_2 (Petrov and Van Breusegem, 2012). The crosstalk between H_2O_2 and Ca^{2+} is associated with different antioxidant defence and plant growth (Hu et al., 2007; Liao et al., 2012). Richards et al., (2014) reported that Ca^{2+} transport-protein regulates H_2O_2-induced Ca^{2+} signature that promotes plant growth and development in *Arabidopsis* and marigold (Liao et al., 2012). H_2O_2 acts on Cys residues of targeted amino acids which leads to protein modifications, thereby altered the genes function (Van Der Reest et al., 2018). Therefore, H_2O_2 has a role of either activation of signalling or a consequence of signalling. All these evidences indicate that H_2O_2 metabolism is regulated by interconnected complex pathways related to stresses. Due to having role in different signalling pathways and in ROS-mediated posttranslational modifications, studies with H_2O_2 has have gained a broader interest (Waszczak et al., 2015). However, the key regulators within these networks that are potentially be applicable to the development of abiotic stress-resistant plants, although studies regarding genetic elements (loci and/or genes) of H_2O_2 in crop plants are very limited. Recently, Sadhukhan et al., (2017) performed a GWAS study to identify loci and genes involved in tolerance pathways for root length of *Arabidopsis* seedlings mediated by toxic level of H_2O_2. It would be interesting to perform such studies with wheat which is a key economic crop worldwide.

Genome wide association study (GWAS) is a genetic tool that has been used to dissect complex traits underlying development, metabolism and stress tolerance for the last few years (Horton et al., 2012; Branham et al., 2016; Julkowska et al., 2016). Following GWAS, candidate gene search and gene ontology (GO) analyses provide a list of promising candidate genes (Daba et al., 2018). Thus, GWAS and GO analyses are powerful tools to uncover the genetic factors induced by H_2O_2 for root-shoot traits. Keeping all the above aspects in mind, the present study was formulated with following specific objectives: (a) to determine the genetic diversity of root-shoot traits induced by H_2O_2, (b) to identify marker and haplotype alleles linked with

contrasting relative value and stress tolerance index (STI) and (c) to identify the candidate loci and genes involved in H_2O_2-mediated tolerance pathways for root-shoot traits using GWAS.

4.3. Materials and methods

4.3.1. Plant materials, growth conditions and treatments

The study material consisted of a diversity panel of 150 cultivars of bread wheat cultivars, over 60% of them are originated from Germany. Others are originated from United States of America (USA), United Kingdom, Mexico, France, Denmark, Serbian, Chili, Australia and Ukraine. A complete list of the cultivars are presented in Supplementary Table 4. S1. The experiment was conducted into a growth chamber. The growth chamber was maintained with 12/12 hours light and dark cycle having the temperature of 22°C-23°C. 15 Seeds per cultivar were surface-sterilized with 5% sodium hypochlorite for 10 minutes followed by washing 5 times with distilled water. Then the seeds were placed into 9 mm petri plates and kept at room temperature for germination. Uniformly germinated seeds were then placed into new petri plates containing blotting paper (Whatman no.2). The seedlings were exposed to the treatment either distilled water (control), or 20 mM H_2O_2 (Sigma, USA). The treatments solution was refreshed in every alternative day. Thus, seedlings were allowed to grow for seven days.

4.3.2. Root-shoot phenotyping

After 7 days of treatment, root length, shoot length, total seedling length, root-shoot ratio, root dry weight, shoot dry weight, and total dry weight were recorded. A measuring tape was used to measure the root and shoot and total length from $n \geq 9$ individual seedlings in millimetre (mm) unit. All weights were recorded by digital balance in milligram (mg). After recording the fresh weights, the dry weights of the samples were recorded by oven dry at 70ºC for 72 hours. H_2O_2 concentration was selected according to Sadhukhan et al. (2017) in *Arabidopsis* with few modifications. The modification was the toxic dose for wheat seedling growth, which was selected based on observation of root-shoot growth in response to 20 mM H_2O_2 in several repeats.

4.3.3. Phenotypic data analysis

Some descriptive statistics including mean, maximum, minimum, and co-efficient of variation (CV %) were performed through R statistical computing software (version 3.6). Mixed model, two-way ANOVA was applied for mean comparison of the traits, where effect of replications were considered as random effect and the genotype and treatments were regarded as fixed effect

(Kadam et al., 2017) using the R program, especially packages namely “nlme”, and “emmeans” (R Development Core Team 2018). The variance components were used for calculating broad sense heritability (H^2). The following formula was used for estimating H^2:

$$\text{Heritability } (H^2) = \frac{Vg}{Vg + \frac{Verr}{r}}$$

Where, Vg is genotypic variance and Verr is the error variance and r is the number of replications.

We estimated relative value and stress tolerance index (STI). To calculate the relative value, mean value of root-shoot traits were used in the following formula:

$$\text{Relative value} = \frac{\text{value under stress conditions}}{\text{value under control conditions}} \ [\%]$$

Thus, relative root length (R_RL), relative shoot length (R_SL), relative shoot fresh weight (R_SFW), relative root fresh weight (R_RFW), and relative root-shoot ratio (R_RSRatio) were recorded. Similarly, we used mean value of traits to calculate STI by using following formula:

$$STI = \frac{(Yww) \text{ x } (Ytd)}{(Xww)^2}$$

Where, Y_{ww} = value of control treatment of a particular cultivar, Y_{td} = value drought treatment of a particular line, X_{ww} = mean value over all cultivars under control condition (Fernandez, 1992).

Thus, STI root length (STI_RL), STI shoot length (STI_SL), STI shoot fresh weight (STI_SFW), and STI root-shoot ratio (STI_RSRatio) were recorded.

To estimate the magnitude of the relationship among attributed traits, pearson's correlation coefficients (r) were calculated using mean values of cultivars in R program and correlation table was made using ‘xtable’ package with the function ‘corstars’. In addition, we categorized our studied panel into two sub-groups: cultivars registered before the year 2000 as ‘traditional’ and cultivars registered after 2000 as ‘modern’. Mean comparison between modern and traditional cultivars was performed through student T-test by MS office excel program 2013 assuming unequal variance for the traits R_SL, STI_SL, R_RSRatio and STI_RSRatio. Other statistical analyses were performed by using R programming software v.3.6. The LD decay pattern of all genomes (A, B, and D) were plotted in R (package, ggplot2).

4.3.4. Genome-wide association studies (GWAS)

A 135K SNP chip representing 24,216 single nucleotide polymorphic (SNP) markers across 21 chromosomes was employed for GWAS analysis. The details of these markers were described in previous publications (Voss-Fels et al., 2019; Dadshani et al., 2021). Missing SNPs exclusion, minor allele frequency (MAF) < 5%, and SNPs data imputation were performed in Trait Analysis by Association, Evolution and Linkage (TASSEL) version 5.2 through LinkImpute (LD-kNNi) method (Money et al., 2015). Then, GWAS was conducted by using TASSEL 5.2 with a compressed MLM that incorporated the population structures and five principal components. Kinship matrix (K) was used as an additive genetic effect and first five principal components as a fixed effect to avoid false positives association and to correct the population structure (Zhang et al., 2010). After the Bonferroni correction, only STI_SL, STI_RSRatio can pass the significant threshold, therefore we avoided this stringent threshold, rather a threshold *P*-value of 0.001 [$-\log_{10}(p) = 3$] was declared as a significant threshold according to previous studies (Tadesse et al., 2015; Gao et al., 2016). After setting this criterion, the SNPs that satisfy the threshold *P*-value ($P \leq 0.001$) were considered as true positives and used for gene search. Manhattan plots were visualized using the R package "CMplot". The phenotypic variation (PV) explained by a marker (r^2) was calculated for the significant SNPs using TASSEL 5.2 (Bradbury et al., 2007).

4.3.5. Linkage disequilibrium (LD) analysis and putative candidate gene search

Haplotype analysis was performed through Haploview 4.2 by selecting significant markers and markers adjacent these according to Barrett et al. (2005). LD block were considered as loci when it displayed in heat-map with upper confidence bounds of D' value exceeded 0.98 and the lower bound exceeded 0.7 (Gabriel et al., 2002). A student's T-test assuming two samples unequal variances was conducted to compare the means of the traits for contrasting haplotypes. However, LD blocks harbouring significant SNPs were defined as the candidate loci, and genes in these loci were assembled. The significant SNPs did not establish any LD block, a 1.0 Mega base pair (Mbp) window on both side of chromosomes was scanned to search putative candidate genes according to Begum et al. (2020). Annotation and gene ontology (GO) was obtained from the Wheat URGI database (https://wheat-urgi.versailles.inra.fr) (Alaux et al., 2018). The genes located the significant SNPs or haplotype block regions were listed and represented as candidate genes in Supplementary Table 4. S3a,b). Further, candidate genes linked with top five significant SNPs (based on *P*-value) were short listed and presented in Table 4. 4.

4.4. Results

4.4.1. Phenotypic analyses unravel the natural genetic variation induced by H_2O_2

In order to assess the impact of H_2O_2 on root-shoot growth eight traits were selected including RL, SL, RSRatio, TL, RFW, SFW, RDW and SDW were assessed. Analysis of variance (ANOVA) revealed that all traits were affected by the H_2O_2 treatment (Table 4. 1). However, a significant effect of genotype (cultivar), treatment, and genotype-treatment interaction was observed for most of the traits except TL and RDW, where only interaction effect was non-significant (Table 4. 1). On average, H_2O_2 stress reduced 29.8% RL, 14.2% of SL, 18.2% of RSRatio, 22.4% of TL, 18.6% of SFW, 25.6% of SDW, 13.2% of RFW and 30.3 % of RDW (Table 4. 1). From these results it was clear that H_2O_2 stress has a strong negative impact on root-shoot growth. Importantly, ANOVA results also revealed that H_2O_2-induced a wider genetic diversity of cultivars for most of the traits except for RFW and RDW.

Pearson correlation revealed fluctuating degrees of correlations among the traits under H_2O_2 treatment (Table 4. 2). High positive association (r = 0.34 to 0.89; $P < 0.05$) were noticed among RLH, SLH, TLH, SFWH, SDWH, and RFWH; whereas negative correlation was observed in RSRatioH, with SLH, SFWH, and SDW (r= -0.07 to -0.35). The trait RDWH was observed very low and negative associations with other traits (RLH, SLH, TLH, SFW and SDW) (r= -0.13 to -0.24), whereas RLH showed high positive correlations with SLH, RSRatioH, TLH, SFWH, SDWH, and RFWH (r= 0.27 to 0.89) (Supplementary Table 4. S2).

4.4.2. High STI and relative value were linked with the traditional sub-group

We assessed H_2O_2 induced root-shoot growth of modern and traditional cultivar sub-groups. The results identified distinct relative and STI of traits between those two sub-groups. It was observed that traditional cultivars had significantly higher (P <0.05) STI_SL, R_RSRatio, STI_RSRatio values than that of modern group except for R_SL which showed the non-significant difference between those two sub-groups (Figure 4. 1a). LD decay pattern was plotted which exhibited a distinguished pattern of LD decay between modern and traditional cultivars (Figure 4. 1e-f).

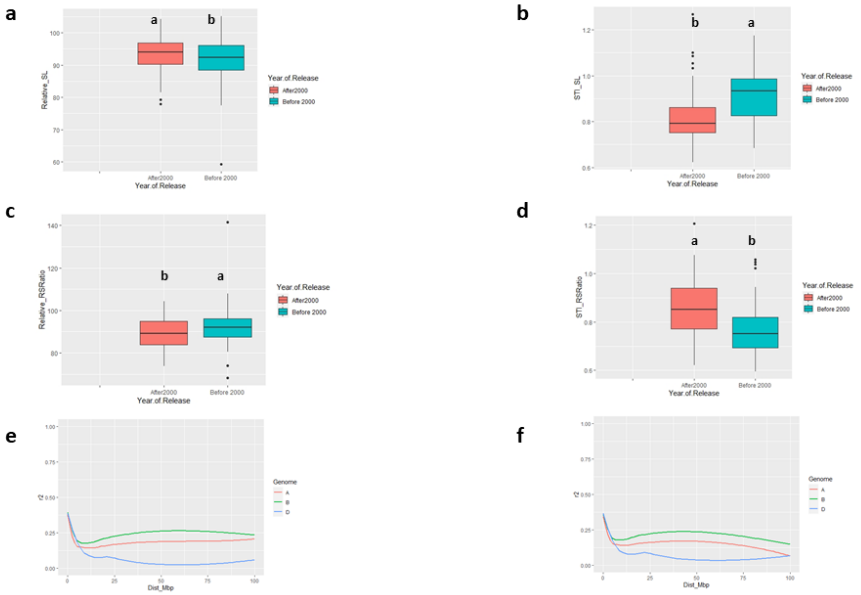

Figure 4.1. Comparison of STI and relative value of sub-groups comprised of the cultivars registered after the year 2000 (modern) and before the year 2000 (traditional). (a) R_SL of modern and traditional cultivars. (b) STI_SL of modern and traditional cultivars. (c) R_RSRatio of modern and traditional cultivars. (d) STI_RSRatio of modern and traditional cultivars. (e-f) is showing the LD decay pattern of studied cultivars of bread wheat across three genome (A, B and D), (e) LD decay pattern of modern cultivars; and (f) LD decay pattern of traditional cultivars. In (a-d), different letters indicate statistical difference at $P < 0.05$.

Table 4.1. Descriptive statistics and analysis of variance based on average phenotypic values of shoot-shoot traits under control and H_2O_2 induced stress conditions

Traits	control					H_2O_2 stress						One-way ANOVA		
	Max	Min	Mean	CV (%)	H^2	Max	Min	Mean	CV (%)	H^2	%R	G	T	G×T
RL	155.92	82.33	113.69	11.52	0.96	134.50	42.78	79.86	18.29	0.93	29.8	***	***	***
SL	150.42	74.00	101.80	14.10	0.92	133.33	43.33	87.31	16.61	0.89	14.2	***	***	***
RSRatio	1.66	0.82	1.13	14.59	0.61	1.75	0.56	0.93	17.54	0.60	18.2	***	***	***
TL	294.33	169.91	215.49	10.55	0.68	260.33	112.26	167.17	15.46	0.68	22.4	***	***	NS
SFW	135.57	57.50	88.96	18.53	0.63	118.00	23.60	72.41	21.70	0.61	18.6	*	***	*
SDW	17.40	4.63	7.94	22.58	0.62	10.43	0.55	5.90	26.53	0.68	25.6	***	***	***
RFW	254.00	87.70	130.41	13.06	0.74	148.70	65.00	113.24	12.71	0.55	13.2	***	***	*
RDW	46.50	9.45	21.58	33.20	0.59	32.71	5.82	15.04	30.99	0.59	30.3	***	***	NS

Note: *p<0.05; ***p<0.0001; NS, Non-Significant. Abbreviations: RL, Root Length; SL, Shoot Length; TL, Total Length; SFW, Shoot Fresh Weight; G=Genotype; T=Treatment; Shoot Dry Weight; RFW, Root Fresh Weight; RDW, Root Dry Weight; %R, % reduction compared to the control; CV, Coefficient of Variation

4.4.3. GWAS analysis uncovered the candidate loci for H_2O_2

Genome-wide mapping was employed to identify H_2O_2-responsive loci underlying the genetic control of the traits. GWAS used the STI and relative values that represents relative reduction percentage of root-shoot traits induced by exogenous H_2O_2 treatment. The compressed mixed linear model (cMLM) was employed which incorporated the population structure and kinship matrix. This model showed fewer false positives rate in comparison to the general linear model (GLM) (Larsson et al., 2013). Next, the marker-trait association (MTA) that satisfied the threshold level of $P = 0.001$, was considered as true positives and significant for investigated relative and STI of traits. MTA identified total 108 significant SNPs that distributed over the wheat genomes (Table 4. 2a, 4.2b; Supplementary Table 4. S4). The linkage disequilibrium (LD) analysis identified the LD blocks contained 17 SNPs that encompassed total of 277 protein-coding genes (Supplementary Table 4. S4). Thirty seven of these genes are short-listed in the Table 4. 4.

4.4.3. Root length

RL induced by H_2O_2 treatment showed a wider phenotypic variation which was represented by R_RL and STI_RL (Figure 4. 2a, 4. 3a). Significant MTA was identified on 1A, 2A, 2B, 3B, 4A, 4B, 5B, 6A, 7B, 7D chromosomes which included total 17 SNP marker for RL (Figure 4. 2a and 4. 2b). Among them, STI_RL is linked with 8 markers and R_RL with 9 markers. These markers showed a phenotypic variation ranged 7.65-8.88% and 7.81-10.25% for R_RL and STI_RL, respectively (Table 4. 2b). In context with 9 markers for R_RL, two markers were found to establish the haplotype block, Rel_RL_3B_Hap1 on 3B chromosome (Figure 4. 2c, e), and one marker formed haplotype block (Com_Hap1) on 4B (Figure 4. 2d, f). The major allele of significant marker for Rel_RL_3B_Hap1 and minor allele for Com_Hap1 exhibited higher R_RL (Figure 4. 1e, f). Single-markers analysis revealed that 83% of minor alleles was linked with significantly higher R_RL. Altogether, 255 protein-coding genes were associated with R_RL (Supplementary Table 4. S3a). 3B chromosome was the hotspot region of MTA. Top five MTA and promising candidate genes are short listed in the Table 4. 4. The top most marker, AX-109990240 (*P*=4.38E-04) was located on 3B chromosome (Table 4. 2b). The linked gene encoded zinc finger protein and showed nucleic acid binding activity (GO: 0003676). Interestingly, within top 5 MTA, the haplotype Com_Hap1 was identified as pleiotropic which overlapped the trait R_RSRatio (Table 4. 3).

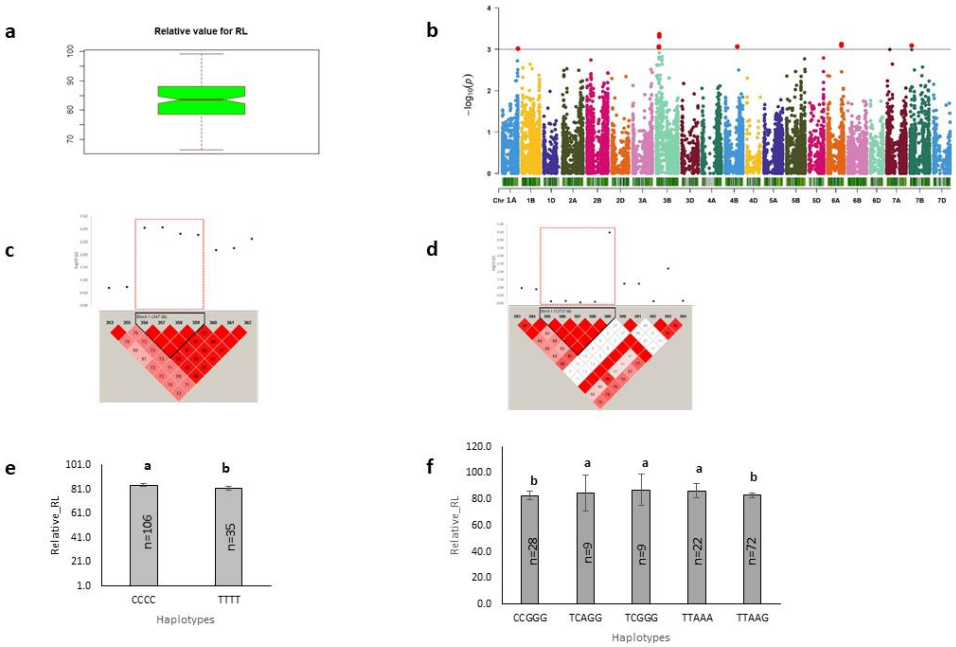

Figure 4.2. Marker-trait associations for R_RL. (a) Box plot showing the distribution of R_RL value; (b) Manhattan plot displaying the marker-trait associations; the horizontal red line indicates threshold level (P =0.001), the dots above this line indicate significant markers. (c) The linkage disequilibrium (LD) heat map illuminating the peak region on chromosome 3B (Rel_RL_3B_Hap1). (d) The linkage disequilibrium (LD) heat map illuminating the peak region on chromosome 4B (Com_Hap1). In (c-d), pair-wise LD map between SNP markers is marked by D′ values, dark red represent 1, whereas white is for 0. The region surrounded by the red dotted line indicate LD block that contain significant SNPs. (e-f) Phenotypic comparison of the haplotype groups established for the significant SNPs as detected by LD block. Different letters indicate statistical difference at $P < 0.05$, n indicates number of genotypes represent each specific haplotype.

Table 4.2a. Significant SNPs associated with STI of different root-shoot traits in bread wheat and marker position, *P*-value (*P*≤ 0.001), phenotypic variance (PV), major, minor (Ma: Mi), and favourable alleles

Traits	Marker	Chr	Position (bp)	P-value	PV (%)	Allele (Ma: Mi)	Fav. allele
STI_RL	AX-158596313	2A	421064707	1.66E-04	10.25	C:T	T
STI_RL	AX-111016876	2A	717417914	4.14E-04	9.07	T:C	T
STI_RL	AX-108742509	2A	718354502	9.03E-04	8.05	A:G	A
STI_RL	AX-158581925	4A	43031174	3.56E-04	9.26	C:T	C
STI_RL	AX-110016919	5B	591062022	8.12E-04	8.18	C:A	C
STI_RL	D_contig78519_72	7D	10724734	9.87E-04	7.81	C:A	C
STI_RSRatio	RAC875_c21906_247	2A	691478630	2.60E-04	8.77	G:A	A
STI_RSRatio	AX-158555653	2A	691479513	2.17E-04	8.91	G:A	A
STI_RSRatio	AX-158555652	2A	691845720	2.43E-04	9.08	C:T	T
STI_RSRatio	RAC875_c52458_454	2A	692755001	9.38E-04	7.13	C:T	T
STI_RSRatio	BobWhite_c17403_635	2A	693241897	9.38E-04	7.13	T:C	C
STI_RSRatio	AX-158572604	2A	706575588	7.03E-04	7.53	G:A	G
STI_RSRatio	AX-158572603	2A	706757509	7.45E-04	7.49	A:G	A
STI_RSRatio	AX-111016876	2A	717417914	8.86E-05	10.58	T:C	T
STI_RSRatio	AX-158557238	2A	717418634	4.86E-04	8.28	T:C	T
STI_RSRatio	AX-109854150	2A	717857707	3.50E-04	8.77	G:T	G
STI_RSRatio	AX-108742509	2A	718354502	1.05E-04	10	A:G	A
STI_RSRatio	AX-158608713	2A	718358893	3.40E-04	8.46	C:T	C
STI_RSRatio	BS00093201_51	2A	718571577	9.76E-04	7.28	A:G	A
STI_RSRatio	AX-110966497	2A	718721301	1.31E-04	9.7	C:T	C
STI_RSRatio	BS00081506_51	2A	718730480	4.28E-04	8.08	C:T	C
STI_RSRatio	AX-109340451	2A	718934808	3.05E-04	8.68	A:G	A
STI_RSRatio	Kukri_c51247_322	3A	140043493	5.21E-04	7.84	C:T	C
STI_RSRatio	AX-108852904	3B	822891332	2.64E-04	8.82	G:A	G
STI_RSRatio	BS00071183_51	3B	823762843	6.00E-04	7.82	A:G	A
STI_RSRatio	AX-158598301	3B	826091387	7.38E-05	10.31	G:A	A
STI_RSRatio	BS00073411_51	3B	829197896	7.51E-04	7.54	T:G	T
STI_RSRatio	AX-111015220	3B	829203418	1.25E-05	12.92	T:C	T
STI_RSRatio	AX-158578652	3B	829293411	4.76E-05	11.05	T:G	T
STI_RSRatio	BS00065603_51	3D	611497215	6.00E-04	7.82	C:T	C

STI_RSRatio	BS00068415_51	3D	612903461	6.63E-04	7.69	G:A	G
STI_RSRatio	AX-158617434	4A	18119033	7.38E-04	7.53	G:A	G
STI_RSRatio	Kukri_rep_c68594_530	4D	12773159	7.77E-04	7.37	A:G	G
STI_SFW	AX-158600273	6A	520581021	8.94E-04	7.98	C:T	C
STI_SFW	AX-158600281	6A	520712811	8.68E-04	8.02	T:G	T
STI_SFW	wsnp_Ku_c4296_7807837	6A	520717537	8.12E-04	8.12	T:C	T
STI_SFW	Excalibur_c54055_694	1D	308455842	5.33E-04	8.78	C:T	C
STI_SFW	AX-158535753	6B	51225226	1.83E-04	10.43	A:G	G
STI_SL	AX-108852904	3B	822891332	3.77E-05	12.87	G:A	G
STI_SL	BS00071183_51	3B	823762843	1.94E-05	13.81	A:G	A
STI_SL	IAAV8659	3B	826081626	1.15E-04	11.07	C:A	C
STI_SL	wsnp_Ra_rep_c75740_73183118	3B	826081626	1.15E-04	11.07	G:T	G
STI_SL	AX-158598301	3B	826091387	1.68E-05	13.86	G:A	A
STI_SL	BS00073411_51	3B	829197896	8.64E-05	11.58	T:G	T
STI_SL	AX-111015220	3B	829203418	7.40E-06	15.49	T:C	T
STI_SL	AX-158578652	3B	829293411	4.15E-05	12.66	T:G	T
STI_SL	BS00065603_51	3D	611497215	1.94E-05	13.81	C:T	C
STI_SL	BS00068415_51	3D	612903461	1.57E-05	14.13	G:A	G

Abbreviations: STI_RSRatio, stress tolerance index root-shoot ratio; STI_RL, stress tolerance index root-length; STI_SL, stress tolerance index shoot length; STI_SFW, stress tolerance index shoot fresh weight

Table 4. 2b. Significant SNPs associated with relative values different root-shoot traits in bread wheat and marker position, *P*-value ($p \leq 0.001$), phenotypic variance (PV), major, minor (Ma: Mi), and favourable alleles

Traits	Marker	Chr	Position (bp)	P-value	PV (%)	Allele (Ma:Mi)	Fav. allele
R_RFW	Kukri_c67721_184	1A	21282106	7.42E-04	9.04	G:A	G
R_RFW	BS00087787_51	1B	50778549	5.23E-04	9.85	C:T	C
R_RFW	BS00084305_51	1B	90992706	6.26E-04	9.89	G:T	G
R_RFW	RAC875_c63067_283	1B	95654954	2.92E-04	10.55	T:C	T
R_RFW	AX-158607168	1B	107000000	2.98E-04	10.71	G:A	G
R_RFW	AX-158570694	1B	116000000	5.59E-04	9.66	T:C	T
R_RFW	Kukri_c29582_126	1B	119000000	2.92E-04	10.55	C:T	C
R_RFW	AX-158606938	1B	223000000	3.98E-04	10.02	G:T	G
R_RFW	Kukri_rep_c105316_262	1B	231000000	3.46E-04	10.28	T:G	T
R_RFW	IAAV902	3A	574000000	5.29E-04	9.66	G:A	G
R_RFW	AX-158603951	4A	535000000	7.05E-04	9.93	G:A	G
R_RFW	Tdurum_contig82473_67	5B	621000000	2.66E-04	10.65	G:A	A
R_RFW	BS00065783_51	5D	69456300	8.02E-05	12.56	T:C	T
R_RFW	Excalibur_c28759_914	6B	716000000	2.96E-04	10.97	A:G	A
R_RFW	AX-158626906	7B	705000000	6.37E-04	9.25	T:C	T
R_RL	AX-89555340	1A	592000000	9.70E-04	7.65	T:C	C
R_RL	wsnp_JD_c2623_3541255	3B	115000000	4.89E-04	8.53	G:T	T
R_RL	AX-109990240	3B	116000000	4.38E-04	8.88	C:T	C
R_RL	AX-158600273	6A	521000000	7.47E-04	7.93	C:T	T
R_RL	AX-158600281	6A	521000000	8.19E-04	7.81	T:G	G
R_RL	wsnp_Ku_c8497_14429303	7B	64728963	8.13E-04	7.89	G:A	A
R_RSRatio	Kukri_c29170_680	2A	693000000	6.94E-04	8.08	A:G	G
R_RSRatio	AX-158533093	3A	444000000	7.36E-04	8.55	A:G	A
R_RSRatio	AX-158523668	3A	445000000	2.37E-04	9.91	C:T	T
R_RSRatio	AX-158523313	3A	462000000	5.05E-04	8.52	C:T	C
R_RSRatio	AX-158533132	3A	478000000	6.31E-04	8.26	G:A	A
R_RSRatio	AX-158548980	3D	534000000	3.85E-04	8.95	T:G	G
R_RSRatio	AX-158582575	4B	510000000	1.66E-04	10.24	A:G	G
R_SFW	AX-110382510	5A	578000000	5.81E-04	10.57	A:G	A
R_SFW	AX-108744896	5A	578000000	5.81E-04	10.57	A:C	A

R_SFW	Ku_c19858_2078	5A	578000000	5.81E-04	10.57	T:C	T
R_SFW	AX-89769139	5A	578000000	3.86E-04	11.35	A:G	A
R_SFW	BS00076246_51	5A	578000000	1.01E-04	13.78	T:C	T
R_SFW	BS00074299_51	5A	578000000	1.01E-04	13.78	T:C	T
R_SFW	Tdurum_contig86202_175	5A	578000000	1.01E-04	13.78	G:A	G
R_SFW	AX-108742709	5A	578000000	1.01E-04	13.78	A:C	A
R_SFW	AX-158589824	6D	3075685	9.60E-04	9.64	G:A	G
R_SL	AX-158521438	1B	6867170	6.38E-04	8.27	C:G	C
R_SL	AX-158532334	2D	535000000	5.85E-04	8.4	A:G	A
R_SL	AX-158521912	2D	542000000	8.63E-04	7.85	C:T	C
R_SL	AX-158582483	4B	661000000	9.65E-04	7.77	G:A	G
R_SL	AX-109884177	5A	37843077	3.16E-04	9.24	T:G	G
R_SL	AX-158544315	7D	87479166	7.72E-04	8.04	G:A	G

Abbreviations: R_RL, relative root length; R_RSRatio, relative root-shoot ratio; R_RFW, relative root fresh weight; R_SFW, relative shoot fresh weight; R_SL, relative shoot length;

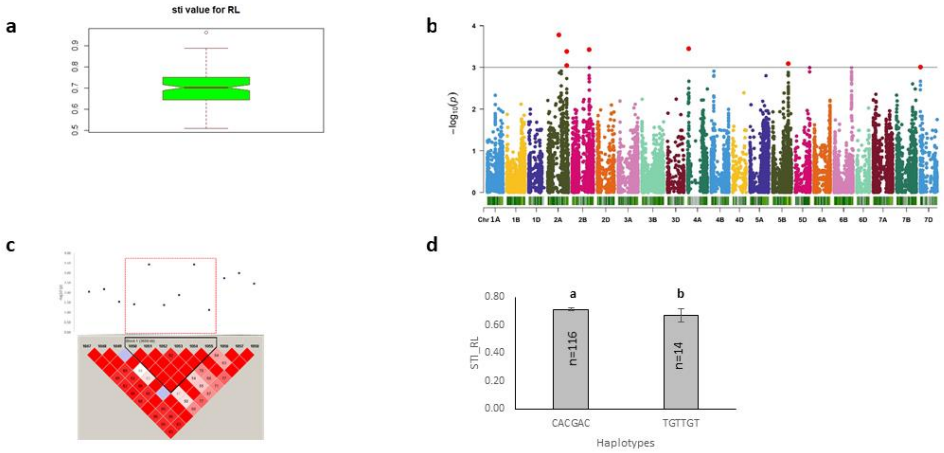

Table 4. 3. Marker-trait associations for STI_RL. (a) Box plot showing the distribution of STI RL_value; (b) Manhattan plot displaying the marker-trait associations; the horizontal red line indicates threshold level (P =0.001), the dots above this line indicate significant markers. (c) The linkage disequilibrium (LD) heat map illuminating the peak region on chromosome 2B (sti_RL_2B_Hap1). In (c), pair-wise LD map between SNP markers is marked by D′ values, dark red represent 1, whereas white is for 0. The region surrounded by the red dotted line indicate LD block that contain significant SNPs. (d) Phenotypic comparison of the haplotype groups established for the significant SNPs as detected by LD block. Different letters indicate statistical difference at $P < 0.05$, n indicates number of genotypes represent each specific haplotype.

The genes associated with remaining four candidate SNPs included bZIP transcription factor, receptor-like kinase, pentatricopeptide repeat-containing protein that were involved in oxidation-reduction, protein phosphorylation, and regulation of transcription functions (Table 4.4). The candidate loci for STI_RL was located on 2A, 2B, 4A, 5B, 7D chromosomes, including AX-158596313 as the top marker located on 2A. The associated gene with the topmost marker encoded a disease resistance protein which was involved in nucleic acid binding function (GO: 0003676). Major allele of single-markers (>80%) were associated with higher STI_RL (Table 4. 2a). Similarly, the major allele of the haplotype sti_RL_2B_Hap1 represented significantly higher STI_RL compared to the minor allele (Figure 4. 3c, d). The haplotype region contained the putative candidate that encoded receptor-like kinase protein (Table 4. 4). However, candidate loci harboured total 172 protein-coding genes for STI_RL (Supplementary Table 4. S3b). The top significant 5 MTA were associated with stress related pathways including protein phosphorylation, protein kinase and ADP binding functions. Notably, other significant marker located on 2A, 7D and 5B chromosomes contained BS-LRR disease resistance protein-coding genes that were involved in ADP binding function (Supplementary Table 4. S3b).

4.4.4. Shoot length

R_SL and STI_SL represented the SL showed a larger phenotypic variation (Figure 4. 4a, 5a). This phenotypic variability was linked with total 23 significant markers distributed across 1A, 1B, 2D, 3B, 3D, 4B, 5A, 5B, and 7D chromosomes and controlled by 352 protein-coding genes (Figure 4. 4b, 4.5b; Supplementary Table 4. 3a, 4.3b).

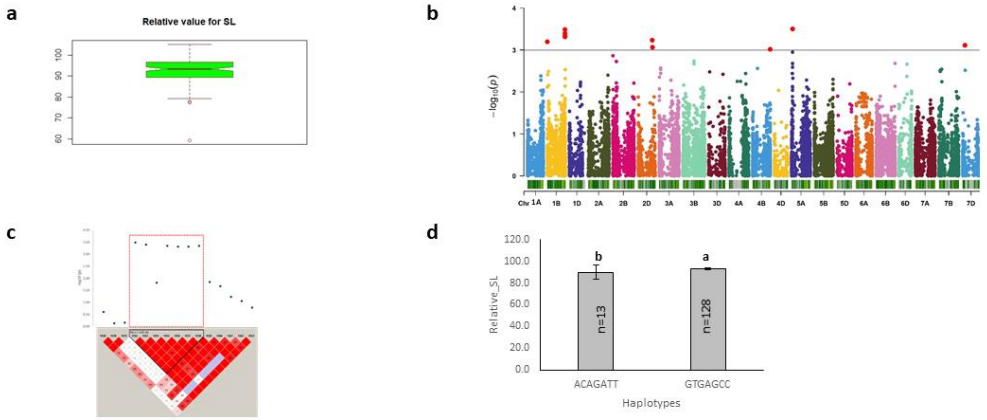

Table 4. 4. Marker-trait associations for R_SL. (a) Box plot showing the distribution of R_SL value; (b) Manhattan plot displaying the marker-trait associations; the horizontal red line indicates threshold level (P =0.001), the dots above this line indicate significant markers. (c) The linkage disequilibrium (LD) heat map illuminating the peak region on chromosome 1B (Rel_SL_1B_Hap1). In (c), pair-wise LD map between SNP markers is marked by D′ values, dark red represent 1, whereas white is for 0. The region surrounded by the red dotted line indicate LD block that contain significant SNPs. (d) Phenotypic comparison of the haplotype groups established for the significant SNPs as detected by LD block. Different letters indicate statistical difference at $P < 0.05$, n indicates number of genotypes represent each specific haplotype.

Among them, 9 and 14 markers that showed phenotypic variation ranged 7.77-9.24 and 11.7-15.49 were associated with R_SL and STI_SL, respectively (Table 4. 2a, 4. 2b). 1B was identified as the hotspot regions which accumulated the highest number of significant markers for R_SL MTA. The haplotype on it was linked with 3 protein coding genes. Major allele of this haplotype and 83% major alleles of single-markers showed higher R_SL (Table 4.2b; Figure 4. 4.c-d). MTA identified the top [P= 3.16E-04] significant marker AX-109884177 on 5A chromosome. This marker was associated with the gene *TraesCS5A01G043000* that was involved in metal ion binding function. One haplotype Rel_SL_1B_Hap1, was linked with the gene *TraesCS1B01G456400* the molecular functions of which was transmembrane transport (Table 4. 4). MTA for STI_SL identified the top most significant (P= 7.40E-06) marker, AX-111015220 on 3B chromosome, and the associated gene had protein phosphorylation activity (GO: 0006468) (Table 4. 4).

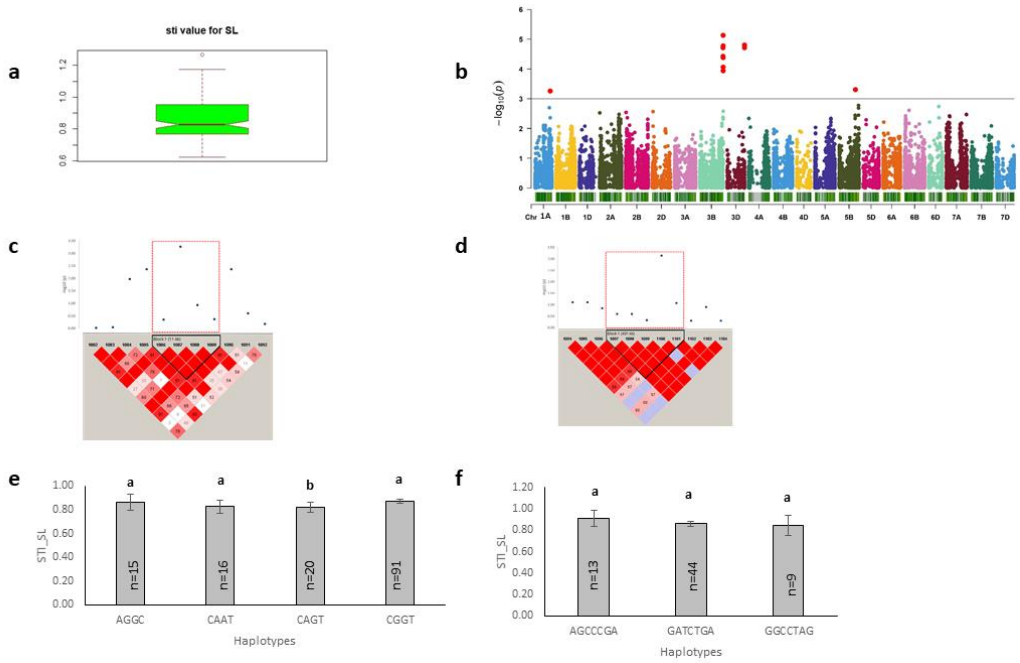

Table 4. 5. Marker-trait associations for STI_SL. (a) Box plot showing the distribution of STI_SL value; (b) Manhattan plot displaying the marker-trait associations; the horizontal red line indicates threshold level ($P = 0.001$), the dots above this line indicate significant markers. (c) The linkage disequilibrium (LD) heat maps illuminating the peak region on chromosome 1A (sti_SL_1A_Hap1). (d) The linkage disequilibrium (LD) heat maps illuminating the peak region on chromosome 5B (sti_SL_5B_Hap1). In (c-d), pair-wise LD map between SNP markers is marked by D′ values, dark red represent 1, whereas white is for 0. The region surrounded by the red dotted line indicate LD block that contain significant SNPs. (e-f) Phenotypic comparison of the haplotype groups established for the significant SNPs as detected by LD block. Different letters indicate statistical difference at $P < 0.05$, n indicates number of genotypes represent each specific haplotype.

Two haplotype blocks sti_SL_1A_Hap1 and sti_SL_5B_Hap1 located on 1A and 5B chromosomes encompassed 2 and 15 protein-coding genes, respectively (Figure 4. 5c, d).

Moreover, pleotropic markers BS00065603_51 and BS00068415_51 located in 3D which overlapped both STI_SL and STI_RSRatio (Table 4. 3). The single markers analysis identified that more 90% major alleles contributed significant higher STI_SL (Table 4. 2a). Top five candidate SNP loci included receptor-like protein kinase, disease resistance protein, aquaporin, NBS-LRR-like resistance protein coding genes (Table 4. 4). These genes were involved in stress related biological processes including protein phosphorylation, transport, and transporter activity.

4.4.5. Root fresh weight

RFW induced by H_2O_2 treatment was represented by R_RFW. Association mapping identified that total 18 markers were distributed on 1A, 1B, 3A, 4A, 5B, 5D, 6B, and 7B chromosomes which linked with 339 protein-coding genes (Table 4.2b; Figure 4. 6a). These markers showed a phenotypic variation ranged 9.25-10.71 % (Table 4. 2b). More than 90% major alleles of

single-markers were linked with high R_RFW (Table 4. 2b). Top most (*P*= 8.02E-05) marker BS00065783_51 lying on 5D chromosome explained 12.56% phenotypic variation. This marker was linked with FAD/NAD (P)-binding oxidoreductase family protein coding gene which was involved in oxidation-reduction process (GO: 0055114) (Table 4. 4).

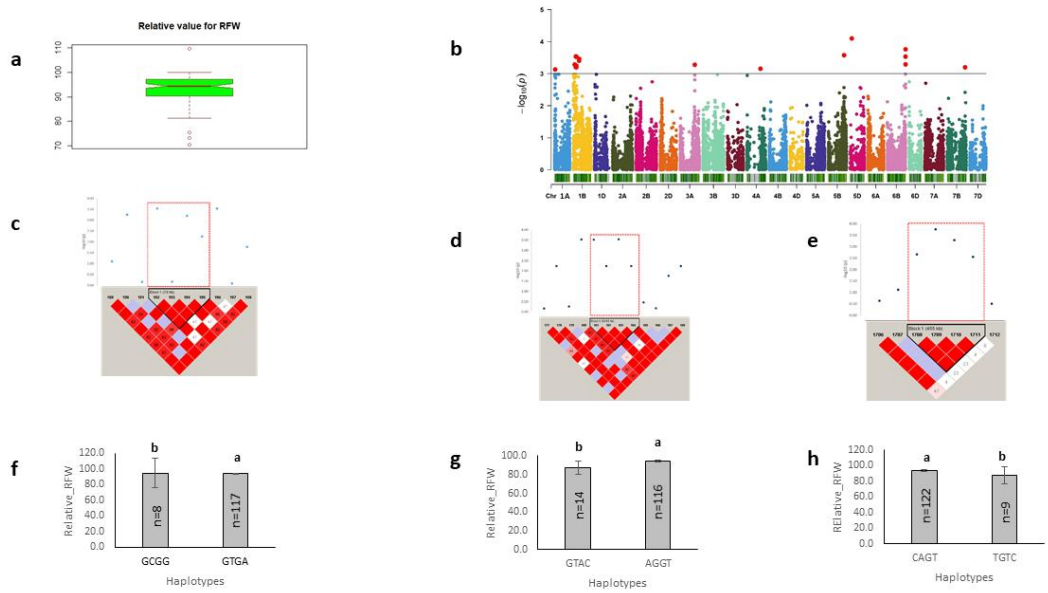

Figure 4.6. Marker-trait associations for R_RFW. (a) Box plot showing the distribution of R_RFW value; (b) Manhattan plot displaying the marker-trait associations; the horizontal red line indicates threshold level (*P* =0.001), the dots above this line indicate significant markers. (c-d) The linkage disequilibrium (LD) heat maps illuminating the peak region on chromosome 1B (Rel_RFW_1B_Hap1 and Rel_RFW_1B_Hap2). (e) The linkage disequilibrium (LD) heat map illuminating the peak region on chromosome 6B (Rel_RFW_6B_Hap1). In (c-e), pair-wise LD map between SNP markers is marked by D′ values, dark red represent 1, whereas white is for 0. The region surrounded by the red dotted line indicate LD block that contain significant SNPs. (f-h) Phenotypic comparison of the haplotype groups established for the significant SNPs as detected by LD block. Different letters indicate statistical difference at $P < 0.05$, n indicates number of genotypes represent each specific haplotype.

The significant marker AX-158607168 located on 1B chromosome was associated with a gene *TraesCS1B01G096200* (*peroxidase*) that was involved in oxidative stress responsive biological process (Supplementary Table 4. S3a). The significant marker AX-158570694 lying on 1A chromosome was associated with a mitogen-activated protein kinase gene which had MAP kinase activity (Supplementary Table 4. S3a). The major allele of haplotypes located on 1B and 6B chromosomes were linked with higher R_RFW (Figure 4. 6c-h). Those haplotypes were associated with the putative genes candidate mainly encoded F-box protein family, receptor-like protein kinase, and pentatricopeptide repeat-containing protein and their biological process included oxidation-reduction process and protein phosphorylation (Table 4. 4).

4.4.6. Shoot fresh weight

SFW was associated with total 18 markers on 1D, 3A, 5A, 5B, 6A, 6B and 6D chromosomes (Table 4.2a, 4.2b Figure 4. 7b, 4.8b). H_2O_2 induced phenotypic variation was represented by R_SFW and STI_SFW (Figure 4.7a, 4.8a). Among identified markers, 6 and 12 markers explained phenotypic variation ranged 7.98-10.43 and 9.64-13.78 for R_SFW and STI_SFW, respectively (Table 4. 2). Top most marker (*P*=1.01E-04), BS00076246_51 was identified for R_SFW, which was linked with the gene *TraesCS5A01G380800* that showed DNA binding function. Major alleles of single-markers showed significantly higher R_SFW. One haplotype was formed on 3A chromosome was linked with 26 protein-coding genes (Figure 4. 7 c, d). The significant markers were mostly associated with putative candidate genes code for DNA repair protein, disease resistance protein, cytochrome P450 family protein that showed biological process including DNA binding, ADP binding, oxidoreductase activity, acting on paired donors, with incorporation or reduction of molecular oxygen (Table 4. 4; Supplementary Table 4. S3a). Top most marker (*P*= 1.83E-04), AX-158535753 was identified for STI_SFW. This marker was linked with a putative candidate gene that encoded for cytochrome P450 family protein and involved in oxidation-reduction process (GO: 0055114). Single-marker analysis identified that 80% major alleles contributed significantly to higher STI_SFW. But the major allele of the haplotype was associated with significantly lower STI_SFW. Top markers were associated with bZIP transcription factor, F-box/LRR-repeat protein which were involved in oxidation-reduction process, transcription factor activity, sequence-specific DNA binding (Table 4. 4).

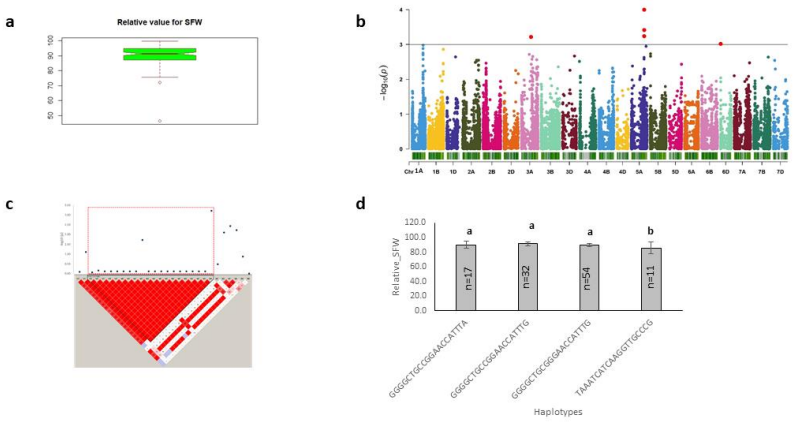

Table 4. 7. Marker-trait associations for R_SFW. (a) Box plot showing the distribution of R_SFW value; (b) Manhattan plot displaying the marker-trait associations; the horizontal red line indicates threshold level (*P* =0.001), the dots above this line indicate significant markers. (c) The linkage disequilibrium (LD) heat map illuminating the peak region on chromosome 3A (Rel_SFW_3A_Hap1). In (c), pair-wise LD map between SNP markers is marked by D′ values, dark red represent 1, whereas white is for 0. The region surrounded by the red dotted line indicate LD block that contain significant SNPs. (d) Phenotypic comparison of the haplotype groups established for the significant SNPs as detected by LD block. Different letters indicate statistical difference at $P < 0.05$, n indicates number of genotypes represent each specific haplotype.

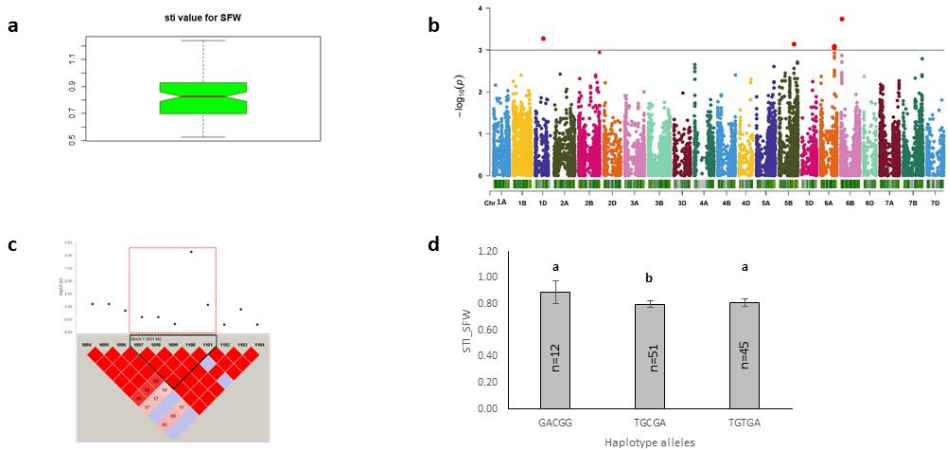

Table 4. 8. Marker-trait associations for STI_SFW. (a) Box plot showing the distribution of STI_SFW value; (b) Manhattan plot displaying the marker-trait associations; the horizontal red line indicates threshold level ($P = 0.001$), the dots above this line indicate significant markers. (c) The linkage disequilibrium (LD) heat map illuminating the peak region on chromosome 5B (sti_SFW_5B_Hap1). In (c), pair-wise LD map between SNP markers is marked by D′ values, dark red represent 1, whereas white is for 0. The region surrounded by the red dotted line indicate LD block that contain significant SNPs. (d) Phenotypic comparison of the haplotype groups established for the significant SNPs as detected by LD block. Different letters indicate statistical difference at $P < 0.05$, n indicates number of genotypes represent each specific haplotype.

4.4.7. Root shoot ratio

Like other traits described above, larger phenotypic variation was observed in RSRatio (Table 4.2 a, 4. 2b; Supplementary Figure 4. S1a, 4. S2a). MTA mapping identified total 45 markers that satisfied the threshold ($P \leq 0.001$). Top five markers were associated with the genes encode for protein phosphatase 2C, ethylene-responsive transcription factor, putative, disease resistance protein which were involved in molecular catalytic activity, DNA binding, and ADP binding functions. Similarly, for STI_RSRatio, more than 70% major alleles of single-markers contributed to high STI_RSRatio (Table 4. 2a, 4. 2b). Top markers were linked with NBS-LRR disease resistance protein, receptor-like protein kinase, aquaporin protein-coding genes. Those genes were involved in protein kinase, ADP binding and transport activity. Overall, GWAS analysed the H_2O_2 induced root-shoot growth variability and identified associated candidate loci and putative candidate genes. The identified genes were involved mostly in metabolic related pathways and functions.

4.4.8. Pleiotropy of candidate loci shared more than one trait

The pleiotropy of candidate loci was assessed to observe whether more than one traits shared common loci. We identified a sum of 11 SNPs that shared both STI and relative value, which were pleiotropic markers. We observed that these significant markers are linked with total 373 protein-coding genes (Table 4. 3). 6 SNPs out of 11, were located on 3B chromosome and coincided with 134 protein coding genes. Those SNPs encompassed both STI_SL and STI_RSRatio. A haplotype block, Com_Hap1 located on 4A chromosome was associated with 157 protein coding genes. This haplotype block was linked with both the traits R_RL and R_RSRatio. Similarly, the marker AX-158600273 and AX-158600281 located in 6A chromosome were identified as a pleotropic marker which was linked with 9 and 2 protein-coding genes for R_RL and STI_SFW, respectively (Table 4. 3).

Table 4. 3. Pleotropic markers located in different chromosomes and the corresponding traits

Marker	Haplotype	Chr	Position (bp)	Traits	No. of genes
AX-108852904	-	3B	822891332	STI_SL and STI_RSRatio	32
BS00071183_51			823762843		13
AX-158598301			826091387		12
BS00073411_51			829197896		19
AX-111015220			829203418		19
AX-158578652			829293411		37
BS00065603_51	-	3D	611497215	STI_SL and STI_RSRatio	40
BS00068415_51		3D	612903461	STI_SL and STI_RSRatio	31
AX-158582574	Com_Hap1	4B	456188724	R_RL and R_RSRatio	157
AX-158600273	-	6A	520581021	R_RL and STI_SFW	9
AX-158600281			520712811		2
AX-111016876		2A	717417914	STI_RL and STI_RSRatio	40
AX-108742509		2A	718354502		7

Abbreviations: R_RL, relative root length; R_RSRatio, relative root-shoot ratio; STI_RSRatio, stress tolerance index root-shoot ratio; STI_RL, stress tolerance index root-length; STI_SL, stress tolerance index shoot length; STI_SFW, stress tolerance index shoot fresh weigh

Table 4. 4. Short-list of putative candidate genes, their gene ontology molecular function and biological process linked with top five significant markers or marker- established haplotype block related to relative and STI of H_2O_2 mediated root-shoot traits

Trait	Marker/Haplotype block	Chr	Candidate gene	Short-Description	Biological Process	Molecular Function
R_RL	AX-109990240	3B	*TraesCS3B01G134400*	Zinc finger family protein	NA	nucleic acid binding (GO:0003676)
	wsnp_JD_c2623_3541255	3B	*TraesCS3B01G132100*	bZIP transcription factor, putative (DUF1664)	NA	NA
	AX-158600273	6A	*TraesCS6A01G287700*	Dof zinc finger protein	regulation of transcription (GO:0006355)	DNA binding (GO:0003677)
	wsnp_Ku_c8497_14429303	7B	*TraesCS7B01G061900*	Receptor-like kinase	protein phosphorylation (GO:0006468)	protein kinase activity (GO:0004672)
	AX-158600281	6A	*TraesCS6A01G288300*	2-oxoglutarate (2OG) and Fe(II)-dependent oxygenase superfamily protein	oxidation-reduction process (GO:0055114)	oxidoreductase activity (GO:0016491)
R_RL, R_RSRatio	Com_Hap1	4B	*TraesCS4B01G208800*	Pentatricopeptide repeat-containing protein	NA	protein binding (GO:0005515)
STI_RL	AX-158596313	2A	*TraesCS2A01G265500*	Disease resistance protein (TIR-NBS-LRR class) family	NA	nucleic acid binding (GO:0003676)
	AX-158581925	4A	*TraesCS4A01G051600*	Protein transport protein GOT1	vesicle-mediated transport (GO:0016192)	NA
	wsnp_JD_c52_87219	2B	*TraesCS2B01G448300*	Receptor-like kinase	protein phosphorylation (GO:0006468)	protein kinase activity (GO:0004672)
	sti_RL_2B_Hap1	2B	*TraesCS4B01G201600*	Receptor-like kinase, putative	protein phosphorylation (GO:0006468)	protein kinase activity (GO:0004672)

STI_RL, STI_RSRatio	AX-111016876	2A	*TraesCS2A01G477200*	NBS-LRR disease resistance protein	NA	ADP binding (GO:0043531)
R_SL	AX-109884177	5A	*TraesCS5A01G043000*	Heavy metal transport/detoxification superfamily protein, putative	metal ion transport (GO:0030001)	metal ion binding (GO:0046872)
	Rel_SL_1B_Hap1	1B	*TraesCS1B01G456400*	S-type anion channel	NA	transmembrane transport (GO:0055085)
STI_SL, STI_RSRatio	AX-111015220	3B	*TraesCS3B01G611100*	Receptor-like protein kinase	protein phosphorylation (GO:0006468)	protein kinase activity (GO:0004672)
STI_SL	BS00068415_51	3D	*TraesCS3D01G541600*	Disease resistance protein (NBS-LRR class) family	NA	ADP binding (GO:0043531)
	AX-158598301	3B	*TraesCS3B01G608500*	Aquaporin	transport (GO:0006810)	transporter activity (GO:0005215)
STI_SL, STI_RSRatio	BS00071183_51	3B	*TraesCS3B01G604800*	NBS-LRR-like resistance protein	NA	ADP binding (GO:0043531)
	BS00065603_51	3D	*TraesCS3D01G540900*	Aquaporin	transporter activity (GO:0005215)	transport (GO:0006810)
R_RSRatio	IAAV4343	3A	*TraesCS3A01G237800*	Protein phosphatase 2c, putative		catalytic activity (GO:0003824)
	AX-158523668	3A	*TraesCS3A01G238300*	Ethylene-responsive transcription factor, putative	regulation of transcription, DNA-templated (GO:0006355)	DNA binding (GO:0003677)
	AX-158548980	3D	*TraesCS3D01G421900*	Disease resistance protein RPM1	NA	ADP binding (GO:0043531)
STI_RSRatio, STI_SL	AX-158578652	3B	*TraesCS3B01G609400*	Cytochrome P450	oxidation-reduction process (GO:0055114)	oxidoreductase activity (GO:0016705)

STI_RSRatio	AX-158598301	3B	*TraesCS3B01G608500*	Aquaporin	transport (GO:0006810)	transporter activity (GO:0005215)
	AX-108742509	2A	*TraesCS2A01G480300*	Thioredoxin	cell redox homeostasis (GO:0045454)	NA
R_RFW	BS00065783_51	5D	*TraesCS5D01G071300*	FAD/NAD(P)-binding oxidoreductase family protein	oxidation-reduction process (GO:0055114)	oxidoreductase activity (GO:0016491)
	AX-158528874	6B	*TraesCS6B01G473100*	F-box protein family	NA	NA
	Tdurum_contig82473_67	5B	*TraesCS5B01G449200*	Receptor-like protein kinase	protein phosphorylation (GO:0006468)	ATP binding (GO:0005524)
	RAC875_c63067_283	1B	*TraesCS1B01G093500*	Pentatricopeptide repeat-containing protein	NA	protein binding (GO:0005515)
R_SFW	BS00074299_51	5A	*TraesCS5A01G380800*	DNA repair protein XRCC4	DNA recombination (GO:0006310)	DNA binding (GO:0003677)
	BS00076246_51	5A	*TraesCS5A01G380800*	DNA repair protein XRCC4	DNA recombination (GO:0006310)	DNA binding (GO:0003677)
	Tdurum_contig86202_175	5A	*TraesCS5A01G380700*	Disease resistance protein (NBS-LRR class) family		ADP binding (GO:0043531)
	AX-108742709	5A	*TraesCS5A01G381100*	Cytochrome P450 family protein, expressed	oxidation-reduction process (GO:0055114)	oxidoreductase activity (GO:0016705)
R_SFW	AX-89769139	5A	*TraesCS5A01G380700*	Disease resistance protein (NBS-LRR class) family	NA	ADP binding (GO:0043531)
	AX-158535753	6B	*TraesCS6B01G074100*	Cytochrome P450 family protein	oxidation-reduction process (GO:0055114)	oxidoreductase activity (GO:0016705)

STI_SFW	Excalibur_c54055_694	1D	*TraesCS1D01G219800*	bZIP transcription factor (DUF630 and DUF632)	NA	NA
	AX-158586104	5B	*TraesCS5B01G382000*	F-box/LRR-repeat protein 17	NA	protein binding (GO:0005515)
	wsnp_Ku_c4296_7807837	6A	*TraesCS6A01G288900*	BZIP transcription factor	transcription factor activity, (GO:0003700)	regulation of transcription (GO:0006355)

Abbreviations: R_RL, relative root length; R_RSRatio, relative root-shoot ratio; STI_RSRatio, stress tolerance index root-shoot ratio; STI_RL, stress tolerance index root-length; STI_SL, stress tolerance index shoot length; R_RFW, relative root fresh weight; R_SFW, relative shoot fresh weight; R_SL, relative shoot length; STI_SFW, stress tolerance index shoot fresh weight

4.5. Discussion

Due to having versatile role in crop both biotic and abiotic stresses, H_2O_2 is steadily gaining more attention in the field of crop biology research. Understanding H_2O_2 regulatory elements in wheat is of particular importance for researcher to reduce the damage derived from stress condition. Several studies focused the signalling role of H_2O_2 in crop plants (Niu and Liao, 2016; Nazir et al., 2020). As it is linked with complex signal transduction networks during stress adaptation, many genetic components are involved in the adaptive mechanisms. The present study identified regulatory components that are linked with tolerance mechanisms induced by H_2O_2 in wheat. A significant treatment effect was observed across the root-shoot traits (RL, SL, RSRatio, TL, SFW, SDW, RFW and RDW). The analysis of variance identified a large genetic variation among the cultivars of the studied panel both under control and H_2O_2 treatment (Table 4. 1). But, H_2O_2 treatment reduced the root-shoot considerably as compared to the control treatment showed wider variation among the cultivars which. Next, the relative value and STI, which represent the relative growth reduction showed a greater variation among the cultivars. These observation indicated that the studied panel has high genetic diversity which is desirable for genetic studies. Our results are supported by a previous study by Sadhukhan et al., (2017) that estimated the significant root length reduction in Arabidopsis induced by H_2O_2 treatment. Our findings were also in agreement with the previous report for elevated dose of H_2O_2 on root-shoot growth and plant dry mass in mustard (Khan et al., 2016).

Moreover, all traits showed moderate to high broad sense heritability in both control and H_2O_2 treatments, which indicated that the phenotypic variation among the traits is controlled by underlying genetic factors (Table 4. 1). The statistical observations including treatment effect and observed phenotypic variation and heritability status of the studied panel were also reported in other traits in previous studies (Voss-Fels et al., 2019; Koua et al., 2021; Siddiqui et al., 2021). In addition, genetic variability status further depicted through the assessment of cultivars under modern and traditional categories. A distinct phenotypic variation of R_SL, STI_SL, R_RSRatio, STI_RSRatio between those two categories was observed, and the underlying LD decay plot exhibited a contrast decay pattern across A, B, and D genomes (Table 4. 2a, 4.2b; Figure 4. 1e, f). These results also indicated that the phenotypic variation between traditional and modern cultivars are linked with the genetic factors. Our findings are supported by a previous report by Reinert et al., (2016), which revealed that phenotypic difference between two genetic sub-group was due underlying genetic distance.

GWAS analysis dissect complex traits and identify the candidate loci and genes which is useful for further genetic study and for functional analysis (Fleury et al., 2010). The present study employed the GWAS and identified the candidate loci linked with H_2O_2 through assessing the H_2O_2 induced STI and relative values. STI and relative values are important indices to assess relative performance of a cultivar under any stress (Sukumaran et al., 2018). Therefore, indices values incorporated in the present GWAS study facilitates to identify true causative loci linked with tolerance mechanism mediated by H_2O_2. We used mixed linear model (MLM) that included five principal components and kinship matrix, which reduce the false discovery rate. Thus, MLM promise a better marker trait association than GLM (Wen et al., 2018).

GWAS identified total 108 MTA that distributed across different chromosomes, those loci are linked with the tolerance mechanism mediated by exogenous H_2O_2 application. For RL, top marker located on 3B and 2A for R_RL and STI_RL, respectively. For SL, the MTA was identified on, 1B, 2D, 4B, 5A, and 7D chromosomes, and on 1A, 3B, 3D and 5B chromosomes including the top marker located on 5A and 3B for R_SL and STI_SL, respectively. Similarly, GWAS identified the MTA across 1A, 1B, 3A, 4A, 5B, 5D, 6B and 7B chromosomes and on 1D, 5B, 6A, and 6B chromosomes including top marker located on 5D and 5A for R_RFW and STI_SFW, respectively. Similarly, MTA for R_RSRatio identified and STI_RSRatio were distributed across different chromosomes. In general, highest number of MTA was identified on B genome and lowest on D genome which is supported by the previous study by Alipour et al., (2017). The identified genetic loci we are reporting here are first time in wheat. The molecular function and biological process of identified candidate genes are involved in ROS signalling pathways.

Azadi et al., (2015) identified yield related QTL on 3B chromosome in wheat under drought condition. We identified top most marker for R_RL on 3B chromosome and linked with a gene encodes for zinc finger family protein that possesses nucleic acid binding function. Jira-Anunkul and Pattanagul, (2021) observed that seed priming and foliar application with H_2O_2 improved the tolerance indices of tiller numbers, number of panicles, number of filled grains, filled grain weight, and grain yield under drought. Therefore, identified loci for hydrogen peroxide on 3B may have linkage with the grain yield related tolerance mechanisms under drought condition. The top most marker of STI_RL is located on 2A chromosome which contains a gene encodes for disease resistance protein. Sadhukhan et al., (2017) reported that a disease resistance protein coding gene N1P1 confers high expression in response to H_2O_2. MTA for R_SL identified the topmost marker on 5A and the linked gene encodes heavy metal

transport/detoxification protein. The top most marker for STI_SL and STI_RSRatio is associated with a receptor-like protein kinase. The gene is involved in protein phosphorylation, protein kinase activity. Plants adaptive mechanisms under stress condition initially begin with phosphorylation of stress related proteins. H_2O_2 causes the phosphorylation of upstream activated MAPK kinase kinase (MAPKKK), which then activate the downstream MAPK kinase. This MAPK cascades translate the signals into post-translational modifications, thus modulate the activity of target proteins (Kovtun et al., 2000). As receptor-like protein kinase involved in this phosphorylation process, our identified gene might have high possibility to be involved in protein phosphorylation process. GWAS identified top most MTA for R_RFW on 5D that harboured a gene which is involved in oxidation-reduction process and oxidoreductase activity. Cellular signalling events are mainly based on redox reactions; therefore, it is plausible that the linked gene of oxidoreductase family protein is directly linked to the cellular redox metabolism, which is corroborated by previous reports (Dietz, 2016; Sellés Vidal et al., 2018). Topmost marker for R_SFW coincided with the gene *TraesCS5A01G380800*, which is involved in DNA binding activities. A previous study identified the molecular function of H_2O_2 was associated with DNA binding activities through expression regulation of the DNA binding proteins (Li et al., 2019). One significant marker (AX-158570694) for R_RFW is linked with mitogen-activated protein kinase encoding gene *TraesCS1B01G104900* (Supplementary Table 4. S3a). The notable effect of H_2O_2 has been documented to induce the expression of TFs and genes responsible for osmolyte synthesis, and activate phosphorylation cascades using mitogen-activated protein kinases (MAPKs) during stress adaptation (Kovtun et al., 2000). During adaptation in drought and other stress, H_2O_2 activates the MAPK pathways. Therefore, the previous report support and suggested that mitogen activated protein kinase gene might be involved in H_2O_2 signalling pathways.

Few significant marker loci are linked with the genes that have DNA and ATP binding activities. Previous study identified that H_2O_2 is associated with expression regulation of the DNA binding proteins (Li et al., 2019). Another study found a positive relationship between H_2O_2 production and energy metabolism (Kibinza et al., 2006). Therefore, those evidence suggest that genes involved in DNA and ATP binding activities might be associated with H_2O_2 signalling. The significant marker BS00068415_51 was associated with both STI_SL and STI_RSRatio. This marker is linked with protein phosphatase family (Supplementary Table 4. S3b). Protein phosphatase family are largely involved in ROS signalling. Adaptive role of protein phosphatase has been investigated under salt stress (Xing et al., 2021). Overall the molecular functions of identified genes included metal ion binding and transmembrane

transport, are involved biologically in stress related pathways including oxidation-reduction process, protein phosphorylation and ADP binding. H_2O_2 can modulate the activities of many components in signalling, such as protein phosphatases, protein kinases and transcription factors

We also observed that major alleles of the haplotype and single markers are linked with higher STI_RL, STI_SL, R_SL, R_SFW, R_RFW, STI_SFW, STI_RSRatio, respectively. Whereas, the minor alleles of single-markers and haplotypes are linked with the higher value of R_RL and R_RSRatio. The alleles linked with high relative value and STI are representing the tolerance mechanism for the root-shoot traits towards the toxic dose of H_2O_2 (Sadhukhan et al., 2017).

4.6. Conclusions

Understanding the H_2O_2 regulatory elements are important to know in depth the players of H_2O_2 signalling under diverse stress condition in plants, although it has not been fully clear yet. The present study revealed a larger genetic diversity induced by toxic dose of H_2O_2, which identified the candidate loci and genes for root-shoot trait by using GWAS. The identified genetic factors for root-shoot traits were distributed in different chromosomes and were linked with the tolerance mechanisms mediated by exogenous H_2O_2 treatment. The study also revealed that, major alleles of significant markers are linked with higher relative and STI for seven traits (except for R_RL and R_RSRatio). Therefore, identified contrasting alleles and putative genes can be incorporated in physiological studies to understand adaptive mechanisms mediated by H_2O_2 in crop.

4.7. References

Alaux M, Rogers J, Letellier T, Flores R, Alfama F, Pommier C, Mohellibi N, Durand S, Kimmel E, Michotey C, et al (2018) Linking the International Wheat Genome Sequencing Consortium bread wheat reference genome sequence to wheat genetic and phenomic data. Genome Biol 19: 111

Alipour H, Bihamta MR, Mohammadi V, Peyghambari SA, Bai G, Zhang G (2017) Genotyping-by-sequencing (GBS) revealed molecular genetic diversity of Iranian wheat landraces and cultivars. Front Plant Sci 8: 1293

Anjum NA, Sharma P, Gill SS, Hasanuzzaman M, Khan EA, Kachhap K, Mohamed AA, Thangavel P, Devmanjuri Devi G, Vasudhevan P, et al (2016) Catalase and ascorbate

peroxidase-representative H 2 O 2-detoxifying heme enzymes in plants. India Env Sci Pollut Res 125: 19002–19029

Azadi A, Mardi M, Hervan EM, Mohammadi SA, Moradi F, Tabatabaee MT, Pirseyedi SM, Ebrahimi M, Fayaz F, Kazemi M, et al (2015) QTL mapping of yield and yield components under normal and salt-stress conditions in bread wheat (triticum aestivum L.). Plant Mol Biol Report 33: 102–120

Barrett JC, Fry B, Maller J, Daly MJ (2005) Haploview: analysis and visualization of LD and haplotype maps. Bioinformatics 21: 263–265

Begum H, Alam MS, Feng Y, Koua P, Ashrafuzzaman M, Shrestha A, Kamruzzaman M, Dadshani S, Ballvora A, Naz AA, et al (2020) Genetic dissection of bread wheat diversity and identification of adaptive loci in response to elevated tropospheric ozone. Plant Cell Environ 43: 2650–2665

Borisova MM, Kozuleva MA, Rudenko NN, Naydov IA, Klenina IB, Ivanov BN (2012) Photosynthetic electron flow to oxygen and diffusion of hydrogen peroxide through the chloroplast envelope via aquaporins. Biochim Biophys Acta - Bioenerg 1817: 1314–1321

Bradbury PJ, Zhang Z, Kroon DE, Casstevens TM, Ramdoss Y, Buckler ES (2007) TASSEL: software for association mapping of complex traits in diverse samples. Bioinformatics 23: 2633–2635

Branham SE, Wright SJ, Reba A, Morrison GD, Randal Linder C (2016) Genome-Wide Association Study in Arabidopsis thaliana of Natural Variation in Seed Oil Melting Point: A Widespread Adaptive Trait in Plants. J Hered 107: 257–265

Brychkova G, Yarmolinsky D, Fluhr R, Sagi M (2012) The determination of sulfite levels and its oxidation in plant leaves. Plant Sci 190: 123–130

Chang Q, Tang H (2014) Optical determination of glucose and hydrogen peroxide using a nanocomposite prepared from glucose oxidase and magnetite nanoparticles immobilized on graphene oxide. Microchim Acta 181: 527–534

Cheng H, Zhang Q, Guo D (2013) Genes that Respond to H 2 O 2 Are Also Evoked Under Light in Arabidopsis. Mol Plant 6: 226–228

Daba SD, Tyagi P, Brown-Guedira G, Mohammadi M (2018) Genome-wide association

studies to identify loci and candidate genes controlling kernel weight and length in a historical United States wheat population. Front Plant Sci 9: 1045

Dadshani S, Mathew B, Ballvora A, Mason AS, Léon J (2021) Detection of breeding signatures in wheat using a linkage disequilibrium-corrected mapping approach. Sci Reports 2021 111 11: 1–12

Deng X-P, Cheng Y-J, Wu X-B, Kwak S-S, Chen W, Eneji AE (2012) Exogenous hydrogen peroxide positively influences root growth and exogenous hydrogen peroxide positively influences root growth and metabolism in leaves of sweet potato seedlings. AJCS 6: 1572–1578

Desikan R, Neill SJ, Hancock JT (2000) Hydrogen peroxide–induced gene expression in Arabidopsis thaliana. Free Radic Biol Med 28: 773–778

Dietz KJ (2016) Thiol-Based Peroxidases and Ascorbate Peroxidases: Why Plants Rely on Multiple Peroxidase Systems in the Photosynthesizing Chloroplast? Moleucles and Cells 39: 20–25

Fernandez GCJ (1992) Effective selection criteria for assessing plant stress tolerance. Adapt food Crop to Temp water Stress. doi: 10.22001/WVC.72511

Fleury D, Jefferies S, Kuchel H, Langridge P (2010) Genetic and genomic tools to improve drought tolerance in wheat. J Exp Bot 61: 3211–3222

Francoz E, Ranocha P, Nguyen-Kim H, Jamet E, Burlat V, Dunand C (2015) Roles of cell wall peroxidases in plant development. Phytochemistry 112: 15–21

Gabriel SB, Schaffner SF, Nguyen H, Moore JM, Roy J, Blumenstiel B, Higgins J, DeFelice M, Lochner A, Faggart M, et al (2002) The structure of haplotype blocks in the human genome. Science (80-) 296: 2225–2229

Gadjev I, Vanderauwera S, Gechev TS, Laloi C, Minkov IN, Shulaev V, Apel K, Inzé D, Mittler R, Van Breusegem F (2006) Transcriptomic Footprints Disclose Specificity of Reactive Oxygen Species Signaling in Arabidopsis. Plant Physiol 141: 436–445

Gao L, Turner MK, Chao S, Kolmer J, Anderson JA (2016) Genome Wide Association Study of Seedling and Adult Plant Leaf Rust Resistance in Elite Spring Wheat Breeding Lines. PLoS One. doi: 10.1371/JOURNAL.PONE.0148671

Horton MW, Hancock AM, Huang YS, Toomajian C, Atwell S, Auton A, Muliyati NW, Platt

A, Sperone FG, Vilhjálmsson BJ, et al (2012) Genome-wide patterns of genetic variation in worldwide Arabidopsis thaliana accessions from the RegMap panel. Nat Genet 2012 442 44: 212–216

Jira-Anunkul W, Pattanagul W (2021) Effects of hydrogen peroxide application on agronomic traits of rice (Oryza sativa L.) under drought stress. Plant, Soil Environ 67 (2021): 221–229

Jubany-Marí T, Munné-Bosch S, López-Carbonell M, Alegre L (2009) Hydrogen peroxide is involved in the acclimation of the Mediterranean shrub, Cistus albidus L., to summer drought. J Exp Bot 60: 107–120

Julkowska MM, Klei K, Fokkens L, Haring MA, Schranz ME, Testerink C (2016) Natural variation in rosette size under salt stress conditions corresponds to developmental differences between Arabidopsis accessions and allelic variation in the LRR-KISS gene. J Exp Bot 67: 2127–2138

Kadam NN, Tamilselvan A, Lawas LMF, Quinones C, Bahuguna RN, Thomson MJ, Dingkuhn M, Raveendran M, Struik PC, Yin X, et al (2017) Genetic Control of Plasticity in Root Morphology and Anatomy of Rice in Response to Water Deficit. Plant Physiol 174: 2302–2315

Khan MIR, Khan NA, Masood A, Per TS, Asgher M (2016) Hydrogen peroxide alleviates nickel-inhibited photosynthetic responses through increase in use-efficiency of nitrogen and sulfur, and glutathione production in mustard. Front Plant Sci 7: 44

Kibinza S, Vinel D, Côme D, Bailly C, Corbineau F (2006) Sunflower seed deterioration as related to moisture content during ageing, energy metabolism and active oxygen species scavenging. Physiol Plant 128: 496–506

Koua AP, Oyiga BC, Baig MM, Léon J, Ballvora A (2021) Breeding driven enrichment of genetic variation for key yield components and grain starch content under drought stress in winter wheat. Front Plant Sci https://www.frontiersin.org/article/10.3389/fpls.2

Kovtun Y, Chiu WL, Tena G, Sheen J (2000) Functional analysis of oxidative stress-activated mitogen-activated protein kinase cascade in plants. Proc Natl Acad Sci U S A 97: 2940–2945

Larsson SJ, Lipka AE, Buckler ES (2013) Lessons from Dwarf8 on the Strengths and Weaknesses of Structured Association Mapping. PLOS Genet 9: e1003246

Li T, Li H, Zhang YX, Liu JY (2011) Identification and analysis of seven H2O2-responsive miRNAs and 32 new miRNAs in the seedlings of rice (Oryza sativa L. ssp. indica). Nucleic Acids Res 39: 2821–2833

Li X, Qiu S, Shi J, Wang S, Wang M, Xu Y, Nie Z, Liu C, Liu C (2019) A new function of copper zinc superoxide dismutase: as a regulatory DNA-binding protein in gene expression in response to intracellular hydrogen peroxide. Nucleic Acids Res 47: 5074–5085

Liao WB, Huang GB, Yu JH, Zhang ML (2012) Nitric oxide and hydrogen peroxide alleviate drought stress in marigold explants and promote its adventitious root development. Plant Physiol Biochem 58: 6–15

Liheng H, Zhiqiang G, Runzhi L (2009) Pretreatment of seed with H2O2 enhances drought tolerance of wheat (Triticum aestivum L.) seedlings. African J Biotechnol 8: 6151–6157

Liu J, He B, Chen Q, Li J, Xiong Q, Yue G, Zhang X, Yang S, Liu H, Liu QH (2016) Direct synthesis of hydrogen peroxide from plasma-water interactions. Sci Reports 2016 61 6: 1–7

Liu J, Macarisin D, Wisniewski M, Sui Y, Droby S, Norelli J, Hershkovitz V (2013) Production of hydrogen peroxide and expression of ROS-generating genes in peach flower petals in response to host and non-host fungal pathogens. Plant Pathol 62: 820–828

Miller G, Schlauch K, Tam R, Cortes D, Torres MA, Shulaev V, Dangl JL, Mittler R (2009) The plant NADPH oxidase RBOHD mediates rapid systemic signaling in response to diverse stimuli. Sci Signal. doi: 10.1126/SCISIGNAL.2000448/SUPPL_FILE/2_RA45_SM.PDF

Money D, Gardner K, Migicovsky Z, Schwaninger H, Zhong GY, Myles S (2015) LinkImpute: Fast and accurate genotype imputation for nonmodel organisms. G3 Genes, Genomes, Genet 5: 2383–2390

Nazir F, Fariduddin Q, Khan TA (2020) Hydrogen peroxide as a signalling molecule in plants and its crosstalk with other plant growth regulators under heavy metal stress. Chemosphere 252: 126486

Neill S, Desikan R, Hancock J (2002) Hydrogen peroxide signalling. Curr Opin Plant Biol 5: 388–395

Neto ADDA, Prisco JT, Enéas-Filho J, Rolim Medeiros JV, Gomes-Filho E (2005) Hydrogen peroxide pre-treatment induces salt-stress acclimation in maize plants. J Plant Physiol 162: 1114–1122

Niu L, Liao W (2016) Hydrogen peroxide signaling in plant development and abiotic responses: Crosstalk with nitric oxide and calcium. Front Plant Sci 7: 230

Petrov VD, Breusegem F Van (2012) Hydrogen peroxide—a central hub for information flow in plant cells. AoB Plants 2012: 14

Pongprayoon W, Roytrakul S, Pichayangkura R, Chadchawan S (2013) The role of hydrogen peroxide in chitosan-induced resistance to osmotic stress in rice (Oryza sativa L.). Plant Growth Regul 70: 159–173

Rao M V., Davis KR (1999) Ozone-induced cell death occurs via two distinct mechanisms in Arabidopsis: the role of salicylic acid. Plant J 17: 603–614

Van Der Reest J, Lilla S, Zheng L, Zanivan S, Gottlieb E (2018) Proteome-wide analysis of cysteine oxidation reveals metabolic sensitivity to redox stress. Nat Commun 2018 91 9: 1–16

Reinert S, Kortz A, Léon J, Naz AA (2016) Genome-wide association mapping in the global diversity set reveals new QTL controlling root system and related shooGenome-wide association mapping in the global diversity set reveals new QTL controlling root system and related shoot variation in barleyt . Front Plant Sci 7: 1061

Richards SL, Laohavisit A, Mortimer JC, Shabala L, Swarbreck SM, Shabala S, Davies JM (2014) Annexin 1 regulates the H2O2-induced calcium signature in Arabidopsis thaliana roots. Plant J 77: 136–145

Rizhsky L, Davletova S, Liang H, Mittler R (2004) The Zinc Finger Protein Zat12 is required for cytosolic ascorbate peroxidase 1 expression during oxidative stress in Arabidopsis. J Biol Chem 279: 11736–11743

Sadhukhan A, Kobayashi Y, Nakano Y, Iuchi S, Kobayashi M, Sahoo L, Koyama H (2017) Genome-wide Association Study Reveals that the Aquaporin NIP1;1 Contributes to Variation in Hydrogen Peroxide Sensitivity in Arabidopsis thaliana. Mol Plant 10: 1082–1094

Sellés Vidal L, Kelly CL, Mordaka PM, Heap JT (2018) Review of NAD(P)H-dependent

oxidoreductases: Properties, engineering and application. Biochim Biophys Acta - Proteins Proteomics 1866: 327–347

Siddiqui MN, Teferi TJ, Ambaw AM, Gabi MT, Koua P, Léon J, Ballvora A (2021) New drought-adaptive loci underlying candidate genes on wheat chromosome 4B with improved photosynthesis and yield responses. Physiol Plant. doi: 10.1111/PPL.13566

Sukumaran S, Reynolds MP, Sansaloni C (2018) Genome-Wide Association Analyses Identify QTL Hotspots for Yield and Component Traits in Durum Wheat Grown under Yield Potential, Drought, and Heat Stress Environments. Front Plant Sci 0: 81

Suzuki N, Mittler R (2006) Reactive oxygen species and temperature stresses: A delicate balance between signaling and destruction. Physiol Plant 126: 45–51

Tadesse W, Ogbonnaya FC, Jighly A, Sanchez-Garcia M, Sohail Q, Rajaram S, Baum M (2015) Genome-wide association mapping of yield and grain quality traits in winter wheat genotypes. PLoS One. doi: 10.1371/journal.pone.0141339

Uchida A, Jagendorf AT, Hibino T, Takabe T, Takabe T (2002) Effects of hydrogen peroxide and nitric oxide on both salt and heat stress tolerance in rice. Plant Sci 163: 515–523

Vanderauwera S, Zimmermann P, Rombauts S, Vandenabeele S, Langebartels C, Gruissem W, Inzé D, Van Breusegem F (2005) Genome-Wide Analysis of Hydrogen Peroxide-Regulated Gene Expression in Arabidopsis Reveals a High Light-Induced Transcriptional Cluster Involved in Anthocyanin Biosynthesis. Plant Physiol 139: 806–821

Voothuluru P, Mäkelä P, Zhu J, Yamaguchi M, Cho IJ, Oliver MJ, Simmonds J, Sharp RE (2020) Apoplastic Hydrogen Peroxide in the Growth Zone of the Maize Primary Root. Increased Levels Differentially Modulate Root Elongation Under Well-Watered and Water-Stressed Conditions. Front Plant Sci 11: 392

Voss-Fels KP, Stahl A, Wittkop B, Lichthardt C, Nagler S, Rose T, Chen T-W, Zetzsche H, Seddig S, Majid Baig M, et al (2019) Breeding improves wheat productivity under contrasting agrochemical input levels. Nat Plants 2019 57 5: 706–714

Wahid A, Sehar S, Perveen M, Gelani S, Basra SMA, Farooq M (2008) Seed pretreatment with hydrogen peroxide improves heat tolerance in maize at germination and seedling growth stages. Seed Sci Technol 36: 633–645

Waszczak C, Akter S, Jacques S, Huang J, Messens J, Van Breusegem F (2015) Oxidative post-translational modifications of cysteine residues in plant signal transduction. J Exp Bot 66: 2923–2934

Wen YJ, Zhang H, Ni YL, Huang B, Zhang J, Feng JY, Wang SB, Dunwell JM, Zhang YM, Wu R (2018) Methodological implementation of mixed linear models in multi-locus genome-wide association studies. Brief Bioinform 19: 700–712

Wu A, Allu AD, Garapati P, Siddiqui H, Dortay H, Zanor MI, Asensi-Fabado MA, Munná-Bosch S, Antonio C, Tohge T, et al (2012) JUNGBRUNNEN1, a reactive oxygen species–responsive NAC transcription factor, regulates longevity in Arabidopsis. Plant Cell 24: 482–506

Wurzinger B, Mair A, Pfister B, Teige M (2011) Cross-talk of calcium-dependent protein kinase and MAP kinase signaling. https://doi.org/104161/psb6114012. doi: 10.4161/PSB.6.1.14012

Xing B, Gu C, Zhang T, Zhang Q, Yu Q, Jiang J, Liu G (2021) Functional Study of BpPP2C1 Revealed Its Role in Salt Stress in Betula platyphylla. Front Plant Sci 11: 2215

Yang H, Mu J, Chen L, Feng J, Hu J, Li L, Zhou JM, Zuo J (2015) S-Nitrosylation Positively Regulates Ascorbate Peroxidase Activity during Plant Stress Responses. Plant Physiol 167: 1604–1615

Zhang M, Zhang S (2022) Mitogen-activated protein kinase cascades in plant signaling. J Integr Plant Biol 64: 301–341

Zhang Z, Ersoz E, Lai CQ, Todhunter RJ, Tiwari HK, Gore MA, Bradbury PJ, Yu J, Arnett DK, Ordovas JM, et al (2010) Mixed linear model approach adapted for genome-wide association studies. Nat Genet. doi: 10.1038/ng.546

Zhou J, Wang J, Shi K, Xia XJ, Zhou YH, Yu JQ (2012) Hydrogen peroxide is involved in the cold acclimation-induced chilling tolerance of tomato plants. Plant Physiol Biochem 60: 141–149

Chapter 5. General discussion

Due to global food demand wheat is currently ranked second after maize and the leading crop in terms of consumption by humans (FAO, 2019). Drought has been documented for crop yield reduction severely. Here, we were interested to know the genetic components for drought-induced proline (Pro) and H_2O_2 accumulation, as they are linked with different adaptive mechanisms under drought and other stress conditions. Genome-wide association studies (GWAS) identified the genetic components that are associated with Pro and H_2O_2 accumulation variation and H_2O_2-induced root-shoot growth variation. However, the key discussions are illustrated in the sub-headings below.

5.1. Diversity panel exhibits augmented phenotypic variation for Pro and H_2O_2 induced by drought and for root-shoot traits induced by H_2O_2

The presence of genetic diversity in a population promises a better adaptation to diverse environments through developing climate-resilient crop varieties (Lukaszewski et al., 2014). This diversity is derived from natural selection and plant evolution (Reinert et al., 2016). Our study found clear plant-to-plant Pro and H_2O_2 content differences under both control and drought treatments, but the variation was wider under the drought stress condition. The effect of genotype and environment interaction was significant, which indicates drought treatment influenced to accumulation of more Pro and H_2O_2. Similarly, the analysis of variance for root-shoot traits (root length, shoot length, root-shoot ratio, total seedling length, shoot fresh weight, shoot dry weight, root fresh weight, and root dry weight) induced by H_2O_2 treatment showed a large phenotypic variation among the cultivars. Treatment H_2O_2 reduced the root-shoot growth considerably as compared to the control treatment which is supported by previous studies (Sadhukhan et al., 2017; Khan et al., 2016). Next, the relative value and stress tolerance index (STI), which represent the relative growth reduction also showed large variation among the cultivars. These observations indicated that our panel is rich in high genetic diversity. High genetic diversity is the product of high heritability. In plant breeding research, heritability possesses an important criterion for selecting traits, the higher heritability across different environments is the prime lead for breeding. We found root-shoot attributes showed moderate to high broad-sense heritability in both control and H_2O_2 treatments in this study. Similarly, a high broad-sense heritability was observed for Pro H_2O_2 under drought treatment. The statistical analyses such as effect of the treatment, phenotypic variation and heritability status of this study are corroborated

by a previous genetic study with drought induced Pro accumulation in sunflower (Khalil et al., 2016). A continuous phenotypic variation was observed for Pro and H_2O_2 content as well as for root-shoot traits in present study induced by H_2O_2, which is indicating polygenic inheritance of the traits. According to Valliyodan et al. (2017), the natural variation among the drought-related traits helps to identify the best resources for genetic studies, their findings suggest the larger genetic diversity of our studied population suitable for genetic as well as genome-wide association studies (GWAS).

Distinct genetic sub-group is a rich source of plant breeding programs to develop climate-resilient crop varieties (Hao et al., 2011). Here we found that the European sub-group showed significantly higher Pro content than the Non-European sub-group under the glasshouse environment. We also observed that Pro accumulation followed a significant difference under-field environment when assessed and compared between modern and traditional sub-groups. The modern sub-group was noticed to accumulate lower Pro than that of the traditional sub-group. Even, the variation of Pro accumulation was wider in the traditional sub-group. In the case of the STI of H_2O_2, the European sub-group exhibited significantly higher STI than Non-European. Next, the LD decay analysis found the genetic distinctness between Europe and Non-European originated sub-groups. Distinct phenotypic variation was also observed in H_2O_2 induced root traits (R_SL, STI_SL, R_RSRatio, STI_RSRatio) for modern and traditional sub-groups and the underlying LD decay plot exhibited a contrast decay pattern across A, B, and D genomes. Our findings are also supported by a previous study by Reinert et al. (2016). They observed the distinct LD decay among the sub-population of barley. Overall, our findings indicates the European as well as the traditional sub-groups are more responsive to drought than the Non-European and traditional sub-groups. The findings will help to understand insight into the genetic factors of those genetic-sub groups underlying Pro and H_2O_2 variation under drought stress.

5.2. GWAS identifies candidate loci and underlying genes in different chromosomes for drought-induced Pro and H_2O_2, and H_2O_2-induced root-shoot traits

GWAS identifies key genetic components controlling a trait of interest and facilitates the understanding role of those components (Visscher et al., 2012). This approach has been successfully implemented in wheat to identify several traits (Verslues et al., 2014; Ueda et al., 2015; Siddiqui et al., 2021; Ahmed et al., 2022). We used the GWAS approach for identifying key

genetic factors of Pro and H_2O_2. The GWAS employed the mixed linear model (MLM) including three to five principal components and a kinship matrix, which reduced the probability of false positives result (Begum et al., 2020). MLM is a better-fitted model than the general linear model and is suitable for metabolites (Ueda et al., 2015). The present study used relative value and STI. STI and relative values are important indices to assess the relative performance of a cultivar under any stress (Sukumaran et al., 2018). Therefore, incorporating indices values in the GWAS study facilitated the identification of true causative loci linked with drought-induced Pro and H_2O_2 and the loci linked with tolerance mechanism mediated by H_2O_2. After considering the threshold level [$-\log_{10}(p) = 3.0$], GWAS identified significant marker-trait association (MTA) for relative Pro values (RPVs) under glasshouse environment, for Pro and H_2O_2 content under drought, and corresponding STI under field environment. MTA was also identified for relative value and STI for root-shoot traits induced by H_2O_2. For the RPVs, the MTA exhibited a consistent significant signal on 1A and 1B regions that harbored a total of 11 SNPs. Under field environment, GWAS identified the top significant MTA for Pro on chromosomes 1A and 5B, and H_2O_2 on 2A, and 1B in response to drought and STI, respectively. Among 143 identified significant MTAs, 36 and 2 were linked with drought and 71 and 34 for STI of Pro and H_2O_2, respectively. For H_2O_2-induced root-shoot traits, MTA was identified on 3B, 2A, 5A, 3B, 5D, 5A, and 6B chromosomes for R_RL, STI_RL, R_SL, STI_SL, R_RFW, R_SFW, STI_SFW, respectively. Overall, the highest number of MTA was observed in the B genome followed by the A, whereas, the D genome harbored the lowest MTA. This result is in agreement with the findings of Alipour et al. (2017). Our result is also supported by a recent study with a genotyping set of 369 Iranian wheat accessions using 16,506 SNPs identified the highest number of SNPs in the B genome, while the lowest number of SNPs were located in D. The lowest number in the D genome is because of the lower frequency of recombination rates (Eltaher et al. 2018).

The candidate genes identified in the present study were mostly involved in metal ion binding, transmembrane transport, oxidation-reduction process, protein phosphorylation, and DNA and ADP binding processes. It has been suggested that the natural variation of a trait in a species might be controlled by genes of the same families in other species (Huang and Salt, 2016). The two top most significant markers for Pro content under drought condition in the field environment coincides with Ras-like protein. Ras protein is a low-molecular-weight GDP/GTP-binding guanine triphosphatase encoded by the Ras gene, which plays a pivotal role in signal transduction of cell

growth, differentiation, and maturation (McCormick, 1995). The haplotypes for Pro accumulation under drought condition and STI are associated with transmembrane protein (TP)- coding genes. TP is especially located in the mitochondrial membrane and is involved in Pro transport. Information regarding the transport protein of Pro is insufficient and needs more study to identify new members. However, few transmembrane proteins have been reported in different species (Wang et al., 2015; Grallath et al., 2005; Fujiwara et al., 2010). Another significant SNP for drought Pro under field environment, BS00009970_51 is associated with calmodulin_binding domain-containing protein. Calmodulin is a ubiquitous calcium-binding protein that can regulate diverse cellular functions by modulating the activity of various enzymes and proteins. A piece of evidence for this was recorded for the gene GmCaM4 in *Arabidopsis*. The overexpression of this gene up-regulated the transcription rate of the Pro-synthesizing P5CS1 enzyme, which conferred salt tolerance by facilitating Pro accumulation (Hyuk Yoo et al., 2004).

We observed few haplotypes and single-markers for STI and RPVs of Pro are associated with F-box protein-coding genes. A large number of F-box protein genes have been identified but the biological functions of only a few genes are available so far and functional roles are largely obscure and unknown (Malik et al., 2020). In plants, the prevalence of a huge number of F-box protein gene members and their involvement in controlling diverse growth and developmental processes make them potential targets for crop improvement. A previous report identified that F-box gene FOA1 carries the Pro-related transcription factors ABF3 and ABRE elements in the promoter region (Peng et al., 2012). F-Box gene has also been reported associated with Pro content in wheat (Li et al., 2018). Genes of the same family have similar functions. This evidence revealed that F-box protein is involved in stresses including drought, and salt in plants, therefore, there might have a possibility of our identified F-box genes are involved in Pro metabolism.

Both STI of Pro and H_2O_2 is associated with cytochrome P450 proteins. The P450s produce H_2O_2 during the reaction cycle, a process known as uncoupling, thus releasing reactive oxygen species. The P450 enzymes are believed to have evolved due to evolutionary adaptations as a result of metabolic and environmental changes in plants. Several other cytochrome P450 families in various plant species play an important role in enhancing drought and salt tolerance (Yan et al., 2016; Tamiru et al., 2015).

Few genes identified in our loci region encode for zinc finger proteins (ZFPs). ZFPs are a large protein family and are mainly involved in abiotic stress tolerance. Previous studies identified their involvement in salt and drought tolerance, Pro biosynthesis, stress responses, and ROS scavenging mechanisms (Luo et al., 2012; Wang et al., 2016). Several genes in our candidate loci regions encode for pentatricopeptide repeat protein. The crucial role of pentatricopeptide repeat proteins has been reported as a positive regulator of plant responses to abiotic stresses and displays a tolerance to drought and salt mediated by the higher level of Pro (Jiang et al., 2015). A previous GWAS identified pentatricopeptide repeat proteins coding genes, which were linked with Pro metabolism in *Arabidopsis* (Verslues et al., 2014). These genes might have a correlation with Pro metabolism in wheat, which is corroborated by Verslues et al.(2014).

Significant locus AX-158596005, responsible for the STI value of H_2O_2, is linked with superoxide dismutase protein. Superoxide dismutase is a ubiquitous antioxidant enzyme that catalytically converts the superoxide radical to hydrogen peroxide (H_2O_2). Its function is reported to be associated with both biotic and abiotic stress including drought, suggesting their association with stress response (Tyagi et al., 2017). Few significant SNPs for STI H_2O_2 are associated with disease resistance proteins. Disease resistance protein has an adaptive role for the plant that is involved in response to stress. A previous study identified that N1P1, a disease resistance coding gene is involved in hydrogen peroxide signaling (Sadhukhan et al., 2017). The topmost significant locus for STI of H_2O_2 is linked with the E3 ubiquitin-protein ligase ORTHRUS 2. The protein of this gene is involved in the protein ubiquitination pathway, which is part of protein modification. A previous report revealed that H_2O_2 causes protein modification, thereby, changing the protein function (Pradhan et al., 2020). Taken together, the present GWAS has successfully screened the natural diversity of wheat to identify novel variants for drought-induced Pro and H_2O_2 and for H_2O_2-induced root-shoot attributes that appear beneficial for improving better adaptation to drought and other stresses. The identified loci regions across different chromosomes and the putative candidate genes for drought-induced Pro and H_2O_2 accumulation and H_2O_2 mediated for root-shoot attributes in wheat will help further genetic and functional studies.

5.3. GWAS uncovers high and low Pro and H_2O_2 associated alleles which could be utilized in crop improvement

Contrasting alleles of traits are an important source of plant breeding programs (Herzig et al., 2018). We identified contrasting alleles of single-markers and haplotypes for RPV under glasshouse condition and STI of Pro and H_2O_2 content under field environment, all of which represents the relative performance of each cultivar in response to drought. Minor alleles containing cultivars are linked with higher Pro and H_2O_2 content under drought as compared to the major allele containing cultivars. The contrasting alleles of topmost significant-markers for RPV's showed that the 'C' allele is contributing to significantly higher RP content than the 'T' allele. Under field environment, the 'C' allele of the topmost significant marker for Pro content is contributing to low STI, whereas the 'T' allele is showing high STI. The cultivar 'Akteur' showed the lowest STI and the 'Centurk' is the highest. Similarly, the topmost significant marker for STI H_2O_2 is linked with a haplotype, the major allele (GTA) which is linked with low STI, and the minor allele (ACG) with high STI. The cultivar 'Urban' has the lowest STI whereas the cultivar 'Mironovs' has the highest. Our results are corroborated by a previous study (Siddiqui et al., 2021), which revealed the contrasting haplotype for photosynthetic activity and grain yield under stress. The cultivars possessing the contrasting alleles for Pro can be further utilized in Pro-mediated genetic improvement of a cultivar in response to drought. In case of H_2O_2 induced root-shoot growth, the major alleles of the haplotypes and single markers are linked with higher STI_RL, STI_SL, R_SL, R_SFW, R_RFW, STI_SFW, STI_RSRatio, respectively. In contrast, the minor alleles are linked with the higher value of R_RL and R_RSRatio. The alleles linked with high relative value and STI might be associated with the tolerance mechanism for the root-shoot traits towards the toxic dose of H_2O_2. These alleles can be incorporated into physiological studies to understand adaptive mechanisms mediated by H_2O_2 in crop plants.

5.4. Comparison of Pro and H_2O_2 associated genomic regions between wheat and *Arabidopsis* reveals the identified loci and genes are new potential candidate for wheat

In the present study, drought was imposed on wheat in both glasshouse and natural field environment. The drought stress was more realistic than other mimic form of drought such as polyethylene glycol-induced drought. Genetic dissection for Pro has been documented in *Arabidopsis* under salt stress condition, the study identified several QTLs/loci regions (Verslues et

al., 2014). We compared those identified loci and genes with wheat, but no homologs were found in the present study. It is known that Pro accumulation from the shoot or aerial part is different from the root even under the same environmental condition (Hayat et al., 2012). In present study aerial part was used for Pro determination in response to drought whereas, the previous study on *Arabidopsis* reported for the root and the stress condition was also different, which might be the reason for having no homolog in the present study. The complete Pro profiling for both root and shoot under the same environmental condition is needed to be performed in wheat in the future to understand the fact precisely. Moreover, different factors such as Pro transporter, transcription factors, proteins, etc. regulate the Pro-related genes and Pro content (Jung et al., 2010; Wang et al., 2014; Aleksza et al., 2017). The involvement of these factors must be different between *Arabidopsis* and wheat for Pro regulation. In addition, evolutionary pathways are also different between *Arabidopsis* and wheat. Wheat is more diversified due to the incorporation of hybrid genomes as well as the introgression of new adaptive alleles from related species under diverse environments for better fitness. Notably, *P5CS1* (*Delta-1-pyrroline-5-carboxylate synthase*) gene has been reported for Pro accumulation in plants (Mattioli et al., 2008). Homologs of this gene are located in wheat between two significant SNPs in 1B chromosome in the present study but far from either of the SNPs and belong to a high LD decay region. Their functional characterizations are yet to be performed. For H_2O_2, no report so far we know described the candidate loci linked with H_2O_2 mediated root-shoot growth in wheat. Therefore, our results suggest that the loci identified in the wheat genome for drought-induced Pro and H_2O_2 accumulation and loci for root-shoot trait linked with H_2O_2 mediated root-shoot growth seem unique.

5.5. Pro and H_2O_2 can be a biomarker under drought stress condition

Pro and H_2O_2 have been known to be correlated positively with drought stress (Forlani et al., 2019). Several studies regarding genetic analyses, transcriptomic and proteomic analyses (Vandenabeele et al., 2003; Xia et al., 2017) identified the impact of Pro and H_2O_2 on stress tolerance. Housekeeping amount Pro enhances signaling pathways associated with plant developmental and maturation process (Mattioli et al., 2020; Jira-Anunkul and Pattanagul, 2021). We estimated the Pro content was about 56 and 11 times high under drought condition as compared to the control treatment in glasshouse and in field environment, respectively. Our findings are in line with a previous study by Sharma and Verslues (2010), which revealed that Pro content under drought stress may exceed up to 100 fold in *Arabidopsis*. Similarly, H_2O_2 content under drought condition

was more than 3 times high as compared to the well-watered control treatment. Our result is supported by a previous report that identified a significant increase in H_2O_2 accumulation under drought treatment (Wang et al., 2012; Chen et al., 2016). Preferentially higher Pro content under stress conditions has also been documented in previous studies on barley and wheat in the epidermis and vascular bundles (Ziijriga et al., 1989; Heerden and Villiers, 2013). This evidence along with our findings suggested that Pro and H_2O_2 can be a reliable biomarker to assess a wheat cultivar under drought.

5.6. Conclusions

Drought is one of the major impediments of crop yield globally. Understanding the genetic basis of plants under drought stress is of prime importance to develop drought tolerant cultivars. This study showed the phenotypic variation of Pro and H_2O_2 in wheat induced by drought. The drought stress caused significantly higher Pro and H_2O_2 accumulation than the control treatment. Pro and H_2O_2 content showed a wider phenotypic variation among the cultivars under drought stress. Pro and H_2O_2 accumulation were also different between European and Non-European, traditional and modern sub- groups. So far we know, this report is the first time regarding the phenotypic variation of Pro and H_2O_2 in wheat using a large number of diverse wheat cultivars. Phenotypic analysis of drought-induced Pro and H_2O_2 accumulation was performed by using GWAS, which revealed significant MTA across different chromosomes. Identified loci and putative candidate genes linked with drought induced Pro and H_2O_2 seem to be reported first time wheat. Therefore, our findings have generated a fundamental basis of loci and genes linked drought-induced Pro and H_2O_2 accumulation in wheat for further molecular analysis. We have identified the contrasting marker alleles associated with relative value and STI of Pro and H_2O_2. These alleles might be important for further genetic improvement of wheat cultivar. Moreover, we studied exogenously applied the toxic dose of H_2O_2 on wheat, which showed a significantly reduced root-shoot growth. Next, a GWAS with relative value and stress STI of root-shoot traits identified the genetic factors that are linked with H_2O_2 induced root- shoot growth. The candidate genes and the contrasting alleles could be utilized in the future for a better understanding of H_2O_2 mediated growth in crops.

5.7. References

Ahmed HGMD, Zeng Y, Iqbal M, Rashid MAR, Raza H, Ullah A, Ali M, Yar MM, Shah AN (2022) Genome-wide association mapping of bread wheat genotypes for sustainable food security and yield potential under limited water conditions. PLoS One 17: e0263263

Aleksza D, Horváth G V., Sándor G, Szabados L (2017) Proline Accumulation Is Regulated by Transcription Factors Associated with Phosphate Starvation. Plant Physiol 175: 555

Alipour H, Bihamta MR, Mohammadi V, Peyghambari SA, Bai G, Zhang G (2017) Genotyping-by-sequencing (GBS) revealed molecular genetic diversity of Iranian wheat landraces and cultivars. Front Plant Sci 8: 1293

Chen D, Wang S, Cao B, Cao D, Leng G, Li H, Yin L, Shan L, Deng X (2016) Genotypic variation in growth and physiological response to drought stress and re-watering reveals the critical role of recovery in drought adaptation in maize seedlings. Front Plant Sci 6: 1241

Eltaher S, Sallam A, Belamkar V, Emara HA, Nower AA, Salem KFM, Poland J, Baenziger PS (2018) Genetic diversity and population structure of F3:6 Nebraska Winter wheat genotypes using genotyping-by-sequencing. Front Genet 9: 76

Forlani G, Trovato M, Funck D, Signorelli S (2019) Regulation of Proline Accumulation and Its Molecular and Physiological Functions in Stress Defence. Osmoprotectant-Mediated Abiotic Stress Toler. Plants. Springer International Publishing, pp 73–97

Fujiwara T, Mitsuya S, Miyake H, Hattori T, Takabe T (2010) Characterization of a novel glycinebetaine/proline transporter gene expressed in the mestome sheath and lateral root cap cells in barley. Planta 232: 133–143

Grallath S, Weimar T, Meyer A, Gumy C, Suter-Grotemeyer M, Neuhaus JM, Rentsch D (2005) The AtProT family. Compatible solute transporters with similar substrate specificity but differential expression patterns. Plant Physiol 137: 117–126

Gupta A, Sarkar AK, Senthil-Kumar M (2016) Global transcriptional analysis reveals unique and shared responses in arabidopsis thaliana exposed to combined drought and pathogen stress. Front Plant Sci 7: 686

Hao C, Wang L, Ge H, Dong Y, Zhang X (2011) Genetic Diversity and Linkage Disequilibrium in Chinese Bread Wheat (Triticum aestivum L.) Revealed by SSR Markers. PLoS One 6: e17279

Hayat S, Hayat Q, Alyemeni MN, Wani AS, Pichtel J, Ahmad A (2012) Role of proline under changing environments: A review. Plant Signal Behav 7: 1456

Herzig P, Maurer A, Draba V, Sharma R, Draicchio F, Bull H, Milne L, Thomas WTB, Flavell AJ, Pillen K (2018) Contrasting genetic regulation of plant development in wild barley grown in two European environments revealed by nested association mapping. J Exp Bot 69: 1517

Hoermiller II, Naegele T, Augustin H, Stutz S, Weckwerth W, Heyer AG (2017) Subcellular reprogramming of metabolism during cold acclimation in Arabidopsis thaliana. Plant Cell Environ 40: 602–610

Huang XY, Salt DEE (2016) Plant Ionomics: From Elemental Profiling to Environmental Adaptation. Mol Plant 9: 787–797

Hyuk Yoo J, Young Park C, Cheol Kim J, Do Heo W, Sun Cheong M, Cheol Park H, Chul Kim M, Cheol Moon B, Soo Choi M, Hwan Kang Y, et al (2004) Direct interaction of a divergent CaM isoform and the transcription factor, MYB2, enhances salt tolerance in Arabidopsis. J Biol Chem 280: 3697–3706

Jiang S-C, Mei C, Liang S, Yu Y-T, Lu K, Wu Z, Wang X-F, Zhang D-P (2015) Crucial roles of the pentatricopeptide repeat protein SOAR1 in Arabidopsis response to drought, salt and cold stresses. Plant Mol Biol 88: 369–385

Jira-Anunkul W, Pattanagul W (2021) Effects of hydrogen peroxide application on agronomic traits of rice (Oryza sativa L.) under drought stress. Plant, Soil Environ 67 (2021): 221–229

Jung Y, Park J, Choi Y, Yang JG, Kim D, Kim BG, Roh K, Lee DH, Auh CK, Lee S (2010) Expression Analysis of Proline Metabolism-related Genes From Halophyte Arabis stelleri under Osmotic Stress Conditions. J Integr Plant Biol 52: 891–903

Khalil F, Rauf S, Monneveux P, Anwar S, Iqbal Z (2016) Genetic analysis of proline concentration under osmotic stress in sunflower (Helianthus annuus L.). Breed Sci 66: 463–470

Li Q, Wang W, Wang W, Zhang G, Liu Y, Wang Y, Wang W (2018) Wheat F-Box Protein Gene TaFBA1 Is Involved in Plant Tolerance to Heat Stress. Front Plant Sci 9: 521

Lukaszewski AJ, Alberti A, Sharpe A, Kilian A, Stanca AM, Keller B, Clavijo BJ, Friebe B, Gill B, Wulff B, et al (2014) A chromosome-based draft sequence of the hexaploid bread wheat (Triticum aestivum) genome. Science (80-). doi: 10.1126/SCIENCE.1251788/SUPPL_FILE/MAYER.SM.PDF

Luo X, Cui N, Zhu Y, Cao L, Zhai H, Cai H, Ji W, Wang X, Zhu D, Li Y, et al (2012) Over-expression of GsZFP1, an ABA-responsive C2H2-type zinc finger protein lacking a QALGGH motif, reduces ABA sensitivity and decreases stomata size. J Plant Physiol 169: 1192–1202

Malik A, Gul A, Amir R, Munir F, Babar MM, Bakhtiar SM, Hayat MQ, Paracha RZ, Khalid Z, Alipour H (2020) Classification and Computational Analysis of Arabidopsis thaliana Sperm Cell-Specific F-Box Protein Gene 3p.AtFBP113. Front Genet 11: 1559

Mattioli R, Marchese D, D'Angeli S, Altamura MM, Costantino P, Trovato M (2008) Modulation of intracellular proline levels affects flowering time and inflorescence architecture in Arabidopsis. Plant Mol Biol 66: 277–288

Mattioli R, Palombi N, Funck D, Trovato M (2020) Proline Accumulation in Pollen Grains as Potential Target for Improved Yield Stability Under Salt Stress. Front Plant Sci 11: 1699

McCormick F (1995) Ras-related proteins in signal transduction and growth control. Mol Reprod Dev 42: 500–506

Mora-Poblete F, Ballesta P, Lobos GA, Molina-Montenegro M, Gleadow R, Ahmar S, Jiménez-Aspee F (2021) Genome-wide association study of cyanogenic glycosides, proline, sugars, and pigments in Eucalyptus cladocalyx after 18 consecutive dry summers. Physiol Plant

172: 1550–1569

Peng J, Yu DS, Wang LQ, Xie MM, Yuan CY, Wang Y, Tang DY, Zhao XY, Liu XM (2012) Arabidopsis F-box gene FOA1 involved in ABA signaling. Sci China Life Sci 55: 497–506

Pradhan S, Ali Babar M, Bai G, Khan J, Shahi D, Avci M, Guo J, McBreen J, Asseng S, Gezan S, et al Genetic dissection of heat-responsive physiological traits to improve adaptation and increase yield potential in soft winter wheat. doi: 10.1186/s12864-020-6717-7

Reinert S, Kortz A, Léon J, Naz AA (2016) Genome-wide association mapping in the global diversity set reveals new QTL controlling root system and related shooGenome-wide association mapping in the global diversity set reveals new QTL controlling root system and related shoot variation in barleyt . Front Plant Sci 7: 1061

Sadhukhan A, Kobayashi Y, Nakano Y, Iuchi S, Kobayashi M, Sahoo L, Koyama H (2017) Genome-wide Association Study Reveals that the Aquaporin NIP1;1 Contributes to Variation in Hydrogen Peroxide Sensitivity in Arabidopsis thaliana. Mol Plant 10: 1082–1094

Sayed MA, Schumann H, Pillen K, Naz AA, Léon J (2012) AB-QTL analysis reveals new alleles associated to proline accumulation and leaf wilting under drought stress conditions in barley (Hordeum vulgare L.). BMC Genet 13: 1–12

Schwacke R, Grallath S, Breitkreuz KE, Stransky E, Stransky H, Frommer WB, Rentsch D (1999) LeProT1, a Transporter for Proline, Glycine Betaine, and g-Amino Butyric Acid in Tomato Pollen. Plant Cell 11: 377

Sharma S, Verslues PE (2010) Mechanisms independent of abscisic acid (ABA) or proline feedback have a predominant role in transcriptional regulation of proline metabolism during low water potential and stress recovery. Plant Cell Environ 33: 1838–1851

Siddiqui MN, Teferi TJ, Ambaw AM, Gabi MT, Koua P, Léon J, Ballvora A (2021) New drought-adaptive loci underlying candidate genes on wheat chromosome 4B with improved photosynthesis and yield responses. Physiol Plant. doi: 10.1111/PPL.13566

Sukumaran S, Reynolds MP, Sansaloni C (2018) Genome-Wide Association Analyses Identify QTL Hotspots for Yield and Component Traits in Durum Wheat Grown under Yield Potential, Drought, and Heat Stress Environments. Front Plant Sci 0: 81

Tyagi S, Sharma S, Taneja M, Shumayla, Kumar R, Sembi JK, Upadhyay SK (2017) Superoxide dismutases in bread wheat (Triticum aestivum L.): Comprehensive characterization and expression analysis during development and, biotic and abiotic stresses. Agri Gene 6: 1–13

Ueda Y, Frimpong F, Qi Y, Matthus E, Wu L, Höller S, Kraska T, Frei M (2015) Genetic dissection of ozone tolerance in rice (Oryza sativa L.) by a genome-wide association study. J Exp Bot 66: 293

Verslues PE, Lasky JR, Juenger TE, Liu TW, Nagaraj Kumar M (2014a) Genome-wide association mapping combined with reverse genetics identifies new effectors of low water potential-induced proline accumulation in Arabidopsis. Plant Physiol. doi: 10.1104/pp.113.224014

Verslues PE, Lasky JR, Juenger TE, Liu TW, Nagaraj Kumar M (2014b) Genome-wide

association mapping combined with reverse genetics identifies new effectors of low water potential-induced proline accumulation in Arabidopsis. Plant Physiol 164: 144–159

Visscher PM, Brown MA, McCarthy MI, Yang J (2012) Five Years of GWAS Discovery. Am J Hum Genet 90: 7–24

Wang F, Tong W, Zhu H, Kong W, Peng R, Liu Q, Yao Q (2016) A novel Cys2/His2 zinc finger protein gene from sweetpotato, IbZFP1, is involved in salt and drought tolerance in transgenic Arabidopsis. Planta 243: 783–797

Wang G, Zhang J, Wang G, Fan X, Sun X, Qin H, Xu N, Zhong M, Qiao Z, Tang Y, et al (2014) Proline responding1 Plays a Critical Role in Regulating General Protein Synthesis and the Cell Cycle in Maize. Plant Cell 26: 2582

Wang H, Tang X, Wang H, Shao HB (2015) Proline accumulation and metabolism-related genes expression profiles in Kosteletzkya virginica seedlings under salt stress. Front Plant Sci 6: 792

Wang S, Liang D, Li C, Hao Y, Ma F, Shu H (2012) Influence of drought stress on the cellular ultrastructure and antioxidant system in leaves of drought-tolerant and drought-sensitive apple rootstocks. Plant Physiol Biochem 51: 81–89

Yan Q, Cui X, Lin S, Gan S, Xing H, Dou D (2016) GmCYP82A3, a Soybean Cytochrome P450 Family Gene Involved in the Jasmonic Acid and Ethylene Signaling Pathway, Enhances Plant Resistance to Biotic and Abiotic Stresses. PLoS One 11: e0162253

Ziijriga GE, Argandora VH, Corcuera LJ (1989) Distribution of glycine-betaine and proline in water stressed and unstressed barley leaves. Phytochemistry 28: 419420

Supplementary Figures

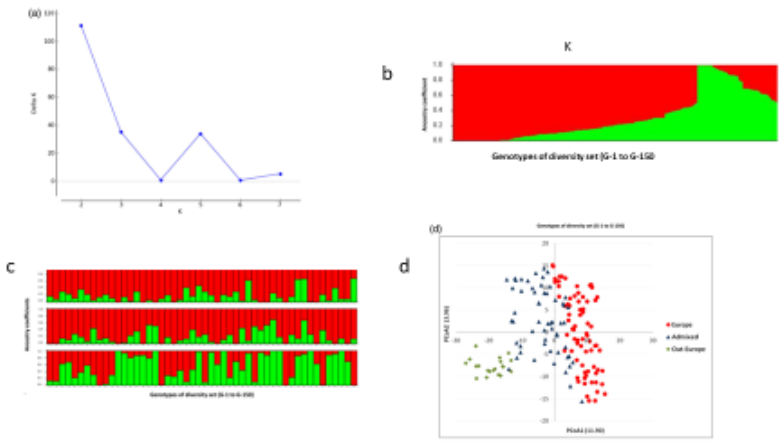

Supplementary Figure 2. S1. The population structure adopted from Begum et al. (2020) to continue proline analysis according to sub-population. Population structure based on ΔK (a). Proportion of ancestry coefficient of sub-populations; sub-population Europe (red) and sub-population out of Europe (green) at K = 2 (b). The proportion of ancestry coefficient of individual genotypes from G-1 to G-150 relative to subpopulation Europe (red) and sub-population out of Europe (green) (c). Principle coordinate analysis (PCoA) of individual genotypes of the diversity set (d).

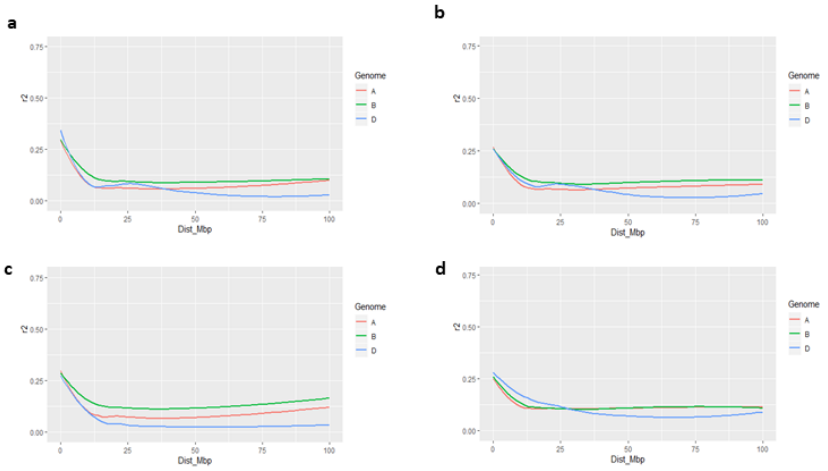

Supplementary Figure 2. S2. Linkage disequilibrium (LD) decay rate of 150 genotypes among whole and sub population across A, B and D genome. Plot of LD decay for whole population (a). Plot of LD decay for Admixture (b). Plot of LD decay for subpopulation Europe (c). Plot of LD decay for subpopulation outside Europe (d).

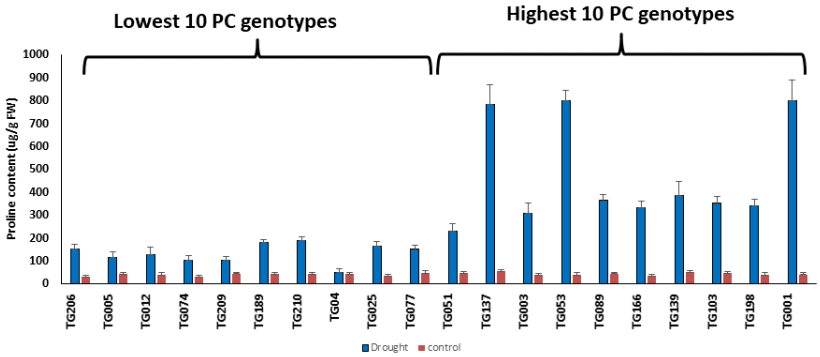

Supplementary Figure 2. S3. Proline values in highest and lowest ten cultivars under drought and control condition, all cultivars showed significantly higher proline under drought condition in comparison to control treatment except for the cultivar TG004 (Claire), which remain non-significant under drought.

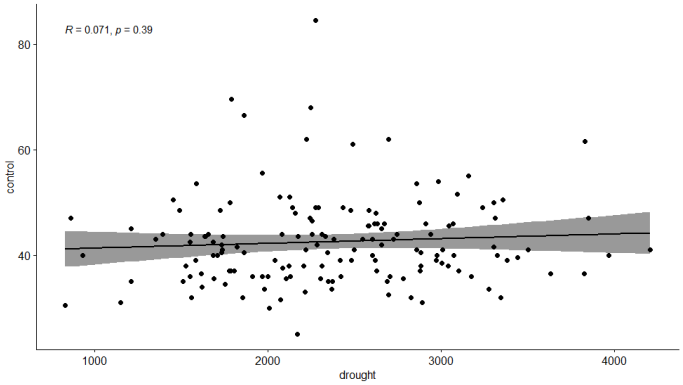

Supplementary Figure 2. S4. Correlation coefficient plot between proline value under drought and control treatment

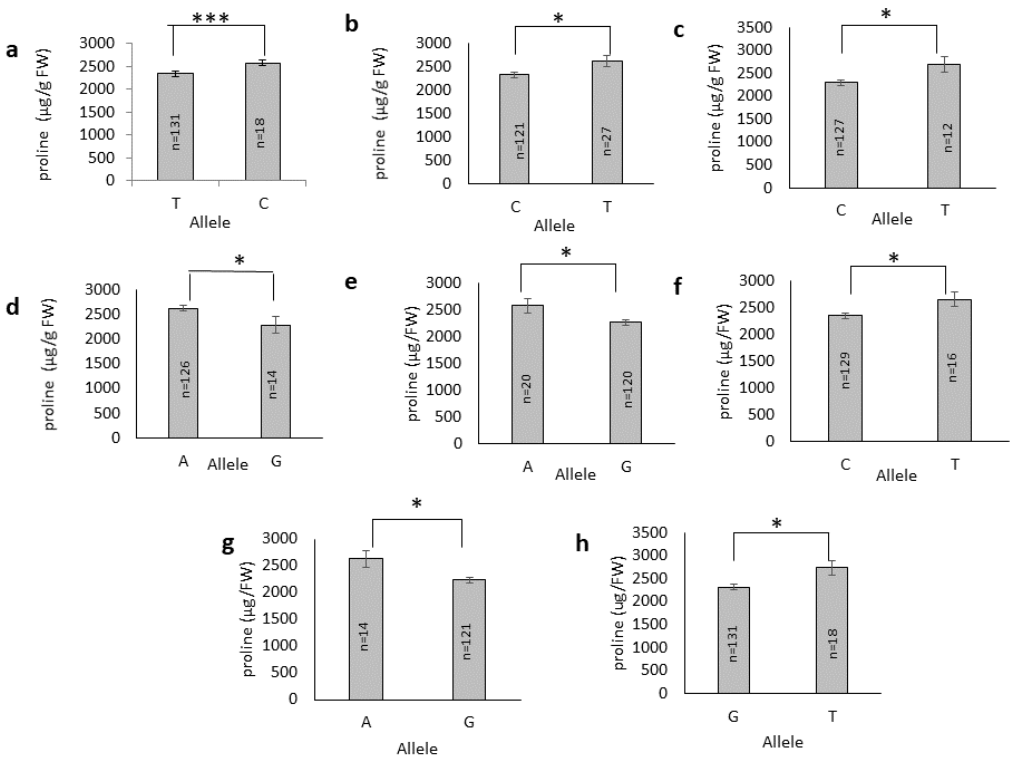

Supplementary Figure 2. S5. Allelic variation of significant single-markers located on chromosome 1B. Comparison of phenotypic values between two allele of top most significant marker JD_c12243_360 shown in panel (a). Comparison of phenotypic values between two allele of 4th rank marker Excalibur_rep_c68921_433 shown in panel (b). Comparison of phenotypic values between two allele of 5th rank marker RAC875_c42715_856 shown in panel (c). Comparison of phenotypic values between two allele of 6th rank marker BobWhite_c13654_447 shown in panel (d). Comparison of phenotypic values between two allele of 7th marker Ex_c4206_502 shown in panel (e). Comparison of phenotypic values between two allele of 8th rank marker BS00022180_51 shown in panel (f). Comparison of phenotypic values between two allele of 10th rank marker Kukri_c2332_1093 shown in panel (g). Single marker analysis located on peak area on chromosome 1A for 9th rank marker Kukri_c37212_1286 and its comparison between two allele (h). Mean values and standard errors are plotted; n indicates the number of lines representing the allele; Mean values and standard errors are plotted; n indicates the number of lines representing the allele *** significant at $p < 0.001$ and * at $p < 0.05$.

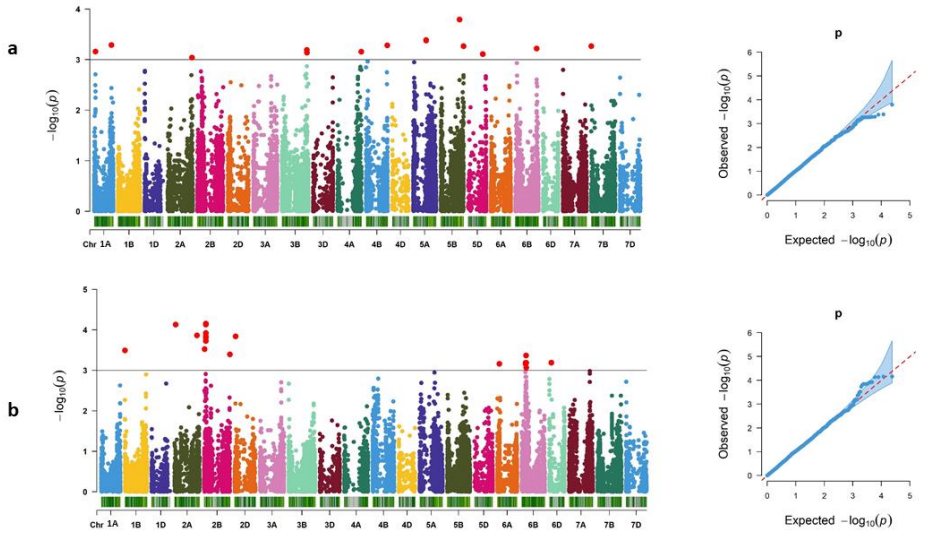

Supplementary Figure 3.S1. Manhattan plots of GWAS conducted on Pro and H_2O_2 content. (a) Manhattan plot (left) and QQplot (right) of proline content under control condition, (b) Manhattan plot (left) and QQplot (right) of hydrogen peroxide content under control condition. $-\log_{10}$ (P) =3.0 is the threshold level for MTA. The red dots on Manhattan plots above the horizontal grey line are representing significant markers

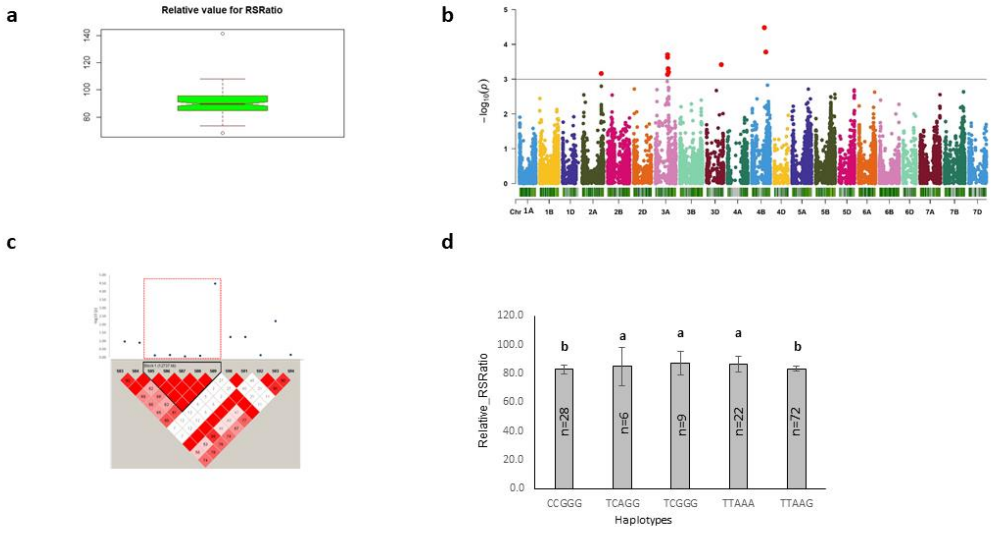

Supplementary Figure 4. S1. Marker-trait associations for R_RSRatio. (a) Box plot showing the distribution of R_RSRatio value; (b) Manhattan plot displaying the marker-trait associations; the horizontal red line indicates threshold level [$-\log_{10}$ (P) =3.0], the dots above this line indicate significant markers. (c) The linkage disequilibrium (LD) heat map illuminating the peak region on chromosome 4B (Com_Hap1). In (c), pair-wise LD map between SNP markers is marked by D′ values, dark red represent 1, whereas white is for 0. The region surrounded by the red dotted line indicate LD block that contain significant SNPs. (d) Phenotypic comparison of the haplotype groups established for the significant SNPs as detected by LD block. Different letters indicate statistical difference at $P < 0.05$, n indicates number of genotypes represent each specific haplotype.

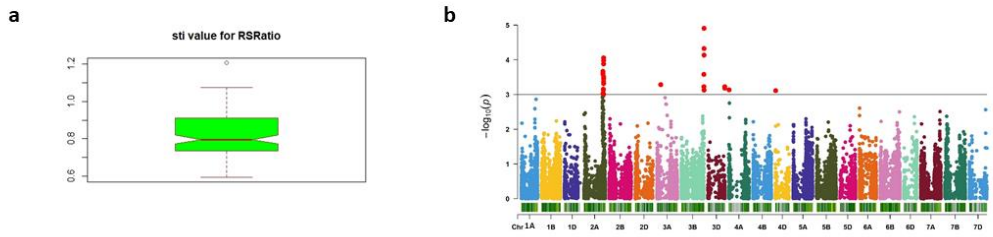

Supplementary Figure 4.S2. Marker-trait associations for STI_RSRatio. (a) Box plot showing the distribution of STI_RSRatio; (b) Manhattan plot displaying the marker-trait associations; the horizontal red line indicates threshold level [$-\log_{10}(P) = 3.0$], the dots above this line indicate significant markers.

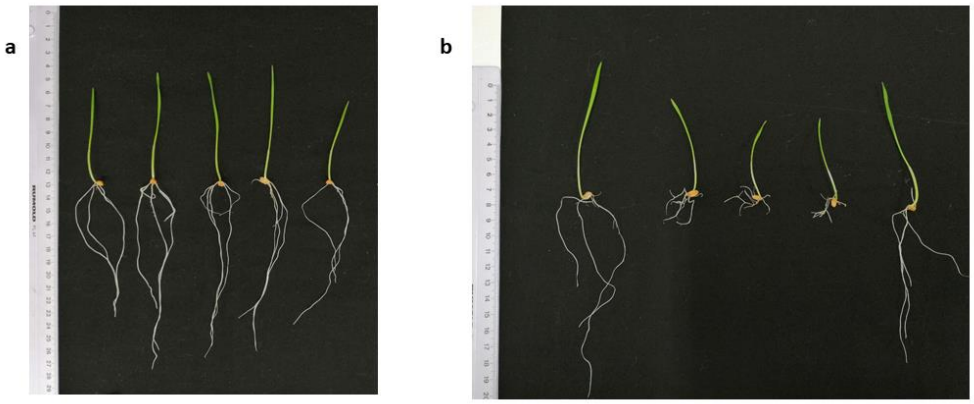

Supplementary Figure 4. S3. Seedling growth of five bread wheat cultivars after 7 days under (a) control and (b) 20 mM H_2O_2 treatment

Supplementary Tables

Supplementary Table 2. S1. List of 150 cultivars used for this study, their local name, origin and year of release

Serial num.	TG number	Local Name	Origin	Year of Release
1	1	Einstein	GB	2004
2	2	Oakley	UK/BE	2008
3	3	Jafet	Deutschland	2008
4	4	Claire	IE/UK	1999
5	5	Rebell	Deutschland	2013
6	6	Memory	Deutschland	2013
7	7	Kurt	Deutschland	2013
8	8	Zappa	Deutschland	2009
9	9	Chevalier	AT, CZ, LT, LU	2005
10	10	Gordian	Deutschland	2013
11	11	Mentor	Deutschland	2012
12	12	Meister	Deutschland	2010
13	13	KWS Santiago	England	2011
14	14	Brigand	GBR	1979
15	15	Profilus	Deutschland	2008
16	16	Durin	Frankreich	Unknown
17	17	KWS Pius	Deutschland	2010
18	18	Paroli	Deutschland	2004
19	19	Estivus	Deutschland	2012
20	21	Desamo	Deutschland	2013
21	22	Carenius	Deutschland	2006
22	23	Mulan	Deutschland	2006
23	25	Nelson	Deutschland	2011
24	26	Patras	Deutschland	2012
25	27	Götz	Deutschland	1978
26	28	Robigus	England	2004
27	29	Anapolis	Deutschland	2013
28	30	Solstice	England	2001
29	32	Capone	Deutschland	2012
30	33	Tabasco	Deutschland	2008
31	35	Cubus	Deutschland	2002
32	36	Edward	Deutschland	2013
33	39	SW Topper	USA	2002
34	41	Jenga	Deutschland	2007
35	42	Linus	Deutschland	2010
36	43	TJB 990-15	GBR	1980
37	44	Forum	DE/EE/PO/SE	2012

38	45	Colonia	DE/BE/HU	2011
39	46	Transit	DE	1994
40	48	Gaucho	USA	1993
41	49	Tarso	Deutschland	1992
42	50	Hermann	Deutschland	2004
43	51	Glaucus	Deutschland	2011
44	53	Atomic	Deutschland	2012
45	54	Tobak	Deutschland	2011
46	56	Manager	Deutschland	2006
47	57	Gourmet	Deutschland	2013
48	58	Limes	Deutschland	2003
49	60	Kalahari	DE/BE	2010
50	63	Zobel	Deutschland	2006
51	66	Global	DE/AT	2009
52	71	Greif	Deutschland	1989
53	74	Skalmeje	Deutschland	2006
54	75	Genius	Deutschland	2010
55	76	Enorm	Deutschland	2002
56	77	Florian	Deutschland	2010
57	78	Skater	Deutschland	2000
58	79	Brilliant	Deutschland	2005
59	84	Maris Huntsman	Deutschland	1975
60	86	Landsknecht	Deutschland	2013
61	87	Sponsor	FR, IE	1994
62	88	Impression	Deutschland	2005
63	89	Winnetou	Deutschland	2002
64	90	Toronto	Deutschland	1990
65	91	Torrild	Deutschland	2005
66	92	Contra	Deutschland	1990
67	93	Schamane	Deutschland	2005
68	94	Granada	Deutschland	1980
69	96	Tommi	Deutschland	2002
70	81	Apertus	Deutschland	2013
71	99	JB Asano	Deutschland	2008
72	100	Kerubino	Deutschland	2004
73	102	Urban	Deutschland	1980
74	103	Orestis	Deutschland	1988
75	104	Flair	Deutschland	1996
76	105	Anthus	Deutschland	2005
77	106	Bombus	Deutschland	2012
78	107	Lucius	Deutschland	2006

79	109	Sorbas	Deutschland	1985
80	112	Magister	Deutschland	2005
81	148	Aristos	Deutschland	1966
82	119	Joss	Deutschland	1972
83	121	Sperber	Deutschland	1982
84	123	Helios	USA	2013
85	124	Obelisk	NE; DE	1987
86	126	Disponent	Deutschland	1975
87	127	Tambor	Deutschland	1993
88	128	Boxer	Deutschland	2013
89	129	Sokrates	Deutschland	2001
90	130	Carisuper	Deutschland	1975
91	131	Rektor	Deutschland	1980
92	134	Alidos	Deutschland	1987
93	188	Cardos	Deutschland	1975
94	136	Akratos	Deutschland	2004
95	137	Knirps		1985
96	139	Oberst	DE	1980
97	140	Cappelle Desprez	FR, CHL, GBR, NL	1946
98	142	Ibis	Deutschland	1991
99	143	Batis	Deutschland	1994
100	145	Akteur	Deutschland	2003
101	151	Astron	Deutschland	1989
102	152	Basalt	Deutschland	1980
103	154	Aron	Deutschland	1992
104	156	Aszita	Deutschland	2005
105	157	Kobold	Deutschland	1978
106	160	Vuka	Deutschland	1975
107	161	Benno	Deutschland	1973
108	163	Aquila	GRB/IT	1979
109	165	Kraka	Deutschland	1982
110	166	Caribo	Deutschland	1968
111	168	Konsul	Deutschland	1990
112	170	Centurk	USA	1971
113	171	NS 22/92	Serbien	Unknown
114	172	Benni multifloret	USA	1980
115	173	Hope	USA	1927
116	174	Vel	USA	Unknown
117	175	Phoenix	AUS	1981
118	176	Mironovska 808	Ukraine	1963
119	177	Caphorn	Frankreich	2000
120	178	Cordiale	England	2003

121	179	Apache	CZ	1997
122	181	Isengrain	FR/SI/ES	1996
123	182	Alixan	Frankreich	2005
124	183	Boregar	Frankreich	2007 2008
125	184	Renesansa	Serbien	1995
126	185	Tremie	ES, FR, IT,	1991
127	187	Triple Dirk "S"	Australien	Unknown
128	189	Soissons	BE, Es, FR, IE, IT; SI	1987
129	190	BCD 1302/83	Moldavien	Unknown
130	191	Arlequin	Frankreich	2007
131	192	Sonalika	Indien	1967
132	193	Camp Remy	Deutschland	1980
133	194	Cajeme 71	Mexico	1971
134	195	Avalon	GBR;	1980
135	196	Ivanka	Serbien	1998
136	197	Pobeda	Serbien	1990
137	198	NS 66/92	Serbien	Unknown
138	199	Mexico 3	Mexico	Unknown
139	200	Orcas	Deutschland	2010
140	201	Nimbus	Deutschland	1975
141	203	Florida	USA	1984
142	205	Highbury	GBR	1968
143	206	Siete Cerros 66	Mexiko	1966
144	207	Kontrast	Deutschland	1990
145	208	WW 4180	Deutschland	2012
146	209	INTRO 615	USA	Unknown
147	210	NS 46/90	Serbien	Unknown
148	211	Mex. 17 bb	Mexico	Unknown
149	212	Lambriego Inia	Chile	1980
150	213	Pegassos	AT,SK	1994

Supplementary Table 2. S2. Highest and lowest 10 proline (µg/g fresh weight) accumulating cultivars under drought condition

SL. No.	TG No.	Local Name	Origin	Year of Release	Proline
Lowest 10 cultivars for proline accumulation under drought					
143	206	Siete Cerros 66	Mexiko	1966	833
5	5	Rebell	Deutschland	2013	863
12	12	Meister	Deutschland	2010	934
53	74	Skalmeje	Deutschland	2006	1150
146	209	INTRO 615	USA	Unknown	1212
128	189	Soissons	BE, Es, FR, IE, IT; SI	1987	1214
147	210	NS 46/90	Serbien	Unknown	1353
4	4	Claire	IE/UK	1999	1395
23	25	Nelson	Deutschland	2011	1456
56	77	Florian	Deutschland	2010	1491
Highest 10 cultivars for proline accumulation under drought					
43	51	Glaucus	Deutschland	2011	3357
95	137	Knirps		1985	3379
3	3	Jafet	Deutschland	2008	3443
44	53	Atomic	Deutschland	2012	3501
63	89	Winnetou	Deutschland	2002	3631
110	166	Caribo	Deutschland	1968	3826
96	139	Oberst	DE	1980	3831
74	103	Orestis	Deutschland	1988	3848
137	198	NS 66/92	Serbien	Unknown	3968
1	1	Einstein	GB	2004	4205

Supplementary Table 2. S3. Proline accumulation under control (Pro_Con), drought condition (Pro_Dro) and relative proline value

Serial no.	TG No.	Pro_Con	Pro_Dro	Relative proline
1	TG001	41	4205	4164
2	TG002	41	2859	2818
3	TG003	39.5	3443	3403.5
4	TG004	44	1395	1351
5	TG005	47	863	816
6	TG006	47	3313	3266
7	TG007	40.5	2343	2302.5
8	TG008	32	2827	2795
9	TG009	44	2254	2210
10	TG010	62	2698	2636
11	TG011	36	2706	2670
12	TG012	40	934	894
13	TG013	37	1807	1770
14	TG014	40	3073	3033
15	TG015	48	2158	2110
16	TG016	25	2170	2145
17	TG017	35.5	1690	1654.5
18	TG018	33	2215	2182
19	TG019	38.5	3005	2966.5
20	TG021	42.5	1687	1644.5
21	TG022	38	2207	2169
22	TG023	37.5	2086	2048.5
23	TG025	50.5	1456	1405.5
24	TG026	37	1780	1743
25	TG027	40	3322	3282
26	TG028	38	2882	2844
27	TG029	51	2126	2075
28	TG030	48.5	2585	2536.5
29	TG032	38	3041	3003
30	TG033	39	2042	2003
31	TG035	42	2657	2615
32	TG036	42.5	1552	1509.5
33	TG039	39	2619	2580
34	TG041	35.5	2303	2267.5
35	TG042	55.5	1970	1914.5
36	TG043	48	2622	2574
37	TG044	50	3305	3255
38	TG045	36	1911	1875
39	TG046	50	2875	2825
40	TG048	49	2277	2228
41	TG049	39	2418	2379
42	TG050	36	1967	1931
43	TG051	50.5	3357	3306.5
44	TG053	41	3501	3460

45	TG054	43.5	2176	2132.5
46	TG056	49	3240	3191
47	TG057	50	1782	1732
48	TG058	62	2224	2162
49	TG060	33.5	2367	2333.5
50	TG063	51	2070	2019
51	TG066	45.5	2578	2532.5
52	TG071	44	2313	2269
53	TG074	31	1150	1119
54	TG075	44	1658	1614
55	TG076	36	3174	3138
56	TG077	48.5	1491	1442.5
57	TG078	53.5	2857	2803.5
58	TG079	41	2498	2457
59	TG081	39	2970	2931
60	TG084	46	2616	2570
61	TG086	36	2130	2094
62	TG087	35.5	2780	2744.5
63	TG088	36.5	3631	3594.5
64	TG089	46	3068	3022
65	TG090	43	2724	2681
66	TG091	38	2124	2086
67	TG092	54	2983	2929
68	TG093	44	2939	2895
69	TG094	49	2141	2092
70	TG096	37	3103	3066
71	TG099	46	2913	2867
72	TG100	46	2674	2628
73	TG102	46.5	2254	2207.5
74	TG103	47	3848	3801
75	TG104	40	2976	2936
76	TG105	41	1736	1695
77	TG106	43.5	2331	2287.5
78	TG107	49	2294	2245
79	TG109	38	2312	2274
80	TG112	40	2602	2562
81	TG119	44	2745	2701
82	TG121	40	1685	1645
83	TG123	68	2247	2179
84	TG124	51.5	3093	3041.5
85	TG126	61	2492	2431
86	TG127	43	2604	2561
87	TG128	44	2082	2038

88	TG129	44	1556	1512
89	TG130	66.5	1865	1798.5
90	TG131	84.5	2274	2189.5
91	TG134	43	2383	2340
92	TG136	40.5	2881	2840.5
93	TG137	69.5	1790	1720.5
94	TG139	45	2655	2610
95	TG140	39	3379	3340
96	TG142	61.5	3831	3769.5
97	TG143	53.5	1589	1535.5
98	TG145	43	2549	2506
99	TG148	40.5	1865	1824.5
100	TG151	33.5	3275	3241.5
101	TG152	38	1527	1489
102	TG154	41.5	3303	3261.5
103	TG156	36.5	1617	1580.5
104	TG157	35	1510	1475
105	TG160	31	2892	2861
106	TG161	35.5	2107	2071.5
107	TG163	41	3010	2969
108	TG165	45.5	3045	2999.5
109	TG166	42	2283	2241
110	TG168	36.5	3826	3789.5
111	TG170	41.5	1823	1781.5
112	TG171	34	1622	1588
113	TG172	31.5	2075	2043.5
114	TG173	43.5	1640	1596.5
115	TG174	40	1708	1668
116	TG175	37	1786	1749
117	TG176	49	2433	2384
118	TG177	36	2422	2386
119	TG178	45.5	2583	2537.5
120	TG179	33.5	1982	1948.5
121	TG181	32	1854	1822
122	TG182	37	2627	2590
123	TG183	39	1585	1546
124	TG184	43.5	1636	1592.5
125	TG185	36	1551	1515
126	TG187	46	2631	2585
127	TG188	48.5	1725	1676.5
128	TG189	35	1214	1179
129	TG190	41	2220	2179
130	TG191	32	3344	3312
131	TG192	32	1561	1529
132	TG193	32.5	2695	2662.5
133	TG194	35	2349	2314

134	TG195	34.5	1756	1721.5
135	TG196	42	1732	1690
136	TG197	35	2373	2338
137	TG198	40	3968	3928
138	TG199	37	2880	2843
139	TG200	55	3159	3104
140	TG201	36	2000	1964
141	TG203	47	2244	2197
142	TG205	43.5	1743	1699.5
143	TG206	30.5	833	802.5
144	TG207	39	2483	2444
145	TG208	30	2008	1978
146	TG209	45	1212	1167
147	TG210	43	1353	1310
148	TG211	40.5	1735	1694.5
149	TG212	48.5	2477	2428.5
150	TG213	35	2687	2652
	Average	42.53	2366.01	
		56	Average 56 times higher proline produced in Dro than background level	
	Dro	Highest	4205	
		Lowest	833	

Supplementary Table 2. S4. List of all genes in significant loci region/in LD block region for relative proline value

SNP	Chr	Gene Name	Description	Molecular function	Biological process
JD_c12243_360	1B	TraesCS1B01G070500	F-box family protein	NA	NA
		TraesCS1B01G070600	F-box family protein	NA	NA
		TraesCS1B01G070700	Ubiquitin activating enzyme E1	ubiquitin-like modifier activating enzyme activity	NA
		TraesCS1B01G070800	Vitamin B12 transporter BtuB	NA	NA
		TraesCS1B01G070900	Ubiquitin activating enzyme E1	ubiquitin-like modifier activating enzyme activity	NA
		TraesCS1B01G071000	F-box family protein	NA	NA
		TraesCS1B01G071100	Vitamin B12 transporter BtuB	NA	NA
		TraesCS1B01G071300	DUF1639 family protein	NA	NA
		TraesCS1B01G071400	Nuclear factor related to kappa-B-binding protein	NA	NA
		TraesCS1B01G071500	Kinesin-like protein	ATP binding	microtubule-based movement
		TraesCS1B01G071600	Pentatricopeptide repeat-containing protein	NA	NA
		TraesCS1B01G071700	Zinc finger family protein	NA	regulation of transcription by RNA polymerase II
		TraesCS1B01G071800	Integral membrane protein, TerC family protein	NA	NA
		TraesCS1B01G072000	Transmembrane protein, putative	NA	NA
		TraesCS1B01G072100	Epsin	NA	NA
		TraesCS1B01G072200	DIS3-like exonuclease 2	enoyl-CoA hydratase activity	fatty acid beta-oxidation
		TraesCS1B01G072300	Pentatricopeptide repeat-containing protein	NA	NA
		TraesCS1B01G072400	Pentatricopeptide repeat-containing protein	NA	NA
		TraesCS1B01G072500	Glucan endo-1,3-beta-glucosidase, putative	hydrolase activity, hydrolyzing O-glycosyl compounds	carbohydrate metabolic process
		TraesCS1B01G072600	Glucan endo-1,3-beta-glucosidase, putative	hydrolase activity, hydrolyzing O-glycosyl compounds	carbohydrate metabolic process
		TraesCS1B01G072700	Pentatricopeptide repeat-containing protein	NA	NA
		TraesCS1B01G072900	Pentatricopeptide repeat-containing protein	NA	NA
		TraesCS1B01G073000	Pentatricopeptide repeat-containing protein	NA	NA
		TraesCS1B01G073100	Pentatricopeptide repeat-containing protein	NA	NA
		TraesCS1B01G073200	Pentatricopeptide repeat-containing protein	NA	NA
		TraesCS1B01G073300	Protein ABIL1	NA	NA

		TraesCS1B01G073600	F-box family protein	NA	SCF-dependent proteasomal ubiquitin-dependent protein catabolic process
		TraesCS1B01G073700	Pyrimidine-specific ribonucleoside hydrolase	purine nucleosidase activity	purine nucleoside catabolic process
		TraesCS1B01G073800	F-box family protein	NA	NA
		TraesCS1B01G073900	Heavy metal transport/detoxification protein	NA	NA
		TraesCS1B01G074300	30S ribosomal protein S4	NA	NA
		TraesCS1B01G074400	tRNA dimethylallyltransferase	protein kinase binding	cellular response to glucose starvation
		TraesCS1B01G074500	DNA/RNA helicase	metal ion binding	NA
		TraesCS1B01G074600	Pentatricopeptide repeat-containing protein	NA	NA
BS00105606_51	1B	TraesCS1B01G070300	Germin-like protein 1	manganese ion binding	chaperone cofactor-dependent protein refolding
		TraesCS1B01G070400	tRNA (guanine-N(1)-)-methyltransferase	NA	NA
		TraesCS1B01G070500	F-box family protein	NA	NA
		TraesCS1B01G070600	F-box family protein	NA	NA
		TraesCS1B01G070700	Ubiquitin activating enzyme E1	ubiquitin-like modifier activating enzyme activity	NA
		TraesCS1B01G070800	Vitamin B12 transporter BtuB	NA	NA
		TraesCS1B01G070900	Ubiquitin activating enzyme E1	ubiquitin-like modifier activating enzyme activity	NA
		TraesCS1B01G071500	Kinesin-like protein	ATP binding	microtubule-based movement
		TraesCS1B01G071600	Pentatricopeptide repeat-containing protein	NA	NA
		TraesCS1B01G071700	Zinc finger family protein	regulation of transcription by RNA polymerase II	carotenoid biosynthetic process
		TraesCS1B01G072700	Pentatricopeptide repeat-containing protein	NA	NA
		TraesCS1B01G072900	Pentatricopeptide repeat-containing protein	NA	NA
		TraesCS1B01G073000	Pentatricopeptide repeat-containing protein	NA	NA
		TraesCS1B01G073100	Pentatricopeptide repeat-containing protein	NA	NA
BS00074962_51	1B	TraesCS1B01G029900	Phloem protein 2-like protein	NA	NA
		TraesCS1B01G030000	TBC1 domain family member	GTPase activator activity	intracellular protein transport
		TraesCS1B01G030100	DNA repair and recombination protein RAD54-like	NA	NA
		TraesCS1B01G030200	F-box family protein	NA	NA
		TraesCS1B01G030300	SKP1-like protein 4	NA	NA
		TraesCS1B01G030400	Beta-galactosidase	beta-galactosidase activity	carbohydrate metabolic process

	TraesCS1B01G030500	cDNA clone:J013058P10, full insert sequence	NA	NA
	TraesCS1B01G030600	calmodulin-binding family protein	NA	NA
	TraesCS1B01G030700	cDNA clone:J013058P10, full insert sequence	NA	NA
	TraesCS1B01G030800	ABC transporter ATP-binding protein	ATPase activity	fatty acid beta-oxidation
	TraesCS1B01G030900	Disease resistance protein	ADP binding	NA
	TraesCS1B01G031000	Dehydration-induced 19-like protein	NA	NA
	TraesCS1B01G031100	tRNA pseudouridine synthase B	pseudouridine synthase activity	mRNA pseudouridine synthesis
	TraesCS1B01G031900	Inhibitor protein	serine-type endopeptidase inhibitor activity	response to wounding
	TraesCS1B01G032000	Receptor-like protein kinase	ATP binding	cell surface receptor signaling pathway
	TraesCS1B01G032100	Protein kinase family protein	transferase activity, transferring acyl groups other than amino-acyl groups	polyketide biosynthetic process
	TraesCS1B01G032200	disease resistance protein (TIR-NBS-LRR class)	NA	NA
	TraesCS1B01G032300	Ankyrin repeat protein family-like protein	4 iron, 4 sulfur cluster binding	NA
	TraesCS1B01G032400	DUF868 family protein (DUF868)	NA	NA
	TraesCS1B01G032500	Kinase family protein	protein serine/threonine kinase activity	intracellular signal transduction
	TraesCS1B01G032600	Ubiquitin-protein ligase, putative	metal ion binding	NA
	TraesCS1B01G032700	NBS-LRR disease resistance protein, putative, expressed	ADP binding	defense response
	TraesCS1B01G032800	ARM repeat superfamily protein	NA	NA
	TraesCS1B01G032900	NBS-LRR disease resistance protein, putative, expressed	NA	NA
	TraesCS1B01G033000	Multicopper oxidase LPR2	oxidoreductase activity	NA
	TraesCS1B01G033100	General transcription factor IIH subunit 5	nucleotide-excision repair, preincision complex assembly	NA
	TraesCS1B01G033200	Cysteine proteinase	cysteine-type endopeptidase activity	proteolysis involved in cellular protein catabolic process
	TraesCS1B01G033300	Guanine nucleotide-binding protein G(k) subunit alpha	nicotinate phosphoribosyltransferase activity	NAD salvage
	TraesCS1B01G033400	Protein phosphatase 2c, putative	protein serine phosphatase activity	NA
	TraesCS1B01G033500	Elongation factor G	GTPase activity	translational elongation
	TraesCS1B01G033600	Leucine--tRNA ligase	NA	NA
	TraesCS1B01G033700	Benzyl alcohol O-benzoyltransferase	transferase activity, transferring acyl groups other than amino-acyl groups	NA

		TraesCS1B01G034600	Disease resistance protein (NBS-LRR class) family	ADP binding	chaperone-mediated protein transport
		TraesCS1B01G034700	Leucine-rich repeat (LRR) family protein	ADP binding	NA
		TraesCS1B01G034800	Heme/hemopexin transporter protein HuxB	NA	NA
		TraesCS1B01G034900	Chymotrypsin inhibitor	serine-type endopeptidase inhibitor activity	response to wounding
		TraesCS1B01G035000	Chymotrypsin inhibitor	serine-type endopeptidase inhibitor activity	response to wounding
Excalibur_rep_c68921_433	1B	TraesCS1B01G070500	F-box family protein	NA	NA
		TraesCS1B01G070600	F-box family protein	NA	NA
		TraesCS1B01G070700	Ubiquitin activating enzyme E1	ubiquitin-like modifier activating enzyme activity	NA
		TraesCS1B01G070800	Vitamin B12 transporter BtuB	NA	NA
		TraesCS1B01G070900	Ubiquitin activating enzyme E1	ubiquitin-like modifier activating enzyme activity	NA
		TraesCS1B01G071000	F-box family protein	NA	NA
		TraesCS1B01G072100	Epsin	clathrin binding	endocytosis
		TraesCS1B01G072200	DIS3-like exonuclease 2	enoyl-CoA hydratase activity	fatty acid beta-oxidation
		TraesCS1B01G072300	Pentatricopeptide repeat-containing protein	NA	NA
		TraesCS1B01G072400	Pentatricopeptide repeat-containing protein	NA	NA
		TraesCS1B01G072500	Glucan endo-1,3-beta-glucosidase, putative	hydrolase activity, hydrolyzing O-glycosyl compounds	carbohydrate metabolic process
		TraesCS1B01G072600	Glucan endo-1,3-beta-glucosidase, putative	hydrolase activity, hydrolyzing O-glycosyl compounds	carbohydrate metabolic process
		TraesCS1B01G072700	Pentatricopeptide repeat-containing protein	NA	NA
		TraesCS1B01G072900	Pentatricopeptide repeat-containing protein	NA	NA
		TraesCS1B01G073000	Pentatricopeptide repeat-containing protein	NA	NA
		TraesCS1B01G073100	Pentatricopeptide repeat-containing protein	NA	NA
		TraesCS1B01G073200	Pentatricopeptide repeat-containing protein	NA	NA
		TraesCS1B01G073300	Protein ABIL1	NA	NA
		TraesCS1B01G073400	S-locus lectin protein kinase family protein	NA	NA
		TraesCS1B01G073500	evolutionarily conserved C-terminal region 6	NA	NA
		TraesCS1B01G073600	F-box family protein	NA	SCF-dependent proteasomal ubiquitin-dependent protein catabolic process
		TraesCS1B01G073700	Pyrimidine-specific ribonucleoside hydrolase	purine nucleosidase activity	purine nucleoside catabolic process
		TraesCS1B01G073800	F-box family protein	NA	NA

		TraesCS1B01G073900	Heavy metal transport/detoxification protein	NA	NA
		TraesCS1B01G074000	Heavy metal transport/detoxification protein	NA	NA
		TraesCS1B01G074100	Heavy metal transport/detoxification superfamily protein, putative	NA	NA
		TraesCS1B01G074200	Heavy metal transport/detoxification protein	NA	NA
		TraesCS1B01G074300	30S ribosomal protein S4	NA	NA
		TraesCS1B01G074400	tRNA dimethylallyltransferase	protein kinase binding	cellular response to glucose starvation
		TraesCS1B01G074500	DNA/RNA helicase	metal ion binding	NA
		TraesCS1B01G074600	Pentatricopeptide repeat-containing protein	NA	NA
RAC875_c42715_856	1B	TraesCS1B01G149300	plant U-box 26	NA	NA
		TraesCS1B01G149400	Ubiquitin carboxyl-terminal hydrolase-like protein	thiol-dependent deubiquitinase	protein deubiquitination
		TraesCS1B01G149500	Prolyl 4-hydroxylase alpha subunit, putative	L-ascorbic acid binding	NA
		TraesCS1B01G149600	Glycerol-3-phosphate acyltransferase	glycerol-3-phosphate 2-O-acyltransferase activity	cutin biosynthetic process
BobWhite_c13654_447	1B	TraesCS1B01G070500	F-box family protein	NA	NA
		TraesCS1B01G070600	F-box family protein	NA	NA
		TraesCS1B01G070700	Ubiquitin activating enzyme E1	ubiquitin-like modifier activating enzyme activity	NA
		TraesCS1B01G070800	Vitamin B12 transporter BtuB	NA	NA
		TraesCS1B01G070900	Ubiquitin activating enzyme E1	ubiquitin-like modifier activating enzyme activity	NA
		TraesCS1B01G071000	F-box family protein	NA	NA
		TraesCS1B01G071100	Vitamin B12 transporter BtuB	NA	NA
		TraesCS1B01G071200	Protein SENSITIVITY TO RED LIGHT REDUCED 1	NA	microtubule-based process
		TraesCS1B01G071300	DUF1639 family protein	NA	NA
		TraesCS1B01G071400	Nuclear factor related to kappa-B-binding protein	NA	NA
		TraesCS1B01G071500	Kinesin-like protein	microtubule binding	microtubule-based movement
		TraesCS1B01G071600	Pentatricopeptide repeat-containing protein	NA	NA
		TraesCS1B01G071700	Zinc finger family protein	NA	regulation of transcription by RNA polymerase II
		TraesCS1B01G072300	Pentatricopeptide repeat-containing protein	NA	NA
		TraesCS1B01G073500	evolutionarily conserved C-terminal region 6	NA	NA
		TraesCS1B01G073600	F-box family protein	NA	SCF-dependent proteasomal ubiquitin-dependent protein catabolic process

		TraesCS1B01G073700	Pyrimidine-specific ribonucleoside hydrolase	purine nucleosidase activity	purine nucleoside catabolic process
		TraesCS1B01G073800	F-box family protein	NA	NA
		TraesCS1B01G073900	Heavy metal transport/detoxification protein	NA	NA
		TraesCS1B01G074000	Heavy metal transport/detoxification protein	NA	NA
		TraesCS1B01G074500	DNA/RNA helicase	metal ion binding	NA
		TraesCS1B01G074600	Pentatricopeptide repeat-containing protein	NA	NA
Ex_c4206_502	1B	TraesCS1B01G401200	F-box protein	NA	NA
		TraesCS1B01G401300	Oligopeptide transporter	oligopeptide transmembrane transporter activity	NA
		TraesCS1B01G401400	Short-chain dehydrogenase/reductase	oxidoreductase activity	NA
		TraesCS1B01G401500	Kinase family protein	ATP binding	phosphorylation of RNA polymerase II C-terminal domain
		TraesCS1B01G401600	Oligopeptide transporter	NA	protein transport
		TraesCS1B01G401700	Myb transcription factor	NA	NA
		TraesCS1B01G401800	Syntaxin, putative	SNAP receptor activity	intracellular protein transport
		TraesCS1B01G401900	Thioredoxin family protein	NA	NA
		TraesCS1B01G402000	Fasciclin-like arabinogalactan-protein-like	NA	plant-type secondary cell wall biogenesis
		TraesCS1B01G402100	Disease resistance protein RPM1	ATP binding	NA
		TraesCS1B01G403500	NBS-LRR disease resistance protein-like	ADP binding	defense response
		TraesCS1B01G403600	50S ribosomal protein L7/L12	structural constituent of ribosome	translation
		TraesCS1B01G403700	ER membrane protein complex subunit 6	NA	autophagosome assembly
		TraesCS1B01G403900	Avr9/Cf-9 rapidly elicited protein	NA	NA
		TraesCS1B01G404000	Phosphatidylserine synthase 2	L-serine-phosphatidylethanolamine phosphatidyltransferase activity	phosphatidylserine biosynthetic process
		TraesCS1B01G404100	Gibberellin-regulated family protein	NA	NA
		TraesCS1B01G404200	Cyclin-D1-binding protein 1	NA	regulation of cell cycle
BS00022180_51	1B	TraesCS1B01G000200	Disease resistance protein RPM1	ADP binding	NA
		TraesCS1B01G000300	Disease resistance protein (NBS-LRR class) family	ADP binding	chaperone-mediated protein transport
		TraesCS1B01G000400	Disease resistance protein (TIR-NBS-LRR class) family	ADP binding	protein ubiquitination
		TraesCS1B01G000500	Disease resistance protein (NBS-LRR class) family	ADP binding	defense response
		TraesCS1B01G000600	50S ribosomal protein L28	structural constituent of ribosome	translation
		TraesCS1B01G000700	Serine/threonine-protein kinase ATM	NA	NA

		TraesCS1B01G000800	Peroxisomal membrane protein PEX14	signaling receptor binding	protein import into peroxisome matrix, docking
		TraesCS1B01G000900	RING-finger ubiquitin ligase	NA	NA
		TraesCS1B01G001000	Tripartite motif-containing protein 29	NA	NA
		TraesCS1B01G001100	Nucleic acid-binding, OB-fold-like protein	NA	NA
		TraesCS1B01G001200	Frigida-like protein	NA	NA
		TraesCS1B01G001400	Pheophorbide a oxygenase family protein with Rieske 2Fe-2S domain-containing protein	NA	NA
		TraesCS1B01G001500	Receptor-like kinase	ATP binding	NA
		TraesCS1B01G001600	Adenylyl cyclase-associated protein 1	NA	NA
		TraesCS1B01G001700	Cytochrome P450	heme binding	NA
		TraesCS1B01G002900	NBS-LRR-like resistance protein	ADP binding	defense response
		TraesCS1B01G003000	Disease resistance protein (TIR-NBS-LRR class) family	NA	NA
		TraesCS1B01G003100	Disease resistance protein (TIR-NBS-LRR class) family	ADP binding	NA
		TraesCS1B01G003200	receptor-like protein kinase 1	ATP binding	NA
		TraesCS1B01G003300	receptor kinase 1	NA	NA
		TraesCS1B01G003400	receptor kinase 1	ATP binding	NA
		TraesCS1B01G003500	TRAF type zinc finger domain containing 1	NA	NA
		TraesCS1B01G003600	Disease resistance protein (NBS-LRR class) family	ADP binding	NA
Kukri_c37212_1286	1A	TraesCS1B01G014800	Pm3-like disease resistance protein	ADP binding	NA
		TraesCS1B01G014900	Pm3-like disease resistance protein	protein serine kinase activity	recognition of pollen
		TraesCS1B01G015000	Disease resistance protein	NA	NA
		TraesCS1B01G015100	S-locus lectin protein kinase family protein	NA	NA
		TraesCS1B01G015200	Myb/SANT-like DNA-binding domain protein	NA	NA
		TraesCS1B01G015300	Pm3-like disease resistance protein	ADP binding	NA
		TraesCS1B01G015400	SNF2 domain-containing protein / helicase domain-containing protein / zinc finger protein-like protein	NA	NA
		TraesCS1B01G015500	cysteine-rich RLK (RECEPTOR-like protein kinase) 37	NA	NA
		TraesCS1B01G015600	S-locus lectin protein kinase family protein	NA	NA
		TraesCS1B01G015700	S-locus lectin protein kinase family protein	NA	NA
		TraesCS1B01G015800	Dirigent protein	oxidoreductase activity	fatty acid biosynthetic process

		TraesCS1B01G015900	Cytochrome P450	heme binding	NA
		TraesCS1B01G016000	Pm3-like disease resistance protein	ADP binding	NA
		TraesCS1B01G016100	Pm3-like disease resistance protein	ADP binding	NA
		TraesCS1B01G016200	E3 ubiquitin-protein ligase SINA-like 2	NA	NA
		TraesCS1B01G016300	Dirigent protein	carbohydrate binding	
		TraesCS1B01G016400	Glucan 1,3-beta-glucosidase	actin filament binding	actin filament bundle assembly
		TraesCS1B01G016500	HXXXD-type acyl-transferase family protein	transferase activity, transferring acyl groups other than amino-acyl groups	NA
		TraesCS1B01G016600	O-methyltransferase-like protein	O-methyltransferase activity	aromatic compound biosynthetic process
		TraesCS1B01G016700	Protein DETOXIFICATION	antiporter activity	NA
		TraesCS1B01G016800	cytochrome oxidase assembly protein	NA	NA
		TraesCS1B01G016900	bZIP transcription factor, putative (DUF1664)	NA	NA
		TraesCS1B01G017000	Dirigent protein	carbohydrate binding	NA
		TraesCS1B01G018200	Arginine decarboxylase	arginine decarboxylase activity	arginine catabolic process
		TraesCS1B01G018300	Serine/threonine-protein kinase	ATP binding	recognition of pollen
		TraesCS1B01G018500	Serine/threonine-protein kinase	ATP binding	recognition of pollen
		TraesCS1B01G018600	Serine/threonine-protein kinase	ATP binding	recognition of pollen
		TraesCS1B01G018700	12-oxophytodienoate reductase-like protein	FMN binding	fatty acid biosynthetic process
		TraesCS1B01G018800	12-oxophytodienoate reductase-like protein	FMN binding	fatty acid biosynthetic process
		TraesCS1B01G018900	Ras-related protein, expressed	GTPase activity	NA
		TraesCS1B01G019000	Disease resistance protein (NBS-LRR class) family	ADP binding	defense response
		TraesCS1B01G019100	Ras-like protein	GTPase activity	regulation of transcription by RNA polymerase II
		TraesCS1B01G019200	Tubulin-specific chaperone cofactor E-like protein	NA	proteasome-mediated ubiquitin-dependent protein catabolic process
		TraesCS1B01G019300	Chaperone protein dnaJ	NA	NA
		TraesCS1B01G019400	Glutathione S-transferase	glutathione transferase activity	NA
		TraesCS1B01G019500	Serine/threonine-protein kinase	ATP binding	recognition of pollen
Kukri_c2332_1093	1B	TraesCS1B01G016100	Pm3-like disease resistance protein	ADP binding	NA
		TraesCS1B01G016200	E3 ubiquitin-protein ligase SINA-like 2	NA	NA
		TraesCS1B01G016300	Dirigent protein	carbohydrate binding	NA
		TraesCS1B01G016400	Glucan 1,3-beta-glucosidase	actin filament binding	actin filament bundle assembly

		TraesCS1B01G016500	HXXXD-type acyl-transferase family protein	transferase activity, transferring acyl groups other than amino-acyl groups	NA
		TraesCS1B01G016600	O-methyltransferase-like protein	O-methyltransferase activity	aromatic compound biosynthetic process
		TraesCS1B01G016700	Protein DETOXIFICATION	antiporter activity	NA
		TraesCS1B01G016800	cytochrome oxidase assembly protein	NA	NA
		TraesCS1B01G016900	bZIP transcription factor, putative (DUF1664)	NA	NA
		TraesCS1B01G017000	Dirigent protein	carbohydrate binding	NA
		TraesCS1B01G017100	Serine/threonine-protein kinase 19	protein serine/threonine kinase activity	protein phosphorylation
		TraesCS1B01G018100	Defensin	defense response	NA
		TraesCS1B01G018200	Arginine decarboxylase	arginine decarboxylase activity	arginine catabolic process
		TraesCS1B01G018300	Serine/threonine-protein kinase	ATP binding	recognition of pollen
		TraesCS1B01G018500	Serine/threonine-protein kinase	ATP binding	recognition of pollen
		TraesCS1B01G018600	Serine/threonine-protein kinase	ATP binding	recognition of pollen
		TraesCS1B01G018700	12-oxophytodienoate reductase-like protein	FMN binding	fatty acid biosynthetic process
		TraesCS1B01G018800	12-oxophytodienoate reductase-like protein	FMN binding	fatty acid biosynthetic process
		TraesCS1B01G018900	Ras-related protein, expressed	GTPase activity	NA
		TraesCS1B01G019000	Disease resistance protein (NBS-LRR class) family	ADP binding	defense response
		TraesCS1B01G019100	Ras-like protein	GTPase activity	regulation of transcription by RNA polymerase II
		TraesCS1B01G019200	Tubulin-specific chaperone cofactor E-like protein	NA	proteasome-mediated ubiquitin-dependent protein catabolic process
		TraesCS1B01G019300	Chaperone protein dnaJ	NA	NA
		TraesCS1B01G019400	Glutathione S-transferase	glutathione binding	NA
		TraesCS1B01G019500	Serine/threonine-protein kinase	protein serine kinase activity	recognition of pollen
		TraesCS1B01G020400	NBS-LRR disease resistance protein, putative, expressed	ADP binding	defense response
		TraesCS1B01G020500	Wall-associated receptor kinase-like protein	ATP binding	NA
		TraesCS1B01G020600	Receptor-like kinase	ATP binding	NA
		TraesCS1B01G020700	Receptor-like kinase protein	ATP binding	NA
		TraesCS1B01G020800	transmembrane protein, putative (DUF594)	NA	NA
BS00083533_51	1B	TraesCS1B01G084500	Receptor-like kinase	ATP binding	defense response to bacterium
		TraesCS1B01G084600	Beta 1, 3 galactosyltransferase	NA	NA

	TraesCS1B01G084700	Dihydrolipoyl dehydrogenase	dihydrolipoyl dehydrogenase activity	cell redox homeostasis
	TraesCS1B01G084800	Pentatricopeptide repeat-containing protein	NA	NA
	TraesCS1B01G084900	TAF RNA polymerase I subunit A	NA	NA
	TraesCS1B01G085000	Kinase family protein	3'-phosphoadenosine 5'-phosphosulfate transmembrane transporter activity	NA
	TraesCS1B01G085300	Pentatricopeptide repeat-containing protein	NA	NA
	TraesCS1B01G085400	Pentatricopeptide repeat-containing protein	NA	NA
	TraesCS1B01G085500	Mitochondrial transcription termination factor family protein, putative	double-stranded DNA binding	DNA-templated transcription, termination
	TraesCS1B01G085600	F-box/LRR-repeat protein	NA	NA
	TraesCS1B01G085700	DHHC-type zinc finger family protein	NA	NA
	TraesCS1B01G085800	Polyribonucleotide nucleotidyltransferase	RNA binding	mRNA processing
	TraesCS1B01G085900	Pentatricopeptide repeat-containing protein	NA	endomembrane system organization

Supplementary Table 2. S5. Gene list of *Ababidopsis thaliana* derived from Verslues et al. 2014 related to proline value and their homologs in wheat

***A. thaliana* (TAIR10)**	**Wheat (A genome)**	**position**	**Description**	**Wheat (B genome)**	
AT4G27720	TraesCS1B02G198500	chr1B:356452352-356456070(-)	Molybdate-anion transporter	TraesCS1A02G182400	chr1A:330082865-330086356(+)
AT5G54940	TraesCS3A02G327200	chr3A:572321308-572323747(-)	Protein translation factor SUI1 homolog	TraesCS3B02G356600	chr3B:566834460-566836799(-)
AT5G54950	TraesCS5A02G505000	chr5A:670406887-670414323(-)	Aconitate hydratase 3, mitochondrial	TraesCS4B02G335100	chr4B:626007336-626012023(-)
AT4G27700	TraesCS5A02G315800	chr5A:526396904-526400499(-)	Rhodanese-like domain-containing protein 14	TraesCS5B02G316400	chr5B:498883332-498887124(-)
AT3G51050	TraesCS2B02G586700	chr2B:773343822-773350031(+)	NA	TraesCS6A02G001600	chr6A:795316-801602(-)
AT3G51090	TraesCS7A02G383300	chr7A:558393101-558398578(+)	Coiled-coil domain-containing protein 90B, mitochondrial	TraesCS7B02G286200	chr7B:521566579-521572697(+)
AT4G27690	TraesCS4A02G164600	chr4A:381219904-381228055(-)	Vacuolar protein sorting-associated protein 26A	TraesCSU02G067300	chrUn:52971115-52974962(+)

AT1G30470	TraesCS2A02G464100	chr2A:709827740-709837331(+)	Serine/threonine-protein phosphatase 6 regulatory subunit 3	TraesCS2B02G485800	chr2B:683021366-683029982(+)
AT4G33250	TraesCS4A02G005900	chr4A:3442130-3445402(+)	Eukaryotic translation initiation factor 3 subunit K	TraesCS4B02G299200	chr4B:585465756-585469091(-)
AT5G55020	TraesCS4A02G458800	chr4A:724399991-724400260(-)	Transcription factor MYB93		
AT1G30480	TraesCS3A02G086900	chr3A:56215736-56218797(-)	DNA-damage-repair/toleration protein DRT111, chloroplastic	TraesCS3B02G102300	chr3B:68899038-68902413(-)
AT5G04820	TraesCS5A02G126300	chr5A:278299188-278300518(-)	Transcription repressor OFP13	TraesCS5B02G125500	chr5B:228270516-228271951(-)

Supplemental table 2. S6. List of SNP loci identified in present study their co-localization with yield QTLs

Marker	Chr	Genetic variance	Physical position		Location on 1B chr
JD_c12243_360	1B	10.01	56879853	Yld.cim-1BS.2 to Yld.cim-1BS.6	44616777 to 71297383
BS00105606_51	1B	10.02	56316838	Yld.cim-1BS.2 to Yld.cim-1BS.6	44616777 to 71297383
BS00074962_51	1B	9.95	15658634	Yld.cim-1BS.1	17892184 to 41,088,103
Excalibur_rep_c68921_433	1B	9.8	2.28E+08		
RAC875_c42715_856	1B	9.55	2.22E+08		
BobWhite_c13654_447	1B	9.65	2.02E+08		
Ex_c4206_502	1B	10.05	6.32E+08		
BS00022180_51	1B	9.2	1203909		
Kukri_c37212_1286	1A	9.71	8242603		
Kukri_c2332_1093	1B	8.9	8675010		
BS00083533_51	1B	9.5	69906151	Yld.cim-1BS.2 to Yld.cim-1BS.6	44616777 to 71297383

Supplementary Table 2. S7. List of cultivars belongs C and T allele and contributed to higher and lower RPVs

Cultivar Name	JD_c12243_360	RPV
Claire	C	1395
Benni multifloret	C	1640
Vuka	C	2107
Anapolis	C	2126
Tommi	C	2141
Profilus	C	2158
Carenius	C	2207
Sperber	C	2247
Einstein	T	4205
Oakley	T	2859
Memory	T	3313
Kurt	T	2343
Zappa	T	2827
Chevalier	T	2254
Gordian	T	2698
Mentor	T	2706
Average	Allele (T)	2003
	Allele (C)	2901
	P value	0.002068

Supplementary Table 3. S1. Brief description of the 184 wheat cultivars used in this study

SL No.	Pro study	H_2O_2 study	Varieties	Year	Origin
1	TG001	TG001	Einstein	2002	UK
2	TG002	TG002	Oakley	2006	UK
3	TG003	-	Jafet	2008	Germany
4	TG005	TG005	Rebell	2013	Germany
5	TG006	-	Memory	2013	Germany
6	TG007	-	Kurt	2013	Germany
7	TG008	TG008	Zappa	2009	Germany
8	TG009	TG009	Chevalie	2006	France
9	TG010	TG010	Gordian	2013	Germany
10	TG011	TG011	Mentor	2012	Germany
11	TG012	TG012	Meister	2010	Germany
12	TG013	TG013	KWS_Sant	2010	England
13	TG014	TG014	Brigand	2002	UK
14	TG015	TG015	Profilus	2008	Germany
15	TG016	TG016	Durin	2006	UK
16	TG018	TG018	Paroli	2004	Germany
17	TG020	TG020	Kronjuwe	1980	Czech Republic
18	TG021	TG021	Desamo	2013	Germany
19	TG022	TG022	Carenius	2006	Germany
20	TG023	TG023	Mulan	2006	Germany
21	TG025	TG025	Nelson	2011	Germany
22	TG027	TG027	Goetz	1978	France
23	TG028	TG028	Robigous	2002	England
24	TG029	TG029	Anapolis	2013	Germany
25	TG030	TG030	Solstice	2001	England
26	TG031	TG031	Biscay	2000	Germany
27	TG032	TG032	Capone	2012	Germany
28	TG033	TG033	Tabasco	2008	Germany
29	TG035	TG035	Cubus	2002	Germany
30	TG036	-	Edward	2013	Germany
31	TG037	TG037	Famulus	2010	Germany
32	TG038	TG038	Dekan	1999	Germany
33	TG039	-	SW_Toppe	2002	Germany
34	TG040	TG040	Matrix	2010	Germany
35	TG041	TG041	Jenga	2007	Germany
36	TG043	-	TJB_990_15	2003	UK
37	TG044	TG044	Forum	2012	Germany
38	TG045	TG045	Colonia	2011	Germany
39	TG046	TG046	Transit	1994	Germany
40	TG047	TG047	Potenzia	2006	Germany
41	TG048	TG048	Gaucho	2005	USA

42	TG049	TG049	Tarso	1994	Germany
43	TG050	TG050	Hermann	2004	Germany
44	TG051	TG051	Glaucus	2011	Germany
45	TG052	TG052	Tuareg	2005	Germany
46	TG053	TG053	Atomic	2012	Germany
47	TG054	TG054	Tobak	2011	Germany
48	TG055	-	Pionier	2013	Germany
49	TG056	TG056	Manager	2006	Germany
50	TG058	TG058	Limes	2003	Germany
51	TG059	TG059	Ritmo	1993	Germany
52	TG060	TG060	Kalahari	2010	Germany
53	TG061	-	Intro	2011	Germany
54	TG062	TG062	Oxal	2010	Germany
55	TG063	-	Zobel	2006	Germany
56	TG065	TG065	Joker	2012	Germany
57	TG066	-	Global	2009	Germany
58	TG067	TG067	Elixer	2012	Germany
59	TG068	TG068	Fedor	2007	Germany
60	TG069	TG069	Türkis	2004	Turkey
61	TG070	TG070	Skagen	2006	Germany
62	TG071	TG071	Greif	1989	Germany
63	TG072	TG072	Esket	2007	Germany
64	TG073	TG073	Primus	2009	Germany
65	TG074	TG074	Skalmeje	2006	Germany
66	TG076	TG076	Enorm	2002	Germany
67	TG078	TG078	Skater	2000	Germany
68	TG079	TG079	Brillant	2005	Germany
69	TG080	-	Inspirat	2007	Germany
70	TG082	TG082	Ellvis	2002	Germany
71	TG084	TG084	Maris_Hu	1975	UK
72	TG085	TG085	SY_Ferry	2012	Germany
73	TG087	TG087	Sponsor	1995	France
74	TG088	TG088	Impressi	2005	Germany
75	TG089	TG089	Winnetou	2002	Germany
76	TG090	TG090	Toronto	1990	Germany
77	TG091	TG091	Torrild	2005	Germany
78	TG092	TG092	Contra	1990	Germany
79	TG093	TG093	Schamane	2005	Germany
80	TG094	TG094	Granada	1980	Germany
81	TG095	TG095	KWS_Coba	2013	Germany
82	TG096	TG096	Tommi	2002	Germany
83	TG097	TG097	Saturn	1973	Germany
84	TG098	TG098	Severin	1980	Belgium
85	TG099	TG099	JB_Asano	2008	Germany

86	TG100	TG100	Kerubino	2004	Czech Republic
87	TG101	TG101	Arktis	2010	Germany
88	TG102	TG102	Urban	1980	Germany
89	TG103	TG103	Orestis	1988	Germany
90	TG104	TG104	Flair	1996	Germany
91	TG105	TG105	Anthus	2005	Germany
92	TG106	TG106	Bombus	2012	Germany
93	TG107	TG107	Lucius	2006	Germany
94	TG108	TG108	Herzog	1986	Germany
95	TG109	TG109	Sorbas	1985	Germany
96	TG110	TG110	Tabor	1979	Germany
97	TG111	-	Terrier	2001	Germany
98	TG112	TG112	Magister	2005	Germany
99	TG113	TG113	Altos	2000	Germany
100	TG114	-	Progress	2000	France
101	TG116	TG116	Avenir	2013	Germany
102	TG117	TG117	Pantus	1966	Germany
103	TG118	TG118	Drifter	1999	Germany
104	TG120	TG120	Kranich	2007	Germany
105	TG121	TG121	Sperber	1982	Germany
106	TG123	TG123	Helios	1980	USA
107	TG124	TG124	Obelisk	1987	Netherlands
108	TG125	TG125	Magnus	2000	Germany
109	TG126	-	Disponen	1975	Germany
110	TG127	TG127	Tambor	1993	Germany
111	TG128	TG128	Boxer	2013	Germany
112	TG129	TG129	Sokrates	2001	Germany
113	TG130	TG130	Carisupe	1975	Germany
114	TG131	TG131	Rektor	1980	Germany
115	TG132	TG132	Alves	2010	Germany
116	TG133	TG133	NaturaSt	2002	Germany
117	TG134	TG134	Alidos	1987	Germany
118	TG135	TG135	Monopol	1975	Germany
119	TG136	TG136	Akratos	2004	Germany
120	TG137	TG137	Knirps	1985	Germany
121	TG138	TG138	Bussard	1990	Germany
122	TG141	TG141	Tiger	2001	Germany
123	TG142	TG142	Ibis	1991	Chile
124	TG143	TG143	Batis	1994	Czech Republic
125	TG144	TG144	Topfit	1972	Germany
126	TG145	TG145	Akteur	2003	Germany
127	TG147	TG147	Asketis	1998	Germany
128	TG148	TG148	Aristos	1997	Germany
129	TG149	TG149	Zentos	1989	Germany

130	TG150	TG150	Diplomat	1966	Germany
131	TG152	TG152	Basalt	1980	Germany
132	TG153	TG153	Kormoran	1973	Germany
133	TG154	TG154	Aron	1992	Germany
134	TG156	TG156	Aszita	2005	Germany
135	TG158	TG158	Carimult	1975	Germany
136	TG159	TG159	Admiral	1968	Germany
137	TG160	TG160	Vuka	1975	Germany
138	TG161	TG161	Benno	1973	Germany
139	TG162	TG162	Apollo	1984	France
140	TG163	TG163	Aquila	1979	Italy
141	TG166	TG166	Caribo	1968	Germany
142	TG167	TG167	Butaro	2009	Germany
143	TG168	TG168	Konsul	1990	Germany
144	TG169	TG169	Ares	1983	Germany
145	TG170	TG170	Centurk	2014	USA
146	TG171	-	NS_22_92	2007	Serbien
147	TG172	TG172	Benni_mu	2015	USA
148	TG173	TG173	Hope	1995	USA
149	TG174	TG174	Vel	2001	Germany
150	TG175	TG175	Phoenix	1981	AUS:New-South-Wales
151	TG176	TG176	Mironovs	1970	Ukraine
152	TG177	TG177	Caphorn	2001	UK
153	TG178	TG178	Cordiale	2005	England
154	TG179	TG179	Apache	1998	Czech Republic
155	TG181	TG181	Isengrai	1997	France
156	TG182	TG182	Alixan	2005	France
157	TG183	TG183	Boregan	2008	France
158	TG185	TG185	Tremie	1992	France
159	TG187	TG187	Triple_d	2016	Australia
160	TG188	TG188	Cardos	1998	Germany
161	TG189	TG189	Soissons	1988	France
162	TG190	TG190	BCD_1302	2012	Maldovien
163	TG191	TG191	Arlequin	2007	France
164	TG192	TG192	Sonalika	1978	Indien
165	TG193	TG193	Camp_Rem	1980	France
166	TG194	-	Cajeme_7	1971	Mexico
167	TG195	-	Avalon	2016	UK
168	TG196	TG196	Ivanka	1999	Serbien
169	TG197	TG197	Pobeda	1998	Serbien
170	TG198	TG198	NS_66_92	2015	Serbien
171	TG199	TG199	Mex_3	2003	Mexico
172	TG200	-	Orcas	2010	Germany

173	TG201	TG201	Nimbus	1975	SE
174	TG203	-	Florida	1985	USA
175	TG204	-	Rumor	2013	Germany
176	TG205	TG205	Highbury	2000	UK
177	TG206	TG206	Siete_Ce	2000	Mexico
178	TG207	TG207	Kontrast	1990	Germany
179	TG208	TG208	WW_4180	2004	Germany
180	TG209	TG209	INTRO_61	2011	USA
181	TG210	-	NS_46_90	2014	Serbien
182	TG211	TG211	Mex_17_b	2009	Mexico
183	TG212	TG212	Lambrieg	2013	Chile
184	TG213	TG213	Pegassos	1994	Germany

Supplementary Table 3. S2. List of cultivars for highest and lowest Pro and H_2O_2 accumulation (µg/g fresh weight) under drought condition

Trait	Variety	Origin	Content	Category
Pro	Zobel	Germany	84.51	L
	Akteur	Germany	98.87	L
	Famulus	Germany	142.66	L
	Alixan	France	198.38	L
	Tremie	France	204.75	L
	KWS_Sant	England	230.31	L
	Progress	France	254.91	L
	Highbury	UK	257.95	L
	Boxer	Germany	275.99	L
	Cardos	Germany	280.11	L
	Meister	Germany	2173.39	H
	Benno	Germany	2227.02	H
	Soissons	France	2283.99	H
	TJB_990_15	UK	2292.80	H
	Torrild	Germany	2304.68	H
	Aquila	Italy	2304.96	H
	Topfit	Germany	2337.09	H
	NS_22_92	Serbien	2361.51	H
	Hope	USA	2395.66	H
	Kurt	Germany	2420.55	H
H_2O_2	Urban	Germany	78.09	L
	Carenius	Germany	86.28	L
	Skalmeje	Germany	89.73	L
	Lambrieg	Chile	90.26	L
	Knirps	Germany	91.09	L
	Kontrast	Germany	91.95	L
	Kronjuwe	Czech Republic	97.82	L

Oxal	Germany	99.06	L
Ludwig	Germany	177.76	H
Bussard	Germany	179.36	H
Carimult	Germany	179.48	H
Benni_mu	USA	179.64	H
Alixan	France	181.11	H
Aszita	Germany	195.60	H
Tremie	France	204.05	H
Batis	Czech Republic	207.04	H
Akratos	Germany	207.13	H
Elixer	Germany	216.53	H

Note: L, low proline; H, High proline; Pro=Proline, H_2O_2= Hydrogen peroxide

Supplementary Table 3. S3. List of alleles and the corresponding cultivars linked with highest and lowest STI for Pro and H_2O_2

Trait	Variety	Category	STI	Alleles	Average value of alleles
proline	Akteur	L	0.66	C	C= 1.51, T= 52.23
	Zobel	L	0.69	C	
	Famulus	L	1.19	C	
	Highbury	L	1.25	C	
	Tremie	L	1.45	C	
	Alixan	L	1.75	C	
	Tommi	L	1.85	C	
	Sokrates	L	1.87	C	
	Greif	L	2.12	C	
	Mulan	L	2.24	C	
	Hope	H	38.36	T	
	Vel	H	40.77	T	
	Camp_Rem	H	49.70	T	
	NS_22_92	H	52.26	T	
	Phoenix	H	53.38	T	
	Benni_mu	H	53.66	T	
	Centurk	H	77.54	T	
H_2O_2	Urban	L	0.73	GTA	GTA= 0.91, ACG= 2.68
	Impressi	L	0.85	GTA	
	Lucius	L	0.86	GTA	
	Robigous	L	0.89	GTA	
	Mulan	L	0.94	GTG	
	Bombus	L	0.95	GTA	
	Cardos	L	1.04	GTA	
	WW_4180	L	1.05	GTA	
	BCD_1302	H	2.20	ACG	
	Esket	H	2.31	GTG	
	Highbury	H	2.36	GCG	
	INTRO_61	H	2.52	ACG	
	Alixan	H	2.69	ACG	
	Tremie	H	3.00	ACG	
	Mironovs	H	3.01	ACG	

Note: Abbreviation: L, low STI; H, High STI

Supplementary Table 3. S4. Mean soil moisture content (m^3m^3) under control and drought treatment

Days	Con	Dro
1	0.191	0.190
2	0.191	0.185
3	0.192	0.160
4	0.190	0.130
5	0.189	0.109
6	0.193	0.080
7	0.191	0.067
8	0.191	0.054
9	0.190	0.054
10	0.190	0.053

Supplementary Table 3. S5. Marker, chromosome (Ch), position, P-value, phenotypic variation (PV), allele, favorable (Fav.) allele, t-test value regarding Pro and H_2O_2 accumulation under control condition

Trait	Marker	Ch	Position	P-value	PV (%)	Allele (Major: Minor)	Fav. Allele	T-test value
Pro	AX-158605765	1A	532785236	5.17E-04	3.70	C:T	T	0.04
	AX-158557326	2A	755978749	9.18E-04	3.33	G:A	G	0.03
	wsnp_Ra_c10710_17570054	3B	775826294	6.44E-04	3.47	G:A	A	0.03
	AX-111014946	3B	776359429	7.33E-04	3.47	C:T	T	0.02
	AX-158598616	4A	739522404	6.99E-04	3.81	G:A	G	0.03
	AX-89647929	4B	660137099	5.25E-04	3.58	A:T	T	<0.01
	RAC875_c25733_2477	5A	398191033	4.22E-04	3.70	A:C	A	0.02
	AX-158524974	5B	588516252	1.62E-04	4.26	A:C	C	<0.01
	Kukri_c637_517	5B	711702379	5.42E-04	3.55	A:C	C	<0.01
	wsnp_Ex_c2207_4136036	5B	712600807	5.42E-04	3.55	G:T	G	0.04
	wsnp_Ku_c16116_24914991	5B	712601710	5.42E-04	3.55	C:A	C	<0.01
	wsnp_RFL_Contig3269_3313084	5D	452214851	7.82E-04	3.41	A:G	G	0.03
	AX-158552604	6B	662515354	6.03E-04	3.54	C:A	A	0.01
H_2O_2	AX-158602322	2A	34152277	1.80E-04	8.22	A:G	G	<0.01
	AX-109950638	2A	699433856	2.06E-04	8.06	G:T	T	<0.01
	AX-110541191	2B	12009445	5.32E-04	7.23	A:C	C	<0.01
	Excalibur_c25043_618	2B	797329571	6.26E-04	7.19	T:C	C	<0.01
	BobWhite_c11059_169	2D	32053537	3.22E-04	7.69	A:C	C	<0.01
	wsnp_BE488206B_Ta_2_1	6D	62502596	5.26E-04	7.00	T:C	T	<0.01

Abbreviations: Pro= Proline, H_2O_2= Hydrogen peroxide

Supplementary Table 3. S6. Haplotypes block, number of markers in haplotype block (NMHB), chromosome (Chr), haplotype block (HB) size, haplotype allele and favorable allele regarding Pro and H_2O_2 accumulation under control condition

Traits	Haplotype block	NMHB	Chr	HB size (bp)	Haplotype alleles	Favorable allele
Pro	Pro_1A_Hap4	3	1A	242151	AGC: GGT	GTT
	Pro_5A_Hap2	3	5A	3884028	GAC: TGC	TGC
	Pro_7B_Hap2	3	7B	595	AGA: GAG	GAG
H_2O_2	HP_1B_Hap3	3	1B	24816	ACG: GTG	ACG
	HP_2B_Hap1	11	1B	2193600	GCGCTGTTTGT: ATATCACCCAT	ATATCACCCAT
	HP_6B_Hap1	4	6B	164905	CTAT: TTGC	TTGC

Abbreviations: Pro= Proline, H_2O_2= Hydrogen peroxide

Supplementary Table 3. S7. Correlation of Pro, H_2O_2 and yield related traits under drought stress condition

	PH	GY	PBW	SDW	SN	KN	TKW	DrH_2O_2
GY	0.11							
PBW	0.23	0.96****						
SDW	0.32*	0.79****	0.89****					
SN	-0.05	0.49***	0.48***	0.53****				
KN	-0.11	0.66****	0.55****	0.48***	0.54****			
TKW	0.14	0.46***	0.52***	0.42**	-0.12	0.18		
DrH_2O_2	0.03	-0.11	-0.06	0.02	0.09	-0.14	-0.25	
DrProl	0.24	-0.21	-0.18	0.1	0.08	-0.06	-0.25	0.25

Note: *p<0.05 (2-tailed); **p<0.01 (2-tailed), and ***p<0.0001 (2-tailed). Abbreviations: GY, grain yield; PBW, plant dry biomass weight; SDW, shoot dry matter weight; SN, spike number; KN, kernels number; TKW, thousand kernel weight (TKW); DrH_2O_2, hydrogen peroxide under Dro stress; DrProl, proline content under Dro stress

Supplementary Table 3.S8a. List of putative candidate genes for Pro content under drought (Dro), control (Con) conditions and for STI

Trait	markers	mrnaid	Human-Readable-Description	GO-IDs-(Description)-via-Interpro
Dro		TraesCS1A01G050800.1	Defensin	GO:0006952 BP: defense response
Dro	1A_AX-110539457	TraesCS1A01G050900.1	Defensin	GO:0006952 BP: defense response
Dro		TraesCS1A01G051000.1	F-box protein	NA
Dro		TraesCS1A01G051600.1	F-box family protein	GO:0005515 MF: protein binding
Dro	1A_AX-158540040_Hap	TraesCS1A01G051700.1	Glycine-rich protein A3	GO:0005509 MF: calcium ion binding;GO:0005544 MF: calcium-dependent phospholipid binding
Dro		TraesCS1A01G051900.1	transmembrane protein	NA
Dro	1A_AX-158569423	TraesCS1A01G015300.1	Ras-like protein	GO:0003924 MF: GTPase activity;GO:0005525 MF: GTP binding
Dro		TraesCS1A01G015900.1	Serine/threonine-protein kinase	GO:0004672 MF: protein kinase activity;GO:0004674 MF: protein serine/threonine kinase activity;GO:0005524 MF: ATP
Dro		TraesCS1A01G016000.1	Serine/threonine-protein kinase	GO:0004672 MF: protein kinase activity;GO:0004674 MF: protein
Dro		TraesCS1A01G016100.1	Serine/threonine-protein kinase	GO:0004672 MF: protein kinase activity;GO:0004674 MF: protein serine/threonine kinase activity;GO:0005524 MF: ATP
Dro		TraesCS1A01G016200.1	Disease resistance protein	GO:0043531 MF: ADP binding
Dro		TraesCS1A01G016300.1	Protein kinase family protein	GO:0004672 MF: protein kinase activity;GO:0004674 MF: protein serine/threonine kinase activity;GO:0005509 MF: calcium ion
Dro		TraesCS1A01G016400.1	NBS-LRR disease resistance protein, putative, expressed	GO:0043531 MF: ADP binding
Dro		TraesCS1A01G016500.1	Chromodomain-helicase-DNA-binding protein 8	NA
Dro		TraesCS1A01G016600.1	Protein kinase family protein	GO:0004672 MF: protein kinase activity;GO:0005509 MF: calcium ion binding;GO:0005515
Dro		TraesCS1A01G016700.1	Receptor-like protein kinase	GO:0004672 MF: protein kinase activity;GO:0005524 MF: ATP binding;GO:0006468 BP: protein phosphorylation
Dro		TraesCS1A01G017100.1	Disease resistance protein RPM1	NA
Dro		TraesCS1A01G017200.1	Serine/threonine-protein kinase	GO:0004672 MF: protein kinase activity
Dro	1A_AX-158595597	TraesCS1A01G015100.1	Chaperone protein dnaJ	NA
Dro	1A_AX-158595597_hap	TraesCS1A01G014400.1	Serine/threonine-protein kinase	GO:0004672 MF: protein kinase activity;
Dro		TraesCS1A01G014500.1	Serine/threonine-protein kinase	GO:0004672 MF: protein kinase activity
Dro	1A_BS00070695_51_Hap	TraesCS1A01G050900.1	Defensin	GO:0006952 BP: defense response
Dro		TraesCS1A01G051000.1	F-box protein	NA
Dro		TraesCS1A01G051100.1	F-box/LRR-repeat protein	NA
Dro		TraesCS1A01G051200.1	Casein kinase I	NA
Dro		TraesCS1A01G051300.1	WEB family protein, chloroplastic	NA

Dro		TraesCS1A01G051600.1	F-box family protein	GO:0005515 MF: protein binding
Dro		TraesCS1A01G051700.1	Glycine-rich protein A3	GO:0005509 MF: calcium ion binding;GO:0005544 MF: calcium-dependent phospholipid binding
Dro	1A_BS00084022_51	TraesCS1A01G049200.1	NADH dehydrogenase subunit 2	NA
Dro		TraesCS1A01G051000.1	F-box protein	NA
Dro		TraesCS1A01G051100.1	F-box/LRR-repeat protein	NA
Dro		TraesCS1A01G051200.1	Casein kinase I	NA
Dro		TraesCS1A01G051900.1	transmembrane protein	NA
Dro	1A_Kukri_c82555_88	TraesCS1A01G052000.1	Wuschel-related homeobox protein	GO:0003677 MF: DNA binding
Dro		TraesCS1A01G052100.1	Calreticulin	GO:0005509 MF: calcium ion binding;
Dro		TraesCS1A01G052200.1	NA	NA
Dro	1A_RFL_Contig1027_442	TraesCS1A01G012900.1	Fatty acid oxidation complex subunit alpha	GO:0003824 MF: catalytic activity;GO:0008152 BP: metabolic process
Dro		TraesCS1A01G013000.1	Disease resistance family protein	GO:0043531 MF: ADP binding
Dro		TraesCS1A01G013000.2	NA	NA
Dro		TraesCS1A01G013100.1	MADS-box transcription factor family protein	GO:0003677 MF: DNA binding;GO:0046983 MF: protein dimerization activity
Dro		TraesCS1A01G013200.1	Ankyrin repeat protein family-like protein	GO:0005515 MF: protein binding
Dro		TraesCS1A01G013900.1	Glutathione s-transferase	GO:0005515 MF: protein binding
Dro		TraesCS1A01G014000.1	Defensin	GO:0006952 BP: defense response
Dro		TraesCS1A01G014100.1	Defensin	GO:0006952 BP: defense response
Dro		TraesCS1A01G014200.1	F-box protein	NA
Dro		TraesCS1A01G014300.1	C2 calcium/lipid-binding and GRAM domain protein	GO:0005515 MF: protein binding
Dro		TraesCS1A01G014400.1	Serine/threonine-protein kinase	GO:0004672 MF: protein kinase activity;GO:0005524 MF: ATP binding;GO:0006468 BP: protein phosphorylation
Dro		TraesCS1A01G014500.1	Serine/threonine-protein kinase	GO:0004672 MF: protein kinase activityBP: protein phosphorylation;GO:0048544 BP: recognition of pollen
Dro		TraesCS3B01G039100.1	MYB transcription factor	GO:0003677 MF: DNA binding
Dro	3B_AX-89548463	TraesCS3B01G039200.1	NBS-LRR disease resistance protein	GO:0043531 MF: ADP binding
Dro		TraesCS3B01G039300.1	Protein DETOXIFICATION	GO:0006855 BP: drug transmembrane transport;GO:0015238 MF: drug transmembrane transporter activity;
Dro		TraesCS3B01G039100.1	MYB transcription factor	GO:0003677 MF: DNA binding
Dro	3B_AX-89747894_Hap	TraesCS3B01G039200.1	NBS-LRR disease resistance protein	GO:0043531 MF: ADP binding
Dro		TraesCS3B01G039300.1	Protein DETOXIFICATION	GO:0006855 BP: drug transmembrane transport
Dro		TraesCS3B01G040200.1	Zinc finger family protein	GO:0003676 MF: nucleic acid binding

Dro	3B_AX-158538340	TraesCS3B01G040300.1	DUF1666 family protein	NA
Dro		TraesCS3B01G040400.1	30S ribosomal protein S10	GO:0003735 MF: structural constituent of ribosome;GO:0005840 CC: ribosome;GO:0006412 BP: translation
Dro		TraesCS3B01G041200.1	Protein NEGATIVE REGULATOR OF RESISTANCE	GO:0010112 BP: regulation of systemic acquired resistance
Dro		TraesCS3B01G041300.1	Disease resistance protein RPM1	GO:0043531 MF: ADP binding
Dro		TraesCS3B01G041400.1	Disease resistance protein (NBS-LRR class) family	GO:0043531 MF: ADP binding
Dro		TraesCS3B01G041500.1	F-box family protein	GO:0005515 MF: protein binding
Dro		TraesCS3B01G041600.1	NA	NA
Dro		TraesCS3B01G041600.2	HIPL1 protein	GO:0003824 MF: catalytic activity;GO:0005975 BP: carbohydrate metabolic process
Dro		TraesCS3B01G040200.1	Zinc finger family protein	GO:0003676 MF: nucleic acid binding
Dro	3B_AX-158541844	TraesCS3B01G040300.1	DUF1666 family protein	NA
Dro		TraesCS3B01G040400.1	30S ribosomal protein S10	GO:0003735 MF: structural constituent of ribosome;GO:0005840 CC: ribosome;GO:0006412 BP: translation
Dro		TraesCS3B01G040500.1	Cytochrome b6-f complex subunit 5	GO:0009512 CC: cytochrome b6f complex
Dro		TraesCS3B01G041400.1	Disease resistance protein (NBS-LRR class) family	GO:0043531 MF: ADP binding
Dro		TraesCS3B01G041500.1	F-box family protein	GO:0005515 MF: protein binding
Dro		TraesCS3B01G041600.1	NA	NA
Dro	3B_CAP12_rep_c3868_270	TraesCS3B01G000900.1	Ankyrin repeat protein family-like protein	GO:0005515 MF: protein binding
Dro		TraesCS3B01G001000.1	Receptor-like protein kinase	GO:0004672 MF: protein kinase activity;GO:0005524 MF: ATP binding;GO:0006468 BP: protein phosphorylation
Dro		TraesCS4A01G049700.1	Syntaxin protein	GO:0016020 CC: membrane;GO:0016192 BP: vesicle-mediated transport;GO:0048193 BP: Golgi vesicle transport
Dro	4A_AX-108953213_Hap	TraesCS4A01G049800.1	60S ribosomal protein L51, mitochondrial	NA
Dro		TraesCS4A01G049900.1	Protein kinase	GO:0004672 MF: protein kinase activity;GO:0005524 MF: ATP binding;
Dro		TraesCS4A01G050000.1	Phosphatase 2C family protein	GO:0003824 MF: catalytic activity;GO:0043169 MF: cation binding
Dro		TraesCS4A01G050100.1	Tetratricopeptide repeat protein 1	GO:0005488 MF: binding;GO:0005515 MF: protein binding
Dro		TraesCS4A01G050200.1	Retinoblastoma-binding protein 5	GO:0005515 MF: protein binding
Dro		TraesCS4A01G053700.1	Plant calmodulin-binding-like protein	GO:0005516 MF: calmodulin binding
Dro	4A_AX-111497637	TraesCS4A01G053800.1	NA	NA
Dro		TraesCS4A01G053800.2	Remorin family protein	NA
Dro		TraesCS4A01G053900.1	Pentatricopeptide repeat-containing protein	NA
Dro		TraesCS4A01G068500.1	Curculin-like mannose-binding lectin family protein	NA

Dro	4A_AX-158549920_Hap	TraesCS4A01G068600.1	Collagen, type IV, alpha 5	NA
Dro		TraesCS4A01G068700.1	Proline-rich protein	NA
Dro		TraesCS4A01G068800.1	NA	NA
Dro		TraesCS4A01G071300.2	26S proteasome non-ATPase regulatory subunit 4	NA
Dro		TraesCS4A01G071400.1	Actin-depolymerizing factor	GO:0003779 MF: actin binding;GO:0005622 CC: intracellular
Dro				
Dro		TraesCS4A01G052800.1	Myb/SANT-like DNA-binding domain protein	NA
Dro	4A_BS00009970_51	TraesCS4A01G052900.1	ATP synthase subunit b	NA
Dro		TraesCS4A01G053000.1	B3 domain-containing protein	GO:0003677 MF: DNA binding
Dro		TraesCS4A01G053000.2	NA	NA
Dro		TraesCS4A01G054900.1	Hexosyltransferase	GO:0016757 MF: transferase activity, transferring glycosyl groups
Dro	4A_wsnp_Ex_c1520_2906995_Hap	TraesCS4A01G055000.1	Leucine-rich repeat receptor protein kinase	GO:0005515 MF: protein binding
Dro		TraesCS4A01G055100.1	Glycosyltransferase	GO:0008152 BP: metabolic process;GO:0016758 MF: transferase activity, transferring hexosyl groups
Dro		TraesCS4A01G055200.1	Alpha amylase inhibitor protein	NA
Dro		TraesCS4A01G055300.1	Tyrosine-specific transport protein, putative	GO:0003333 BP: amino acid transmembrane transport
Dro		TraesCS5A01G254800.1	DUF2431 domain protein	NA
Dro	5A_wsnp_Ex_c57094	TraesCS5A01G254900.1	DUF2431 domain protein	NA
Dro		TraesCS6B01G472400.1	integral membrane metal-binding family protein (DUF2296)	NA
Dro	6B_RAC875_c49751_75	TraesCS6B01G472400.2	NA	NA
Dro		TraesCS6B01G472500.1	alpha-1,3-mannosyl-glycoprotein beta-1,2-N-acetylglucosaminyltransferase	NA
Dro		TraesCS6B01G472600.1	proton-dependent oligopeptide transport (POT) family protein	NA
Dro		TraesCS6B01G472700.1	ATP-dependent RNA helicase	GO:0003676 MF: nucleic acid binding;GO:0005524 MF: ATP binding
Dro		TraesCS6B01G472800.1	Calcium uniporter protein, mitochondrial	NA
Dro		TraesCS6B01G472900.1	NA	NA
Dro		TraesCS6B01G472900.2	integral membrane metal-binding family protein (DUF2296)	NA
Dro		TraesCS6B01G472900.3	NA	NA
Dro		TraesCS6B01G473000.1	Mitochondrial intermediate peptidase	GO:0004222 MF: metalloendopeptidase activity;GO:0006508 BP: proteolysis
Dro		TraesCS6B01G473100.1	F-box protein family	NA

Dro		TraesCS6D01G401000.1	60 kDa chaperonin	NA
Dro	6D_AX-110033836_Hap	TraesCS6D01G401100.1	Pentatricopeptide repeat-containing protein	GO:0005515 MF: protein binding
Dro		TraesCS6D01G401200.1	Protease	NA
Dro		TraesCS6D01G401300.1	Plant invertase/pectin methylesterase inhibitor superfamily protein	GO:0004857 MF: enzyme inhibitor activity
Dro		TraesCS6D01G401400.1	Plant invertase/pectin methylesterase inhibitor	GO:0004857 MF: enzyme inhibitor activity
Dro		TraesCS6D01G401500.1	Mitochondrial intermediate peptidase	GO:0004222 MF: metalloendopeptidase activity;GO:0006508 BP: proteolysis
Dro		TraesCS6D01G401600.1	Response regulator	GO:0000160 BP: phosphorelay signal transduction system
Dro		TraesCS6D01G401700.1	integral membrane metal-binding family protein (DUF2296)	NA
Dro		TraesCS6D01G401800.1	Cell surface glycoprotein CD200 receptor 4	NA
Dro		TraesCS6D01G396800.1	Disease resistance protein (NBS-LRR class) family	GO:0043531 MF: ADP binding
Dro	6D_Excalibur_c2991_320	TraesCS6D01G396900.1	NA	NA
Dro		TraesCS6D01G396900.2	Receptor-like protein kinase	GO:0004672 MF: protein kinase activity; binding;GO:0005524 MF: ATP binding;GO:0006468 BP: protein phosphorylation
Dro		TraesCS6D01G397500.1	calcium-dependent protein kinase 18	NA
Dro		TraesCS6D01G397600.1	F-box family protein	GO:0005515 MF: protein binding
Dro		TraesCS6D01G397600.2	NA	NA
Dro		TraesCS6D01G397700.1	Protein kinase superfamily protein	NA
Dro		TraesCS6D01G397800.1	NA	NA
Dro		TraesCS6D01G397800.2	Gibberellin-regulated family protein	NA
Dro		TraesCS6D01G402400.1	RING/U-box superfamily protein	NA
Dro		TraesCS6D01G402500.1	70 kDa heat shock protein	NA
Dro		TraesCS7B01G122600.2	Aquaporin	GO:0005215 MF: transporter activity;GO:0006810 BP: transport;GO:0016020 CC: membrane
Dro	7B_AX-158593686_Hap	TraesCS7B01G122700.1	Non-lysosomal glucosylceramidase	NA
Dro		TraesCS7B01G122800.1	Receptor-like protein kinase	GO:0004672 MF: protein kinase activity;GO:0005524 MF: ATP binding;GO:0006468 BP: protein phosphorylation
Dro		TraesCS7B01G122900.1	Zinc finger family protein	GO:0003676 MF: nucleic acid binding
Dro		TraesCS7B01G123000.1	Glycosyltransferase	GO:0008152 BP: metabolic process;GO:0016758 MF: transferase activity, transferring hexosyl groups
Dro		TraesCS7B01G123100.1	Glycosyltransferase	GO:0008152 BP: metabolic process
Dro		TraesCS7B01G123200.1	U-box domain-containing protein 33	NA
Dro		TraesCS7B01G123300.1	U-box domain-containing family protein	NA

Dro		TraesCS7B01G123400.1	Protein kinase	GO:0004672 MF: protein kinase activity;GO:0005524 MF: ATP binding;GO:0006468 BP: protein phosphorylation
		TraesCS2A01G582700.1	Pentatricopeptide repeat protein	GO:0003676 MF: nucleic acid binding;GO:0005515 MF: protein binding
STI	2A_AX-110412102	TraesCS2A01G582700.2	NA	NA
STI		TraesCS2A01G582800.1	Hydrophobic family protein	GO:0016021 CC: integral component of membrane
STI		TraesCS2A01G582900.1	RNA-binding protein	GO:0003676 MF: nucleic acid binding
STI		TraesCS2A01G583000.1	CCR4-NOT transcription complex family protein	GO:0003676 MF: nucleic acid binding
STI		TraesCS2A01G583100.1	Eukaryotic aspartyl protease family protein, putative	GO:0004190 MF: aspartic-type endopeptidase activity;GO:0006508 BP: proteolysis
STI		TraesCS2A01G585200.1	Disease resistance protein (TIR-NBS-LRR class) family	GO:0043531 MF: ADP binding
STI		TraesCS2A01G585300.1	F-box family protein	NA
STI		TraesCS2A01G585400.1	UBX domain-containing protein	NA
STI		TraesCS2A01G585500.1	NA	NA
STI		TraesCS2A01G585500.2	F-box family protein	GO:0005515 MF: protein binding
STI		TraesCS2A01G585600.1	Heat shock 70 kDa protein	NA
STI		TraesCS2A01G585700.1	Actin-related protein	NA
STI		TraesCS2A01G585800.1	Choline transporter-related family protein	NA
STI		TraesCS2A01G585800.2	NA	NA
STI		TraesCS2A01G585900.1	NA	NA
STI		TraesCS2A01G586000.1	F-box family protein	GO:0005515 MF: protein binding
STI		TraesCS2A01G586000.2	NA	NA
STI		TraesCS2A01G586000.3	NA	NA
STI		TraesCS2A01G586100.1	Acyl-CoA-binding domain-containing protein	GO:0000062 MF: fatty-acyl-CoA binding;GO:0005515 MF: protein binding
STI		TraesCS2A01G586200.1	2-oxoglutarate (2OG) and Fe(II)-dependent oxygenase superfamily protein	NA
STI		TraesCS2A01G586300.1	Ubiquitin-conjugating enzyme E2	NA
STI				
STI		TraesCS2B01G439400.1	Heavy metal transport/detoxification superfamily protein	GO:0030001 BP: metal ion transport;GO:0046872 MF: metal ion binding
STI	2B_AX-158540981	TraesCS2B01G439500.1	APO protein	GO:0003723 MF: RNA binding
STI		TraesCS2B01G439600.1	F-box protein	NA
STI		TraesCS2B01G439700.1	cysteine-rich/transmembrane domain A-like protein	NA

STI		TraesCS2B01G439800.1	cysteine-rich/transmembrane domain A-like protein	NA
STI		TraesCS2B01G440700.1	Cysteine protease, putative	GO:0006508 BP: proteolysis;GO:0008234 MF: cysteine-type peptidase activity
STI		TraesCS2B01G440800.1	Cytochrome P450, putative	GO:0005506 MF: iron ion binding;GO:0016705 MF: oxidoreductase activity
STI		TraesCS2B01G440900.1	MADS-box transcription factor	GO:0003677 MF: DNA binding;GO:0003700 MF: transcription factor activity, sequence-specific DNA binding
STI		TraesCS2B01G441000.1	Dehydrogenase	NA
STI		TraesCS2B01G441100.1	Potassium transporter	GO:0015079 MF: potassium ion transmembrane transporter activity;GO:0016020 CC: membrane;GO:0071805 BP: potassium ion transmembrane transport
STI		TraesCS2B01G441100.2	NA	NA
STI		TraesCS2B01G441200.1	GRF zinc finger-containing protein-like protein	GO:0008270 MF: zinc ion binding
STI		TraesCS2B01G441300.1	F-box protein	GO:0005515 MF: protein binding
STI		TraesCS3A01G479800.1	Pleiotropic drug resistance ABC transporter	GO:0005524 MF: ATP binding;GO:0016020 CC: membrane;GO:0016887 MF: ATPase activity
STI	3A_AX-158523479	TraesCS3A01G479900.1	Expansin protein	GO:0005576 CC: extracellular region;GO:0019953 BP: sexual reproduction
STI		TraesCS3A01G480000.1	Expansin protein	GO:0005576 CC: extracellular region;GO:0019953 BP: sexual reproduction
STI		TraesCS3A01G480100.1	Cytochrome P450, putative, expressed	GO:0005506 MF: iron ion binding;GO:0016705 MF: oxidoreductase activity, acting on paired donors, with incorporation or reduction of molecular oxygen;
STI		TraesCS3A01G480200.1	Endo-1,3-beta-glucanase	GO:0004553 MF: hydrolase activity, hydrolyzing O-glycosyl compounds;GO:0005975 BP: carbohydrate metabolic process
STI		TraesCS3A01G480300.1	Endo-1,3-beta-glucanase	GO:0004553 MF: hydrolase activity, hydrolyzing O-glycosyl compounds;GO:0005975 BP: carbohydrate metabolic process
STI		TraesCS3A01G480400.1	Beta-1,3-glucanase	GO:0004553 MF: hydrolase activity, hydrolyzing O-glycosyl compounds;GO:0005975 BP: carbohydrate metabolic process
STI		TraesCS3A01G480500.1	Bax inhibitor-1 family protein	NA
STI	3B_AX-110362575_Hap	TraesCS3B01G475900.1	NA	NA
STI		TraesCS3B01G475900.2	Aspartokinase	GO:0004072 MF: aspartate kinase activity;GO:0008152 BP: metabolic process;
STI		TraesCS3B01G476000.1	Transcription factor Inducer of CBF expression 1	GO:0046983 MF: protein dimerization activity
STI		TraesCS3B01G476000.2	NA	NA
STI		TraesCS3B01G476100.1	Coiled-coil domain-containing protein SCD2	NA
STI		TraesCS3B01G476200.1	Defensin	GO:0006952 BP: defense response
STI		TraesCS3B01G476300.1	Defensin-like protein	GO:0006952 BP: defense response
STI		TraesCS3B01G476400.1	Ribosomal RNA apurinic site specific lyase-like protein	NA
STI		TraesCS3B01G476500.1	F-box protein	NA
STI		TraesCS3B01G476600.1	methyl-coenzyme M reductase II subunit gamma, putative (DUF3741)	NA

STI		TraesCS3B01G476700.1	Auxin response factor	NA
STI		TraesCS3B01G476800.1	Prefoldin subunit 5	NA
STI		TraesCS3B01G476900.1	F-box protein family	GO:0005515 MF: protein binding
STI		TraesCS3B01G477000.1	E3 ubiquitin protein ligase drip2	NA
STI		TraesCS3B01G477100.1	NA	NA
STI		TraesCS3B01G041700.1	Alpha-glucosidase	GO:0003824 MF: catalytic activity;GO:0004553 MF: hydrolase activity, hydrolyzing O-glycosyl compounds;
STI	3B_AX-111526074_Hap	TraesCS3B01G475800.1	Auxin response factor	GO:0003677 MF: DNA binding;GO:0005515 MF: protein binding;
STI	3B_AX-158548691	TraesCS3B01G475900.1	NA	NA
STI		TraesCS3B01G475900.2	Aspartokinase	GO:0004072 MF: aspartate kinase activity;GO:0008152 BP: metabolic process;GO:0008652
STI		TraesCS3B01G476000.1	Transcription factor Inducer of CBF expression 1	GO:0046983 MF: protein dimerization activity
STI		TraesCS3B01G476400.1	Ribosomal RNA apurinic site specific lyase-like protein	NA
STI		TraesCS3B01G476500.1	F-box protein	NA
STI		TraesCS3B01G476800.1	Prefoldin subunit 5	NA
STI		TraesCS3B01G476900.1	F-box protein family	GO:0005515 MF: protein binding
STI		TraesCS3B01G477000.1	E3 ubiquitin protein ligase drip2	NA
STI		TraesCS3B01G477100.1	NA	NA
STI		TraesCS3B01G477100.2	8-amino-7-oxononanoate synthase	GO:0003824 MF: catalytic activity;GO:0008152 BP: metabolic process;GO:0009058 BP: biosynthetic process;
STI		TraesCS3B01G477400.1	Kinase family protein	GO:0004672 MF: protein kinase activity;GO:0005524 MF: ATP binding;GO:0006468 BP: protein phosphorylation
STI		TraesCS3B01G477500.1	cDNA clone:J013058P10, full insert sequence	NA
STI		TraesCS3B01G477600.1	cDNA clone:J013058P10, full insert sequence	NA
STI		TraesCS3B01G476900.1	F-box protein family	GO:0005515 MF: protein binding
STI	3B_Ku_c1575_338	TraesCS3B01G477000.1	E3 ubiquitin protein ligase drip2	NA
STI		TraesCS3B01G477100.1	NA	NA
STI		TraesCS3B01G477100.2	8-amino-7-oxononanoate synthase	GO:0003824 MF: catalytic activity;GO:0008152 BP: metabolic process;
STI		TraesCS3B01G477400.1	Kinase family protein	GO:0004672 MF: protein kinase activity;GO:0005524 MF: ATP binding;GO:0006468 BP: protein phosphorylation
STI		TraesCS3B01G477500.1	cDNA clone:J013058P10, full insert sequence	NA
STI		TraesCS3B01G477600.1	cDNA clone:J013058P10, full insert sequence	NA
STI		TraesCS3B01G477700.1	Short-chain dehydrogenase/reductase family protein	GO:0016491 MF: oxidoreductase activity

STI		TraesCS3B01G479300.1	NBS-LRR-like resistance protein	NA
STI		TraesCS3B01G479400.1	HTH-type transcriptional activator RhaR	NA
STI		TraesCS3B01G479500.1	2-oxoglutarate (2OG) and Fe(II)-dependent oxygenase superfamily protein	GO:0016491 MF: oxidoreductase activity;GO:0055114 BP: oxidation-reduction process
STI		TraesCS3B01G479600.1	5'-methylthioadenosine/S-adenosylhomocysteine nucleosidase	GO:0003824 MF: catalytic activity;GO:0009116 BP: nucleoside metabolic process
STI				
STI		TraesCS4B01G292500.1	Transcription initiation factor IIE subunit beta	GO:0005673 CC: transcription factor TFIIE complex;GO:0006367 BP: transcription initiation from RNA polymerase II promoter
STI	4B_AX-108829152_Hap	TraesCS4B01G292600.1	N-acetyltransferase, putative	GO:0008080 MF: N-acetyltransferase activity
STI		TraesCS4B01G292700.1	Transmembrane protein, putative	NA
STI		TraesCS4B01G292800.1	BnaC08g32970D protein	NA
STI		TraesCS4B01G292900.1	AP2-like ethylene-responsive transcription factor	GO:0003677 MF: DNA binding;GO:0003700 MF: transcription factor activity,
STI		TraesCS4B01G293000.1	DUF538 family protein, putative (Protein of unknown function, DUF538)	NA
STI		TraesCS4B01G293100.1	DUF538 family protein, putative (Protein of unknown function, DUF538)	NA
STI		TraesCS4B01G293200.1	DUF538 family protein (Protein of unknown function, DUF538)	NA
STI		TraesCS4B01G293300.1	Carboxypeptidase	GO:0004185 MF: serine-type carboxypeptidase activity;GO:0006508 BP: proteolysis
STI		TraesCS4B01G293400.1	E3 Ubiquitin ligase	GO:0004842 MF: ubiquitin-protein transferase activity;GO:0005515 MF: protein binding
STI		TraesCS4B01G293500.1	Membrane lipoprotein, putative	NA
STI		TraesCS4B01G293600.1	NA	NA
STI		TraesCS4B01G293600.2	NA	NA
STI		TraesCS4B01G374900.1	GTP binding Elongation factor Tu family protein	NA
STI	4B_AX-109516903_Hap	TraesCS4B01G375000.1	2-phosphoglycerate kinase, putative, expressed	NA
STI		TraesCS4B01G375100.1	CCR4-NOT transcription complex subunit 1	NA
STI		TraesCS5A01G234100.1	HVA22-like protein	NA
STI	5A_AX-158550762	TraesCS5A01G234200.1	1-aminocyclopropane-1-carboxylate oxidase	GO:0016491 MF: oxidoreductase activity;GO:0055114 BP: oxidation-reduction process
STI		TraesCS5A01G234300.1	1-aminocyclopropane-1-carboxylate oxidase	GO:0016491 MF: oxidoreductase activity;GO:0055114 BP: oxidation-reduction process
STI		TraesCS5A01G234300.2	NA	NA

STI		TraesCS5A01G234400.1	Protein disulfide isomerase	GO:0016853 MF: isomerase activity;GO:0045454 BP: cell redox homeostasis
STI		TraesCS5A01G234500.1	DNA-binding storekeeper protein-related transcriptional regulator, putative	GO:0006355 BP: regulation of transcription, DNA-templated
STI		TraesCS5A01G234600.1	DUF1644 family protein	NA
STI		TraesCS5A01G234700.1	LysM domain-containing GPI-anchored protein 1	NA
STI		TraesCS5A01G234800.1	Aspartic proteinase nepenthesin-1	GO:0004190 MF: aspartic-type endopeptidase activity;GO:0006508 BP: proteolysis
STI		TraesCS5A01G234900.1	FBD-associated F-box protein	GO:0005515 MF: protein binding
STI		TraesCS5A01G235000.1	Aspartic proteinase nepenthesin-1	GO:0004190 MF: aspartic-type endopeptidase activity;GO:0006508 BP: proteolysis
STI		TraesCS5A01G235100.1	F-box protein (DUF295)	NA
STI		TraesCS5A01G235200.1	Ripening-related protein	NA
STI		TraesCS5A01G235300.1	NA	NA
STI		TraesCS5A01G235300.2	NA	NA
STI		TraesCS5A01G235300.3	NA	NA
STI		TraesCS5A01G235300.4	Hexosyltransferase	GO:0006486 BP: protein glycosylation;GO:0008378 MF: galactosyltransferase activity;GO:0016020 CC: membrane
STI		TraesCS5A01G235400.1	Transmembrane protein 50A	NA
STI		TraesCS5A01G235400.2	NA	NA
STI		TraesCS5A01G236400.2	NA	NA
STI		TraesCS5A01G236500.1	F-box protein-like	GO:0005515 MF: protein binding
STI		TraesCS5A01G236600.1	Carbonic anhydrase, putative	GO:0004089 MF: carbonate dehydratase activity;GO:0006730 BP: one-carbon metabolic process;GO:0008270 MF: zinc ion binding
STI		TraesCS5A01G236700.1	Mitochondrial carrier family	NA
STI		TraesCS5A01G236800.1	Acyl-[acyl-carrier-protein] desaturase	GO:0006631 BP: fatty acid metabolic process
STI		TraesCS5A01G516700.1	Non-specific lipid-transfer protein	NA
STI	5A_AX-158585060_Hap	TraesCS5A01G516800.1	Basic-leucine zipper (bZIP) transcription factor family protein	NA
STI		TraesCS5A01G516800.2	NA	NA
STI		TraesCS5A01G516900.1	Heavy metal transport/detoxification superfamily protein	GO:0030001 BP: metal ion transport;GO:0046872 MF: metal ion binding
STI		TraesCS5A01G517000.1	Dihydroflavonol-4-reductase	GO:0003824 MF: catalytic activity;GO:0050662 MF: coenzyme binding
STI		TraesCS5B01G306800.1	Basic helix loop helix (BHLH) family transcription factor	GO:0046983 MF: protein dimerization activity
STI	5B_AX-158525047	TraesCS5B01G306900.1	NA	NA
STI		TraesCS5B01G307000.1	Basic helix loop helix (BHLH) family transcription factor	GO:0046983 MF: protein dimerization activity

STI		TraesCS5B01G307100.1	Basic helix loop helix (BHLH) family transcription factor	GO:0046983 MF: protein dimerization activity
STI		TraesCS5B01G307200.1	DNA polymerase delta subunit 4	GO:0005634 CC: nucleus;GO:0006260 BP: DNA replication
STI		TraesCS5B01G320200.1	Protein STAY-GREEN, chloroplastic	NA
STI	5B_Excalibur_c9846_458_Hap	TraesCS5B01G320300.1	60S ribosomal protein L44	GO:0003735 MF: structural constituent of ribosome;GO:0005622 CC: intracellular;GO:0005840 CC: ribosome;GO:0006412 BP: translation
STI		TraesCS5B01G320400.1	Late embryogenesis abundant (LEA) hydroxyproline-rich glycoprotein family	NA
STI		TraesCS5B01G320500.1	Pseudo response regulator	GO:0000160 BP: phosphorelay signal transduction system;GO:0005515 MF: protein binding
STI		TraesCS5B01G320600.1	Pentatricopeptide repeat-containing protein	GO:0005515 MF: protein binding
STI				
STI		TraesCS5B01G388200.1	NA	NA
STI	5B_Excalibur_c18492_249_Hap	TraesCS5B01G388200.2	Orotidine 5'-phosphate decarboxylase	NA
STI		TraesCS5B01G388300.1	Transmembrane emp24 domain-containing protein	GO:0006810 BP: transport;GO:0016021 CC: integral component of membrane
STI		TraesCS5B01G388400.1	ATP synthase subunit alpha	GO:0005524 MF: ATP binding;GO:0015986 BP: ATP synthesis coupled proton transport
STI		TraesCS5B01G388500.1	NADH-ubiquinone oxidoreductase chain 6	NA
STI		TraesCS5B01G388600.1	NADH-ubiquinone oxidoreductase chain 6	GO:0008137 MF: NADH dehydrogenase (ubiquinone) activity;GO:0055114 BP: oxidation-reduction process
STI		TraesCS5B01G388700.1	Glycosyltransferase	GO:0008152 BP: metabolic process;GO:0016758 MF: transferase activity, transferring hexosyl groups
STI		TraesCS5B01G388800.1	HXXXD-type acyl-transferase family protein, putative	GO:0016747 MF: transferase activity, transferring acyl groups other than amino-acyl groups
STI		TraesCS5B01G321000.1	Beta-1,3-glucanase	GO:0004553 MF: hydrolase activity, hydrolyzing O-glycosyl compounds;GO:0005975 BP: carbohydrate metabolic process
STI	5B_Excalibur_rep_c67473_264_Hap	TraesCS5B01G321100.1	Ornithine carbamoyltransferase	NA
STI		TraesCS5B01G321200.1	Cysteine-rich protein	NA
STI		TraesCS5B01G321300.1	Leucine-rich repeat protein kinase family protein	NA
STI		TraesCS5B01G321600.1	Purple acid phosphatase	GO:0016787 MF: hydrolase activity
STI		TraesCS5B01G321700.1	Inactive purple acid phosphatase-like protein	GO:0016787 MF: hydrolase activity
STI		TraesCS5B01G305100.1	Formin-like protein	NA
STI	5B_GENE_3437_148	TraesCS5B01G305200.1	Acyl-coenzyme A thioesterase 9, mitochondrial	NA
STI		TraesCS5B01G305300.1	Glycosyltransferase	GO:0008152 BP: metabolic process;GO:0016758 MF: transferase activity, transferring hexosyl groups
STI		TraesCS5B01G305700.1	Ankyrin repeat-containing protein	GO:0005515 MF: protein binding

STI		TraesCS5B01G305800.1	Inositol-tetrakisphosphate 1-kinase 4	NA
STI		TraesCS5B01G305900.1	Inositol-tetrakisphosphate 1-kinase	GO:0000287 MF: magnesium ion binding;GO:0005524 MF: ATP binding;GO:0005622
STI		TraesCS5B01G303500.1	Sister chromatid cohesion 1 protein 3	GO:0000228 CC: nuclear chromosome;GO:0005515 MF: protein binding
STI	5B_Jagger_c3991_101	TraesCS5B01G303600.1	Sister chromatid cohesion 1 protein 3	GO:0000228 CC: nuclear chromosome;GO:0005515 MF: protein binding
STI		TraesCS5B01G303700.1	NADP-dependent alkenal double bond reductase	GO:0016491 MF: oxidoreductase activity;GO:0055114 BP: oxidation-reduction process
STI		TraesCS5B01G303800.1	NADP-dependent alkenal double bond reductase	GO:0016491 MF: oxidoreductase activity;GO:0055114 BP: oxidation-reduction process
STI		TraesCS5B01G303900.1	Alanine--tRNA ligase	GO:0000166 MF: nucleotide binding;GO:0004813 MF: alanine-tRNA ligase activity;
STI		TraesCS5B01G304000.1	NA	NA
STI		TraesCS5B01G304000.2	F-box protein	GO:0005515 MF: protein binding
STI		TraesCS5B01G304100.1	Ornithine decarboxylase	GO:0003824 MF: catalytic activity;GO:0006596 BP: polyamine biosynthetic process
STI		TraesCS5B01G304200.1	Ornithine decarboxylase	GO:0003824 MF: catalytic activity;GO:0006596 BP: polyamine biosynthetic process
STI		TraesCS5B01G304300.1	Agmatine coumaroyltransferase-2	GO:0016747 MF: transferase activity, transferring acyl groups other than amino-acyl groups
STI		TraesCS5B01G304400.1	C2 domain-containing protein / GRAM domain-containing protein	GO:0005515 MF: protein binding
STI		TraesCS5B01G304500.1	F-box protein	GO:0005515 MF: protein binding
STI		TraesCS5B01G304600.1	F-box protein	GO:0005515 MF: protein binding
STI		TraesCS5B01G304700.1	Ethylene-responsive transcription factor	GO:0003677 MF: DNA binding
STI		TraesCS5B01G304800.1	cytochrome P450, family 702, subfamily A, polypeptide 6	NA
STI		TraesCS5B01G304900.1	NBS-LRR disease resistance protein	GO:0043531 MF: ADP binding
STI		TraesCS5B01G305000.1	CsAtPR5	NA
STI		TraesCS5B01G385300.1	E3 ubiquitin protein ligase DRIP2	GO:0005515 MF: protein binding;GO:0008270 MF: zinc ion binding
STI	5B_Kukri_rep_c103366_421_Hap	TraesCS5B01G385400.1	response regulator 1	GO:0000160 BP: phosphorelay signal transduction system
STI		TraesCS5B01G385400.2	NA	NA
STI		TraesCS5B01G385500.1	BTB/POZ domain containing protein, expressed	GO:0005515 MF: protein binding
STI		TraesCS5B01G385600.1	BTB/POZ domain containing protein, expressed	GO:0005515 MF: protein binding
STI		TraesCS5B01G387300.1	ATP sulfurylase (Sulfate adenylyltransferase)	GO:0000103 BP: sulfate assimilation;GO:0004781 MF: sulfate adenylyltransferase (ATP) activity
STI		TraesCS5B01G387400.1	F-box family protein	GO:0005515 MF: protein binding
STI		TraesCS5B01G387500.1	NA	NA
STI		TraesCS5B01G387500.2	Kinase	GO:0004672 MF: protein kinase activity;GO:0005515 MF: protein binding;GO:0005524 MF: ATP binding

STI		TraesCS5B01G387500.3	NA	NA
STI		TraesCS5B01G387600.1	General transcription factor 3C polypeptide 3	GO:0005515 MF: protein binding
STI		TraesCS5B01G387700.1	Stem-specific protein TSJT1	NA
STI		TraesCS5B01G503300.1	VQ motif family protein, expressed	NA
STI	5B_Tdurum_contig44115_720_Hap	TraesCS5B01G503400.1	DNA polymerase epsilon catalytic subunit A, putative	NA
STI		TraesCS5B01G503500.1	Dirigent protein	NA
STI		TraesCS5B01G503600.1	DNA polymerase epsilon catalytic subunit A, putative	NA
STI		TraesCS5B01G503700.1	DNA polymerase epsilon catalytic subunit A, putative	NA
STI		TraesCS5B01G387600.1	General transcription factor 3C polypeptide 3	GO:0005515 MF: protein binding
STI	5B_wsnp_Ex_c1343_2568829_Hap	TraesCS5B01G387700.1	Stem-specific protein TSJT1	NA
STI		TraesCS6A01G149700.1	GMP synthase [glutamine-hydrolyzing]	NA
STI	6A_AX-158588213	TraesCS6A01G149800.1	HD domain-containing protein 2	NA
STI		TraesCS6A01G149900.1	Kinase	GO:0004672 MF: protein kinase activity;GO:0005524 MF: ATP binding;GO:0006468 BP: protein phosphorylation
STI		TraesCS6A01G149900.2	NA	NA
STI		TraesCS6A01G150000.1	Fatty acid hydroxylase superfamily	GO:0005506 MF: iron ion binding;GO:0008610 BP: lipid biosynthetic process;GO:0016491 MF: oxidoreductase activity;GO:0055114 BP: oxidation-reduction process
STI		TraesCS6A01G150100.1	Flavin-containing monooxygenase	GO:0004499 MF: N,N-dimethylaniline monooxygenase activity
STI		TraesCS6A01G150200.1	Basic helix-loop-helix transcription factor	GO:0046983 MF: protein dimerization activity
STI		TraesCS6A01G150300.1	DNA-directed RNA polymerase subunit beta	GO:0003677 MF: DNA binding
STI		TraesCS6A01G150500.1	Protein CYPRO4	GO:0005515 MF: protein binding
STI		TraesCS6A01G150600.1	Protein transport protein Sec61 subunit gamma	GO:0006605 BP: protein targeting;GO:0006886 BP: intracellular protein transport;GO:0016020 CC: membrane
STI		TraesCS6A01G150700.1	Flavin-containing monooxygenase	GO:0055114 BP: oxidation-reduction process
Con	1A_AX-158605765	TraesCS1A01G343200.1	ATP-binding cassette transporter subfamily A member	GO:0005524 MF: ATP binding;GO:0016887 MF: ATPase activity
Con		TraesCS1A01G343300.1	Auxin-responsive protein	GO:0005515 MF: protein binding
Con		TraesCS1A01G343400.1	Profilin	GO:0003779 MF: actin binding
Con		TraesCS1A01G343400.2	NA	NA
Con		TraesCS1A01G344200.1	F-box family protein	GO:0005515 MF: protein binding
Con		TraesCS1A01G344300.1	Protein kinase, putative	GO:0004672 MF: protein kinase activity;GO:0005515 MF: protein binding;GO:0005524 MF: ATP binding;GO:0006468 BP: protein phosphorylation

Con		TraesCS1A01G346400.1	Pentatricopeptide repeat-containing protein	GO:0005515 MF: protein binding;GO:0008270 MF: zinc ion binding
Con		TraesCS1A01G346500.1	Zinc finger CCCH domain-containing protein	GO:0046872 MF: metal ion binding
Con		TraesCS1A01G346600.1	Calcium homeostasis regulator CHoR1	NA
Con		TraesCS1A01G346700.1	F-box protein	GO:0005515 MF: protein binding
Con		TraesCS1A01G346800.1	NA	NA
Con		TraesCS1A01G346800.2	NA	NA
Con		TraesCS1A01G346800.3	Reticulon-like protein	NA
Con		TraesCS1A01G346900.1	Ring finger protein, putative	GO:0005515 MF: protein binding;GO:0008270 MF: zinc ion binding
Con		TraesCS1A01G347000.1	Late embryogenesis abundant hydroxyproline-rich glycoprotein	NA
Con		TraesCS1A01G347900.1	DNA replication complex GINS protein PSF3	NA
Con		TraesCS1A01G348000.1	Early nodulin-like protein	GO:0009055 MF: electron carrier activity
Con		TraesCS1A01G348100.1	Zinc finger protein	GO:0003676 MF: nucleic acid binding;GO:0008270 MF: zinc ion binding
Con		TraesCS1A01G348200.1	Zinc finger protein	GO:0003676 MF: nucleic acid binding;GO:0008270 MF: zinc ion binding
Con		TraesCS1A01G348300.1	50S ribosomal protein L20	GO:0005622 CC: intracellular;GO:0005840 CC: ribosome;GO:0006412 BP: translation;GO:0019843 MF: rRNA binding
Con		TraesCS1A01G348400.1	26S proteasome non-ATPase regulatory subunit 1	GO:0000502 CC: proteasome complex;GO:0005488 MF: binding;
Con		TraesCS1A01G348500.1	Malate dehydrogenase	GO:0003824 MF: catalytic activity;GO:0005975 BP: carbohydrate metabolic process;
Con		TraesCS1A01G348600.1	WRKY family transcription factor	;GO:0006355 BP: regulation of transcription, DNA-templated;GO:0043565 MF: sequence-specific DNA binding
Con	1A_wsnp_CAP12_c2438_1180601_Hap	TraesCS1A01G058800.1	Amino acid transporter, putative	NA
Con		TraesCS2A01G546000.1	RING/U-box superfamily protein	GO:0005515 MF: protein binding;GO:0008270 MF: zinc ion binding;GO:0046872 MF: metal ion binding
Con	2A_AX-158557326	TraesCS2A01G546100.1	hyaluronan mediated motility receptor-like protein	NA
Con		TraesCS2A01G546200.1	Cytochrome P450 family protein, expressed	GO:0005506 MF: iron ion binding;GO:0016705 MF: oxidoreductase activity, acting on paired donors, with incorporation or reduction of molecular oxygen;
Con		TraesCS2A01G546300.1	Cysteine proteinase	GO:0006508 BP: proteolysis;GO:0008234 MF: cysteine-type peptidase activity
Con		TraesCS2A01G546400.1	Cytochrome P450 family protein, expressed	GO:0005506 MF: iron ion binding;GO:0016705 MF: oxidoreductase activity
Con		TraesCS2A01G546500.1	Cytochrome P450 family protein, expressed	GO:0005506 MF: iron ion binding;GO:0016705 MF: oxidoreductase activity, acting on paired donors, with incorporation or reduction of molecular oxygen;
Con		TraesCS2A01G546600.1	Cytochrome P450 family protein, expressed	GO:0005506 MF: iron ion binding;GO:0016705 MF: oxidoreductase activity,
Con		TraesCS2A01G546700.1	Cysteine proteinase	GO:0006508 BP: proteolysis;GO:0008234 MF: cysteine-type peptidase activity
Con		TraesCS2A01G547600.1	Cytochrome P450, putative	GO:0005506 MF: iron ion binding;GO:0016705 MF: oxidoreductase activity,

Con				
Con		TraesCS3B01G536000.1	F-box family protein	NA
Con	3B_AX-111014946	TraesCS3B01G536100.1	Glutathione S-transferase	GO:0005515 MF: protein binding
Con		TraesCS3B01G536200.1	Calcium binding protein	GO:0005509 MF: calcium ion binding
Con		TraesCS3B01G536300.1	P-loop containing nucleoside triphosphate hydrolases superfamily protein	NA
Con		TraesCS3B01G536400.1	Phytochromobilin:ferredoxin oxidoreductase	GO:0050897 MF: cobalt ion binding;GO:0055114 BP: oxidation-reduction process
Con		TraesCS3B01G536500.1	7-dehydrocholesterol reductase	GO:0016020 CC: membrane;GO:0016628 MF: oxidoreductase activity
Con		TraesCS3B01G536600.1	Calmodulin-like family protein	GO:0005509 MF: calcium ion binding
Con				
Con		TraesCS3B01G535100.1	GRAS family transcription factor containing protein	NA
Con	3B_wsnp_Ra_c10710	TraesCS3B01G535200.1	NA	NA
Con		TraesCS3B01G535300.1	Glutathione S-transferase	GO:0005515 MF: protein binding
Con	4A_AX-158598616	TraesCS4A01G483900.1	Receptor-like kinase	GO:0004672 MF: protein kinase activity;GO:0005524 MF: ATP binding;GO:0006468 BP: protein phosphorylation
Con		TraesCS4A01G484000.1	Receptor-like protein kinase	GO:0004672 MF: protein kinase activity;GO:0005524 MF: ATP binding;GO:0006468 BP: protein phosphorylation
Con		TraesCS4A01G484000.2	NA	NA
Con		TraesCS4A01G484100.1	F-box family protein	GO:0005515 MF: protein binding
Con		TraesCS4A01G484200.1	Protein yippee-like	NA
Con		TraesCS4A01G484300.1	NA	NA
Con		TraesCS4A01G485100.1	Cytochrome P450 family protein, expressed	GO:0005506 MF: iron ion binding
Con		TraesCS4A01G485200.1	ATP-dependent caseinolytic (Clp) protease/crotonase family protein	NA
Con		TraesCS4A01G485300.1	Transducin/WD40 repeat-like superfamily protein	GO:0005515 MF: protein binding
Con		TraesCS4B01G375000.1	2-phosphoglycerate kinase, putative, expressed	NA
Con	4B_AX-89647929	TraesCS4B01G375100.1	CCR4-NOT transcription complex subunit 1	NA
Con		TraesCS4B01G375200.1	Expansin protein	
Con		TraesCS4B01G375300.1	Serine/threonine-protein kinase	GO:0004672 MF: protein kinase activity;GO:0004674 MF: protein serine/threonine kinase activity;GO:0005524 MF: ATP binding;GO:0006468 BP: protein phosphorylation;GO:0048544 BP: recognition of pollen
Con		TraesCS4B01G375400.1	Serine/threonine-protein kinase	GO:0004672 MF: protein kinase activity;GO:0004674 MF: protein serine/threonine kinase activity
Con		TraesCS4B01G375500.1	Serine/threonine-protein kinase	GO:0048544 BP: recognition of pollen

Con		TraesCS4B01G375600.1	Expansin protein	GO:0005576 CC: extracellular region;GO:0019953 BP: sexual reproduction
Con	5A_AX-89333764_Hap	TraesCS5A01G194900.2	Transmembrane protein, putative	NA
Con		TraesCS5A01G195000.1	NA	NA
Con		TraesCS5A01G195000.2	Wd repeat protein	GO:0005515 MF: protein binding
Con		TraesCS5A01G195100.1	NA	NA
Con		TraesCS5A01G195100.2	Agmatine deiminase	GO:0004668 MF: protein-arginine deiminase activity;GO:0009446 BP: putrescine biosynthetic process;
Con		TraesCS5A01G195100.3	NA	NA
Con		TraesCS5A01G195200.1	Skp1-like protein 1a	NA
Con		TraesCS5A01G195300.1	NA	NA
Con		TraesCS5A01G193900.1	Alcohol dehydrogenase	GO:0008270 MF: zinc ion binding;GO:0016491 MF: oxidoreductase activity;GO:0055114 BP: oxidation-reduction process
Con	5A_RAC875_c25733_2477	TraesCS5A01G194000.1	TP53-regulated inhibitor of apoptosis 1	NA
Con		TraesCS5A01G194100.1	NA	NA
Con		TraesCS5A01G194100.2	NA	NA
Con		TraesCS5A01G194100.3	Aminopeptidase	GO:0008237 MF: metallopeptidase activity;GO:0008270 MF: zinc ion binding
Con		TraesCS5A01G194200.1	Aminopeptidase	GO:0008237 MF: metallopeptidase activity;GO:0008270 MF: zinc ion binding
Con	5B_AX-158524974	TraesCS5B01G412700.1	Tubulin alpha chain	GO:0003924 MF: GTPase activity;
Con		TraesCS5B01G412800.1	F-box family protein	GO:0005515 MF: protein binding
Con		TraesCS5B01G412900.1	Pectin acetylesterase	GO:0016787 MF: hydrolase activity
Con		TraesCS5B01G413000.1	NADH-quinone oxidoreductase subunit I	GO:0016020 CC: membrane;
Con		TraesCS5B01G413000.2	NA	NA
Con		TraesCS5B01G414200.1	Cytochrome P450	GO:0005506 MF: iron ion binding;
Con		TraesCS5B01G414300.1	Cinnamoyl CoA reductase	GO:0003824 MF: catalytic activity;GO:0050662 MF: coenzyme binding
Con		TraesCS5B01G414400.1	Cytochrome P450	GO:0005506 MF: iron ion binding;
Con		TraesCS5B01G414800.1	F-box family protein	GO:0005515 MF: protein binding
Con		TraesCS5B01G414900.1	Succinate dehydrogenase [ubiquinone] flavoprotein subunit, mitochondrial	GO:0006099 BP: tricarboxylic acid cycle;GO:0016491 MF: oxidoreductase activity;
Con		TraesCS5B01G566700.1	Flavin-containing monooxygenase	GO:0016491 MF: oxidoreductase activity;GO:0055114 BP: oxidation-reduction process
Con	5B_Kukri_c637_517	TraesCS5B01G566800.1	NA	NA
Con		TraesCS5B01G566900.1	Disease resistance protein (NBS-LRR class) family	GO:0043531 MF: ADP binding

Con		TraesCS5B01G567000.1	Disease resistance protein (NBS-LRR class) family	GO:0043531 MF: ADP binding
Con		TraesCS5B01G568200.1	Disease resistance protein (NBS-LRR class) family	GO:0043531 MF: ADP binding
Con		TraesCS5B01G568300.1	Acetyl-coenzyme A carboxylase carboxyl transferase subunit beta, chloroplastic	GO:0006508 BP: proteolysis;GO:0008234 MF: cysteine-type peptidase activity
Con	5B_wsnp_Ex_c2207_4136036	TraesCS5B01G569000.1	Disease resistance protein (NBS-LRR class) family	GO:0043531 MF: ADP binding
Con		TraesCS5B01G569100.1	NBS-LRR disease resistance protein-like protein	GO:0043531 MF: ADP binding
Con		TraesCS5B01G570200.1	Cytochrome P450	GO:0005506 MF: iron ion binding;GO:0016705 MF: oxidoreductase activity,
Con		TraesCS5B01G570200.2	NA	NA
Con		TraesCS5B01G570300.1	Cytochrome P450	GO:0005506 MF: iron ion binding;GO:0016705 MF: oxidoreductase activity,
Con		TraesCS5B01G570400.1	Acyl transferase	GO:0016747 MF: transferase activity, transferring acyl groups other than amino-acyl groups
Con		TraesCS5B01G570500.1	translocase inner membrane subunit 44-1	NA
Con		TraesCS5B01G570600.1	NBS-LRR disease resistance protein-like protein	GO:0043531 MF: ADP binding
Con		TraesCS5B01G570700.1	Methyl-CpG-binding domain-containing protein 9	NA
Con		TraesCS5B01G570800.1	Aquaporin	GO:0005215 MF: transporter activity;GO:0006810 BP: transport;GO:0016020 CC: membrane
Con		TraesCS5B01G570900.1	Invertase inhibitor	GO:0004857 MF: enzyme inhibitor activity
Con	5B_wsnp_Ku_c16116_24914991	TraesCS5B01G571400.1	RNA binding protein, putative	GO:0003676 MF: nucleic acid binding
Con		TraesCS5B01G571500.1	F-box protein	GO:0005515 MF: protein binding
Con		TraesCS5B01G571600.1	Pentatricopeptide repeat-containing protein	GO:0005515 MF: protein binding
Con		TraesCS5B01G572000.1	dentin sialophosphoprotein	GO:0005515 MF: protein binding
Con		TraesCS5B01G572100.1	Late embryogenesis abundant (LEA) hydroxyproline-rich glycoprotein family	NA
Con	5D_wsnp_RFL_Contig3269_3313084	TraesCS5D01G381200.1	Serine protease SplB	NA
Con		TraesCS5D01G381300.1	EEIG1/EHBP1 N-terminal domain-containing protein	NA
Con		TraesCS5D01G381400.1	Cytosolic 5-nucleotidase	GO:0000287 MF: magnesium ion binding;GO:0005737 CC: cytoplasm;GO:0008253 MF: 5'-nucleotidase activity
Con		TraesCS5D01G381500.1	Histidine--tRNA ligase	GO:0005524 MF: ATP binding;GO:0005737 CC: cytoplasm;GO:0006427 BP: histidyl-tRNA aminoacylation
Con		TraesCS6B01G386700.1	Cytochrome b-c1 complex subunit 8	GO:0005743 CC: mitochondrial inner membrane;
Con	6B_AX-158552604	TraesCS6B01G386800.1	Structural maintenance of chromosomes protein	NA

Con		TraesCS6B01G386900.1	Mediator of RNA polymerase II transcription subunit 23	NA
Con		TraesCS6B01G387000.1	Isopentenyl-diphosphate delta-isomerase	GO:0016787 MF: hydrolase activity
Con	7B_Kukri_c46310_84 _Hap	TraesCS7B01G003100.2	NA	NA
Con		TraesCS7B01G003200.1	Kinase family protein	GO:0004672 MF: protein kinase activity
Con		TraesCS7B01G003300.1	Disease resistance protein (NBS-LRR class) family	GO:0043531 MF: ADP binding
Con		TraesCS7B01G003400.1	NBS-LRR disease resistance protein-like	GO:0043531 MF: ADP binding

Supplementary Table 3. 8b. List of putative candidate genes for H_2O_2 content under drought (Dro), control (Con) conditions and for STI

Trait	Marker	mrnaid	Human-Readable-Description	GO-IDs-(Description)-via-Interpro
	Kukri_c79308_278	TraesCS1B01G007900.1	E3 ubiquitin-protein ligase ORTHRUS 2	GO:0005515 MF: protein binding;
	AX-158569774	TraesCS1B01G435800.1	Glutamate--tRNA ligase	GO:0005515 MF: protein binding
		TraesCS1B01G435900.1	Sugar transporter protein	GO:0005215 MF: transporter activity
		TraesCS1B01G436300.1	3-ketoacyl-CoA synthase	GO:0003824 MF: catalytic activity
		TraesCS1B01G436500.1	Iron-sulfur cluster assembly protein	GO:0005506 MF: iron ion binding;GO:0016226 BP: iron-sulfur cluster assembly;GO:0051536 MF: iron-sulfur cluster binding
		TraesCS1B01G436700.1	50S ribosomal protein L7/L12	GO:0003735 MF: structural constituent of ribosome
		TraesCS1B01G436800.1	MYB transcription factor	GO:0003677 MF: DNA binding
		TraesCS1B01G437200.1	F-box protein	GO:0005515 MF: protein binding
		TraesCS1B01G437300.1	F-box protein	GO:0005515 MF: protein binding
STI , Con		TraesCS1B01G437600.1	Serine protease	GO:0004252 MF: serine-type endopeptidase activity;GO:0005515 MF: protein binding;GO:0006508 BP: proteolysis
		TraesCS1B01G437700.1	F-box family protein	GO:0005515 MF: protein binding
		TraesCS1B01G437900.1	Leucine-rich repeat receptor-like protein kinase family protein, putative	GO:0005515 MF: protein binding
		TraesCS1B01G438000.1	Leucine-rich repeat receptor-like protein kinase family protein	GO:0005515 MF: protein binding
		TraesCS1B01G438300.1	Disease resistance protein (NBS-LRR class) family	GO:0043531 MF: ADP binding

		TraesCS1B01G438500.1	Disease resistance protein (NBS-LRR class) family	GO:0043531 MF: ADP binding
		TraesCS1B01G438600.1	Disease resistance protein (TIR-NBS-LRR class) family	GO:0043531 MF: ADP binding
		TraesCS1B01G438800.1	Disease resistance protein (TIR-NBS-LRR class) family	GO:0043531 MF: ADP binding
		TraesCS1B01G438900.1	F-box family protein	GO:0005515 MF: protein binding
		TraesCS1B01G439000.1	Leucine-rich repeat receptor-like protein kinase family protein	GO:0005515 MF: protein binding
		TraesCS1B01G439100.1	Disease resistance protein (TIR-NBS-LRR class) family	GO:0043531 MF: ADP binding
		TraesCS1B01G439200.2	Disease resistance protein RPP8	GO:0043531 MF: ADP binding
		TraesCS1B01G439300.1	Disease resistance protein (TIR-NBS-LRR class) family	GO:0043531 MF: ADP binding
		TraesCS1B01G439400.1	Disease resistance protein (TIR-NBS-LRR class) family	GO:0043531 MF: ADP binding
		TraesCS1B01G439500.1	F-box domain containing protein	GO:0005515 MF: protein binding
		TraesCS1B01G439800.1	G-box binding factor	GO:0003700 MF: transcription factor activity,
STI	AX-89670926	TraesCS1B01G381500.1	Late embryogenesis abundant protein	NA
		TraesCS1B01G381600.1	StAR-related lipid transfer protein	GO:0008289 MF: lipid binding
	AX-86183817	TraesCS1B01G381700.1	Late embryogenesis abundant protein	NA
		TraesCS1B01G381800.1	Late embryogenesis abundant protein	NA
		TraesCS1B01G381900.1	Saposin B domain protein	GO:0006629 BP: lipid metabolic process
		TraesCS1B01G382000.1	Lys-63-specific deubiquitinase BRCC36	GO:0005515 MF: protein binding
		TraesCS1B01G382200.2	Pectin lyase-like superfamily protein	GO:0004650 MF: polygalacturonase activity;GO:0005975 BP: carbohydrate metabolic process
		TraesCS1B01G382300.1	Pectin lyase-like superfamily protein	GO:0005975 BP: carbohydrate metabolic process
	AX-110434034	TraesCS1B01G382400.1	Protein MATERNALLY EXPRESSED GENE 1	NA
	AX-158569774	TraesCS1B01G435800.1	Glutamate--tRNA ligase	NA
		TraesCS1B01G435900.1	Sugar transporter protein	GO:0005215 MF: transporter activity
		TraesCS1B01G436300.1	3-ketoacyl-CoA synthase	GO:0003824 MF: catalytic activity
		TraesCS1B01G436500.1	Iron-sulfur cluster assembly protein	GO:0005506 MF: iron ion binding;
		TraesCS1B01G436700.1	50S ribosomal protein L7/L12	GO:0003735 MF: structural constituent of ribosome
		TraesCS1B01G436800.1	MYB transcription factor	GO:0003677 MF: DNA binding
		TraesCS1B01G437200.1	F-box protein	GO:0005515 MF: protein binding
		TraesCS1B01G437300.1	F-box protein	GO:0005515 MF: protein binding
		TraesCS1B01G437600.1	Serine protease	GO:0004252 MF: serine-type endopeptidase activity

		TraesCS1B01G437700.1	F-box family protein	GO:0005515 MF: protein binding
		TraesCS1B01G437900.1	Leucine-rich repeat receptor-like protein kinase family protein, putative	GO:0005515 MF: protein binding
		TraesCS1B01G438000.1	Leucine-rich repeat receptor-like protein kinase family protein	GO:0005515 MF: protein binding
		TraesCS1B01G438500.1	Disease resistance protein (NBS-LRR class) family	GO:0043531 MF: ADP binding
		TraesCS1B01G438600.1	Disease resistance protein (TIR-NBS-LRR class) family	GO:0043531 MF: ADP binding
		TraesCS1B01G438800.1	Disease resistance protein (TIR-NBS-LRR class) family	GO:0043531 MF: ADP binding
		TraesCS1B01G438900.1	F-box family protein	GO:0005515 MF: protein binding
		TraesCS1B01G439000.1	Leucine-rich repeat receptor-like protein kinase family protein	GO:0005515 MF: protein binding
		TraesCS1B01G439100.1	Disease resistance protein (TIR-NBS-LRR class) family	GO:0043531 MF: ADP binding
		TraesCS1B01G439200.2	Disease resistance protein RPP8	GO:0043531 MF: ADP binding
		TraesCS1B01G439300.1	Disease resistance protein (TIR-NBS-LRR class) family	GO:0043531 MF: ADP binding
		TraesCS1B01G439400.1	Disease resistance protein (TIR-NBS-LRR class) family	GO:0043531 MF: ADP binding
		TraesCS1B01G439500.1	F-box domain containing protein	GO:0005515 MF: protein binding
		TraesCS1B01G439800.1	G-box binding factor	GO:0003700 MF: transcription factor activity, transcription,
	AX-158602322	TraesCS2A01G074900.1	Dioxygenase-related protein	GO:0016702 MF: oxidoreductase activity
		TraesCS2A01G075000.1	Germin-like protein	GO:0030145 MF: manganese ion binding
		TraesCS2A01G075100.1	F-box family protein	GO:0005515 MF: protein binding
		TraesCS2A01G075200.1	1-deoxy-D-xylulose-5-phosphate synthase, Transketolase	GO:0003824 MF: catalytic activity
		TraesCS2A01G075300.1	Acyl-[acyl-carrier-protein] desaturase	GO:0006631 BP: fatty acid metabolic process
		TraesCS2A01G075400.1	Acyl-[acyl-carrier-protein] desaturase	GO:0006631 BP: fatty acid metabolic process
		TraesCS2A01G075500.1	Acyl-[acyl-carrier-protein] desaturase	GO:0006631 BP: fatty acid metabolic process
		TraesCS2A01G075800.1	Methyl-CpG-binding domain protein	GO:0003677 MF: DNA binding
		TraesCS2A01G076100.1	IAA-amino acid hydrolase ILR1	GO:0008152 BP: metabolic process;GO:0016787 MF: hydrolase activity
		TraesCS2A01G076500.1	Cytochrome P450	GO:0005506 MF: iron ion binding
		TraesCS2A01G076600.1	L-lactate dehydrogenase	GO:0003824 MF: catalytic activity
		TraesCS2A01G076700.1	Elongation factor 1 alpha	GO:0003924 MF: GTPase activity;GO:0005525 MF: GTP binding
STI, Con		TraesCS2A01G076800.1	FBD-associated F-box protein	GO:0005515 MF: protein binding
	AX-158596005	TraesCS2A01G534600.1	Cytochrome P450	GO:0005506 MF: iron ion binding

		TraesCS2A01G534800.1	Ethylene-responsive transcription factor	GO:0003677 MF: DNA binding
		TraesCS2A01G534900.1	Protein DETOXIFICATION	GO:0006855 BP: drug transmembrane transport
		TraesCS2A01G535100.1	5555-protein kinase	GO:0004672 MF: protein kinase activity
STI		TraesCS2A01G535300.1	Copalyl diphosphate synthase	GO:0008152 BP: metabolic process
		TraesCS2A01G536000.1	ATP synthase subunit 9, mitochondrial	GO:0015078 MF: hydrogen ion transmembrane transporter activity
		TraesCS2A01G536100.1	Non-specific 5555 protein kinase	GO:0004672 MF: protein kinase activity;GO:0005524 MF: ATP binding
		TraesCS2A01G536200.1	Sulfotransferase	GO:0008146 MF: sulfotransferase activity
		TraesCS2A01G536300.1	5555-protein kinase	GO:0004672 MF: protein kinase activity
		TraesCS2A01G536400.1	5555-protein kinase	GO:0004672 MF: protein kinase activity
		TraesCS2A01G536500.2	5555-protein kinase	GO:0004672 MF: protein kinase activity
		TraesCS2A01G536800.1	5555-protein kinase	GO:0004672 MF: protein kinase activity;GO:0006468 BP: protein phosphorylation
		TraesCS2A01G537000.1	5555-protein kinase	GO:0004672 MF: protein kinase activity
		TraesCS2A01G537100.1	Superoxide dismutase	GO:0004784 MF: superoxide dismutase activity
	Kukri_c30020_302	TraesCS2A01G537300.1	5555-protein kinase	NA
		TraesCS2A01G537400.1	Sulfotransferase	GO:0008146 MF: sulfotransferase activity
		TraesCS2A01G537500.1	Sulfotransferase	GO:0008146 MF: sulfotransferase activity
		TraesCS2A01G537600.1	5555-protein kinase	GO:0048544 BP: recognition of pollen
		TraesCS2A01G537700.1	5555-protein kinase	GO:0004672 MF: protein kinase activity
		TraesCS2A01G537800.1	Leucine-rich repeat protein kinase-like	NA
		TraesCS2A01G537900.2	5555-protein kinase	GO:0004672 MF: protein kinase activity
		TraesCS2A01G538000.1	Exocyst complex component, putative	GO:0006887 BP: exocytosis
		TraesCS2A01G538100.1	5555-protein kinase	GO:0004672 MF: protein kinase activity
		TraesCS2A01G538200.3	5555-protein kinase	GO:0004672 MF: protein kinase activity
		TraesCS2A01G538300.1	5555-protein kinase	GO:0006468 BP: protein phosphorylation
		TraesCS2A01G538400.1	Cysteine protease, putative	GO:0006508 BP: proteolysis;GO:0008234 MF: cysteine-type peptidase activity
		TraesCS2A01G538500.1	basic helix-loop-helix (bHLH) DNA-binding superfamily protein	GO:0046983 MF: protein dimerization activity
		TraesCS2A01G538600.1	2-oxoglutarate (2OG) and Fe(II)-dependent oxygenase superfamily protein	GO:0016491 MF: oxidoreductase activity;GO:0055114 BP: oxidation-reduction process
		TraesCS2A01G538700.1	2-oxoglutarate (2OG) and Fe(II)-dependent oxygenase superfamily protein	GO:0016491 MF: oxidoreductase activity;GO:0055114 BP: oxidation-reduction process

	TraesCS2A01G538800.2	Ubiquitin carboxyl-terminal hydrolase	GO:0006511 BP: ubiquitin-dependent protein catabolic process
	TraesCS2A01G539000.1	Heavy metal transport/detoxification superfamily protein	GO:0030001 BP: metal ion transport;GO:0046872 MF: metal ion binding
	TraesCS2A01G539100.1	Heavy metal transport/detoxification superfamily protein	GO:0030001 BP: metal ion transport;GO:0046872 MF: metal ion binding
	TraesCS2A01G539200.1	Phosphoglycerate kinase	GO:0004618 MF: phosphoglycerate kinase activity
	TraesCS2A01G539300.1	Heavy metal transport/detoxification superfamily protein	GO:0030001 BP: metal ion transport;GO:0046872 MF: metal ion binding
	TraesCS2A01G539400.1	Heavy metal transport/detoxification superfamily protein	GO:0030001 BP: metal ion transport;GO:0046872 MF: metal ion binding
	TraesCS2A01G539500.1	Heavy metal transport/detoxification superfamily protein	GO:0030001 BP: metal ion transport;GO:0046872 MF: metal ion binding
	TraesCS2A01G539600.1	Heavy metal transport/detoxification superfamily protein	GO:0030001 BP: metal ion transport
	TraesCS2A01G539700.1	Actin-related family protein	GO:0005515 MF: protein binding
AX-158575274	TraesCS2B01G090100.1	1-deoxy-D-xylulose-5-phosphate synthase, Transketolase	GO:0003824 MF: catalytic activity
	TraesCS2B01G090200.1	F-box family protein	GO:0005515 MF: protein binding
	TraesCS2B01G090300.1	Germin-like protein	GO:0030145 MF: manganese ion binding
	TraesCS2B01G090400.1	Acyl-[acyl-carrier-protein] desaturase	GO:0006631 BP: fatty acid metabolic process
	TraesCS2B01G090500.1	F-box family protein	GO:0005515 MF: protein binding
	TraesCS2B01G090600.2	Methyl-CpG-binding domain protein	GO:0003677 MF: DNA binding
	TraesCS2B01G090700.1	Acyl-[acyl-carrier-protein] desaturase	GO:0006631 BP: fatty acid metabolic process
	TraesCS2B01G091000.1	IAA-amino acid hydrolase ILR1	GO:0008152 BP: metabolic process;GO:0016787 MF: hydrolase activity
	TraesCS2B01G091100.1	carboxyl-terminal peptidase (DUF239)	NA
	TraesCS2B01G091200.1	IAA-amino acid hydrolase ILR1	GO:0008152 BP: metabolic process;GO:0016787 MF: hydrolase activity
	TraesCS2B01G091300.1	Amine oxidase	GO:0005507 MF: copper ion binding
	TraesCS2B01G091400.1	L-lactate dehydrogenase	GO:0003824 MF: catalytic activity;
	TraesCS2B01G091500.1	Cytochrome P450	GO:0005506 MF: iron ion binding
	TraesCS2B01G091600.1	Elongation factor 1 alpha	GO:0003924 MF: GTPase activity
	TraesCS2B01G091700.1	FBD-associated F-box protein	GO:0005515 MF: protein binding
AX-158575274,	TraesCS2B01G090100.1	1-deoxy-D-xylulose-5-phosphate synthase, Transketolase	GO:0003824 MF: catalytic activity
AX-158547448	TraesCS2B01G090200.1	F-box family protein	GO:0005515 MF: protein binding
AX-158597348	TraesCS2B01G090300.1	Germin-like protein	GO:0030145 MF: manganese ion binding;GO:0045735 MF: nutrient reservoir activity
BS00009807_51	TraesCS2B01G090400.1	Acyl-[acyl-carrier-protein] desaturase	GO:0006631 BP: fatty acid metabolic process
IAAV3165	TraesCS2B01G090500.1	F-box family protein	GO:0005515 MF: protein binding

wsnp_Ex_c10596_17293192	TraesCS2B01G090600.2	Methyl-CpG-binding domain protein	GO:0003677 MF: DNA binding
wsnp_Ex_c10596_17293363	TraesCS2B01G090700.1	Acyl-[acyl-carrier-protein] desaturase	GO:0006631 BP: fatty acid metabolic process
BS00010055_51	TraesCS2B01G090700.2	NA	NA
AX-158562505	TraesCS2B01G091000.1	IAA-amino acid hydrolase ILR1	GO:0008152 BP: metabolic process;GO:0016787 MF: hydrolase activity
	TraesCS2B01G091100.1	carboxyl-terminal peptidase (DUF239)	NA
	TraesCS2B01G091200.1	IAA-amino acid hydrolase ILR1	GO:0008152 BP: metabolic process;GO:0016787 MF: hydrolase activity
	TraesCS2B01G091300.1	Amine oxidase	GO:0005507 MF: copper ion binding
	TraesCS2B01G091400.1	L-lactate dehydrogenase	GO:0003824 MF: catalytic activity
	TraesCS2B01G091500.1	Cytochrome P450	GO:0016705 MF: oxidoreductase activity,
	TraesCS2B01G091600.1	Elongation factor 1 alpha	GO:0003924 MF: GTPase activity;GO:0005525 MF: GTP binding
	TraesCS2B01G091700.1	FBD-associated F-box protein	GO:0005515 MF: protein binding
AX-158597022	TraesCS2B01G566600.1	RING/U-box superfamily protein	GO:0005515 MF: protein binding;GO:0008270 MF: zinc ion binding
wsnp_BG605258B_Ta_2_7	TraesCS2B01G566700.1	RING/U-box superfamily protein	GO:0005515 MF: protein binding;GO:0008270 MF: zinc ion binding
AX-158597024	TraesCS2B01G566800.1	Non-specific 5555 protein kinase	GO:0005524 MF: ATP binding;GO:0006468 BP: protein phosphorylation;
AX-111058839	TraesCS2B01G566900.1	5555-protein kinase	GO:0004672 MF: protein kinase activity;GO:0006468 BP: protein phosphorylation
	TraesCS2B01G567000.1	5555-protein kinase	GO:0004674 MF: protein serine/threonine kinase activity
	TraesCS2B01G567100.4	5555-protein kinase	GO:0004672 MF: protein kinase activity
	TraesCS2B01G567500.2	5555-protein kinase	GO:0004672 MF: protein kinase activity
	TraesCS2B01G567600.1	Superoxide dismutase	GO:0004784 MF: superoxide dismutase activity
	TraesCS2B01G567700.1	5555-protein kinase	GO:0004672 MF: protein kinase activity
	TraesCS2B01G567800.1	5555-protein kinase	GO:0004672 MF: protein kinase activity
	TraesCS2B01G567900.1	Non-specific 5555 protein kinase	GO:0004672 MF: protein kinase activity
	TraesCS2B01G568000.1	5555-protein kinase	GO:0004672 MF: protein kinase activity
	TraesCS2B01G568100.1	Sulfotransferase	GO:0008146 MF: sulfotransferase activity
	TraesCS2B01G568200.1	Sulfotransferase	GO:0008146 MF: sulfotransferase activity
	TraesCS2B01G568300.1	Sulfotransferase	GO:0008146 MF: sulfotransferase activity
	TraesCS2B01G568400.1	Cyanidin-3-O-glucoside 2-O-glucuronosyltransferase	NA
	TraesCS2B01G568500.1	5555-protein kinase	GO:0004672 MF: protein kinase activity
	TraesCS2B01G568600.1	5555-protein kinase	GO:0004672 MF: protein kinase activity

	TraesCS2B01G568700.1	basic helix-loop-helix (bHLH) DNA-binding superfamily protein	GO:0046983 MF: protein dimerization activity
	TraesCS2B01G568800.1	2-oxoglutarate (2OG) and Fe(II)-dependent oxygenase superfamily protein	GO:0016491 MF: oxidoreductase activity;GO:0055114 BP: oxidation-reduction process
	TraesCS2B01G568900.1	2-oxoglutarate (2OG) and Fe(II)-dependent oxygenase superfamily protein	GO:0016491 MF: oxidoreductase activity;GO:0055114 BP: oxidation-reduction process
Excalibur_c9752_289	TraesCS2B01G569400.1	Heavy metal transport/detoxification superfamily protein	GO:0030001 BP: metal ion transport;GO:0046872 MF: metal ion binding
	TraesCS2B01G569500.1	Heavy metal transport/detoxification superfamily protein	GO:0030001 BP: metal ion transport;GO:0046872 MF: metal ion binding
	TraesCS2B01G569600.1	Heavy metal transport/detoxification superfamily protein	GO:0030001 BP: metal ion transport;GO:0046872 MF: metal ion binding
	TraesCS2B01G569700.1	Cortactin-binding protein 2	NA
	TraesCS2B01G569800.1	Heavy metal transport/detoxification superfamily protein	GO:0030001 BP: metal ion transport;GO:0046872 MF: metal ion binding
	TraesCS2B01G569900.1	F-box family protein	GO:0005515 MF: protein binding
	TraesCS2B01G570000.1	Actin-related family protein	GO:0005515 MF: protein binding
	TraesCS2B01G570100.1	Ubiquitin-conjugating enzyme E2	NA
	TraesCS2B01G570200.1	50S ribosomal protein L16	GO:0003735 MF: structural constituent of ribosome
	TraesCS2B01G570300.1	Regulatory protein recX	GO:0006282 BP: regulation of DNA repair
	TraesCS2B01G570400.1	NA	NA
	TraesCS2B01G570400.2	2-aminoethanethiol dioxygenase	GO:0016702 MF: oxidoreductase activity
	TraesCS2B01G570500.1	phosphatidylinositol 4-kinase gamma-like protein	GO:0016301 MF: kinase activity
	TraesCS2B01G570600.1	Thiol-disulfide oxidoreductase DCC	NA
AX-158597023	TraesCS2B01G570700.1	F-box protein	GO:0005515 MF: protein binding
	TraesCS2B01G570800.2	Gibberellin 3-beta-hydroxylase	GO:0016491 MF: oxidoreductase activity;GO:0055114 BP: oxidation-reduction process
	TraesCS2B01G570900.1	Gibberellin 3-beta-hydroxylase 2	GO:0016491 MF: oxidoreductase activity;GO:0055114 BP: oxidation-reduction process
	TraesCS2B01G571000.1	Cysteine protease, putative	GO:0006508 BP: proteolysis;GO:0008234 MF: cysteine-type peptidase activity
	TraesCS2B01G571100.1	Exocyst complex component, putative	GO:0000145 CC: exocyst;GO:0006887 BP: exocytosis
	TraesCS2B01G571200.1	Exocyst subunit EXO70 family protein	GO:0000145 CC: exocyst;GO:0006887 BP: exocytosis
	TraesCS2B01G571300.1	Exocyst complex component, putative	GO:0000145 CC: exocyst;GO:0006887 BP: exocytosis
	TraesCS2B01G571400.1	UTP--glucose-1-phosphate uridylyltransferase	GO:0008152 BP: metabolic process;GO:0070569 MF: uridylyltransferase activity
	TraesCS2B01G571500.1	Exocyst complex component, putative	GO:0000145 CC: exocyst;GO:0006887 BP: exocytosis
	TraesCS2B01G571600.1	Exocyst complex component, putative	GO:0000145 CC: exocyst;GO:0006887 BP: exocytosis

	TraesCS2B01G572400.1	FAD-binding Berberine family protein, putative	GO:0003824 MF: catalytic activity
	TraesCS2B01G572500.1	Ethylene-responsive transcription factor, putative	GO:0003677 MF: DNA binding
AX-158596842	TraesCS2B01G627300.1	CsAtPR5	NA
	TraesCS2B01G627700.1	C2H2-like zinc finger protein	GO:0003676 MF: nucleic acid binding
	TraesCS2B01G628100.1	Receptor-like protein kinase	GO:0005524 MF: ATP binding;GO:0006468 BP: protein phosphorylation
	TraesCS2B01G628200.1	Receptor-like protein kinase	GO:0005524 MF: ATP binding;GO:0006468 BP: protein phosphorylation
	TraesCS2B01G628300.1	lectin-receptor kinase	GO:0005524 MF: ATP binding;GO:0006468 BP: protein phosphorylation
	TraesCS2B01G628500.1	2-oxoglutarate (2OG) and Fe(II)-dependent oxygenase-like protein	GO:0016491 MF: oxidoreductase activity;GO:0055114 BP: oxidation-reduction process
	TraesCS2B01G628600.2	Zinc finger protein ZPR1	GO:0008270 MF: zinc ion binding
	TraesCS2B01G628700.2	Tetratricopeptide repeat	GO:0005515 MF: protein binding
	TraesCS2B01G628900.1	Glycosyltransferase	GO:0008152 BP: metabolic process
	TraesCS2B01G629300.1	Mitochondrial transcription termination factor-like	GO:0003690 MF: double-stranded DNA binding
	TraesCS2B01G629400.1	Disease resistance protein RPM1	GO:0043531 MF: ADP binding
	TraesCS2B01G629500.1	Disease resistance protein RPM1	GO:0043531 MF: ADP binding
	TraesCS2B01G629800.1	Disease resistance protein RPM1	GO:0043531 MF: ADP binding
BobWhite_c11059_169	TraesCS2D01G073800.1	F-box family protein	GO:0005515 MF: protein binding
	TraesCS2D01G073900.1	1-deoxy-D-xylulose-5-phosphate synthase, Transketolase	GO:0003824 MF: catalytic activity
	TraesCS2D01G074000.1	Acyl-[acyl-carrier-protein] desaturase	GO:0006631 BP: fatty acid metabolic process
	TraesCS2D01G074100.1	Acyl-[acyl-carrier-protein] desaturase	GO:0006631 BP: fatty acid metabolic process
	TraesCS2D01G074200.1	Acyl-[acyl-carrier-protein] desaturase	GO:0006631 BP: fatty acid metabolic process
	TraesCS2D01G074300.1	Methyl-CpG-binding domain protein	GO:0003677 MF: DNA binding
	TraesCS2D01G076000.1	Strictosidine synthase	GO:0009058 BP: biosynthetic process
	TraesCS2D01G076200.1	Strictosidine synthase	GO:0009058 BP: biosynthetic process
	TraesCS2D01G076300.1	Strictosidine synthase	GO:0009058 BP: biosynthetic process
	TraesCS2D01G076400.1	Strictosidine synthase	GO:0009058 BP: biosynthetic process
	TraesCS2D01G076600.1	Dof zinc finger protein	GO:0003677 MF: DNA binding
	TraesCS2D01G076700.1	Kinase family protein	GO:0016567 BP: protein ubiquitination
	TraesCS2D01G076900.1	2-oxoglutarate dehydrogenase E1 component family protein	GO:0004591 MF: oxoglutarate dehydrogenase
	TraesCS2D01G077000.1	Telomere repeat-binding factor like-protein	GO:0003677 MF: DNA binding

wsnp_RFL_Contig4402_5154408	TraesCS2D01G541900.1	Thiol-disulfide oxidoreductase DCC	NA
	TraesCS2D01G542000.1	Cysteine protease	GO:0006508 BP: proteolysis;GO:0008234 MF: cysteine-type peptidase activity
	TraesCS2D01G542100.1	Gibberellin 3-beta-hydroxylase 2	GO:0016491 MF: oxidoreductase activity
	TraesCS2D01G542200.1	Cysteine protease, putative	GO:0006508 BP: proteolysis;GO:0008234 MF: cysteine-type peptidase activity
	TraesCS2D01G542300.1	Exocyst complex component, putative	GO:0000145 CC: exocyst;GO:0006887 BP: exocytosis
	TraesCS2D01G542400.1	Exocyst complex protein EXO70	GO:0000145 CC: exocyst;GO:0006887 BP: exocytosis
	TraesCS2D01G542500.1	Exocyst complex component, putative	GO:0000145 CC: exocyst;GO:0006887 BP: exocytosis
	TraesCS2D01G542600.1	Ubiquinol oxidase	GO:0009916 MF: alternative oxidase activity
	TraesCS2D01G543700.1	FAD-binding Berberine family protein, putative	GO:0003824 MF: catalytic activity
	TraesCS2D01G543800.1	Myb/SANT-like DNA-binding domain protein	NA
	TraesCS2D01G543900.1	Ethylene-responsive transcription factor, putative	GO:0003677 MF: DNA binding
	TraesCS2D01G544000.1	EH domain-containing protein 1	GO:0005509 MF: calcium ion binding
	TraesCS2D01G544200.1	Acyl-protein thioesterase 1	GO:0016787 MF: hydrolase activity
	TraesCS2D01G544300.1	Acyl-protein thioesterase 1	GO:0016787 MF: hydrolase activity
	TraesCS2D01G544400.1	Purple acid phosphatase	GO:0016787 MF: hydrolase activity
	TraesCS2D01G544500.1	BTB/POZ/MATH-domain protein	GO:0005515 MF: protein binding
	TraesCS2D01G544600.1	Acyl-protein thioesterase 1	GO:0016787 MF: hydrolase activity
	TraesCS2D01G544700.1	BTB/POZ/MATH-domain protein	GO:0005515 MF: protein binding
	TraesCS2D01G544800.1	Cysteine protease	GO:0006508 BP: proteolysis
	TraesCS2D01G544900.1	BTB/POZ domain containing protein, expressed	GO:0005515 MF: protein binding
Tdurum_contig42636_995	TraesCS5B01G307800.1	Serine carboxypeptidase family protein	GO:0004185 MF: serine-type carboxypeptidase activity
	TraesCS5B01G307900.1	CoA ligase	GO:0003824 MF: catalytic activity;GO:0008152 BP: metabolic process
	TraesCS5B01G308000.1	F-box family protein	GO:0005515 MF: protein binding
	TraesCS5B01G308100.1	Eukaryotic translation initiation factor 3 subunit G	GO:0003676 MF: nucleic acid binding
	TraesCS5B01G308200.1	Cytochrome P450 family protein	GO:0005506 MF: iron ion binding
	TraesCS5B01G308300.1	Cytochrome P450 family protein, expressed	GO:0005506 MF: iron ion binding
	TraesCS5B01G308400.1	Ethylene-responsive transcription factor	GO:0003677 MF: DNA binding
	TraesCS5B01G308500.1	Ring finger protein, putative	GO:0005515 MF: protein binding
	TraesCS5B01G308600.1	Ring finger protein, putative	GO:0005515 MF: protein binding

		TraesCS5B01G308700.1	Ring finger protein, putative	GO:0005515 MF: protein binding;GO:0008270 MF: zinc ion binding
		TraesCS5B01G308800.1	Transcription factor	GO:0003700 MF: transcription factor activity
		TraesCS5B01G309100.1	Bile acid sodium symporter	GO:0016020 CC: membrane
		TraesCS5B01G309200.1	Disease resistance protein (NBS-LRR class) family	GO:0043531 MF: ADP binding
		TraesCS5B01G309300.1	Alpha-L-fucosidase 1	GO:0004560 MF: alpha-L-fucosidase activity;GO:0005975 BP: carbohydrate metabolic process
		TraesCS5B01G309500.1	ATP-dependent RNA helicase	GO:0003676 MF: nucleic acid binding
		TraesCS5B01G309700.1	Alpha-L-fucosidase 1	GO:0004560 MF: alpha-L-fucosidase activity;GO:0005975 BP: carbohydrate metabolic process
		TraesCS5B01G309800.1	3-ketoacyl-CoA synthase	GO:0003824 MF: catalytic activity
		TraesCS5B01G309900.1	3-ketoacyl-CoA synthase	GO:0003824 MF: catalytic activity
		TraesCS5B01G310100.1	Tropinone reductase-like protein	GO:0016491 MF: oxidoreductase activity
		TraesCS5B01G310200.1	F-box protein family	GO:0005515 MF: protein binding
		TraesCS5B01G310300.1	F-box family protein	GO:0005515 MF: protein binding
		TraesCS5B01G310400.1	ATPase ASNA1 homolog	GO:0005524 MF: ATP binding;GO:0016887 MF: ATPase activity
		TraesCS5B01G310500.1	SPX domain-like protein	GO:0055085 BP: transmembrane transport
		TraesCS5B01G310600.1	Mannosyltransferase	GO:0016757 MF: transferase activity, transferring glycosyl groups
		TraesCS5B01G310700.1	Flap endonuclease 1	GO:0003677 MF: DNA binding
		TraesCS5B01G310800.1	CRT-binding factor	GO:0003677 MF: DNA binding
		TraesCS5B01G310900.1	CRT-binding factor	GO:0003677 MF: DNA binding
		TraesCS5B01G311200.1	CRT-binding factor	GO:0003677 MF: DNA binding
STI	AX-109306349	TraesCS6D01G007800.1	receptor kinase 1	GO:0006468 BP: protein phosphorylation
Dro	AX-158557366	TraesCS2A01G530100.1	Cytochrome P450 family protein, expressed	GO:0005506 MF: iron ion binding
		TraesCS2A01G530200.1	Cytochrome P450 family protein, expressed	GO:0005506 MF: iron ion binding
		TraesCS2A01G530800.1	Histidine--tRNA ligase	GO:0004821 MF: histidine-tRNA ligase activity
		TraesCS2A01G532600.1	5555-protein kinase	GO:0004672 MF: protein kinase activity;GO:0005524 MF: ATP binding
		TraesCS2A01G532800.1	Diacylglycerol kinase	GO:0003951 MF: NAD+ kinase activity
		TraesCS2A01G533000.1	Protein kinase	GO:0004672 MF: protein kinase activity;GO:0005524 MF: ATP binding;GO:0006468 BP: protein phosphorylation
		TraesCS2A01G533100.1	Exocyst complex component, putative	GO:0000145 CC: exocyst;GO:0006887 BP: exocytosis
		TraesCS2A01G533200.1	Flavin-containing monooxygenase	GO:0016491 MF: oxidoreductase activity
		TraesCS2A01G533400.1	5555-protein kinase	GO:0004674 MF: protein serine/threonine kinase activity
		TraesCS2A01G533500.1	Cytochrome P450	GO:0005506 MF: iron ion binding

		TraesCS2A01G533600.1	F-box family protein	GO:0005515 MF: protein binding
		TraesCS2A01G533700.1	Cytochrome P450	GO:0005506 MF: iron ion binding
		TraesCS2A01G533800.1	Invertase inhibitor	GO:0004857 MF: enzyme inhibitor activity
		TraesCS2A01G533900.1	Heme oxygenase 1	GO:0004392 MF: heme oxygenase (decyclizing) activity
		TraesCS2A01G534100.1	5555-protein kinase	GO:0004672 MF: protein kinase activity
		TraesCS2A01G534200.1	Transcription factor	GO:0003700 MF: transcription factor activity, sequence-specific DNA binding
		TraesCS2A01G534300.1	Transcription factor	GO:0003700 MF: transcription factor activity
		TraesCS2A01G534400.2	5555-protein kinase	GO:0004672 MF: protein kinase activity
Dro	AX-158550818	TraesCS5A01G548900.1	DNA topoisomerase	NA
		TraesCS5A01G549100.1	Agmatine coumaroyltransferase-2	GO:0016747 MF: transferase activity, transferring acyl groups other than amino-acyl groups
		TraesCS5A01G549200.1	Polyphenol oxidase	GO:0008152 BP: metabolic process;GO:0016491 MF: oxidoreductase activity
		TraesCS5A01G549400.1	Glycosyltransferase	GO:0008152 BP: metabolic process
		TraesCS5A01G549500.1	Organic cation transporter protein	GO:0055085 BP: transmembrane transport
		TraesCS5A01G549600.1	Polyamine oxidase	GO:0016491 MF: oxidoreductase activity
		TraesCS5A01G549700.1	Homeobox leucine-zipper protein	GO:0003677 MF: DNA binding
		TraesCS5A01G549800.1	Tyrosine decarboxylase	GO:0003824 MF: catalytic activity
		TraesCS5A01G549900.1	Malate dehydrogenase	GO:0005975 BP: carbohydrate metabolic process
		TraesCS5A01G550100.1	Peroxidase	GO:0055114 BP: oxidation-reduction process
		TraesCS5A01G550200.1	Peroxidase	GO:0055114 BP: oxidation-reduction process
		TraesCS5A01G550300.1	Peroxidase	GO:0055114 BP: oxidation-reduction process
		TraesCS5A01G550400.1	Peroxidase	GO:0055114 BP: oxidation-reduction process
		TraesCS5A01G550500.1	Peroxidase	GO:0055114 BP: oxidation-reduction process
		TraesCS5A01G550600.1	Peroxidase	GO:0004601 MF: peroxidase activity
		TraesCS5A01G550700.1	Heat shock transcription factor	GO:0003700 MF: transcription factor activity, sequence-specific DNA binding
		TraesCS5A01G551700.1	Polyubiquitin	GO:0005515 MF: protein binding
		TraesCS5A01G551800.1	F-box family protein	GO:0005515 MF: protein binding
		TraesCS5A01G552200.1	Receptor-like protein kinase	GO:0004672 MF: protein kinase activity;GO:0005524 MF: ATP binding;GO:0006468 BP: protein phosphorylation
		TraesCS5A01G552300.1	rRNA N-glycosidase	GO:0017148 BP: negative regulation of translation
		TraesCS5A01G552400.1	Nicotianamine synthase	GO:0030410 MF: nicotianamine synthase activity
		TraesCS5A01G552500.1	rRNA N-glycosidase	GO:0017148 BP: negative regulation of translation;GO:0030598 MF: rRNA N-glycosylase activity

		TraesCS5A01G552600.1	Kinase interacting (KIP1-like) family protein	GO:0003779 MF: actin binding
		TraesCS5A01G552900.1	Cytochrome P450	GO:0005506 MF: iron ion binding
		TraesCS5A01G553000.1	Cytochrome P450	GO:0005506 MF: iron ion binding
		TraesCS5A01G553100.1	Glycosyltransferase	GO:0008152 BP: metabolic process;GO:0016758 MF: transferase activity, transferring hexosyl groups
		TraesCS5A01G553200.1	Protein DETOXIFICATION	GO:0006855 BP: drug transmembrane transport
		TraesCS5A01G553300.3	DNA (Cytosine-5-)-methyltransferase	GO:0005515 MF: protein binding;GO:0006306 BP: DNA methylation
		TraesCS5A01G553900.1	Replication factor C subunit, putative	GO:0003677 MF: DNA binding;GO:0006260 BP: DNA replication
		TraesCS5A01G554000.1	Cytochrome P450-like protein	GO:0005506 MF: iron ion binding;
		TraesCS5A01G554100.1	Heavy metal transport/detoxification superfamily protein	GO:0030001 BP: metal ion transport;GO:0046872 MF: metal ion binding
		TraesCS5A01G554200.1	Beta-amylase	GO:0000272 BP: polysaccharide catabolic process
		TraesCS5A01G555800.1	Arginine/serine-rich splicing factor	GO:0003676 MF: nucleic acid binding
		TraesCS5A01G555900.1	ABC transporter family protein	GO:0005524 MF: ATP binding
		TraesCS5A01G557200.1	Cytochrome P450-like protein	GO:0016705 MF: oxidoreductase activity, acting on paired donors, with incorporation or reduction of molecular oxygen
		TraesCS5A01G557300.1	AP-2 complex subunit alpha-2	GO:0005488 MF: binding;GO:0006886 BP: intracellular protein transport
		TraesCS5A01G557400.1	Zinc finger CCCH domain protein	GO:0003677 MF: DNA binding;GO:0005515 MF: protein binding;GO:0008270 MF: zinc ion binding
		TraesCS5A01G557600.1	Cysteine proteinase inhibitor	GO:0004869 MF: cysteine-type endopeptidase inhibitor activity
		TraesCS5A01G558300.1	5555-protein kinase	GO:0004672 MF: protein kinase activity
Con	AX-109950638	TraesCS2A01G449000.1	Glucose-induced degradation protein 8-like protein	NA
		TraesCS2A01G449200.1	Zinc finger family protein	GO:0003676 MF: nucleic acid binding
Con	AX-110541191	TraesCS2B01G023700.1	Ankyrin repeat family protein	NA
		TraesCS2B01G025000.1	Apyrase	GO:0016787 MF: hydrolase activity
		TraesCS2B01G025100.1	Disease resistance protein RGA2	NA
		TraesCS2B01G025300.1	NB-ARC domain-containing disease resistance protein	NA
		TraesCS2B01G025400.1	NB-ARC domain-containing disease resistance protein	NA
		TraesCS2B01G025500.1	receptor kinase 1	GO:0004672 MF: protein kinase activity;GO:0005524 MF: ATP binding;GO:0006468 BP: protein phosphorylation
		TraesCS2B01G025600.1	NB-ARC domain-containing disease resistance protein	NA
		TraesCS2B01G025800.1	NB-ARC domain-containing disease resistance protein	NA
		TraesCS2B01G027100.1	NB-ARC domain-containing disease resistance protein	NA

		TraesCS2B01G027200.1	NB-ARC domain-containing disease resistance protein	NA
		TraesCS2B01G027300.1	Apyrase	GO:0016787 MF: hydrolase activity
Con	Excalibur_c25043_618	TraesCS2B01G622200.1	Chitinase	GO:0004568 MF: chitinase activity
		TraesCS2B01G622300.1	DNA-directed RNA polymerase subunit	GO:0003677 MF: DNA binding
		TraesCS2B01G624600.1	Oligopeptide transporter, putative	GO:0055085 BP: transmembrane transport
		TraesCS2B01G624900.2	disease resistance protein (TIR-NBS-LRR class)	GO:0005515 MF: protein binding
		TraesCS2B01G625000.1	Dirigent protein	NA
		TraesCS2B01G625200.1	Receptor-kinase, putative	GO:0004672 MF: protein kinase activity
		TraesCS2B01G625300.1	E3 ubiquitin-protein ligase	GO:0005515 MF: protein binding;GO:0008270 MF: zinc ion binding
		TraesCS2B01G625400.1	NBS-LRR-like resistance protein	GO:0043531 MF: ADP binding
		TraesCS2B01G625500.1	NBS-LRR-like resistance protein	GO:0043531 MF: ADP binding
		TraesCS2B01G625700.1	Werner Syndrome-like exonuclease	GO:0003676 MF: nucleic acid binding
	BobWhite_c11059_169	TraesCS2D01G073800.1	F-box family protein	GO:0005515 MF: protein binding
		TraesCS2D01G073900.1	1-deoxy-D-xylulose-5-phosphate synthase, Transketolase	GO:0003824 MF: catalytic activity
		TraesCS2D01G074000.1	Acyl-[acyl-carrier-protein] desaturase	GO:0006631 BP: fatty acid metabolic process
		TraesCS2D01G076700.1	Kinase family protein	GO:0004672 MF: protein kinase activity
		TraesCS2D01G076900.1	2-oxoglutarate dehydrogenase E1 component family protein	GO:0004591 MF: oxoglutarate dehydrogenase
		TraesCS2D01G077000.1	Telomere repeat-binding factor like-protein	GO:0003677 MF: DNA binding
Con	Tdurum_contig21737_203	TraesCS6B01G138700.1	Glucan endo-1,3-beta-glucosidase 3	NA
Con	wsnp_BE488206B_Ta_2_1	TraesCS6D01G097900.1	low-molecular-weight cysteine-rich 48	NA
		TraesCS6D01G100300.1	NBS-LRR-like resistance protein	GO:0043531 MF: ADP binding

Supplementary Table 3.S9. Gene list of *Ababidopsis thaliana* related to Pro and their homologs in wheat are described in table 2. S5.

Supplementary Table 4. S1. Cultivars used in this study are described in supplementary table 2.S1.

Supplementary Table 4. S2. Pearson correlation coefficients among root-shoot related traits under H_2O_2 treatment of the evaluated wheat association panel

Traits	RLH	SLH	RSRatio_H	TLH	SFWH	SDWH	RFWH
RLH							
SLH	0.58****						
RSRatioH	0.49****	-0.40****					
TLH	0.89****	0.89****	0.05				
SFWH	0.54****	0.86****	-0.35***	0.78****			
SDWH	0.27**	0.38****	-0.07	0.36****	0.37****		
RFWH	0.30***	0.30***	0.01	0.34****	0.44****	0.11	
RDWH	-0.23**	-0.19*	0.07	-0.24**	-0.13	-0.14	0.16

Note: p <0.0001 '****'; p <0.001 '***'; p < 0.01 '**'; p <0.05 '*'. Abbreviations: RLH, Root Length H_2O_2 stress; SLH, Shoot Length H_2O_2 stress, RSRatioH, Root Shoot Ratio H_2O_2 stress; TLH, Total Length H_2O_2 stress; SFWH, Shoot Fresh Weight H_2O_2 stress; SDWH, Shoot Dry Weight H_2O_2 stress; RFWH, Root Fresh Weight H_2O_2 stress; RDWC, Root Dry Weight H_2O_2 stress

Supplementary Table 4. S3a: List of significant Haplotypes/SNPs for relative values and corresponding chromosomal position and their linked candidate genes in 1Mb span up and down stream regions

Trait	Marker	Hap	Ch	Pos (Mbp)	mrnaid	Human-Readable-Description	GO-IDs-(Description)-via-Interpro
R_RFW	Kukri_c67721_184		1A	21	TraesCS1A01G036600	Rotundifolia-like protein	NA
					TraesCS1A01G036800	F-box family protein	GO:0005515 MF: protein binding
					TraesCS1A01G037100	F-box protein	GO:0005515 MF: protein binding
					TraesCS1A01G037400	Cation/H(+) antiporter	GO:0055085 BP: transmembrane transport
					TraesCS1A01G037700	Phenylalanine ammonia-lyase	GO:0003824 MF: catalytic activity
					TraesCS1A01G037800	Phenylalanine ammonia-lyase	GO:0003824 MF: catalytic activity
					TraesCS1A01G038100	Histone H2A	GO:0003677 MF: DNA binding
					TraesCS1A01G038200	Histone H2A	GO:0003677 MF: DNA binding
					TraesCS1A01G039100	TF-B3 domain-containing protein	GO:0003677 , MF: DNA binding
					TraesCS1A01G039700	ABC transporter, putative	GO:0005524 MF: ATP binding
					TraesCS1A01G039800	3-ketoacyl-CoA synthase	GO:0003824 MF: catalytic activity
					TraesCS1A01G040100	Zinc finger family protein	GO:0003676 MF: nucleic acid binding
					TraesCS1A01G040200	Zinc finger family protein	GO:0003676 MF: nucleic acid binding
R_RL	AX-89555340		1A	591	TraesCS1A01G442200	Flavonoid 3'-hydroxylase	GO:0020037 MF: heme binding
					TraesCS1A01G442600	Protein kinase family protein	GO:0006468 BP: protein phosphorylation
					TraesCS1A01G442800	Protein kinase family protein	GO:0004672 MF: protein kinase activity
					TraesCS1A01G442900	F-box family protein	GO:0005515 MF: protein binding
					TraesCS1A01G443100	Protein kinase	GO:0004672 MF: protein kinase activity
					TraesCS1A01G444100	Response regulator	GO:0000160 BP: phosphorelay signal transduction system
					TraesCS1A01G444200	Zinc finger protein CONSTANS	GO:0005515 MF: protein binding
					TraesCS1A01G444300	Nucleoside diphosphate kinase	GO:0004550 MF: nucleoside diphosphate kinase activity
					TraesCS1A01G444400	Zinc finger protein CONSTANS	GO:0005515 MF: protein binding
					TraesCS1A01G444900	Ring finger protein, putative	GO:0005515 MF: protein binding
R_RFW	AX-158570694		1B	115	TraesCS1B01G104900	Mitogen-activated protein kinase	GO:0004672 MF: protein kinase activity
R_RFW	AX-158606938		1B	223	TraesCS1B01G149400	Ubiquitin carboxyl-terminal hydrolase-like protein	GO:0004843 MF: thiol-dependent ubiquitin-specific protease activity
					TraesCS1B01G149500	Prolyl 4-hydroxylase alpha subunit, putative	GO:0005506 MF: iron ion binding
					TraesCS1B01G149600	Glycerol-3-phosphate acyltransferase	GO:0008152 BP: metabolic process

				TraesCS1B01G149700	DNA mismatch repair protein mutS	GO:0030983 MF: mismatched DNA binding
R_RFW	AX-158607168	1B	106	TraesCS1B01G096200	Peroxidase	GO:0004601 MF: peroxidase activity
				TraesCS1B01G096300	Peroxidase	GO:0004601 MF: peroxidase activity
				TraesCS1B01G096400	Peroxidase	GO:0004601 MF: peroxidase activity
				TraesCS1B01G096600	Peroxidase	GO:0004601 MF: peroxidase activity
				TraesCS1B01G096800	Peroxidase	GO:0004601 MF: peroxidase activity
				TraesCS1B01G096900	Peroxidase	GO:0004601 MF: peroxidase activity
				TraesCS1B01G097200	Glutathione S-transferase	GO:0005515 MF: protein binding
				TraesCS1B01G097400	Glutathione S-transferase	GO:0005515 MF: protein binding
				TraesCS1B01G097500	Myb-like transcription factor	GO:0003677 MF: DNA binding
				TraesCS1B01G099000	ABC transporter B family protein	GO:0005524 MF: ATP binding
				TraesCS1B01G099600	Aspartic proteinase	GO:0004190 MF: aspartic-type endopeptidase activity
R_RFW	BS00084305_51	1B	90	TraesCS1B01G089500	BTB/POZ domain containing protein	GO:0005515 MF: protein binding
				TraesCS1B01G089800	Mitochondrial pyruvate carrier	GO:0005743 CC: mitochondrial inner membrane
				TraesCS1B01G090000	Mitochondrial pyruvate carrier	GO:0005743 CC: mitochondrial inner membrane
				TraesCS1B01G090100	Receptor-like protein kinase	GO:0004672 MF: protein kinase activity
				TraesCS1B01G090600	Aminotransferase like protein	GO:0003824 MF: catalytic activity
				TraesCS1B01G090700	Endoglucanase	GO:0003824 MF: catalytic activity
R_RFW	BS00087787_51	1B	50	TraesCS1B01G065200	NADH-ubiquinone oxidoreductase chain 1	GO:0055114 BP: oxidation-reduction process
				TraesCS1B01G065600	NADH-ubiquinone oxidoreductase chain 1	GO:0055114 BP: oxidation-reduction process
				TraesCS1B01G065700	Nuclear pore complex protein Nup107	GO:0005643 CC: nuclear pore
				TraesCS1B01G065800	E3 ubiquitin-protein ligase RNF14	GO:0003676 MF: nucleic acid binding
				TraesCS1B01G065900	Arginine/serine-rich splicing factor, putative	GO:0003676 MF: nucleic acid binding
				TraesCS1B01G066000	ABC transporter G family member	GO:0005524 MF: ATP binding
				TraesCS1B01G066300	Peptidyl-prolyl cis-trans isomerase	GO:0004864 MF: protein phosphatase inhibitor activity
				TraesCS1B01G067000	Defensin-like protein	GO:0006952 BP: defense response
				TraesCS1B01G067100	Defensin	GO:0006952 BP: defense response
				TraesCS1B01G067300	Defensin	GO:0006952 BP: defense response
				TraesCS1B01G067400	F-box protein	GO:0005515 MF: protein binding

R__RFW	Excalibur_c7954_672 and	Rel_RFW_1B_Hap1	1B	117	TraesCS1B01G105300	O-acyltransferase	NA
R_RFW	Kukri_c29582_126		1B	118	TraesCS1B01G106700	ATP-dependent RNA helicase, putative	GO:0046872 MF: metal ion binding
					TraesCS1B01G106800	Zinc finger homeodomain protein	GO:0003677 MF: DNA binding
					TraesCS1B01G107000	Serine/threonine-protein phosphatase	GO:0004721 MF: phosphoprotein phosphatase activity
					TraesCS1B01G107100	Ankyrin repeat domain-containing protein 2	GO:0005515 MF: protein binding
					TraesCS1B01G107200	DNA repair helicase	GO:0003676 MF: nucleic acid binding
					TraesCS1B01G107400	Agmatine coumaroyltransferase-1	GO:0016747 MF: transferase activity, transferring acyl groups other than amino-acyl groups
R_RFW	Kukri_rep_c105316_262		1B	230	TraesCS1B01G150400	NA	NA
					TraesCS1B01G150600	Zinc finger CCCH domain protein	GO:0046872 MF: metal ion binding
R_RFW	RAC875_c28894_526 and	Rel_RFW_1B_Hap2	1B	106	TraesCS1B01G099300	polyadenylate-binding protein 1-B-binding protein	NA
	wsnp_Ex_c11976_19193550	Rel_RFW_1B_Hap2	1B	109	TraesCS1B01G099400	Polyadenylate-binding protein 1-B-binding protein	NA
					TraesCS1B01G099600	Aspartic proteinase	GO:0004190 MF: aspartic-type endopeptidase activity
					TraesCS1B01G100000	Chitinase	GO:0016998 BP: cell wall macromolecule catabolic process
					TraesCS1B01G100100	Low temperature and salt responsive protein	GO:0016021 CC: integral component of membrane
					TraesCS1B01G100200	Bushy growth protein	GO:0000228 CC: nuclear chromosome
					TraesCS1B01G100300	Auxin-responsive protein	GO:0005515 MF: protein binding
					TraesCS1B01G100400	Basic helix-loop-helix transcription factor	GO:0046983 MF: protein dimerization activity
					TraesCS1B01G100600	MYB transcription factor	GO:0003677 MF: DNA binding
					TraesCS1B01G100800	RNA-binding family protein	GO:0003676 MF: nucleic acid binding
					TraesCS1B01G101600	tRNA/rRNA methyltransferase family protein	GO:0003723 MF: RNA binding
					TraesCS1B01G101700	RING/U-box superfamily protein, putative	GO:0005515 MF: protein binding
					TraesCS1B01G101800	2,3-bisphosphoglycerate-dependent phosphoglycerate mutase	GO:0003824 MF: catalytic activity
R_RFW	RAC875_c63067_283		1B	95	TraesCS1B01G093300	G-patch domain containing protein	GO:0003676 MF: nucleic acid binding
					TraesCS1B01G093500	Pentatricopeptide repeat-containing protein	GO:0005515 MF: protein binding
					TraesCS1B01G093600	Long-Chain Acyl-CoA Synthetase	GO:0008152 BP: metabolic process
					TraesCS1B01G093800	Receptor-like protein kinase	GO:0004672 MF: protein kinase activity

					TraesCS1B01G093900	DNA-directed RNA polymerase III subunit RPC3	GO:0003677 MF: DNA binding
					TraesCS1B01G094000	FBD-associated F-box protein	GO:0005515 MF: protein binding
					TraesCS1B01G094200	Formin-like protein	GO:0005515 MF: protein binding
					TraesCS1B01G094300	Phosphate translocator	GO:0005215 MF: transporter activity
					TraesCS1B01G094500	MYB transcription factor	GO:0003677 MF: DNA binding
					TraesCS1B01G094600	Nitrogen regulatory protein P-II-like protein	GO:0006808 BP: regulation of nitrogen utilization
R_SL	AX-158521438		1B	6	TraesCS1B01G012100	Pm3-like disease resistance protein	GO:0043531 MF: ADP binding
					TraesCS1B01G012200	Pm3-like disease resistance protein	GO:0043531 MF: ADP binding
					TraesCS1B01G012300	Ankyrin repeat protein family-like protein	GO:0005515 MF: protein binding
					TraesCS1B01G012400	Pm3-like disease resistance protein	GO:0043531 MF: ADP binding
					TraesCS1B01G012500	Disease resistance protein (TIR-NBS-LRR class) family	GO:0043531 MF: ADP binding
					TraesCS1B01G012600	NBS-LRR class disease resistance protein	GO:0043531 MF: ADP binding
					TraesCS1B01G012700	Disease resistance protein (TIR-NBS-LRR class) family	GO:0043531 MF: ADP binding
					TraesCS1B01G012800	Pm3-like disease resistance protein	GO:0043531 MF: ADP binding
					TraesCS1B01G014300	HXXXD-type acyl-transferase family protein	GO:0016747 MF: transferase activity, transferring acyl groups other than amino-acyl groups
					TraesCS1B01G014400	disease resistance family protein / LRR family protein	GO:0043531 MF: ADP binding
					TraesCS1B01G014500	disease resistance family protein / LRR family protein	GO:0043531 MF: ADP binding
					TraesCS1B01G014800	Pm3-like disease resistance protein	GO:0043531 MF: ADP binding
					TraesCS1B01G014900	Pm3-like disease resistance protein	GO:0043531 MF: ADP binding
					TraesCS1B01G015300	Pm3-like disease resistance protein	GO:0043531 MF: ADP binding
					TraesCS1B01G015900	Cytochrome P450	GO:0005506 MF: iron ion binding
					TraesCS1B01G016000	Pm3-like disease resistance protein	GO:0043531 MF: ADP binding
					TraesCS1B01G016100	Pm3-like disease resistance protein	GO:0043531 MF: ADP binding
R_SL	AX-158540096	Rel_SL_1B_Hap1	1B	671	TraesCS1B01G456400	S-type anion channel	GO:0016021 CC: integral component of membrane;GO:0055085 BP: transmembrane transport
R_SL	AX-158560878	Rel_SL_1B_Hap1	1B	670	TraesCS1B01G456500	S-type anion channel	GO:0016021 CC: integral component of membrane;GO:0055085 BP: transmembrane transport
R_SL	Tdurum_contig94450_255	Rel_SL_1B_Hap1	1B	671	TraesCS1B01G456600	Protein ABIL1	NA
R_RSRatio	Kukri_c29170_680		2A	693	TraesCS2A01G442300	p-loop containing nucleoside triphosphate hydrolases superfamily protein, putative	GO:0005515 MF: protein binding;GO:0005524 MF: ATP binding

				TraesCS2A01G442500	Basic helix loop helix (BHLH) family transcription factor	GO:0046983 MF: protein dimerization activity
				TraesCS2A01G443000	Kinase, putative	GO:0004672 MF: protein kinase activity
				TraesCS2A01G443100	LEAFY-like protein	GO:0003677 MF: DNA binding
				TraesCS2A01G443200	50S ribosomal protein L11	GO:0003735 MF: structural constituent of ribosome
				TraesCS2A01G443600	Peptide transporter	GO:0005215 MF: transporter activity
				TraesCS2A01G443700	Peptide transporter	GO:0005215 MF: transporter activity
				TraesCS2A01G443800	WRKY transcription factor	GO:0003700 MF: transcription factor activity, sequence-specific DNA binding
R_SL	AX-158532334	2D	534	TraesCS2D01G419900	GRF zinc finger protein	GO:0008270 MF: zinc ion binding
				TraesCS2D01G420000	GRF zinc finger-containing protein-like protein	GO:0008270 MF: zinc ion binding
				TraesCS2D01G420100	SKP1-like protein	GO:0006511 BP: ubiquitin-dependent protein catabolic process
				TraesCS2D01G420400	ABC subfamily C transporter	GO:0005524 MF: ATP binding
				TraesCS2D01G420500	Armadillo/beta-catenin-like repeat family protein, expressed	GO:0005488 MF: binding
				TraesCS2D01G420800	F-box family protein	GO:0005515 MF: protein binding
				TraesCS2D01G420900	Pathogenesis-related protein 1	GO:0006952 BP: defense response
				TraesCS2D01G421000	Werner Syndrome-like exonuclease	GO:0003676 MF: nucleic acid binding
				TraesCS2D01G421100	Methyl-CpG-binding domain protein	GO:0003677 MF: DNA binding
				TraesCS2D01G421600	Leucine-rich repeat receptor-like protein kinase family protein	GO:0005515 MF: protein binding
				TraesCS2D01G421900	F-box family protein	GO:0005515 MF: protein binding
				TraesCS2D01G422000	Zinc transporter	GO:0005385 MF: zinc ion transmembrane transporter activity
				TraesCS2D01G422100	Vacuolar ATPase assembly integral membrane protein VMA21 homolog	GO:0070072 BP: vacuolar proton-transporting V-type ATPase complex assembly
				TraesCS2D01G422200	Pentatricopeptide repeat-containing protein	GO:0005515 MF: protein binding
				TraesCS2D01G422300	Cytochrome P450	GO:0005506 MF: iron ion binding
				TraesCS2D01G422400	Alcohol dehydrogenase, putative	GO:0008270 MF: zinc ion binding
				TraesCS2D01G422600	Coatomer subunit epsilon	GO:0005198 MF: structural molecule activity
R_SL	AX-158521912	2D	542	TraesCS2D01G429400	Serine/arginine repetitive matrix protein 2, putative isoform 1	NA
				TraesCS2D01G429700	Cytochrome P450	GO:0005506 MF: iron ion binding
				TraesCS2D01G429800	DNA ligase	GO:0003677 MF: DNA binding

				TraesCS2D01G429900	ELKS/Rab6-interacting/CAST family protein	GO:0005515 MF: protein binding
R_RSRatio	AX-158523313	3A	462	TraesCS3A01G246300	Serine/threonine-protein kinase	GO:0004672 MF: protein kinase activity
R_RSRatio	AX-158523668	3A	444	TraesCS3A01G238100	NAD-dependent deacetylase sirtuin-6	NA
				TraesCS3A01G238300	Ethylene-responsive transcription factor, putative	GO:0003677 MF: DNA binding
R_RSRatio	AX-158533093	3A	444	TraesCS3A01G232800	Pentatricopeptide repeat-containing protein	GO:0005515 MF: protein binding
				TraesCS3A01G233100	F-box protein	GO:0005515 MF: protein binding
				TraesCS3A01G233300	ADP,ATP carrier protein	GO:0005471 MF: ATP:ADP antiporter activity
				TraesCS3A01G233800	Potassium channel	GO:0005216 MF: ion channel activity
				TraesCS3A01G234400	Transcription initiation factor TFIID subunit 7	GO:0005669 CC: transcription factor TFIID complex
				TraesCS3A01G234500	Transcription factor GTE4	GO:0005044 MF: scavenger receptor activity
				TraesCS3A01G234600	Transcription factor GTE4-like protein	GO:0005515 MF: protein binding
				TraesCS3A01G234700	WD repeat protein	GO:0005515 MF: protein binding
				TraesCS3A01G234800	Malate dehydrogenase	GO:0003824 MF: catalytic activity oxidation-reduction process
				TraesCS3A01G234900	GDSL esterase/lipase	GO:0016788 MF: hydrolase activity, acting on ester bonds
				TraesCS3A01G235000	GDSL esterase/lipase	GO:0016788 MF: hydrolase activity, acting on ester bonds
				TraesCS3A01G235100	GDSL esterase/lipase	GO:0006629 BP: lipid metabolic process
				TraesCS3A01G235200	Pentatricopeptide repeat-containing protein	GO:0005515 MF: protein binding
				TraesCS3A01G235300	Phospholipase A1	GO:0006629 BP: lipid metabolic process
				TraesCS3A01G235400	Phospholipase A1	GO:0006629 BP: lipid metabolic process
				TraesCS3A01G235500	GDSL esterase/lipase	GO:0016788 MF: hydrolase activity, acting on ester bonds
				TraesCS3A01G235700	Phospholipase A1	GO:0006629 BP: lipid metabolic process
				TraesCS3A01G236500	Transducin/WD40 repeat-like superfamily protein	GO:0005515 MF: protein binding
				TraesCS3A01G236700	CTP synthase	GO:0003883 MF: CTP synthase activity
				TraesCS3A01G237400	Kinase family protein	GO:0004672 MF: protein kinase activity
				TraesCS3A01G237700	Long-Chain Acyl-CoA Synthetase	GO:0003824 MF: catalytic activity
R_RSRatio	AX-158533132	3A	477	TraesCS3A01G254900	Subtilisin-like protease	GO:0004252 MF: serine-type endopeptidase activity
				TraesCS3A01G255100	Carboxyl methyltransferase	GO:0008168 MF: methyltransferase activity
				TraesCS3A01G255200	Epoxide hydrolase 2	GO:0003824 MF: catalytic activity
				TraesCS3A01G255300	Bidirectional sugar transporter SWEET	GO:0016021 CC: integral component of membrane

					TraesCS3A01G255600	Protein kinase-like	GO:0004672 MF: protein kinase activity
					TraesCS3A01G255700	Protein kinase-like	GO:0004672 MF: protein kinase activity
					TraesCS3A01G255800	GMP synthase [glutamine-hydrolyzing]	GO:0003922 MF: GMP synthase (glutamine-hydrolyzing) activity
					TraesCS3A01G255900	ABC transporter ATP-binding protein	GO:0005524 MF: ATP binding
					TraesCS3A01G256000	RNA polymerase II transcriptional coactivator KELP	GO:0003677 MF: DNA binding
					TraesCS3A01G256100	Proliferating cell nuclear antigen	GO:0003677 MF: DNA binding
					TraesCS3A01G256200	Protein kinase-like	GO:0004672 MF: protein kinase activity
					TraesCS3A01G256300	Protein kinase-like	GO:0004672 MF: protein kinase activity
					TraesCS3A01G256600	Strictosidine synthase family protein	GO:0009058 BP: biosynthetic process
					TraesCS3A01G256700	FBD-associated F-box protein	GO:0005515 MF: protein binding
					TraesCS3A01G256800	Flavin-containing monooxygenase	GO:0016491 MF: oxidoreductase activity
					TraesCS3A01G256900	SWAP (Suppressor-of-White-APricot)/surp domain-containing protein	GO:0003723 MF: RNA binding
R_RSRatio	IAAV4343		3A	444	TraesCS3A01G237800	Protein phosphatase 2c, putative	GO:0003824 MF: catalytic activity
R_SFW	AX-158532834	Rel_SFW_3A_Hap1	3A	434	TraesCS3A01G230200	Exostosin family protein	NA
					TraesCS3A01G230400	Dual-specificity RNA methyltransferase RlmN	GO:0003824 MF: catalytic activity
					TraesCS3A01G230500	Kinase family protein	GO:0004672 MF: protein kinase activity
					TraesCS3A01G230700	Bifunctional dihydroflavonol 4-reductase/flavanone 4-reductase isoform 2	GO:0016021 CC: integral component of membrane
					TraesCS3A01G231200	F-box/kelch-repeat protein	GO:0005515 MF: protein binding
					TraesCS3A01G231400	Single-stranded DNA-binding protein	GO:0003697 MF: single-stranded DNA binding
					TraesCS3A01G231500	Auxin efflux carrier component	GO:0016021 CC: integral component of membrane
					TraesCS3A01G231600	Homeobox associated leucine zipper protein	GO:0003677 MF: DNA binding
					TraesCS3A01G231700	Mitogen-activated protein kinase	GO:0004672 MF: protein kinase activity
					TraesCS3A01G232100	Zinc finger protein ZPR1	GO:0008270 MF: zinc ion binding
					TraesCS3A01G232300	Elongation factor	GO:0003924 MF: GTPase activity
					TraesCS3A01G232500	Zinc finger CCCH domain protein	GO:0046872 MF: metal ion binding
					TraesCS3A01G232600	Flavin-containing monooxygenase	GO:0004499 MF: N,N-dimethylaniline monooxygenase activity
					TraesCS3A01G232700	Sodium Bile acid symporter family	GO:0016020 CC: membrane

R_RFW	IAAV902		3A	574	TraesCS3A01G328100	Ethylene-responsive transcription factor, putative	GO:0003677 MF: DNA binding
					TraesCS3A01G328700	DNA-3-methyladenine glycosylase	GO:0003824 MF: catalytic activity
					TraesCS3A01G329100	Transportin-1	GO:0005488 MF: binding
					TraesCS3A01G329200	Serine carboxypeptidase family protein, expressed	GO:0004185 MF: serine-type carboxypeptidase activity
					TraesCS3A01G329600	Pentatricopeptide repeat-containing protein	GO:0005515 MF: protein binding
					TraesCS3A01G329700	Purple acid phosphatase	GO:0003993 MF: acid phosphatase activity
					TraesCS3A01G330200	DNA-(apurinic or apyrimidinic site) lyase	GO:0003677 MF: DNA binding
					TraesCS3A01G330300	DNA-(apurinic or apyrimidinic site) lyase	GO:0003677 MF: DNA binding
					TraesCS3A01G330500	Beta-1,3-glucanase	GO:0004553 MF: hydrolase activity, hydrolyzing O-glycosyl compounds
R_RL	AX-109990240		3B	115	TraesCS3B01G132400	3'-N-debenzoyl-2'-deoxytaxol N-benzoyltransferase	GO:0016747 MF: transferase activity, transferring acyl groups other than amino-acyl groups
					TraesCS3B01G132500	Extracellular ribonuclease	GO:0004518 MF: nuclease activity
					TraesCS3B01G133000	F-box protein	GO:0005515 MF: protein binding
					TraesCS3B01G133100	Histone-lysine N-methyltransferase	GO:0005515 MF: protein binding
					TraesCS3B01G133400	Alkaline alpha-galactosidase seed imbibition protein	GO:0003824 MF: catalytic activity
					TraesCS3B01G133600	Cytochrome P450 family protein, expressed	GO:0005506 MF: iron ion binding
					TraesCS3B01G133700	Cytochrome P450 family protein, expressed	GO:0005506 MF: iron ion binding
					TraesCS3B01G134100	Cytochrome P450 family protein	;GO:0055114 BP: oxidation-reduction process
					TraesCS3B01G134200	Nuclear factor Y subunit C	GO:0046982 MF: protein heterodimerization activity
					TraesCS3B01G134300	Type I inositol-1,4,5-trisphosphate 5-phosphatase 1	GO:0046856 BP: phosphatidylinositol dephosphorylation
					TraesCS3B01G134400	Zinc finger family protein	GO:0003676 MF: nucleic acid binding
					TraesCS3B01G134500	Zinc finger family protein	GO:0003676 MF: nucleic acid binding
					TraesCS3B01G134700	Ankyrin repeat protein-like	GO:0005515 MF: protein binding
R_RL	BobWhite_c10402_140	Rel_RL_3B_Hap1	3B	100	TraesCS3B01G125400	Pollen-specific protein SF21	NA
R_RL	wsnp_JD_c2623_3541255		3B	114	TraesCS3B01G131500	Ubiquitin-conjugating enzyme E2-like protein	NA
					TraesCS3B01G131700.9	Homeobox protein, putative	GO:0003677 MF: DNA binding
					TraesCS3B01G132000	FACT complex subunit SSRP1	GO:0003677 MF: DNA binding
					TraesCS3B01G132200	FAD-binding Berberine family protein	GO:0003824 MF: catalytic activity

					TraesCS3B01G132300	Glutamine--tRNA ligase	GO:0000166 MF: nucleotide binding
					TraesCS3B01G132400	3'-N-debenzoyl-2'-deoxytaxol N-benzoyltransferase	GO:0016747 MF: transferase activity, transferring acyl groups other than amino-acyl groups
					TraesCS3B01G132500	Extracellular ribonuclease	GO:0004518 MF: nuclease activity
					TraesCS3B01G133000	F-box protein	GO:0005515 MF: protein binding
					TraesCS3B01G133100	Histone-lysine N-methyltransferase	GO:0005515 MF: protein binding;GO:0008270 MF: zinc ion binding
R_RSRatio	AX-158548980		3D	533	TraesCS3D01G420700	RING/U-box superfamily protein	GO:0005515 MF: protein binding;GO:0008270 MF: zinc ion binding
					TraesCS3D01G420900	RING/U-box superfamily protein	GO:0005515 MF: protein binding;GO:0008270 MF: zinc ion binding
					TraesCS3D01G421000	RING/U-box superfamily protein	GO:0005515 MF: protein binding;GO:0008270 MF: zinc ion binding
					TraesCS3D01G421100	RING/U-box superfamily protein	GO:0005515 MF: protein binding;GO:0008270 MF: zinc ion binding
					TraesCS3D01G421200	RING/U-box superfamily protein	GO:0005515 MF: protein binding;GO:0008270 MF: zinc ion binding
					TraesCS3D01G421600	Auxin efflux carrier component	GO:0016021 CC: integral component of membrane
					TraesCS3D01G421800	F-box domain containing protein	GO:0005515 MF: protein binding
					TraesCS3D01G421900	Disease resistance protein RPM1	GO:0043531 MF: ADP binding
					TraesCS3D01G422000	F-box family protein	GO:0005515 MF: protein binding
					TraesCS3D01G422100	F-box family protein	GO:0005515 MF: protein binding
R_RFW	AX-158603951		4A	534	TraesCS4A01G225700	Gibberellin receptor GID1a	GO:0008152 BP: metabolic process
					TraesCS4A01G226000	ATP-dependent Clp protease ATP-binding subunit	GO:0005524 MF: ATP binding
					TraesCS4A01G226100	Serine carboxypeptidase family protein, expressed	GO:0004185 MF: serine-type carboxypeptidase activity
					TraesCS4A01G226300	Protein phosphatase 2c, putative	GO:0003824 MF: catalytic activity
					TraesCS4A01G226400	Non-lysosomal glucosylceramidase	GO:0003824 MF: catalytic activity
					TraesCS4A01G226700	Heat-shock protein, putative	NA
					TraesCS4A01G226800	Zinc finger-homeodomain protein 1	GO:0003677 MF: DNA binding
					TraesCS4A01G227100	Glucuronoxylan 4-O-methyltransferase	GO:0045492 BP: xylan biosynthetic process
					TraesCS4A01G227200	Protein kinase-like protein	GO:0004672 MF: protein kinase activity
					TraesCS4A01G227300	Chlorophyll a/b binding protein domain-containing protein	GO:0008942 MF: nitrite reductase [NAD(P)H] activity
					TraesCS4A01G227400	ethylene-responsive transcription factor	GO:0003677 MF: DNA binding
R_RL	AX-158582574	Com_Hap1	4B	456	TraesCS4B01G200500	Serine/threonine-protein kinase	NA
R_RSRatio	AX-158582574	Com_Hap1	4B	456	TraesCS4B01G200600	ABC transporter G family member	GO:0005524 MF: ATP binding

TraesCS4B01G201100	Integrator complex subunit 4	GO:0005488 MF: binding
TraesCS4B01G201500	Calcium-transporting ATPase	GO:0000166 MF: nucleotide binding
TraesCS4B01G201600	Receptor-like kinase, putative	GO:0004672 MF: protein kinase activity
TraesCS4B01G201800	Cytosine-specific methyltransferase	GO:0003682 MF: chromatin binding
TraesCS4B01G201900	Werner Syndrome-like exonuclease	GO:0003676 MF: nucleic acid binding
TraesCS4B01G202000	Cytochrome P450	GO:0005506 MF: iron ion binding
TraesCS4B01G202300	Ankyrin repeat-containing protein	GO:0005515 MF: protein binding
TraesCS4B01G203300	Kinesin-like protein	GO:0003777 MF: microtubule motor activity
TraesCS4B01G203400	Zinc finger family protein	GO:0003676 MF: nucleic acid binding
TraesCS4B01G203500	3'-5' exonuclease domain-containing protein	GO:0003676 MF: nucleic acid binding
TraesCS4B01G204300	RNA-binding family protein	GO:0003676 MF: nucleic acid binding
TraesCS4B01G204400	Histone H2B	GO:0003677 MF: DNA binding
TraesCS4B01G204500	ATP synthase subunit b	GO:0015078 MF: hydrogen ion transmembrane transporter activity
TraesCS4B01G204600	RNA binding protein	GO:0003676 MF: nucleic acid binding
TraesCS4B01G204700	Acyl-CoA N-acyltransferase with RING/FYVE/PHD-type zinc finger protein	GO:0008080 MF: N-acetyltransferase activity
TraesCS4B01G204800	Polyadenylate-binding protein	GO:0003676 MF: nucleic acid binding
TraesCS4B01G204900	ADP-ribosylation factor GTPase-activating protein	GO:0005096 MF: GTPase activator activity
TraesCS4B01G205000	RNA-binding family protein	GO:0003676 MF: nucleic acid binding
TraesCS4B01G205400	NAD(P)H dehydrogenase (Quinone)	GO:0003955 MF: NAD(P)H dehydrogenase (quinone) activity
TraesCS4B01G205900	Guanosine nucleotide diphosphate dissociation inhibitor	GO:0005092 MF: GDP-dissociation inhibitor activity
TraesCS4B01G206800	Dof zinc finger protein	GO:0003677 MF: DNA binding
TraesCS4B01G208800	Pentatricopeptide repeat-containing protein	GO:0005515 MF: protein binding
TraesCS4B01G208900	Hsp70 nucleotide exchange factor fes1	GO:0005488 MF: binding
TraesCS4B01G209100	RING/U-box superfamily protein	GO:0005515 MF: protein binding
TraesCS4B01G210300	Mannose-1-phosphate guanyltransferase, putative	GO:0009058 BP: biosynthetic process
TraesCS4B01G210600	Kinase family protein	GO:0004672 MF: protein kinase activity
TraesCS4B01G210800	Serine/threonine-protein phosphatase	GO:0016787 MF: hydrolase activity
TraesCS4B01G210900	LIM domain-containing protein 1	GO:0008270 MF: zinc ion binding

				TraesCS4B01G211000	Mitochondrial carrier protein, expressed	GO:0055085 BP: transmembrane transport
				TraesCS4B01G212600	LIM domain-containing protein	GO:0008270 MF: zinc ion binding
				TraesCS4B01G212900	Ubiquitin-like-specific protease ESD4	GO:0006508 BP: proteolysis
				TraesCS4B01G213200	SH3 domain containing protein, expressed	GO:0005488 MF: binding
				TraesCS4B01G213400	RNA-binding family protein	GO:0003676 MF: nucleic acid binding
				TraesCS4B01G213600	50S ribosomal protein L4	GO:0003735 MF: structural constituent of ribosome
				TraesCS4B01G213900	Josephin, putative, expressed	GO:0004843 MF: thiol-dependent ubiquitin-specific protease activity
				TraesCS4B01G214100	Holliday junction ATP-dependent DNA helicase RuvB	GO:0005524 MF: ATP binding
				TraesCS4B01G214200	BTB/POZ domain-containing protein	GO:0005515 MF: protein binding
				TraesCS4B01G214400	C2H2-like zinc finger protein	GO:0003676 MF: nucleic acid binding
				TraesCS4B01G214500	Anthranilate synthase	GO:0000162 BP: tryptophan biosynthetic process
				TraesCS4B01G214800	LAG1 longevity assurance-like protein	GO:0005783 CC: endoplasmic reticulum
				TraesCS4B01G215000	Calcium-binding EF hand family protein, putative, expressed	GO:0005509 MF: calcium ion binding
				TraesCS4B01G215100	S-ribonuclease binding protein	GO:0004842 MF: ubiquitin-protein transferase activity
				TraesCS4B01G215300	Strictosidine synthase family protein	GO:0009058 BP: biosynthetic process
				TraesCS4B01G215500	Splicing factor 3A subunit 2	GO:0003676 MF: nucleic acid binding
				TraesCS4B01G215800	ethylene-responsive transcription factor	GO:0003677 MF: DNA binding
				TraesCS4B01G216000	Serine/threonine-protein kinase	GO:0004672 MF: protein kinase activity
R_RSRatio	AX-158582575	4B	509	TraesCS4B01G245900	Protein CRABS CLAW, putative	GO:0007275 BP: multicellular organism development
				TraesCS4B01G246100	Mitotic checkpoint protein bub3.1	GO:0005515 MF: protein binding
				TraesCS4B01G246400	Expansin	GO:0005576 CC: extracellular region
				TraesCS4B01G246500	Expansin	GO:0005576 CC: extracellular region
				TraesCS4B01G246600	Expansin	GO:0005576 CC: extracellular region
R_SL	AX-158582483	4B	661	TraesCS4B01G377100	Germin-like protein	GO:0030145 MF: manganese ion binding
				TraesCS4B01G377200	Germin-like protein	GO:0030145 MF: manganese ion binding
				TraesCS4B01G378000	Germin-like protein	GO:0030145 MF: manganese ion binding
				TraesCS4B01G379000	Alkyl transferase	GO:0016765 MF: transferase activity, transferring alkyl or aryl (other than methyl) groups
				TraesCS4B01G379200	Calcineurin B-like protein	GO:0005509 MF: calcium ion binding

				TraesCS4B01G379300	Casein kinase II subunit beta	GO:0005956 CC: protein kinase CK2 complex
				TraesCS4B01G379500	Pterin-4-alpha-carbinolamine dehydratase, putative	GO:0006729 BP: tetrahydrobiopterin biosynthetic process
				TraesCS4B01G379600	Invertase inhibitor	GO:0004857 MF: enzyme inhibitor activity
				TraesCS4B01G379800	Man1-Src1p-carboxy-terminal domain protein	GO:0005639 CC: integral component of nuclear inner membrane
				TraesCS4B01G379900	Ribose-phosphate pyrophosphokinase	GO:0000287 MF: magnesium ion binding
				TraesCS4B01G380000	Protein NRT1/ PTR FAMILY 5.1	GO:0005215 MF: transporter activity
				TraesCS4B01G380100	C2 domain-containing family protein	GO:0005515 MF: protein binding
				TraesCS4B01G380200	CAAX protease self-immunity protein	GO:0016020 CC: membrane
				TraesCS4B01G380800	ATP-dependent chaperone ClpB	GO:0005524 MF: ATP binding
				TraesCS4B01G380900	RING/U-box superfamily protein	GO:0005515 MF: protein binding
				TraesCS4B01G381000	RING-finger ubiquitin ligase	GO:0005515 MF: protein binding
				TraesCS4B01G381100	RING/U-box superfamily protein	GO:0005515 MF: protein binding
				TraesCS4B01G381200	Divalent metal cation transporter MntH	GO:0005215 MF: transporter activity
				TraesCS4B01G381300	Carboxyl methyltransferase	GO:0008168 MF: methyltransferase activity
				TraesCS4B01G382300	Cytochrome P450	;GO:0055114 BP: oxidation-reduction process
				TraesCS4B01G382400	Phosphatase 2C family protein	GO:0003824 MF: catalytic activity
R_SFW	AX-108742709	5A	578	TraesCS5A01G381000	WRKY transcription factor	GO:0003700 MF: transcription factor activity, sequence-specific DNA binding
				TraesCS5A01G381100	Cytochrome P450 family protein, expressed	GO:0005506 MF: iron ion binding
R_SFW	AX-108744896	5A	577	TraesCS5A01G379500	Chalcone synthase	GO:0003824 MF: catalytic activity
				TraesCS5A01G379600	Chalcone synthase	GO:0003824 MF: catalytic activity
				TraesCS5A01G379700	Chalcone synthase	GO:0003824 MF: catalytic activity
				TraesCS5A01G380100	Deoxyhypusine synthase, putative, expressed	GO:0008612 BP: peptidyl-lysine modification to peptidyl-hypusine
R_SFW	AX-110382510	5A	577	TraesCS5A01G379500	Chalcone synthase	GO:0003824 MF: catalytic activity
				TraesCS5A01G379600	Chalcone synthase	GO:0003824 MF: catalytic activity
				TraesCS5A01G379700	Chalcone synthase	GO:0003824 MF: catalytic activity
				TraesCS5A01G380100	Deoxyhypusine synthase, putative, expressed	GO:0008612 BP: peptidyl-lysine modification to peptidyl-hypusine
				TraesCS5A01G380200	F-box protein	GO:0005515 MF: protein binding
				TraesCS5A01G380300	Deoxyhypusine synthase	GO:0008612 BP: peptidyl-lysine modification to peptidyl-hypusine

				TraesCS5A01G380400	CWF19-like protein 2	GO:0003824 MF: catalytic activity
				TraesCS5A01G380500	LEM3 (Ligand-effect modulator 3)-like	GO:0016020 CC: membrane
				TraesCS5A01G380600	Vacuolar sorting-associated protein 18-like protein	GO:0005515 MF: protein binding
				TraesCS5A01G380700	Disease resistance protein (NBS-LRR class) family	GO:0043531 MF: ADP binding
				TraesCS5A01G380800	DNA repair protein XRCC4	GO:0003677 MF: DNA binding
				TraesCS5A01G380900	Basic helix-loop-helix transcription factor	GO:0046983 MF: protein dimerization activity
				TraesCS5A01G381000	WRKY transcription factor	GO:0003700 MF: transcription factor activity, sequence-specific DNA binding
				TraesCS5A01G381100	Cytochrome P450 family protein, expressed	GO:0005506 MF: iron ion binding
R_SFW	AX-89769139	5A	578	TraesCS5A01G380500	LEM3 (Ligand-effect modulator 3)-like	GO:0016020 CC: membrane
				TraesCS5A01G380600	Vacuolar sorting-associated protein 18-like protein	GO:0005515 MF: protein binding
				TraesCS5A01G380700	Disease resistance protein (NBS-LRR class) family	GO:0043531 MF: ADP binding
				TraesCS5A01G380800	DNA repair protein XRCC4	GO:0003677 MF: DNA binding
R_SFW	BS00074299_51	5A	578	TraesCS5A01G380800	DNA repair protein XRCC4	GO:0003677 MF: DNA binding
R_SFW	BS00076246_51	5A	578	TraesCS5A01G380800	DNA repair protein XRCC4	GO:0003677 MF: DNA binding
R_SFW	Ku_c19858_2078	5A	577	TraesCS5A01G380200	F-box protein	GO:0005515 MF: protein binding
				TraesCS5A01G380300	Deoxyhypusine synthase	GO:0008612 BP: peptidyl-lysine modification to peptidyl-hypusine
				TraesCS5A01G380400	CWF19-like protein 2	GO:0003824 MF: catalytic activity
R_SFW	Tdurum_contig86202_175	5A	578	TraesCS5A01G380700	Disease resistance protein (NBS-LRR class) family	GO:0043531 MF: ADP binding
				TraesCS5A01G380800	DNA repair protein XRCC4	GO:0003677 MF: DNA binding
R_SL	AX-109884177	5A	37	TraesCS5A01G040900	BTB/POZ domain containing protein, expressed	GO:0005515 MF: protein binding
				TraesCS5A01G041000	BTB/POZ and MATH domain-containing protein 1	GO:0005515 MF: protein binding
				TraesCS5A01G041100	Guanosine nucleotide diphosphate dissociation inhibitor	GO:0005092 MF: GDP-dissociation inhibitor activity
				TraesCS5A01G041300	BTB/POZ and MATH domain-containing protein 2	GO:0005515 MF: protein binding
				TraesCS5A01G042400	Eukaryotic translation initiation factor 3 subunit A	GO:0005515 MF: protein binding
				TraesCS5A01G042600	BTB/POZ domain-containing protein	GO:0005515 MF: protein binding
				TraesCS5A01G042700	Histone-lysine N-methyltransferase	GO:0005515 MF: protein binding
				TraesCS5A01G042800	Glutamate receptor	GO:0004930 MF: G-protein coupled receptor activity

				TraesCS5A01G042900	Cationic amino acid transporter, putative	GO:0003333 BP: amino acid transmembrane transport
				TraesCS5A01G043000	Heavy metal transport/detoxification superfamily protein, putative	GO:0030001 BP: metal ion transport
R_RFW	Tdurum_contig82473_67	5B	620	TraesCS5B01G447800	Cytosine-specific methyltransferase	GO:0003682 MF: chromatin binding
				TraesCS5B01G448000	Expansin	GO:0005576 CC: extracellular region
				TraesCS5B01G448100	30S ribosomal protein S19	GO:0003723 MF: RNA binding
				TraesCS5B01G448200	Histone H1	GO:0003677 MF: DNA binding
				TraesCS5B01G448400	Histone H1	GO:0000786 CC: nucleosome
				TraesCS5B01G448500	Histone H1	GO:0000786 CC: nucleosome
				TraesCS5B01G448600	Kinase-like	GO:0004672 MF: protein kinase activity
				TraesCS5B01G448700	Mitochondrial transcription termination factor-like	GO:0003690 MF: double-stranded DNA binding
				TraesCS5B01G449000	Histone H1	GO:0000786 CC: nucleosome
				TraesCS5B01G449200	Receptor-like protein kinase	GO:0004672 MF: protein kinase activity
				TraesCS5B01G449300	Receptor-like protein kinase	GO:0004672 MF: protein kinase activity
R_RFW	BS00065783_51	5D	69	TraesCS5D01G070700	WRKY transcription factor	GO:0003700 MF: transcription factor activity, sequence-specific DNA binding
				TraesCS5D01G070800	Aminotransferase	GO:0003824 MF: catalytic activity
				TraesCS5D01G070900	GTP 3',8-cyclase	GO:0003824 MF: catalytic activity
				TraesCS5D01G071000	RNA-binding KH domain-containing protein	GO:0003676 MF: nucleic acid binding
				TraesCS5D01G071100	N-carbamyl-L-amino acid amidohydrolase	GO:0008152 BP: metabolic process
				TraesCS5D01G071200	Cinnamoyl-CoA reductase 4	GO:0003824 MF: catalytic activity
				TraesCS5D01G071300	FAD/NAD(P)-binding oxidoreductase family protein	GO:0016491 MF: oxidoreductase activity
				TraesCS5D01G071400	Gamma-tubulin complex component	GO:0000226 BP: microtubule cytoskeleton organization
				TraesCS5D01G071500	WAT1-related protein	GO:0016021 CC: integral component of membrane
				TraesCS5D01G071600	Splicing factor U2AF, large subunit	GO:0003676 MF: nucleic acid binding
				TraesCS5D01G071700	Splicing factor U2AF, large subunit	GO:0003676 MF: nucleic acid binding
				TraesCS6A01G287700	Dof zinc finger protein	GO:0003677 MF: DNA binding
				TraesCS6A01G288000	Acetolactate synthase	GO:0000287 MF: magnesium ion binding
				TraesCS6A01G288100	Basic helix-loop-helix transcription factor	GO:0046983 MF: protein dimerization activity

R_RL	AX-158600281		6A	520	TraesCS6A01G288300	2-oxoglutarate (2OG) and Fe(II)-dependent oxygenase superfamily protein	GO:0016491 MF: oxidoreductase activity
					TraesCS6A01G288400	2-oxoglutarate (2OG) and Fe(II)-dependent oxygenase superfamily protein	GO:0016491 MF: oxidoreductase activity
R_RFW	AX-158528874	6B_Hap1	6B	720	TraesCS6B01G473000	Mitochondrial intermediate peptidase	GO:0004222 MF: metalloendopeptidase activity
	BS00011795_51	6B_Hap1	6B	720	TraesCS6B01G473100	F-box protein family	NA
					TraesCS6B01G473200	Pectinesterase inhibitor	GO:0004857 MF: enzyme inhibitor activity
					TraesCS6B01G473300	Plant invertase/pectin methylesterase inhibitor superfamily protein	GO:0004857 MF: enzyme inhibitor activity
					TraesCS6B01G473500	Pentatricopeptide repeat-containing protein	GO:0005515 MF: protein binding
R_RFW	Excalibur_c28759_914		6B	716	TraesCS6B01G462100	Transcription factor, putative	NA
					TraesCS6B01G462300	Peroxidase	GO:0004601 MF: peroxidase activity
					TraesCS6B01G462500	4-hydroxybenzoate octaprenyltransferase	GO:0004659 MF: prenyltransferase activity GO:0016021 CC: integral component of membrane
					TraesCS6B01G462600	Receptor-kinase, putative	GO:0004672 MF: protein kinase activity
					TraesCS6B01G462700	Replication protein A 32 kDa subunit	GO:0003677 MF: DNA binding
					TraesCS6B01G462900	Tyrosine--tRNA ligase	GO:0000166 MF: nucleotide binding
					TraesCS6B01G463000	Calcium-dependent lipid-binding (CaLB domain) family protein	GO:0005515 MF: protein binding
					TraesCS6B01G463200	F-box protein	GO:0005515 MF: protein binding
					TraesCS6B01G463500	Disease resistance protein RPM1	GO:0043531 MF: ADP binding
					TraesCS6B01G463600	Disease resistance protein RPM1	GO:0043531 MF: ADP binding
					TraesCS6B01G463700	Disease resistance protein RPM1	GO:0043531 MF: ADP binding
					TraesCS6B01G463800	Disease resistance protein (NBS-LRR class) family	GO:0043531 MF: ADP binding
					TraesCS6B01G463900	Disease resistance protein RPM1	GO:0043531 MF: ADP binding
					TraesCS6B01G464000	Disease resistance protein RPM1	GO:0043531 MF: ADP binding
					TraesCS6B01G464200	Disease resistance protein RPM1	GO:0043531 MF: ADP binding
					TraesCS6B01G464300	Disease resistance protein RPM1	GO:0043531 MF: ADP binding
					TraesCS6B01G464400	Disease resistance protein RPM1	GO:0043531 MF: ADP binding
					TraesCS6B01G464500	Disease resistance protein RPM1	GO:0043531 MF: ADP binding
					TraesCS6B01G464600	NADH-ubiquinone oxidoreductase chain 6	GO:0008137 MF: NADH dehydrogenase (ubiquinone) activity
					TraesCS6B01G464800	12-oxophytodienoate reductase-like protein	GO:0003824 MF: catalytic activity

				TraesCS6B01G464900	Disease resistance protein RPM1	GO:0043531 MF: ADP binding
				TraesCS6B01G465000	Disease resistance protein (NBS-LRR class) family	GO:0043531 MF: ADP binding
				TraesCS6B01G465100	Disease resistance protein RPM1	GO:0043531 MF: ADP binding
				TraesCS6B01G465600	Protein kinase family protein	GO:0004672 MF: protein kinase activity
				TraesCS6B01G465700	receptor kinase 1	GO:0004672 MF: protein kinase activity
				TraesCS6B01G465800	Disease resistance protein RPM1	GO:0043531 MF: ADP binding
				TraesCS6B01G465900	BTB/POZ domain containing protein	GO:0005515 MF: protein binding
				TraesCS6B01G466000	receptor kinase 2	GO:0004672 MF: protein kinase activity
				TraesCS6B01G466200	Inhibitor protein	GO:0004867 MF: serine-type endopeptidase inhibitor activity
R_SFW	AX-158589824	6D	3	TraesCS6D01G004100	F-box family protein	GO:0005515 MF: protein binding
				TraesCS6D01G004300	Anthocyanidin synthase	GO:0016491 MF: oxidoreductase activity
				TraesCS6D01G004600	Protein disulfide-isomerase	GO:0045454 BP: cell redox homeostasis
				TraesCS6D01G004700	Protein disulfide-isomerase	GO:0005783 CC: endoplasmic reticulum;
				TraesCS6D01G004800	tetratricopeptide repeat (TPR)-containing protein	GO:0005515 MF: protein binding
				TraesCS6D01G005100	RING/U-box superfamily protein	GO:0008270 MF: zinc ion binding
				TraesCS6D01G005200	Protein disulfide-isomerase	GO:0005783 CC: endoplasmic reticulum
				TraesCS6D01G005300	NBS-LRR-like resistance protein	GO:0043531 MF: ADP binding
				TraesCS6D01G005600	E3 ubiquitin-protein ligase	GO:0004842 MF: ubiquitin-protein transferase activity
				TraesCS6D01G005800	Leucine-rich repeat receptor-like protein kinase family protein	GO:0005515 MF: protein binding
				TraesCS6D01G005900	Leucine-rich repeat receptor-like protein kinase family protein	GO:0005515 MF: protein binding
				TraesCS6D01G006000	Leucine-rich repeat receptor-like protein kinase family protein	GO:0005515 MF: protein binding
				TraesCS6D01G006100	F-box protein	GO:0005515 MF: protein binding
				TraesCS6D01G006400	F-box protein	GO:0005515 MF: protein binding
				TraesCS6D01G006500	Terpene cyclase/mutase family member	GO:0016866 MF: intramolecular transferase activity
				TraesCS6D01G009500	Bidirectional sugar transporter SWEET	GO:0016021 CC: integral component of membrane
				TraesCS6D01G009600	Bidirectional sugar transporter SWEET	GO:0016021 CC: integral component of membrane
				TraesCS6D01G009700	Bidirectional sugar transporter SWEET	GO:0016021 CC: integral component of membrane
				TraesCS6D01G009800	WAT1-related protein	GO:0016020 CC: membrane

				TraesCS6D01G009900	WAT1-related protein	GO:0016020 CC: membrane
				TraesCS6D01G010000	F-box family protein	GO:0005515 MF: protein binding
				TraesCS6D01G010100	Lipoxygenase	GO:0005515 MF: protein binding
				TraesCS6D01G010600	F-box family protein	GO:0005515 MF: protein binding
R_RFW	AX-158626906	7B	704	TraesCS7B01G004400	Apyrase	GO:0016787 MF: hydrolase activity
				TraesCS7B01G004700	Flavin-containing monooxygenase	GO:0004499 MF: N,N-dimethylaniline monooxygenase activity
				TraesCS7B01G004800	HXXXD-type acyl-transferase-like protein	GO:0016747 MF: transferase activity, transferring acyl groups other than amino-acyl groups
				TraesCS7B01G004900	NAC domain protein	GO:0003677 MF: DNA binding
				TraesCS7B01G005000	RNA-binding family protein	GO:0003676 MF: nucleic acid binding
				TraesCS7B01G005100	Anthocyanin 5-aromatic acyltransferase	GO:0016747 MF: transferase activity, transferring acyl groups other than amino-acyl groups
				TraesCS7B01G005200	Pleiotropic drug resistance ABC transporter	GO:0005524 MF: ATP binding
				TraesCS7B01G005400	DNA repair radA-like protein	GO:0003677 MF: DNA binding
				TraesCS7B01G005500	ATP-dependent 6-phosphofructokinase	GO:0003872 MF: 6-phosphofructokinase activity
				TraesCS7B01G005600	B3 domain-containing protein family	GO:0003677 MF: DNA binding
				TraesCS7B01G005700	Ubiquitin-like modifier-activating enzyme 5	GO:0008641 MF: small protein activating enzyme activity
				TraesCS7B01G005900	NBS-LRR disease resistance protein-like	GO:0043531 MF: ADP binding
				TraesCS7B01G006000	Dual specificity protein phosphatase family protein	GO:0004725 MF: protein tyrosine phosphatase activity
				TraesCS7B01G006100	3-ketoacyl-CoA synthase	GO:0003824 MF: catalytic activity
				TraesCS7B01G006200	3-ketoacyl-CoA synthase	GO:0003824 MF: catalytic activity
				TraesCS7B01G006300	3-ketoacyl-CoA synthase	GO:0003824 MF: catalytic activity
				TraesCS7B01G006400	Zinc finger, B-box	GO:0005622 CC: intracellular;
				TraesCS7B01G006600	Photosynthetic NDH subcomplex B 3	GO:0009055 MF: electron carrier activity
				TraesCS7B01G006700	Ubiquinone biosynthesis O-methyltransferase	GO:0006744 BP: ubiquinone biosynthetic process
				TraesCS7B01G007000	GDSL esterase/lipase	GO:0016788 MF: hydrolase activity, acting on ester bonds
				TraesCS7B01G007300	WAT1-related protein	GO:0016020 CC: membrane
R_RL	wsnp_Ku_c8497_14429303	7B	64	TraesCS7B01G061100	Ring finger protein, putative	GO:0005515 MF: protein binding
				TraesCS7B01G061200	Haloacid dehalogenase-like hydrolase superfamily protein	GO:0008253 MF: 5'-nucleotidase activity
				TraesCS7B01G061300	Histone H3	GO:0000786 CC: nucleosome

					TraesCS7B01G061400	Exocyst complex component, putative	GO:0000145 CC: exocyst
					TraesCS7B01G061600	Pectinesterase	GO:0004857 MF: enzyme inhibitor activity
					TraesCS7B01G061900	Receptor-like kinase	GO:0004672 MF: protein kinase activity
					TraesCS7B01G062100	Basic helix-loop-helix transcription factor	GO:0046983 MF: protein dimerization activity
					TraesCS7B01G062200	Ethylene-responsive transcription factor	GO:0003677 MF: DNA binding
R_SL	AX-158544315		7D	87	TraesCS7D01G135100	Sulfiredoxin	NA
					TraesCS7D01G135200	MYB-related transcription factor	GO:0003677 MF: DNA binding
					TraesCS7D01G135300	MYB-related transcription factor	GO:0003677 MF: DNA binding
					TraesCS7D01G135500	MYB-related transcription factor	GO:0003677 MF: DNA binding
					TraesCS7D01G136600	Cytochrome b6-f complex subunit 6	GO:0009055 MF: electron carrier activity
					TraesCS7D01G136700	Protein kinase family protein	GO:0004672 MF: protein kinase activity
					TraesCS7D01G137100	3'-N-debenzoyl-2'-deoxytaxol N-benzoyltransferase	GO:0016747 MF: transferase activity, transferring acyl groups other than amino-acyl groups
					TraesCS7D01G137200	Pheophorbide a oxygenase, chloroplastic	GO:0010277 MF: chlorophyllide a oxygenase [overall] activity
					TraesCS7D01G137900	Zinc knuckle family protein, expressed	GO:0003676 MF: nucleic acid binding

Supplementary Table 4. S3b: list of significant Haplotypes/SNPs for STI values, corresponding chromosomal position and their linked candidate genes in 1Mb span up and down stream regions

Trait	Marker	Hap	Ch	Pos (Mbp)	mrnaid	Description	GO-IDs-(Description)-via-Interpro
STI_SL	AX-158595571	sti_SL_1A_Hap1	1A	535	TraesCS1A01G350400	Heat shock transcription factor	GO:0003700 MF: transcription factor activity
					TraesCS1A01G350500	Non-specific serine/threonine protein kinase	GO:0004672 MF: protein kinase activity
STI_SFW	Excalibur_c54055_694		1D	308	TraesCS1D01G219800	bZIP transcription factor (DUF630 and DUF632)	NA
					TraesCS1D01G220100	Kinase family protein	GO:0004672 MF: protein kinase activity
					TraesCS1D01G220300	Phospholipase a1-chloroplastic-like	GO:0006629 BP: lipid metabolic process
					TraesCS1D01G220400	Serine hydroxymethyltransferase	GO:0003824 MF: catalytic activity
					TraesCS1D01G220500	MYB-related transcription factor	GO:0003677 MF: DNA binding

				TraesCS1D01G220600	Dual specificity protein phosphatase	GO:0004725 MF: protein tyrosine phosphatase activity
				TraesCS1D01G220900	Homeobox-leucine zipper family protein	GO:0003677 MF: DNA binding
				TraesCS1D01G221000	Myb transcription factor	GO:0003677 MF: DNA binding
				TraesCS1D01G221500	ethylene-responsive transcription factor	GO:0003677 MF: DNA binding
STI_RL	AX-158596313	2A	421	TraesCS2A01G264800	Two-component response regulator	GO:0003677 MF: DNA binding
				TraesCS2A01G264900	L-ascorbate oxidase-like protein	GO:0005507 MF: copper ion binding
				TraesCS2A01G265300	F-box family protein-like protein	GO:0005515 MF: protein binding
				TraesCS2A01G265500	Disease resistance protein (TIR-NBS-LRR class) family	GO:0003676 MF: nucleic acid binding
				TraesCS2A01G265600	F-box family protein	GO:0005515 MF: protein binding
STI_RL	AX-111016876	2A	717	TraesCS2A01G477000	Pathogenesis-related protein 1	GO:0006952 BP: defense response
				TraesCS2A01G477200	NBS-LRR disease resistance protein	GO:0043531 MF: ADP binding
				TraesCS2A01G477400	GDSL esterase/lipase	GO:0016788 MF: hydrolase activity, acting on ester bonds
				TraesCS2A01G477500	Pentatricopeptide repeat-containing protein	GO:0005515 MF: protein binding
				TraesCS2A01G477600	Non-specific lipid-transfer protein	GO:0006869 BP: lipid transport
				TraesCS2A01G479100	Cyclin family protein	GO:0000079 BP: regulation of cyclin-dependent protein serine/threonine kinase activity
				TraesCS2A01G480100	NBS-LRR disease resistance protein, putative, expressed	GO:0043531 MF: ADP binding
				TraesCS2A01G480300	Thioredoxin	GO:0045454 BP: cell redox homeostasis
				TraesCS2A01G480400	NBS-LRR disease resistance protein	GO:0043531 MF: ADP binding
STI_RL	AX-108742509	2A	718	TraesCS2A01G480100	NBS-LRR disease resistance protein, putative, expressed	GO:0043531 MF: ADP binding
				TraesCS2A01G480200	Divalent-cation tolerance protein CutA	GO:0010038 BP: response to metal ion
				TraesCS2A01G480300	Thioredoxin	GO:0045454 BP: cell redox homeostasis
				TraesCS2A01G480400	NBS-LRR disease resistance protein	GO:0043531 MF: ADP binding
				TraesCS2A01G480500	Kinesin-like protein	GO:0003777 MF: microtubule motor activity
				TraesCS2A01G480600	Kinase-like	GO:0004672 MF: protein kinase activity
STI_RS Ratio	RAC875_c21906_247	2A	691	TraesCS2A01G439200	Acylphosphatase	NA
				TraesCS2A01G439400	Ubiquinol oxidase	GO:0009916 MF: alternative oxidase activity
				TraesCS2A01G439500	Glucan endo-1,3-beta-glucosidase	GO:0004553 MF: hydrolase activity, hydrolyzing O-glycosyl compounds
				TraesCS2A01G439800	Cytochrome P450	GO:0005506 MF: iron ion binding
				TraesCS2A01G440900	O-methyltransferase family protein, expressed	GO:0008168 MF: methyltransferase activity

				TraesCS2A01G441100	O-methyltransferase-like protein	GO:0008168 MF: methyltransferase activity
				TraesCS2A01G441300	Myb family transcription factor family protein	GO:0003677 MF: DNA binding
				TraesCS2A01G442200	HXXXD-type acyl-transferase family protein	GO:0016747 MF: transferase activity, transferring acyl groups other than amino-acyl groups
STI_RS Ratio	AX-158555653	2A	691	TraesCS2A01G441600	Wound-induced basic	NA
STI_RS Ratio	AX-158555652	2A	691	TraesCS2A01G439800	Cytochrome P450	GO:0005506 MF: iron ion binding
				TraesCS2A01G440000	WD-repeat cell cycle regulatory protein	GO:0005515 MF: protein binding
				TraesCS2A01G440900	O-methyltransferase family protein, expressed	GO:0008168 MF: methyltransferase activity
				TraesCS2A01G441100	O-methyltransferase-like protein	GO:0008168 MF: methyltransferase activity
				TraesCS2A01G441300	Myb family transcription factor family protein	GO:0003677 MF: DNA binding
				TraesCS2A01G442200	HXXXD-type acyl-transferase family protein	GO:0016747 MF: transferase activity, transferring acyl groups other than amino-acyl groups
				TraesCS2A01G442300	p-loop containing nucleoside triphosphate hydrolases superfamily protein, putative	GO:0005515 MF: protein binding
				TraesCS2A01G442500	Basic helix loop helix (BHLH) family transcription factor	GO:0046983 MF: protein dimerization activity
				TraesCS2A01G442600	Glycosyltransferase	GO:0016757 MF: transferase activity, transferring glycosyl groups
				TraesCS2A01G442700	Basic helix-loop-helix (BHLH) Transcription Factor	GO:0046983 MF: protein dimerization activity
STI_RS Ratio	RAC875_c52458_454	2A	692	TraesCS2A01G442900	Receptor-like protein kinase	GO:0004672 MF: protein kinase activity
				TraesCS2A01G443000	Kinase, putative	GO:0004672 MF: protein kinase activity
STI_RS Ratio	BobWhite_c17403_635	2A	693	TraesCS2A01G443200	50S ribosomal protein L11	GO:0003735 MF: structural constituent of ribosome
STI_RS Ratio	AX-158572604	2A	706	TraesCS2A01G457000	RING/U-box superfamily protein	NA
				TraesCS2A01G457300	Prefoldin subunit 2	GO:0006457 BP: protein folding
				TraesCS2A01G457500	Structural maintenance of chromosomes protein	GO:0005515 MF: protein binding
				TraesCS2A01G457600	ATP-dependent zinc metalloprotease FtsH	GO:0005524 MF: ATP binding
				TraesCS2A01G457700	Calcium-dependent lipid-binding (CaLB domain) family protein	GO:0005515 MF: protein binding
				TraesCS2A01G458700	BTB/POZ domain containing protein, expressed	GO:0005515 MF: protein binding
				TraesCS2A01G458800	Ubiquitin	GO:0003735 MF: structural constituent of ribosome
				TraesCS2A01G458900	Expansin protein	GO:0005576 CC: extracellular region
				TraesCS2A01G459000	30S ribosomal protein S11	GO:0003735 MF: structural constituent of ribosome
				TraesCS2A01G459100	NBS-LRR disease resistance protein	GO:0043531 MF: ADP binding
				TraesCS2A01G459200	MADS-box transcription factor family protein	GO:0003677 MF: DNA binding

				TraesCS2A01G459600	Imidazoleglycerol-phosphate dehydratase	GO:0000105 BP: histidine biosynthetic process
				TraesCS2A01G460400	UDP-glucose 4-epimerase, putative	GO:0003978 MF: UDP-glucose 4-epimerase activity
				TraesCS2A01G460700	B3 domain-containing protein	GO:0003677 MF: DNA binding
				TraesCS2A01G461600	Gamma-soluble NSF attachment protein	GO:0005515 MF: protein binding
				TraesCS2A01G461700	Basic helix-loop-helix transcription factor	GO:0046983 MF: protein dimerization activity
STI_RS Ratio	AX-158572603	2A	706	TraesCS2A01G461800	Receptor-like kinase	GO:0004672 MF: protein kinase activity
				TraesCS2A01G461900	Leucine-rich repeat receptor-like protein kinase family protein	GO:0005515 MF: protein binding
STI_RS Ratio	AX-111016876	2A	717	TraesCS2A01G477000	Pathogenesis-related protein 1	GO:0006952 BP: defense response
				TraesCS2A01G477200	NBS-LRR disease resistance protein	GO:0043531 MF: ADP binding
				TraesCS2A01G477400	GDSL esterase/lipase	GO:0016788 MF: hydrolase activity, acting on ester bonds
				TraesCS2A01G477500	Pentatricopeptide repeat-containing protein	GO:0005515 MF: protein binding
				TraesCS2A01G478000	Histone-lysine N-methyltransferase	GO:0005515 MF: protein binding
				TraesCS2A01G478100	Linalool synthase, chloroplastic	GO:0000287 MF: magnesium ion binding
				TraesCS2A01G478500	Beta-glucosidase	GO:0004553 MF: hydrolase activity, hydrolyzing O-glycosyl compounds
				TraesCS2A01G478700	Glycosyltransferase	GO:0008152 BP: metabolic process
				TraesCS2A01G478800	Histone-lysine N-methyltransferase	GO:0005515 MF: protein binding
				TraesCS2A01G478900	Glycosyltransferase	GO:0008152 BP: metabolic process
				TraesCS2A01G479100	Cyclin family protein	GO:0000079 BP: regulation of cyclin-dependent protein serine/threonine kinase activity
				TraesCS2A01G480100	NBS-LRR disease resistance protein, putative, expressed	GO:0043531 MF: ADP binding
				TraesCS2A01G480200	Divalent-cation tolerance protein CutA	GO:0010038 BP: response to metal ion
				TraesCS2A01G480300	Thioredoxin	GO:0045454 BP: cell redox homeostasis
				TraesCS2A01G480400	NBS-LRR disease resistance protein	GO:0043531 MF: ADP binding
				TraesCS2A01G480600	Kinase-like	GO:0004672 MF: protein kinase activity
				TraesCS2A01G480900	Glycosyltransferase	GO:0016757 MF: transferase activity, transferring glycosyl groups
STI_RS Ratio	AX-158557238	2A	717	TraesCS2A01G479100	Cyclin family protein	GO:0000079 BP: regulation of cyclin-dependent protein serine/threonine kinase activity
				TraesCS2A01G479500	Histone-lysine N-methyltransferase	GO:0005515 MF: protein binding
				TraesCS2A01G479700	Invertase/pectin methylesterase inhibitor family protein	GO:0004857 MF: enzyme inhibitor activity
				TraesCS2A01G479900	SNF2 domain-containing protein / helicase domain-containing protein / zinc finger protein-like protein	GO:0005515 MF: protein binding

				TraesCS2A01G480100	NBS-LRR disease resistance protein, putative, expressed	GO:0043531 MF: ADP binding
				TraesCS2A01G480200	Divalent-cation tolerance protein CutA	GO:0010038 BP: response to metal ion
				TraesCS2A01G480300	Thioredoxin	GO:0045454 BP: cell redox homeostasis
				TraesCS2A01G480400	NBS-LRR disease resistance protein	GO:0043531 MF: ADP binding
				TraesCS2A01G480500	Kinesin-like protein	GO:0003777 MF: microtubule motor activity
				TraesCS2A01G480600	Kinase-like	GO:0004672 MF: protein kinase activity
				TraesCS2A01G480900	Glycosyltransferase	GO:0016757 MF: transferase activity, transferring glycosyl groups
STI_RS Ratio	AX-109854150	2A	717	TraesCS2A01G477900	Aldehyde dehydrogenase	GO:0004491 MF: methylmalonate-semialdehyde dehydrogenase (acylating) activity
				TraesCS2A01G478000	Histone-lysine N-methyltransferase	GO:0005515 MF: protein binding
				TraesCS2A01G478100	Linalool synthase, chloroplastic	GO:0000287 MF: magnesium ion binding
				TraesCS2A01G478500	Beta-glucosidase	GO:0004553 MF: hydrolase activity, hydrolyzing O-glycosyl compounds
				TraesCS2A01G478700	Glycosyltransferase	GO:0008152 BP: metabolic process
				TraesCS2A01G478800	Histone-lysine N-methyltransferase	GO:0005515 MF: protein binding
				TraesCS2A01G478900	Glycosyltransferase	GO:0008152 BP: metabolic process
				TraesCS2A01G479000	Phosphatidylinositol-4-phosphate 5-kinase, putative	GO:0005524 MF: ATP binding
				TraesCS2A01G479100	Cyclin family protein	GO:0000079 BP: regulation of cyclin-dependent protein serine/threonine kinase activity
STI_RS Ratio	AX-108742509	2A	718	TraesCS2A01G480100	NBS-LRR disease resistance protein, putative, expressed	GO:0043531 MF: ADP binding
				TraesCS2A01G480200	Divalent-cation tolerance protein CutA	GO:0010038 BP: response to metal ion
				TraesCS2A01G480300	Thioredoxin	GO:0045454 BP: cell redox homeostasis
				TraesCS2A01G480400	NBS-LRR disease resistance protein	GO:0043531 MF: ADP binding
				TraesCS2A01G480500	Kinesin-like protein	GO:0003777 MF: microtubule motor activity
				TraesCS2A01G480600	Kinase-like	GO:0004672 MF: protein kinase activity
STI_RS Ratio	AX-158608713	2A	718	TraesCS2A01G480800	Serine/threonine-protein kinase	NA
				TraesCS2A01G480900	Glycosyltransferase	GO:0016757 MF: transferase activity, transferring glycosyl groups
				TraesCS2A01G481000	Protein SDA1-like protein	GO:0005488 MF: binding
STI_RS Ratio	BS00093201_51	2A	718	TraesCS2A01G481100	At4g28290	NA
				TraesCS2A01G481200	Anthocyanidin reductase	GO:0003824 MF: catalytic activity
				TraesCS2A01G481300	Anthocyanidin reductase	GO:0003824 MF: catalytic activity

STI_RS Ratio	AX-110966497		2A	718	TraesCS2A01G481400	Anthocyanidin reductase	GO:0003824 MF: catalytic activity
STI_RS Ratio	BS00081506_51		2A	718	TraesCS2A01G481500	Anthocyanidin reductase	GO:0003824 MF: catalytic activity
					TraesCS2A01G481700	Anthocyanidin reductase	GO:0003824 MF: catalytic activity
STI_RS Ratio	AX-109340451		2A	718	TraesCS2A01G481800	Anthocyanidin reductase	GO:0003824 MF: catalytic activity
					TraesCS2A01G481900	Anthocyanidin reductase	GO:0003824 MF: catalytic activity
					TraesCS2A01G483300	Pleiotropic drug resistance ABC transporter	GO:0005524 MF: ATP binding
					TraesCS2A01G483400	Organic cation transporter-like protein	GO:0005215 MF: transporter activity
					TraesCS2A01G483500	Organic cation transporter protein	GO:0005215 MF: transporter activity
					TraesCS2A01G483700	Organic cation transporter protein	GO:0005215 MF: transporter activity
					TraesCS2A01G484700	basic helix-loop-helix (bHLH) DNA-binding superfamily protein	GO:0046983 MF: protein dimerization activity
					TraesCS2A01G484800	Serine/threonine-protein kinase	GO:0004672 MF: protein kinase activity
					TraesCS2A01G484900	Serine/threonine-protein kinase	GO:0004672 MF: protein kinase activity
STI_RL	wsnp_JD_c52_87219	sti_RL_2B_Hap1	2B	640	TraesCS2B01G447700	alpha/beta-Hydrolases superfamily protein	NA
	Excalibur_c11392_1193	sti_RL_2B_Hap1	2B	641	TraesCS2B01G447800	Late embryogenesis abundant protein family protein	NA
					TraesCS2B01G447900	Yellow stripe-like transporter 17	GO:0055085 BP: transmembrane transport
					TraesCS2B01G448100	Ethylene-responsive transcription factor	GO:0003677 MF: DNA binding
					TraesCS2B01G449000	30S ribosomal protein S8	GO:0003735 MF: structural constituent of ribosome
					TraesCS2B01G449100	Transporter-related family protein	GO:0005215 MF: transporter activity
					TraesCS2B01G449200	Protein phosphatase 2c, putative	GO:0003824 MF: catalytic activity
					TraesCS2B01G449300	Pumilio-like protein	GO:0003723 MF: RNA binding
					TraesCS2B01G449400	Pumilio-like protein	GO:0003723 MF: RNA binding
					TraesCS2B01G450100	Cytochrome P450	GO:0005506 MF: iron ion binding
					TraesCS2B01G450200	Cytochrome P450	GO:0005506 MF: iron ion binding
					TraesCS2B01G450800	26S proteasome non-ATPase regulatory subunit 1	GO:0000502 CC: proteasome complex
STI_RS Ratio	Kukri_c51247_322		3A	140	TraesCS3A01G151100	Peptidyl-prolyl cis-trans isomerase	GO:0000413 BP: protein peptidyl-prolyl isomerization
					TraesCS3A01G151300	ATP-dependent zinc metalloprotease FtsH 1	GO:0005524 MF: ATP binding
					TraesCS3A01G151400	S-type anion channel	GO:0016021 CC: integral component of membrane
					TraesCS3A01G151500	F-box family protein	GO:0005515 MF: protein binding
STI_SL	AX-108852904		3B	822	TraesCS3B01G601500	11S globulin seed storage protein 2	GO:0045735 MF: nutrient reservoir activity

				TraesCS3B01G601600	Metallothionein	GO:0046872 MF: metal ion binding
				TraesCS3B01G601700	Metallothionein	GO:0046872 MF: metal ion binding
				TraesCS3B01G603200	SKP1-like protein	GO:0006511 BP: ubiquitin-dependent protein catabolic process
				TraesCS3B01G604000	Protein phosphatase 2C family protein	GO:0003824 MF: catalytic activity
				TraesCS3B01G604100	NBS-LRR disease resistance protein	GO:0043531 MF: ADP binding
				TraesCS3B01G604300	rRNA N-glycosidase	GO:0017148 BP: negative regulation of translation
				TraesCS3B01G604500	NBS-LRR resistance-like protein	GO:0043531 MF: ADP binding
				TraesCS3B01G604600	Disease resistance protein (NBS-LRR class) family	GO:0043531 MF: ADP binding
STI_SL	BS00071183_51	3B	823	TraesCS3B01G604700	External alternative NAD(P)H-ubiquinone oxidoreductase B2, mitochondrial	GO:0016491 MF: oxidoreductase activity
				TraesCS3B01G604800	NBS-LRR-like resistance protein	GO:0043531 MF: ADP binding
				TraesCS3B01G604900	Disease resistance protein (NBS-LRR class) family	GO:0017148 BP: negative regulation of translation
				TraesCS3B01G605100	Kinase interacting (KIP1-like) family protein	GO:0003779 MF: actin binding
				TraesCS3B01G605700	Lipoxygenase	GO:0005515 MF: protein binding
STI_SL	IAAV8659	3B	826	TraesCS3B01G606000	F-box protein	NA
				TraesCS3B01G606400	Aspartic proteinase nepenthesin-1	GO:0004190 MF: aspartic-type endopeptidase activity
				TraesCS3B01G606700	Disease resistance protein (TIR-NBS-LRR class) family	GO:0043531 MF: ADP binding
				TraesCS3B01G606800	rRNA N-glycosidase	GO:0017148 BP: negative regulation of translation
				TraesCS3B01G607400	Plant/T31B5-30 protein	GO:0008152 BP: metabolic process
STI_SL	wsnp_Ra_rep_c75740_73183118	3B	826	826.0816	Chaperone protein dnaJ	NA
STI_SL	AX-158598301	3B	826	TraesCS3B01G607500	Chaperone protein dnaJ	NA
				TraesCS3B01G607600	ABC transporter B family protein	GO:0005524 MF: ATP binding
				TraesCS3B01G607700	Disease resistance protein RPP13	GO:0043531 MF: ADP binding
				TraesCS3B01G608400	GDSL esterase/lipase	GO:0016788 MF: hydrolase activity, acting on ester bonds
				TraesCS3B01G608500	Aquaporin	GO:0005215 MF: transporter activity
				TraesCS3B01G608600	MADS-box transcription factor	GO:0003677 MF: DNA binding
STI_SL	BS00073411_51	3B	829	TraesCS3B01G608900	Dof zinc finger protein	GO:0003677 MF: DNA binding
				TraesCS3B01G609000	Dof zinc finger protein	GO:0003677 MF: DNA binding
				TraesCS3B01G609100	Dof zinc finger protein	GO:0003677 MF: DNA binding
				TraesCS3B01G609300	F-box protein-like protein	GO:0005515 MF: protein binding

				TraesCS3B01G610200	Pectin acetylesterase	GO:0016787 MF: hydrolase activity
				TraesCS3B01G610300	Pectin acetylesterase	GO:0016787 MF: hydrolase activity
				TraesCS3B01G610400	Pectin acetylesterase	GO:0016787 MF: hydrolase activity
				TraesCS3B01G610600	Pectin acetylesterase	GO:0016787 MF: hydrolase activity
				TraesCS3B01G610700	B3 domain-containing protein	GO:0003677 MF: DNA binding
STI_SL	AX-111015220	3B	829	TraesCS3B01G610800	Histone H2A	GO:0003677 MF: DNA binding
				TraesCS3B01G610900	RNA-binding protein	GO:0003676 MF: nucleic acid binding
				TraesCS3B01G611100	Receptor-like protein kinase	GO:0004672 MF: protein kinase activity
				TraesCS3B01G611300	Histone H2A	GO:0003677 MF: DNA binding
				TraesCS3B01G611600	Soluble inorganic pyrophosphatase	GO:0000287 MF: magnesium ion binding
				TraesCS3B01G612600	Transcription factor, MADS-box	GO:0003677 MF: DNA binding
				TraesCS3B01G612700	Transcription factor, MADS-box	GO:0003677 MF: DNA binding
STI_SL	AX-158578652	3B	829	TraesCS3B01G609100	Dof zinc finger protein	GO:0003677 MF: DNA binding
				TraesCS3B01G609300	F-box protein-like protein	GO:0005515 MF: protein binding
				TraesCS3B01G609400	Cytochrome P450	GO:0005506 MF: iron ion binding
				TraesCS3B01G609500	Ankyrin repeat family protein	GO:0005515 MF: protein binding
				TraesCS3B01G609600	Cytochrome P450	GO:0005506 MF: iron ion binding
				TraesCS3B01G609900	Pre-mRNA-splicing factor ISY1-like protein	GO:0000350 BP: generation of catalytic spliceosome for second transesterification step
				TraesCS3B01G611900	Ubiquitin family protein	GO:0005515 MF: protein binding
				TraesCS3B01G612000	O-methyltransferase	GO:0008168 MF: methyltransferase activity
				TraesCS3B01G612200	MYB transcription factor	GO:0003677 MF: DNA binding
				TraesCS3B01G612300	Transcription factor, MADS-box	GO:0003677 MF: DNA binding
				TraesCS3B01G612400	Transcription factor, MADS-box	GO:0003677 MF: DNA binding
				TraesCS3B01G612500	Transcription factor, MADS-box	GO:0003677 MF: DNA binding
				TraesCS3B01G612600	Transcription factor, MADS-box	GO:0003677 MF: DNA binding
				TraesCS3B01G612700	Transcription factor, MADS-box	GO:0003677 MF: DNA binding
STI_RS Ratio	AX-108852904	3B	822	TraesCS3B01G601500	11S globulin seed storage protein 2	GO:0045735 MF: nutrient reservoir activity
				TraesCS3B01G601600	Metallothionein	GO:0046872 MF: metal ion binding
				TraesCS3B01G601700	Metallothionein	GO:0046872 MF: metal ion binding
				TraesCS3B01G601800	Metallothionein	GO:0046872 MF: metal ion binding

				TraesCS3B01G602000	30S ribosomal protein S17	GO:0003735 MF: structural constituent of ribosome
				TraesCS3B01G602100	30S ribosomal protein S19	GO:0003723 MF: RNA binding
				TraesCS3B01G603800	Kinase-like protein	GO:0004672 MF: protein kinase activity
				TraesCS3B01G603900	GATA transcription factor, putative	GO:0003700 MF: transcription factor activity, sequence-specific DNA binding
				TraesCS3B01G604000	Protein phosphatase 2C family protein	GO:0003824 MF: catalytic activity
				TraesCS3B01G604100	NBS-LRR disease resistance protein	GO:0043531 MF: ADP binding
				TraesCS3B01G604300	rRNA N-glycosidase	GO:0017148 BP: negative regulation of translation
				TraesCS3B01G604500	NBS-LRR resistance-like protein	GO:0043531 MF: ADP binding
				TraesCS3B01G604600	Disease resistance protein (NBS-LRR class) family	GO:0043531 MF: ADP binding
STI_RS Ratio	BS00071183_ 51	3B	823	TraesCS3B01G604700	External alternative NAD(P)H-ubiquinone oxidoreductase B2, mitochondrial	GO:0016491 MF: oxidoreductase activity
				TraesCS3B01G604800	NBS-LRR-like resistance protein	GO:0043531 MF: ADP binding
				TraesCS3B01G604900	Disease resistance protein (NBS-LRR class) family	GO:0017148 BP: negative regulation of translation
				TraesCS3B01G605100	Kinase interacting (KIP1-like) family protein	GO:0003779 MF: actin binding
STI_RS Ratio	AX- 158598301	3B	826	TraesCS3B01G607500	Chaperone protein dnaJ	NA
				TraesCS3B01G607600	ABC transporter B family protein	GO:0005524 MF: ATP binding
				TraesCS3B01G607700	Disease resistance protein RPP13	GO:0043531 MF: ADP binding
				TraesCS3B01G608400	GDSL esterase/lipase	GO:0016788 MF: hydrolase activity, acting on ester bonds
				TraesCS3B01G608500	Aquaporin	GO:0005215 MF: transporter activity
				TraesCS3B01G608600	MADS-box transcription factor	GO:0003677 MF: DNA binding
STI_RS Ratio	BS00073411_ 51	3B	829	TraesCS3B01G608900	Dof zinc finger protein	GO:0003677 MF: DNA binding
				TraesCS3B01G609000	Dof zinc finger protein	GO:0003677 MF: DNA binding
				TraesCS3B01G609100	Dof zinc finger protein	GO:0003677 MF: DNA binding
				TraesCS3B01G610700	B3 domain-containing protein	GO:0003677 MF: DNA binding
STI_RS Ratio	AX- 111015220	3B	829	TraesCS3B01G610800	Histone H2A	GO:0000786 CC: nucleosome
				TraesCS3B01G610900	RNA-binding protein	GO:0003676 MF: nucleic acid binding
				TraesCS3B01G611100	Receptor-like protein kinase	GO:0004672 MF: protein kinase activity
				TraesCS3B01G611300	Histone H2A	GO:0003677 MF: DNA binding
				TraesCS3B01G612300	Transcription factor, MADS-box	GO:0003677 MF: DNA binding
				TraesCS3B01G612400	Transcription factor, MADS-box	GO:0003677 MF: DNA binding

				TraesCS3B01G612500	Transcription factor, MADS-box	GO:0003677 MF: DNA binding
				TraesCS3B01G612600	Transcription factor, MADS-box	GO:0003677 MF: DNA binding
				TraesCS3B01G612700	Transcription factor, MADS-box	GO:0003677 MF: DNA binding
STI_RS Ratio	AX-158578652	3B	829	TraesCS3B01G609100	Dof zinc finger protein	GO:0003677 MF: DNA binding
				TraesCS3B01G609300	F-box protein-like protein	GO:0005515 MF: protein binding
				TraesCS3B01G609400	Cytochrome P450	GO:0005506 MF: iron ion binding
				TraesCS3B01G609500	Ankyrin repeat family protein	GO:0005515 MF: protein binding
				TraesCS3B01G609600	Cytochrome P450	GO:0005506 MF: iron ion binding
				TraesCS3B01G609900	Pre-mRNA-splicing factor ISY1-like protein	GO:0000350 BP: generation of catalytic spliceosome for second transesterification step
				TraesCS3B01G612400	Transcription factor, MADS-box	GO:0003677 MF: DNA binding
				TraesCS3B01G612500	Transcription factor, MADS-box	GO:0003677 MF: DNA binding
				TraesCS3B01G612600	Transcription factor, MADS-box	GO:0003677 MF: DNA binding
				TraesCS3B01G612700	Transcription factor, MADS-box	GO:0003677 MF: DNA binding
STI_SL and STI_RS Ratio	BS00065603_51	3D	611	TraesCS3D01G537400	Dof zinc finger protein	GO:0003677 MF: DNA binding
				TraesCS3D01G537500	Dof zinc finger protein	GO:0003677 MF: DNA binding
				TraesCS3D01G537700	F-box protein-like protein	GO:0005515 MF: protein binding
				TraesCS3D01G537800	Cytochrome P450	GO:0005506 MF: iron ion binding
				TraesCS3D01G538900	Pectin acetylesterase	GO:0016787 MF: hydrolase activity
				TraesCS3D01G539100	Pectin acetylesterase	GO:0016787 MF: hydrolase activity
				TraesCS3D01G539200	B3 domain-containing protein	GO:0003677 MF: DNA binding
				TraesCS3D01G540900	Aquaporin	GO:0005215 MF: transporter activity
STI_SL and	BS00068415_51	3D	612	TraesCS3D01G541500	Disease resistance protein RPP13	NA
				TraesCS3D01G541600	Disease resistance protein (NBS-LRR class) family	GO:0043531 MF: ADP binding
				TraesCS3D01G541700	ABC transporter B family protein	GO:0005524 MF: ATP binding
				TraesCS3D01G542000	Pectinesterase inhibitor	GO:0004857 MF: enzyme inhibitor activity
				TraesCS3D01G542300	Protein kinase-like protein	GO:0004672 MF: protein kinase activity
				TraesCS3D01G542400	lectin-receptor kinase	GO:0004672 MF: protein kinase activity
				TraesCS3D01G542500	Disease resistance protein (TIR-NBS-LRR class) family	NA
				TraesCS3D01G543800	Serine/threonine-protein kinase ATM	GO:0003676 MF: nucleic acid binding

					TraesCS3D01G543900	Kinase-like protein	GO:0004672 MF: protein kinase activity
					TraesCS3D01G544100	Phosphatase 2C family protein	GO:0003824 MF: catalytic activity;GO:0043169 MF: cation binding
STI_RL	AX-158581925		4A	43	TraesCS4A01G051300	Cyclin family protein	GO:0005634 CC: nucleus
					TraesCS4A01G051400	Mannose-1-phosphate guanyltransferase	GO:0009058 BP: biosynthetic process
					TraesCS4A01G051600	Protein transport protein GOT1	GO:0016192 BP: vesicle-mediated transport
					TraesCS4A01G052000	Cysteine proteinase inhibitor	GO:0004869 MF: cysteine-type endopeptidase inhibitor activity
					TraesCS4A01G052100	Cysteine proteinase inhibitor	GO:0004869 MF: cysteine-type endopeptidase inhibitor activity
					TraesCS4A01G052200	Beta-xylosidase, putative	GO:0004553 MF: hydrolase activity, hydrolyzing O-glycosyl compounds
STI_RS Ratio	AX-158617434		4A	18	TraesCS4A01G024900	CASP-like protein	NA
					TraesCS4A01G025900	Serine protease HtrA-like	GO:0005515 MF: protein binding
					TraesCS4A01G026000	Werner Syndrome-like exonuclease	GO:0003676 MF: nucleic acid binding
					TraesCS4A01G026100	receptor kinase 1	GO:0004672 MF: protein kinase activity
					TraesCS4A01G026200	Serine/threonine-protein kinase	GO:0004672 MF: protein kinase activity
					TraesCS4A01G026300	receptor kinase 1	GO:0004672 MF: protein kinase activity
STI_RS Ratio	Kukri_rep_c68594_530		4D	12	TraesCS4D01G026700	5'-AMP-activated protein kinase subunit beta-1	NA
					TraesCS4D01G026800	NRT1/PTR family protein 2.2	GO:0005215 MF: transporter activity
					TraesCS4D01G026900	Hexosyltransferase	GO:0016757 MF: transferase activity, transferring glycosyl groups
STI_RL	AX-110016919		5B	591	TraesCS5B01G415900	N-acetylglucosaminyl-phosphatidylinositol biosynthetic protein gpi1	GO:0006506 BP: GPI anchor biosynthetic process
					TraesCS5B01G416800	NBS-LRR disease resistance protein, putative, expressed	GO:0043531 MF: ADP binding
					TraesCS5B01G416900	Calmodulin-binding protein, putative, expressed	GO:0005516 MF: calmodulin binding
					TraesCS5B01G417000	receptor kinase 1	GO:0004672 MF: protein kinase activity
					TraesCS5B01G417200	Calmodulin-binding protein, putative, expressed	GO:0005516 MF: calmodulin binding
					TraesCS5B01G417300	Calmodulin-binding protein, putative, expressed	GO:0005516 MF: calmodulin binding
STI_SL	Excalibur_c5329_1335	sti_SL_5B_Hap1	5B	580	TraesCS5B01G403700	Chitinase	GO:0004568 MF: chitinase activity
					TraesCS5B01G403800	GDSL esterase/lipase	GO:0016788 MF: hydrolase activity, acting on ester bonds
					TraesCS5B01G403900	Upstream activation factor subunit spp27	GO:0005515 MF: protein binding
					TraesCS5B01G404000	Phosphatase 2C family protein	GO:0003824 MF: catalytic activity
					TraesCS5B01G404200	Peroxidase	GO:0004601 MF: peroxidase activity

STI_SFW	AX-158586104	sti_SFW_5B_Hap1	5B	560	TraesCS5B01G382000	NA	NA
					TraesCS5B01G382000	F-box/LRR-repeat protein 17	GO:0005515 MF: protein binding
STI_SFW	AX-158600273		6A	520	TraesCS6A01G287400	Nuclear transcription factor Y subunit B	GO:0046982 MF: protein heterodimerization activity
					TraesCS6A01G287700	Dof zinc finger protein	GO:0003677 MF: DNA binding
					TraesCS6A01G288000	Acetolactate synthase	GO:0000287 MF: magnesium ion binding
					TraesCS6A01G288100	Basic helix-loop-helix transcription factor	GO:0046983 MF: protein dimerization activity
STI_SFW	AX-158600281		6A	520	TraesCS6A01G288300	2-oxoglutarate (2OG) and Fe(II)-dependent oxygenase superfamily protein	GO:0016491 MF: oxidoreductase activity
					TraesCS6A01G288400	2-oxoglutarate (2OG) and Fe(II)-dependent oxygenase superfamily protein	GO:0016491 MF: oxidoreductase activity
STI_SFW	wsnp_Ku_c4296_7807837		6A	520	520.7175	NBS-LRR-like resistance protein	NA
					TraesCS6A01G289500	Receptor-like kinase	GO:0004672 MF: protein kinase activity
					TraesCS6A01G289600	H/ACA ribonucleoprotein complex subunit 2-like protein	GO:0003723 MF: RNA binding
					TraesCS6A01G289800	Tetraspanin family protein	GO:0016021 CC: integral component of membrane
STI_SFW	AX-158535753		6B	51	TraesCS6B01G074400	F-box family protein	GO:0005515 MF: protein binding
					TraesCS6B01G074500	F-box family protein	GO:0005515 MF: protein binding
					TraesCS6B01G074700	F-box family protein	GO:0005515 MF: protein binding
					TraesCS6B01G075200	NAC domain protein	GO:0003677 MF: DNA binding
					TraesCS6B01G075400	F-box family protein	GO:0005515 MF: protein binding
					TraesCS6B01G075500	F-box family protein	GO:0005515 MF: protein binding
					TraesCS6B01G075600	NBS-LRR disease resistance protein-like protein	GO:0043531 MF: ADP binding
					TraesCS6B01G075700	NBS-LRR disease resistance protein-like protein	GO:0043531 MF: ADP binding
STI_RL	D_contig78519_72		7D	10	TraesCS7D01G021200	Protein kinase family protein	GO:0004672 MF: protein kinase activity
					TraesCS7D01G021300	Disease resistance protein (NBS-LRR class) family	NA
					TraesCS7D01G021600	F-box protein	GO:0005515 MF: protein binding
					TraesCS7D01G021700	F-box protein	GO:0005515 MF: protein binding
					TraesCS7D01G021800	F-box protein	GO:0005515 MF: protein binding
					TraesCS7D01G021900	disease resistance family protein / LRR family protein	NA
					TraesCS7D01G022000	receptor-like protein kinase 1	GO:0004672 MF: protein kinase activity
					TraesCS7D01G022100	Disease resistance protein (NBS-LRR class) family	GO:0043531 MF: ADP binding
					TraesCS7D01G022200	Protein kinase family protein	GO:0004672 MF: protein kinase activity

	TraesCS7D01G022300	Disease resistance protein (NBS-LRR class) family	GO:0005515 MF: protein binding
	TraesCS7D01G022400	Disease resistance protein (NBS-LRR class) family	GO:0003677 MF: DNA binding
	TraesCS7D01G024500	Cytochrome P450 family protein, expressed	GO:0005506 MF: iron ion binding
	TraesCS7D01G024700	NBS-LRR resistance-like protein	GO:0043531 MF: ADP binding
	TraesCS7D01G024900	Disease resistance protein (NBS-LRR class) family	GO:0043531 MF: ADP binding

Supplementary Table 4. S4. The haplotype blocks associated with different traits and their chromosomal positions and alleles

Trait	Haplotype block	Significant marker (s)	NMHB	Chr	No. of Genes	Favorable allele
STI_SL	sti_SL_1A_Hap1	AX-158595571	4	1A	2	CGGT
STI_RL	sti_RL_2B_Hap1	wsnp_JD_c52_87219, Excalibur_c11392_1193	6	2B	31	CACGAC
STI_SL	sti_SL_5B_Hap1	Excalibur_c5329_1335	7	5B	15	AGCCCGA
STI_SFW	sti_SFW_5B_Hap1	AX-158586104	5	5B	3	GACGG
R_RFW	Rel_RFW_1B_Hap1	Excalibur_c7954_672	4	1B	1	GCGG
R_RFW	Rel_RFW_1B_Hap2	RAC875_c28894_526, wsnp_Ex_c11976_19193550	4	1B	29	AGGT
R_SL	Rel_SL_1B_Hap1	AX-158540096, AX-158560878, Tdurum_contig94450_255	7	1B	3	GTGAGCC
R_SFW	Rel_SFW_3A_Hap1	AX-158532834	19	3A	26	GGGGCTGCCGGA ACCATTTA
R_RL	Rel_RL_3B_Hap1	BobWhite_c10402_140, wsnp_JD_c30422_23944042	4	3B	1	CCCC
R_RFW	Rel_RFW_6B_Hap1	AX-158528874, BS00011795_51	4	6B	9	CAGT
R_RL, R_RSRatio	Com_Hap1	AX-158582574	5	4B	157	TCGGG

Abbreviations: NMHB, number of markers in haplotype block; Chr, chromosome; R_SL, relative shoot length; STI_RL, stress tolerance index root length; STI_SFW, stress tolerance shoot fresh weight; STI_SFW, stress tolerance index shoot fresh weight; R_RL, relative root length; R_RFW, relative root fresh weight; R_RSRatio, relative root-shoot ratio